Cainozoic deformation of Iberia

A model for intraplate mountain building and basin development based on analogue modelling

Javier Fernández Lozano

UTRECHT STUDIES IN EARTH SCIENCES
No. 013

The research presented in this thesis was carried out at:

The Netherlands Research Centre for Integrated Solid Earth Sciences (ISES)
De Boelelaan 1085
1081 HV Amsterdam
The Netherlands

Instituto de Geociencias (IGEO)
Facultad de Ciencias Geológicas
Universidad Complutense de Madrid
José Antonio Novais 12
28040 Madrid
España

Departamento de Geodinámica
Facultad de Ciencias Geológicas
Universidad Complutense de Madrid
José Antonio Novais 12
28040 Madrid
España

Members of the dissertation committee:

Prof. Dr. Manel Fernández
Departamento de Geofísica y Tectónica, Instituto de Ciencias de la Terra Jaume Almera, Barcelona, Spain

Prof. Dr. Jan-Diederik Van Wees
Department of Tectonics and Structural Geology, VU University Amsterdam, The Netherlands

Prof. Dr. Evgenii Burov
Laboratoire de Tectonique, Université Pierre et Marie Curie (UPMC) Paris, France

Dr. Antonio Casas-Sainz
Departamento de Ciencias de la Tierra. Universidad de Zaragoza Zaragoza, Spain

Dr. Fred Beekman
Department of Earth Sciences, Utrecht University Utrecht, The Netherlands

ISBN: 978-90-6266-294-4

Printed by Wöhrmann Print Service, Zutphen

Cover image: *Composite image consisting of the filtered topography of an analogue experiment draped over a digital elevation model of Iberia emphasizing the relationship between topography and folding of the lithosphere.*

Cainozoic deformation of Iberia

A model for intraplate mountain building and basin development based on analogue modelling

Cenozoïsche intraplaat deformatie van Iberië

Een analoge modelstudie voor de vorming van gebergten en sedimentaire bekkens
(met een samenvatting in het Nederlands)

Deformación Cenozoica de Iberia

Un modelo para la formación montañosa y desarrollo de cuencas intraplaca basado en la modelación análoga
(con un resumen en Castellano)

Proefschrift

ter verkrijging van de graad van doctor aan de Universiteit Utrecht op gezag van de rector magnificus, prof.dr. G.J. van der Zwaan, ingevolge het besluit van het college voor promoties in het openbaar te verdedigen op dinsdag 1 mei 2012 des middags te 2.30 uur

door

Javier Fernández Lozano

geboren op 11 juni 1982
te *Madrid, Spanje*

Promotoren: Prof. dr. S.A.P.L. Cloetingh
Prof. dr. G. De Vicente
Co-promotoren: Prof. dr. D. Sokoutis
Dr. E. Willingshofer

This thesis was accomplished with financial support from Universidad Complutense de Madrid (Spain), the Spanish National Research Program: CGL2006-13926-CO-01-02 Topo-Iberia Foreland and Consolider Ingenio 2006 Topo-Iberia CSD20006-00041, as well as The Netherlands Research Centre for Integrated Solid Earth Sciences (ISES).

Nothing can remain inmense if it can be measured

Hannah Arendt, (1958). The Human Condition

Contents

1 Cainozoic intra-plate mountain building in Iberia 1

1.1 Introduction 1
1.2 Early evidences of intra-plate topography 4
1.3 Different hypothesis for intraplate mountain building in Iberia 4
1.4 Scope of this thesis 6
1.5 Thesis outline 7

2 Fundamental aspects of folding 9

2.1 Introduction 9
2.2 Mechanisms of folding development 10
2.2.1 Folding of single-layer systems 10
2.2.2 Folding of multilayer systems 12
2.3 Folding-faulting relationships 13
2.4 Lithospheric folding 14
2.4.1 Global distribution 16
2.4.2 Continental lithosphere 17
2.4.3 Oceanic lithosphere 18
2.5 Folding of the Ibero-African lithosphere 19

3 Cainozoic deformation of Iberia: a model for intra-plate mountain building and basin development based on analogue modelling 21

3.1 Introduction 21
3.2 Cainozoic deformation and plate reorganisation 22
3.3 The role of late-Variscan tectonic structures 28
3.4 Distribution of mountain ranges and related basins 34
3.4.1 Alpine evolution of intra-plate mountain ranges 34
3.4.1.1 Northern Spain 34
3.4.1.2 Central Iberia 36
3.4.1.3 Atlantic margin 40
3.4.2 Cainozoic intra-plate basins 45

3.4.2.1 Ebro Basin 45
3.4.2.2 Duero Basin 49
3.4.2.3 Tagus Basin 50
3.4.2.4 Minor intra-plate basins 52
3.5 The Iberian lithosphere 54
3.5.1 Crustal structure and topography 54
3.5.2 Thermal structure and rheology 57
3.6 Analogue modelling set-up 60
3.6.1 Geometry, rheology and scaling 60
3.6.2 Simplifications and general assumptions 62
3.7 Modelling results 64
3.7.1 Crust-mantle coupling 64
3.7.1.1 Model IBERIA-I: weak crust-mantle coupling (convergence rate 0.5 cm/h) 64
3.7.1.2 Model IBERIA-II: strong crust-mantle coupling (convergence rate 1cm/h) 67
3.7.2 Rheology of the lower crust and upper mantle 67
3.7.2.1 Model IBERIA-III: strong lower crust, weak upper mantle 67
3.7.3 Influence of an indenter 69
3.7.3.1 Model IBERIA-IV 69
3.7.3.2 Model IBERIA-V 69
3.7.3.3 Model IBERIA-VI 73
3.7.4 Role of model size 73
3.7.4.1 Model IBERIA-VII 73
3.7.4.2 Model IBERIA-VIII 73
3.8. Discussion of modelling results 76
3.8.1 Relationship of folding and faulting 76
3.8.2 Experimental Moho depth and surface topography 77
3.8.3 Implications for mountain building and basin development in Iberia 79
3.8.3.1 Basement uplift controlled by lithosphere folding amplification 79
3.8.3.2 Intra-mountain evolution,

migration and subsequent basin disconnection:
a broken foreland basin model 81
3.9 Conclusions 83

4 Integration of gravity and topography analysis in analogue modelling: understanding lateral strength variations in Iberia and their influence on intra-plate mountain building 85

4.1 Introduction 85
4.2 Surface structure and lithospheric configuration of Iberia 86
4.3 Integrating analogue modelling with spectral analysis of gravity and topography 87
4.3.1 Analogue modelling 87
4.3.2 Gravity interpretation of physical experiments 88
4.3.2.1 Fundamentals of gravity 88
4.3.2.2 Corrections to gravity observations 91
4.3.2.3 Geological factors and assumptions 93
4.3.2.4 Gravity modelling 93
4.3.3 Fourier analysis of periodic functions 95
4.3.3.1 Data processing 97
4.4 Modelling results 98
4.4.1 Model with homogeneous strong lithosphere (IBERIA-I) 98
4.4.2 Model with lateral strength variations (IBERIA-XIX) 98
4.4.3 Model with lateral strength variations and E-W Mesozoic depocentres (IBERIA-X) 103
4.5 Discussion 106
4.5.1 Lithosphere strength variations and topography 106
4.5.2 The role of late-Variscan structures during Cainozoic deformation of Iberia: do they really influence folding? 108
4.6 Conclusions 111

5 Strain partitioning and intra-plate deformation: the role of lateral strength variations in Central Iberia 113

5.1 Introduction 113

5.2 Geological framework 114
5.3 Analogue modelling experiments 118
5.4 Modelling results 120
5.4.1 Model without depocentres (IBERIA-XIX) 122
5.4.2 Model with E-W Mesozoic depocentres (IBERIA-X) 124
5.5 Discussion 125
5.5.1 Influence of lateral lithospheric strength changes on mode of deformation 125
5.5.2 Strain partitioning within intra-plate domains 126
5.6 Conclusions 127

6 Discussion and conclusions 129
6.1 Introduction 130
6.2 Folding of de-coupled lithosphere 130
6.2.1 Ibero-Atlas mountain belt 132
6.2.2 Tien Shan Mountains in Central Asia 136
6.3 Crustal architecture of intra-plate folded lithosphere: The role of pre-existent tectonic structures 139
6.3.1 The Mérida Andes (western Venezuela) 139
6.3.2 Comparison with Iberia 139
6.4 Basin response to active intra-plate mantle deformation 141
6.5 Conclusions: a new model for Intra-plate mountain building and basin development in Iberia. 141

7 References 143

Summary 163

Samenvatting 167

Resumen 171

Acknowledgements 175

Chapter 1

Cainozoic Intra-plate mountain building in Iberia

The overall average topography of Iberia, rising over 600 m, represents the highest mean elevation in Europe far from the Alpine front. Such high elevation contrasts with the presence of sedimentary basins that are present above the highest average topography in the intra-plate Europe (such as the Duero ~900 and Tagus basins ~750 m). In addition to vertical hypsometric differences observed in Iberia, another striking feature concerns the general mountain trends and their regular periodicity towards the west. Topographic trends had a major influence on river drainage systems arrangement. In general, catchment areas also tend to occur parallel to the main mountain fronts. However, the influence of major tectonic structures and deep processes may also have contributed to the present-day topographic configuration. This chapter introduces the main features that define the topography of Iberia, its main differences and peculiarities. Moreover, the principal theories behind the mechanism (s) for intra-plate mountain building and basin development within the Iberian Peninsula are reviewed. Accordingly, this thesis focuses on the study of large-scale folding through a series of analogue models, validatded by integrating gravity and topography interpretation of the modelling results, in order to link surface and deep Earth processes. The aim of this thesis is to contribute to a better understanding of the observed differences in pattern of relief in Iberian, describing the mechanisms of mountain building. Special attention is paid on the lithosphere structure as a result of lithospheric folding. The conclusions in this chapter represent the outline for this thesis, following a detailed description of the upcoming sections.

1.1 Introduction

The Iberian Peninsula constitutes the western most margin of the European continent. Commonly, the whole Peninsula has been called Iberian micro-continent due to its geometry and configuration (acting as an independent plate during most of the Mesozoic Era and early Tertiary Era).

Geographically, Iberia is characterised by a series of mountain belts mostly trending E-W and NE-SW. Moreover, the main mountain reliefs are bordered by inter-mountain basins (like the Duero, Ebro and the Tagus-Madrid Basin), and several small intra-mountain basins that configure the Peninsula relief. The average of overall topography is 660 m. Nevertheless, significant differences of elevation are recorded between the mountain ranges and their relative

subordinate basins. For instance, the presence of relative high elevation of the Tagus (>700 m) and Duero Basins (~900 m), contrast with the low altitudes found along northwestern Spain (Terra-Chá reliefs in Galicia ~500 m). According to *Casas-Sainz and De Vicente* (2009b), the present-day topographic differences in Iberia result from Cainozoic compression and Neogene extension along the eastern border, leading to a general topographic tilting towards the Atlantic margin. These major changes in topography raise the question whether differences between mountain range systems and associated basins are related to surface or deep tectonic processes and their potential implications for climatic change conditions.

A feature that distinguishes the Iberian landscape from any other intra-plate setting in the world is the presence of an elongated drainage pattern following parallel orientations between the different basins [Fig.1.1]. Moreover, the E-W marked river pattern becomes controlled by the position and uplift of the surrounding mountain ranges. Although the drainage system tends to change along structural features leading to strong river incision all over the Iberian Massif following mainly NW-SE, NE-SW and N-S late-Variscan structures along the Sierra Morena, the Spanish Central System and the north west Galicia margin, respectively (Arthaud and Matte, 1977) [Fig.2.1a].

Aerial pictures portray the presence of fluvial capture mechanisms allowed by differential erosion rate, rock type, tectonic uplift and climate perturbations which may impose important controls on catchment processes. A good example is shown by small rivers diverging to the Ebro basin that become captured by the Tagus drainage system [Fig.2.1a]. Differences in depth of the basement between broad basins may also have perturbed the direction of the main drainage systems acting as sedimentary thresholds. Besides recent neotectonic movements that were able to control the evolution of fluvial patterns, inherited Mesozoic features may have influenced the actual river position and incision. A good example is found along the lower part of the Guadiana River.

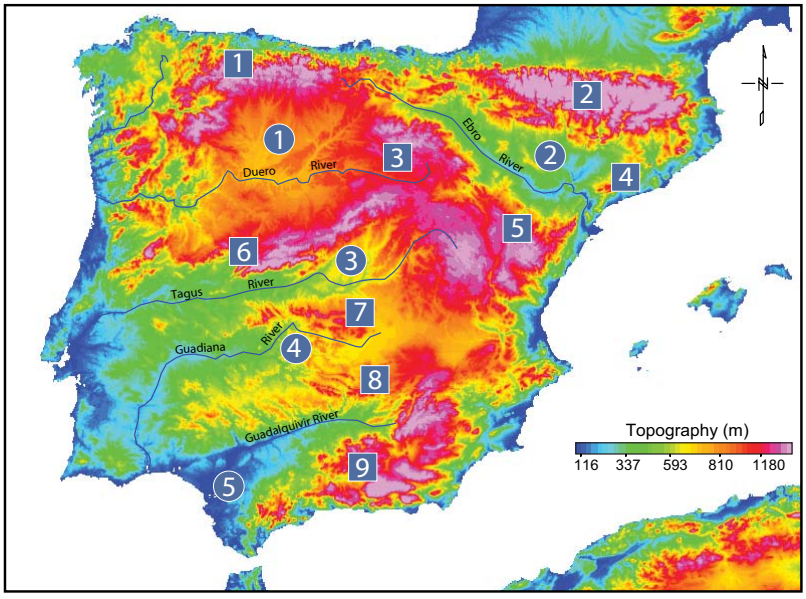

Figure 1.1: *Topographic map of Iberia showing the main reliefs. Circles: main basins 1) Duero Basin, 2) Ebro Basin, 3) Tagus Basin, 4) Badajoz Basin and 5) Guadalquivir Basin. Squares: main mountain ranges; 1) Cantabrian Mountains, 2) Pyrenees, 3) Demanda-Cameros, 4) Catalan-Coastal Ranges, 5) Montalban, 6) Spanish Central System, 7) Guadalupe-Montanchez Sierras and Toledo Mountains, 8) Sierra Morena, 9) Betics.*

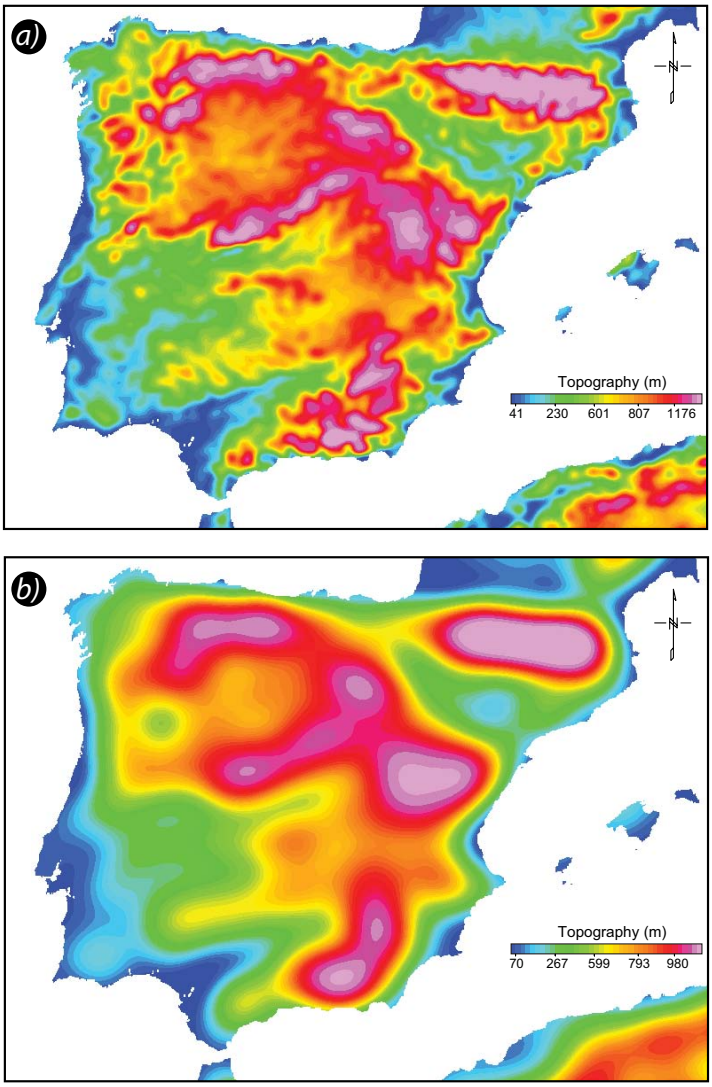

Figure 1.2: *Filtered topography at 50 km showing the imprint of Variscan deformation along N-S, E-W, NE-SW and NW-SE tectonic structures. (c) Map of Iberia showing the filtered topography at 250 km, indicating a series of periodic uplifts in western Iberia that clearly correlate from north to south with the Cantabrian Mountains, The Spanish Central System and Sierra Morena, respectively.*

It is believed that the river may have had occupied a broad plateau in southern Spain, during an endoreic stage of evolution related to lithospheric flexure induced by rift-shoulder uplift of the western part of the Iberian Massif during the Mesozoic opening of the Atlantic mid-ocean ridge (*Stapel et al.,* 1996; *Martín-González et al.,* 2006; *Ghorbal et al.,* 2008). Such uplift may have also influenced the straight pattern of topography along the western margin as suggested by *Tejero et al.* (2010). The topographic map shown in [Fig.2.1b] shows E-W to NE-SW periodic trends along the western part of Iberia, from north to south: Pyrenean-Cantabrian mountains, the Spanish Central System and Sierra Morena, respectively. However, towards the

east NW-SE to E-W and in some cases NE-SW trends are found along the Iberian Chain and the Catalan Ranges. However, little is known about the mechanism that led to the present-day distribution and orientation of mountain ranges in Iberia. In such a context, several hypotheses have been put forward to explain the observed relief. The aim of this thesis is to gain insight into the surface pattern of relief and deep processes involved in the development and evolution of intra-plate mountain ranges and subordinate basins in Spain. It provides an understanding of the effect of rheological lithosphere variations and the importance of late-Variscan pre-existent fractures that may have controlled the final configuration of topography.

1.2 Early evidences of intra-plate topography

After the beginning of plate reorganization in the late Cretaceous, the northern Iberian basins, where shallow marine and continental sediments were deposited, became isolated. As a result, several small epeiric seas were formed prior to the onset of the raising Pyrenean Orogen (e.g. Basque Basin, Tremp Basin). The formation of the Pyrenees lasted for nearly 50 My. giving raise to the so called Pyrenean Mountains. The evolution of the Orogen is linked to the N-directed continental collision among the European and Iberian plates (*Roure et al.,* 1989; *Choukroune,* 1992). Once the collision took place, the plate boundary unexpectedly moved towards southern Iberia (early Miocene onwards, *Kampschuur and Rondeel,* 1975; *Maldonado et al.,* 1999). The ongoing collision between Iberia and Africa during the Neogene squeezed the Alboran crustal-block, forced by the movement of Africa to the North and pushed away by the tectonic stretching of the Western Mediterranean. However, recent fission track data and structural data, have suggested that the overall topography of the Iberian plate interior was already uplifted by the time the Betic Orogen was formed. These data estimates the age of uplift of Northern Iberia as Paleogene (Cantabrian Mountains, early Eocene; Galaico-Leoneses Mountains, early Miocene), Central Iberia (Spanish Central System, Eocene-Oligocene and Miocene; Iberian Chain, Eocene-Oligocene) (*De Bruijne and Andriessen,* 2000; *Barbero et al.,* 2005; *Del Rio et al.,* 2009; *Martín-González et al.,* 2011). Therefore, despite the mechanism that may have influenced the formation of topography remains unknown, it appears clear that the age of uplift is subsequently the final result of the stress transmission from the Pyrenean border prior to the collision and formation of the Betic Orogen. For this reason and in order to prevent any further correlation with the Betics, this thesis does not deal with the post-Miocene tectonic evolution of the micro-plate. Consequently, the main focus of the text is paid to the intra-plate formation of topography as a result of the N-S Pyrenean shortening that took place in Iberia during the Cainozoic.

1.3 Different hypothesis for intraplate mountain building in Iberia

Several tectonic processes have been proposed for explaining the actual distribution of mountain ranges and related basins in Iberia. However, there is not a single model that could successfully explain the observed intra-plate topography, and therefore, the most likely scenario may result from the interaction of several of these processes. So far, the five most important mechanisms proposed are:

» **Block rotation model**. The actual topography of the central part of Spain would be the result of strain localisation along late-Variscan faults which led to block rotation and fault reorganisation probably linked to thickening of the lower crust under the Spanish Central System (*Vegas et al.,* 1990). However, despite this hypothesis successfully explains morphological characters like distribution of intra-mountain basins, or the rotation of

tectonic structures, it is exclusively based on previous studies focusing on a small area in central eastern Iberia (*Banda et al.,* 1981; *Banda et al.,* 1983 and *Vegas and Suriñach,* 1987). In addition, some other hypotheses trying to explain the topography (differential sink, compression-decompression, doming of the Castellano-Extremeña domain or romb-horst hypothesis as it was argued by *Hernández-Pacheco* (1923); *Birot and Solé-Sabaris* (1954); *Alía-Medina* (1976) and *Portero and Aznar* (1984), focus exclusively to the region of the Central System, therefore they wont be mentioned here. However, more information could be find in *Ubanell* (1994) and references therein.

» **Mid-crustal detachment**. This hypothesis assumes the presence of a large-scale mid-crustal detachment affecting the Iberian Range and Central System rooted at the Pyrenees and Betic Cordillera (*Banks and Warburton,* 1991). However, gravity modelling studies and palinspastic reconstructions do not support the existence of mid-crustal detachments with large horizontal displacements (*Salas and Casas,* 1993; *Guimerá et al.,* 2004).

» **Extension-inversion coupling mechanism**. Crustal reorganisation and lithosphere thermo-mechanical re-adjustments between stretched areas in the east and the relative stable Variscan lithosphere to the west occurred as a result of early Miocene extension along the Valencia Trough (*Vergés and Fernández,* 2006); crustal thinning and thermal anomalies that affected eastern Iberia (probably closely related to the rifting episode that extended across western and central Europe (*Ziegler and Dezes,* 2006), and subsequent tectonic inversion (late Pyrenean to early Betic tectonic phase) during early-late Miocene. Unlike previously proposed models, it successfully explains the thermal anomalies and lateral changes of lithospheric thickness. However, this model does not correlate surface processes with large-scale deep processes. Furthermore, this model can not accurately link the Tertiary coeval-evolution of several mountain ranges under a single lithosphere mechanism, and turns into several processes occurring since Palaeozoic Era to explain the overall topography.

» **Thick vs. thin-skinned tectonics**. This mechanism proposed by *De Vicente et al.* (1992) and *Guimerá et al.* (2004), is based on the crustal thickness distribution within the plate interior. Gravity data show low values in areas where basin inversion took place (i.e. Iberian Chain, northern Cantabrian Border). These areas are affected by crustal thickening (by thick and thin-skinned tectonics deformation) providing a gravity minimum. This mechanism may explain high topography in areas like the Spanish Central System or the Iberian Chain where several detachment levels at crustal-scale induce crustal thickening (*Guimerá and González,* 1998; *De Vicente et al.,* 2007; *De Vicente et al.,* 2009b). Nevertheless, it cannot account for the observed lower crust thickening (>4 km) along the Central Range, unless a mechanism of crustal flow is involved. Unfortunately, there is not enough seismic data to confirm the rheological and tectonic mode of deformation of the Iberian lower crust. On the other hand this hypothesis may not explain the regular periodicity of the signals provided by crustal thickness, topography and Bouguer gravity anomalies.

» **Lithospheric folding**. The actual E-W to NE-SW distribution of mountain ranges in western Iberia follows a periodic pattern as it can be inferred from Figure 2.1b. Numerical models carried out by *Cloetingh et al.* (2002), suggest the presence of large-scale folding to explain the observed periodicity as a result of compressional stresses during the Betics phase of Alpine deformation. Following the line of large-scale folding, *Vegas* (2005a) and *De Vicente and Vegas* (2009a) have correlated the actual asymmetry observed in topography with the onset of alpine deformation, which in turn, mostly took place during Oligocene-Miocene times (Pyrenean phase). These authors assumed that much of the present-day topographic configuration was already formed before the latest stage of the Alpine cycle in Iberia as a result of strain partitioning (folding and faulting) [Fig.3.1]. However, this model

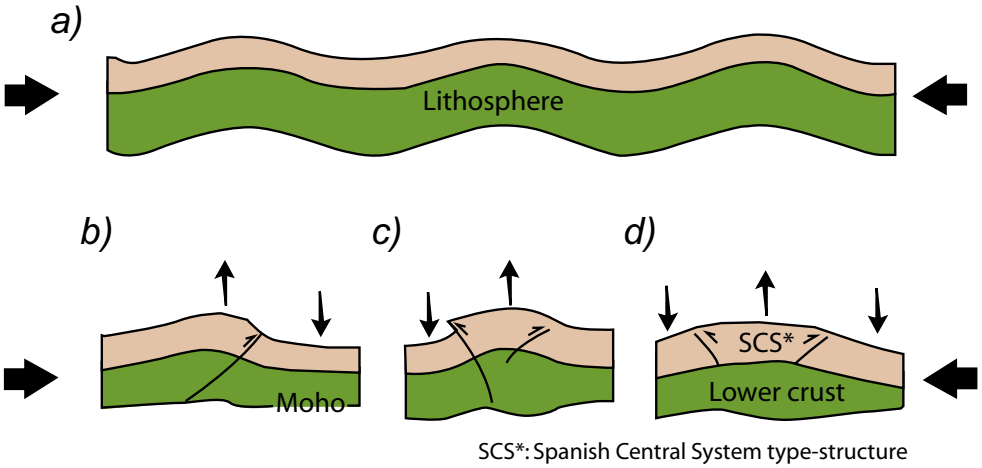

Figure 3.1: *(a) Illustrates the mechanism of "buckling" during horizontal shortening. (b, c and d) Tectonic relationships between faulting and folding during the shortening episode. Arrows show the direction of convergence. Modified from Vegas (2005).*

does not explain the non-periodic pattern of topography and active Miocene extension observed in eastern Spain.

1.4 Scope of this thesis

The long-term topography in Iberia is still a matter of debate. However, a major effort has been made in order to link surface expressions with deep Earth processes. Recently, *De Vicente and Vegas* (2009a) have argued that N-S compression during the Alpine Orogeny (Pyrenean stage) led to a series of periodic basement uplifts, previously called lithosphere folds by *Cloetingh et al.* (2002). These large-scale folds may have been influenced by Miocene extension that took place along the eastern margin of Iberia during the opening of the Valencia Trough (*Gaspar-Escribano et al.,* 2003). However, recent studies raise the question whether tectonic inversion and subsequent thickening of a hot lithosphere (as a result of the Mesozoic extension), could have dismantled such large-scale folds (*Fernández-Lozano et al.,* 2010), whereas these folds may continue along the Atlantic platform in the west (*Muñoz-Martín et al.,* 2010).

The aim of this thesis is: first, to infer through a series of analogue experiments the favourable conditions for buckling of the lithosphere. Well known differences on lithosphere strength from west to east have been related to the presence of inherited tectonic structures and lateral changes of the thermo-mechanical properties of the lithosphere prior to compression (*Guimerá and González,* 1998; *Vergés and Fernández,* 2006). Therefore, a series of analogue models were performed in order to investigate the response of the lithosphere under lateral strength changes, combined with the presence of major pre-existent late-Variscan structures that may have played an important role on strain localisation. Secondly, whether the pattern of topography is periodic or not, it may indicate the presence of large-scale folding. Furthermore, this thesis presents a new methodology developed over the analogue modelling results based on the interplay between gravity and topography, which aims to distinguish the presence of periodic patterns based on the spectral analysis of waveforms. The compiled maps of the Moho, gravity

and topography from the models are compared to nature in order to observe possible differences that may aim to distinguish the processes of folding and crustal thickening. Finally, this thesis aims to resolve questions concerning multi-phase deformational stages invoked to understand the topographic trends, investigating whether a single mechanism of strain-partitioning is able to explain the current patterns of topography developed during the Pyrenean stage of the Alpine Orogeny in Iberia.

1.5 Thesis outline

The tectonic framework and evolution of the Iberian micro-plate is still a matter of debate. Despite geological interpretations based on the micro-plate as a self-entity during Mesozoic plate-rotation, most recently, the mechanism of intraplate mountain building has considered the role of adjacent plates during Cainozoic Era (Europe to the north and Africa to the south, respectively). This thesis integrates geological and geophysical data in order to address the interpretation of present-day configuration of topography including surface to deep earth lithospheric processes.

Satellite pictures from Iberia provide an overview of a peculiar topography. Differences between western and eastern Iberia can be defined in terms of orientation and periodicity of mountain belts. Chapter 1 introduces some aspects of the peculiarities from the Iberian topography, paying special attention to the different hypotheses concerning mountain building and basin development of the Iberian plate interior.

Chapter 2 focuses on the mechanism of folding. Concepts and ideas are reviewed, related to ductile deformation of single and multi-layer systems and long-term relationships between faulting and folding. Additionally, this chapter deals with different mechanisms of lithosphere deformation, and in particular, the process of large-scale folding, both under extension and compression in order to distinguish processes that may cause the same surface expression.

The N-S distribution of mountain ranges precluding the timing and advance of deformation towards the plate interior is presented in Chapter 3. Starting with the first steps of the early Mesozoic evolution of the Iberian plate, this chapter goes through the final episodes of mountain building episode during the Cainozoic. Moreover, this chapter describes the key areas that may help to understand present-day topography in Iberia. Geological and geophysical data are presented to provide the reader with the latest and more relevant advances in the knowledge of the Iberian Peninsula. In addition, a full description of surface and deep Earth data concerning the thermo-mechanical state of the Iberian lithosphere is given in terms of rheological properties, composition and state of stress. The presented data provides detailed information that aimed to carry out a series of analogue models that are scaled-replicas of nature. These models aim to better understand the mechanism involved in the process of intra-plate mountain building, as well as, the state of (de)-coupling of the Iberian lithosphere.

Chapter 4 centres on a more complete understanding of the mechanisms involving intra-plate deformation based on the integration of gravity and topography data, applied to analogue modelling results. In addition to the previous models presented in Chapter 3, the effect of inherited late-Variscan faults is investigated, which may have played a key role on the final configuration of mountain ranges in Iberia during the Cainozoic. Moreover, experiments were implemented by adding lateral strength variations, representing thermo-mechanical differences from the western Variscan (cold and strong lithosphere), to the eastern Mesozoic rift-related lithosphere (rather hot and weak at the beginning of the Cainozoic). Whether the present-day

methodology applied to the analogue modelling technique, which is based on the interpretation of topography, gravity data and depth to Moho maps. In addition, a comparison is made between gravity and topography through the spectral analysis to distinguish between periodic and non-periodic signals. A periodic pattern of the signals (gravity and topography) found during the spectral analysis, may indicate the presence of large-scale folds. On the contrary, if hardly any periodicity is observed, this could be related to a different mechanism, i.e. crustal thickening by thrusting or flow at lower crustal levels. Furthermore, the model topography which was obtained through laser scanning was filtered following the results of the spectral analysis at the suggested wavelengths. The results reflect the effect of mantle deformation on the surface of the models. Consequently, an accurate comparison between models and Iberia will aim to understand the mechanism that lead to the present-day configuration of intra-plate mountain belts.

By the end of the above chapter, the most likely thermo-mechanical state of the Iberian lithosphere has been presented, examining the effect of large-scale folding on present-day configuration of topography. Differences on lithosphere strength and the role of pre-existent faults would be discussed in terms of intra-plate mountain building. However, there is still some uncertainty about the influence of several stress-fields on topographic trends. Therefore, in order to distinguish between a single or multiple stress-fields that may have influenced the final configuration of topography in Iberia, as well as, re-activation of pre-existent tectonic structures, this thesis integrates analogue models and analysis of particle displacement field over the models surface. Chapter 5 provides full details about the evolution of Central Iberia. Analogue models were carried out in order to distinguish the effects of strain partitioning at surface scale from differences on lithospheric strength during a single episode of N-S Alpine convergence. Moreover, detailed mapping of surface deformation of the models by applying the new advances on the Particle Image Velocimetry technique (PIV). The results are compared with the gravity and Moho surface anomalies which aimed to investigate the lithosphere mode of deformation providing clues on the mechanism of intra-plate mountain building and basin development that may have occurred under a single stress field.

The final chapter (Summary) aims to put the findings of this thesis into the context of Cainozoic tectonics in the Iberian Peninsula and includes a comparison of specific factors which may have controlled the mechanism of mountain building and basin formation in Spain. This chapter, therefore, focuses on the mechanism that governs the actual distribution of mountain ranges from east to west Iberia, but also covers other areas of intra-plate topography that may have involved lithospheric-scale folding such as the Moroccan Atlas or Central Asia.

Chapter 2

Fundamental aspects of folding

The effect of tectonic forces on rock layers can lead to rock failure and folding. Depending on the rock rheology, temperature, and pressure, the prevailing mechanism of deformation may change as it is the case of rock behaviour at different depths or under different conditions of pore fluid pressure. Folding is a common mechanism of deformation developed under tectonic forces or during sedimentation. It may also occur under different tectonic regimes. However, folds are mostly formed by shortening of existing layers. They have been often classified based on their shapes, size or fold wavelengths. In this chapter the theory of folding is reviewed. This chapter presents the most straightforward cases (folding of a single layer) and comparison with a multilayer system, from small to large-scale processes of folding. Particularly, different mechanisms for large-scale folding have been proposed affecting both, oceanic and continental lithospheres. Therefore, I provide a global classification that locates the proposed areas where lithosphere folds may occur. The chapter concludes with a broad overview of lithospheric folds affecting the Ibero-African area.

2.1 Introduction

Folding represents an effective mechanism for rock deformation in nature and has been identified as a primary response to tectonic forces, either under compression or extension. Therefore, under the same amount of shortening, folding requires a minor amount of work than thrusting (*Davis and Reynolds,* 1984). As a result, the first response to horizontal compression in nature is folding of a stiff layer. In general, it is assumed that folds develop along rock layers containing planar features or internal heterogeneities (*Ramberg,* 1967 and *Ramsay and Huber,* 1987). In addition, depending on the apply forces across the layering (i.e. horizontal or planar and vertical forces) three different mechanisms of folding can be defined: i) a mechanism of buckling results from forces parallel to the layer; ii) when forces are applied at a high angle or orthogonal to the layers a bending mechanism prevails; iii) finally, flexural-slip folds are those where layering exerts a strong influence in the folding of a rock sequence, subsequently, the flexing of layers is followed by slipping or flow between layers (*Donath and Parker,* 1964). Although, the end shape might be the result of one or more fold mechanism [Fig 2.1].

Folding mechanisms are influenced by several factors that occur during deformation, such as: the temperature, pressure, presence of fluids and rheological rock properties which in

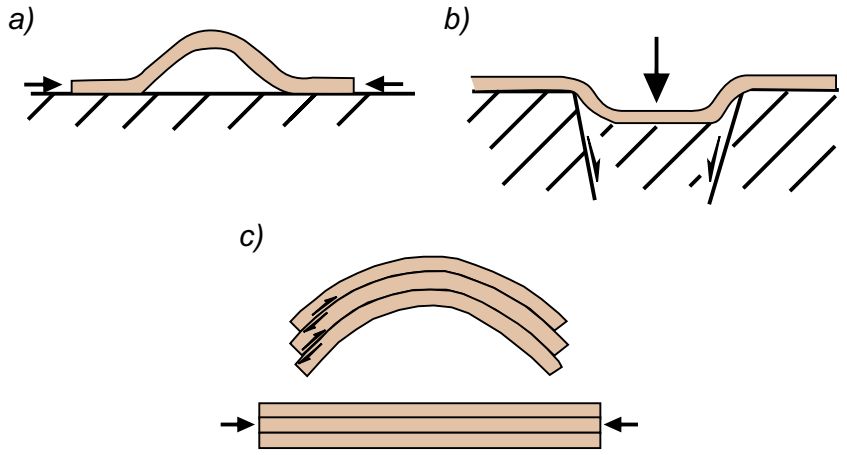

Figure 2.1 *Principal folding mechanism in nature. (a) Buckling; (b) Passive bending and (c) Flexural-slip (see a detailed explanation in the text).*

turn depends on composition, temperature and pressure. (*Ranalli,* 1995; *Stüwe,* 2007). Several laboratory experiments have been performed to address the mechanisms that govern folding of single and multilayered rocks. Among others, the studies carried out by *Biot et al.* (1961); *Hudleston* (1973); *Cobbold* (1975); *Schmid and Podladchikov (*2006); *Treagus and Fletcher* (2009).

The following section introduces some of the first insights on folding through laboratory analyses.

2.2 Mechanisms of folding development

The mechanism of folding has been extensively studied to address large-scale geodynamic process. Since the earliest experiments carried out by *James Hall* (1812) to simulate the folding of strata as observed in some outcrops along the eastern coast of Scotland [Fig 2.2], new studies have been attempted to understand the behaviour of the rocks under compression and extension (*Davy and Cobbold,* 1991; *Brun and Beslier,* 1996).

Most of the studies addressing folding mechanisms are commonly used to constrain the geometry of large-scale folds. Therefore, a better understanding on the effect of confinement layers, thickness/dip relations and amplitude/wavelength ratios has been investigated through a series of analogue and numerical experiments involving single and multilayer bodies. A brief outline on the fundamentals of single and multilayered folding systems is given in the following section.

2.2.1 Folding of single-layer systems

Studies dealing with single embedded layers have successfully reproduced the behaviour and effect of rock properties under certain boundary conditions (i.e. changes on layer thickness, viscosity etc). Good examples were shown by *Biot* (1961), *Sherwin and Chapple* (1968), *Smith* (1975), *Smith* (1977) and *Cobbold* (1975). These experiments have shown that horizontal shortening localised buckling, induced by a heterogeneity within the layer, which can be of structural and compositional nature [Fig 2.3].

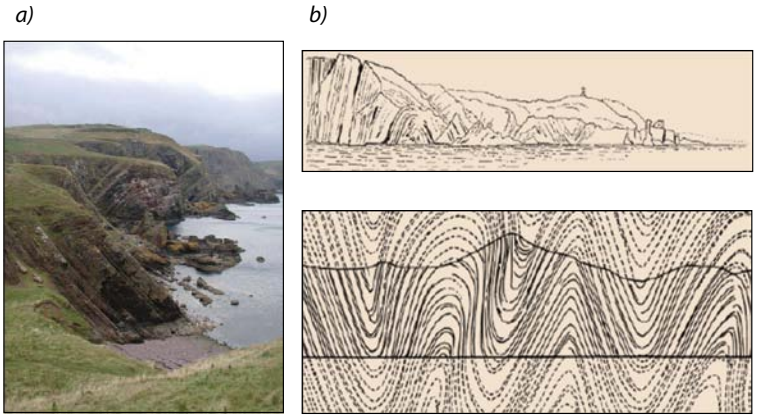

Figure 2.2 *(a) Asymmetrical fault-related tilting of coastal plain syncline along the coast of St. Abb´s Head (Scotland). (b) Original drawings and modelling results from James Hall experiments (1812) based on outcrops from figure (a).*

In spite of this disturbance, further deformation led to a series of folds ranging in amplitude from the central part of the models to the sides. Therefore, folding-growth extends laterally producing regular periodic undulations. Moreover, the geometry of folding (i.e. parallel or similar) also depends on the viscosity contrast, the degree of shortening and the initial wavelength/thickness ratio (*Sherwin and Chapple,* 1968; *Hudleston and Stephansson,* 1973). However, shortening is often not parallel to the principal stresses, an assumption made in former buckling theories. Furthermore, *Treagus* (1973) has shown that the obliquity of principal stresses causes folding asymmetry, therefore, leading to internal cleavage refraction. Despite the above mentioned facts, the equation governing the wavelength of a single folded layer depends mainly on viscosity (η) and thickness (t) given by the relation:

$$W = 2t\pi \sqrt[3]{\frac{\eta_1}{6\eta_2}} \qquad [2.1]$$

where the dominant wavelength for Newtonian bodies (*W*) is given by the Biot-Ramberg equation, where *t* is the thickness of the competent layer, η_1 is the viscosity of the competent layer and η_2 is the viscosity of the host material (*Ramberg,* 1967).

It could be argued, that folding of a single layer embedded in a soft matrix may lead to the development of a series of buckling folds with different characteristics depending on the rheologies of the materials. *Jeng and Huang* (2008) have performed a series of analytical models showing that, the strain rate does not influence the fold-form for a viscous layer embedded in viscous matrix. In order to evaluate the effect of the competence layer contrast between layer and matrix, they studied the relationship between both, elastic and the viscous materials leading to the conclusion that after deformation, folding might have the same wavelength versus the lateral shortening relationship. These models are in agreement with the results of finite element modelling obtained by *Hudleston and Lan* (1994). In addition, according to *Schmalholz et al.* (2002), for a single layer embedded within a viscous matrix, material flow becomes controlled by the so-called Argand number (Ar), which is a measure of the ratio between the stress arising from thickness contrasts (e.g. crustal thickness) and the stress required to deform the material at surface strain rates (*England and McKenzie,* 1982):

$$Ar = \frac{\Delta\rho g H}{2\mu_{eff}\varepsilon_B} = \frac{\Delta\rho g H}{B\dot{\varepsilon}_B^{1/n}} \qquad [2.2]$$

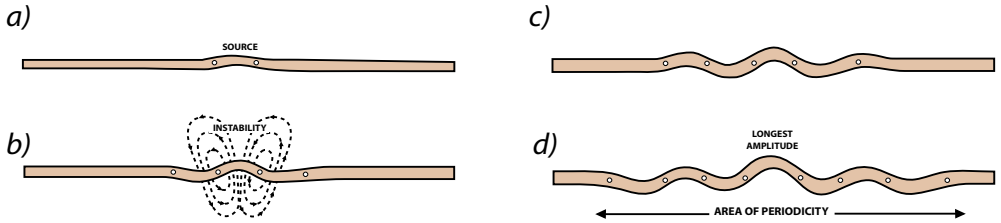

Figure 2.3 *Serial buckling of a single layer after Cobbold (1975), illustrating perturbation flow-lines (INSTABILITY). The experimental result shows that buckling may not occur across the entire model but progressively propagates laterally from the source.*

Where r is the density, g the gravity acceleration, H is the thickness of the layer, μ_{eff} the effective viscosity, ε_B is the absolute value of the mean layer-parallel strain rate and $B = 2\mu_{eff}$ if n = 1 with μ_{eff} being the viscosity of the layer.

Consequently, if Ar is small (i.e. high effective viscosity), the flow is governed by boundary conditions (lengths, thickness, etc). However, if the Argand number is high, the forces related to crustal thickness variations dominate the system and consequently, the effective viscosity cannot account for supporting elevation. Therefore, different modes of folding can be inferred according to the diagram shown in Figure 2.4: matrix-controlled folding provides information about the effective viscosity contrast between the folded layer and the matrix; gravity-controlled folding provides information about the Argand number, and detachment folding provides information about the thickness of the detachment zone (*Schmalholz et al.,* 2002). Subsequently, folding of single layers involves a series of geometrical and rheological complexities that could influence their shape, amplitude and wavelength during horizontal shortening, which sometimes is difficult to predict.

2.2.2 Folding of multilayer systems

Similarly to single layer folds, folding of multilayer systems initiate at singular points under compression (*Watkinson,* 1976). Analogue models have shown that the mechanism of folding develops during the initial stages of compression leading to a series of buckles without local isostatic compensation. Consequently, buckling influences and localises faulting at the inflexion points of buckles and thickness variations finally occur.

The style of crustal thickening in multilayer rocks is therefore controlled by the relative initial thicknesses and resistances of the layers (*Davy and Cobbold,* 1991; *Martinod and Davy,* 1992).

Multilayered systems have been extensively studied by analytical and numerical modelling. In general, these models show the evolution of folding under strain regimes between competent layers embedded in a soft matrix. In fact, stacked multilayers exhibit a large variety of fold shapes comprising kink-bands, chevrons, angular folds, etc. The amplitude and wavelength is clearly dependent on the material property contrasts but also on the number of layers and their relative thickness ratios (*Schmid and Podladchikov*, 2006).

Recently, laboratory experiments carried out by *Treagus and Fletcher* (2009) have shown the control of thick competent layers on the folding of a multilayer system as a primary element for preventing folding. Therefore, the parameters of thickness and viscosity may be able to control the geometry and style of folding reproducing a large range of fold shapes that occur

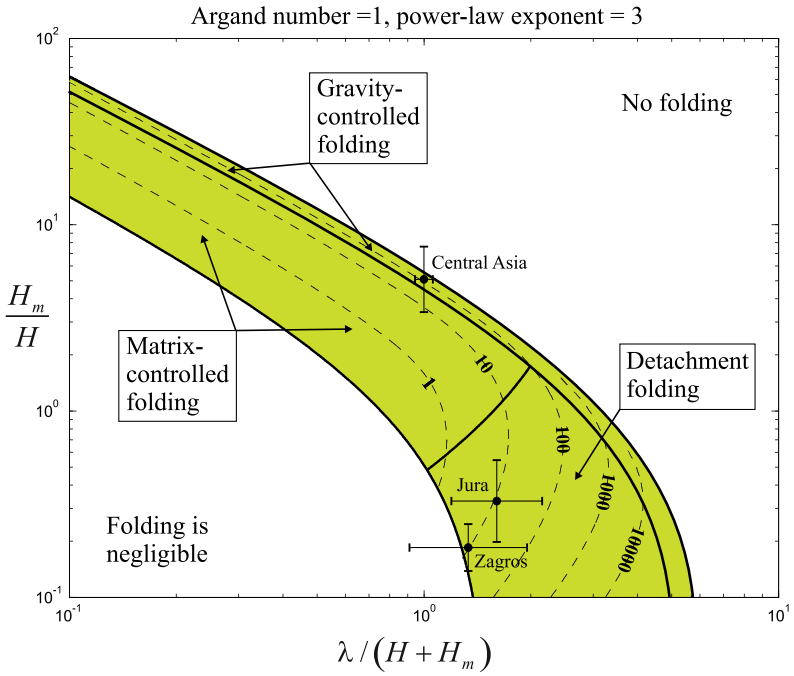

Figure 2.4 *Modes of folding for a given value of the Argand number (Ar) and the power law exponent (n) of the layer material, according to Schmalholz et al. (2002).* H_m/H *represents the ratio of matrix thickness to layer thickness and* $\lambda/(H + H_m)$ *the ratio of wavelength to total thickness. The dashed lines are contour lines of the effective viscosity contrast* (μ_{eff}/μ_m *is given by the numbers on the dashed lines) between layer and matrix. The active folding mode is determined by the mode that provides the slowest amplification rate.*

in natural multilayer systems.

2.3 Folding-faulting relationships

The interaction between folding and faulting has been a matter of debate during the last decades. For example, it is still not well understood, which parameters governing the vergence of structures and the mechanisms that control the geometry and shape of faults in fold-and-thrust belts. This sub-chapter deals with the feasible mechanisms that could help to understand the relationships between folding and faulting and vice-versa under compression.

Analytical and numerical experiments have been employed to obtain a comprehensive view of structures developed in nature. Since analytical models have the possibility to extend to 4D, they enable the reproduction of extensive areas covering a broad range of surface and deep processes. In addition, the models based on brittle-ductile systems reproduce structures which differ from structures observed in brittle models. Lithospheric scale-models allow the reproduction of folding since a free surface (asthenosphere) is able to accommodate deformation of the lithospheric system allowing ductile thickening. Therefore, they represent a good tool to study folding-faulting relationships. Subsequently, experiments carried out by *Davy and Cobbold* (1991); *Sokoutis et al.* (2005) and *Fernández-Lozano et al.* (2010) show that thrusts form within the brittle layers at the inflection points of the folds affecting the ductile layers. The main observed structures are pop-ups and pop-downs. However, additional single faults and

blind thrust are also observed. It is important to mention that the geometry, spacing and style of thrusting are also influenced by the strength of the ductile layers which in turn represents vertical rheological variations. Consequently, asymmetry of the structures is clearly constrained by the viscosity of the ductile layers underneath.

In addition, a series of brittle-ductile thrust wedge experiments (*Smit et al.,* 2003; *Bonini,* 2007a), were performed to solve the parameters governing the thrust vergence. However, they could not conclude firmly the mechanism that influences the dominating vergence. Nevertheless, they found that controlling the orientation of the fold axis, basal friction and décollement effectively influence the pattern of deformation and structural vergence. Moreover, the study of *Smit* (2005) suggests that the evolution of transient faults to master fault during deformation is controlled by the ductile layers below. The above author shows the influence of the basal angle wedge on the structural polarity of the thrust system (foreland-hinterland verging thrust faults). Even although several studies deal with folding and faulting inter-relations, there is general agreement that the mechanism that controls geometry and style of faulting does not simply depend on the brittle-ductile coupling.

2.4 Lithospheric folding

The Plate Tectonics theory is based on the concept of a rigid lithosphere underlain by a ductile asthenosphere. However, the theory cannot successfully explain the presence of intra-plate mountain belts and seismicity. On the contrary, it is believed that the Earth system is characterised by far-field stresses that are transferred from plate boundaries through the main plate interiors either through both, continental as well as oceanic domains (*Zoback et al.,* 1989; *Cloetingh et al.,* 1995). As a result, intra-plate deformation takes place, giving rise to mountain building, uplift and tectonic inversion of basins. Crustal thickening and lithosphere buckling are considered among the most common mechanisms for intraplate deformation (*Stephenson et al.,* 1990; *Burov et al.,* 1993; *Ziegler et al.,* 1995; *Cloetingh et al.,* 1999; *Bourgeois et al.,* 2007).

The presence of large-scale folds affecting the entire lithosphere is generally attributed to areas under subsidence or uplift in the plate interiors, which follow a certain periodicity. However, it is rather difficult to differentiate between the processes that influence the mechanism of folding, e.g. lithosphere instabilities in *Martinod and Davy* (1994). Recently, *Bourgeois et al.* (2007), have argued for considerable differences on the lithosphere-folding mechanisms. The above authors have claimed the distinction of geometrical signatures provided by the processes of rifting, foreland flexural bending, intra-plate buckling and up-welling of asthenospheric thermal anomalies.

For example, the stretching of the lithosphere as a direct consequence of rifting may lead to a mechanism of necking (a well-known process based on pinch-and-swell structures affecting the lower crust and lithosphere mantle) [Fig 2.5a].

Analogue models have shown that thinning of the lithosphere favours the raising of hot mantle material which may transfer the heat from the passively uplifted asthenosphere, leading in turn to a density decrease of the lithosphere. Consequently, the up-warping of the lithosphere around would involve vertical isostatic movements (*Brun et al.,* 1994; *Brun,* 1999).

Another mechanism is related to flexural folding of the foreland along orogenic fronts (*Doglioni et al.,* 1994), which reflects flexural bending of an elastic lithospheric plate by the weight of an orogenic wedge [Fig 2.5b]. In spite of the importance of the above mentioned

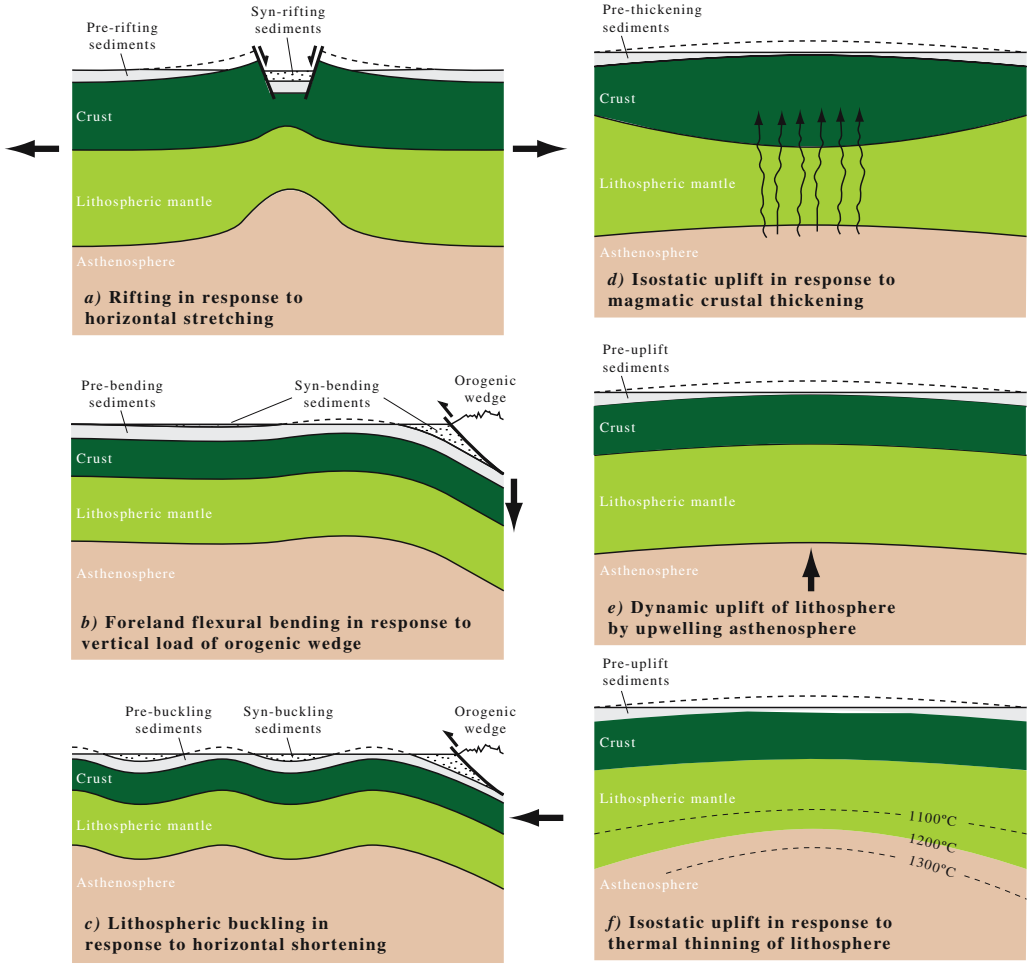

Figure 2.5 *Summarizes different mechanism for lithosphere deformation: (a) rifting; (b) foreland bulge; (c) lithosphere buckling; (d) magmatic crustal thickening; (e) Dynamic uplift and (f) isostatic uplift in response to thermal thinning of the lithosphere. After Bourgeois et al. (2007).*

models in some parts of the world, a widely invoked process is represented by lithosphere folding senso-stricto and usually referred as "buckling", as a result of plate convergence. This mechanism may help to explain periodic undulations (*Cloetingh et al.,* 1999) reflected by the Moho that would account for areas subjected to subsidence and uplift revealed by gravity and topographic signals within plate interiors (*Stephenson and Cloetingh,* 1991; *Burov et al.,* 1993). The conceptual model of lithospheric folding is shown in Figure 2.6a and b. It has mainly been proposed for intra-plate areas both, in continental and oceanic lithospere, such as central Asia, Iberia or the Alpine foreland (*Burov et al.,* 1990; *Burov and Molnar,* 1998; *Ziegler and Dèzes,* 2007).

A totally different scenario, according to *Bourgeois et al.* (2007), where the presence of thermal anomalies caused by up-welling of hot asthenospheric material, may also produce long-wavelength deformation of the lithosphere by magmatic crustal thickening, bulging of the crust by buoyancy of hot asthenosphere and isostatic uplift in response to thermal thinning of the

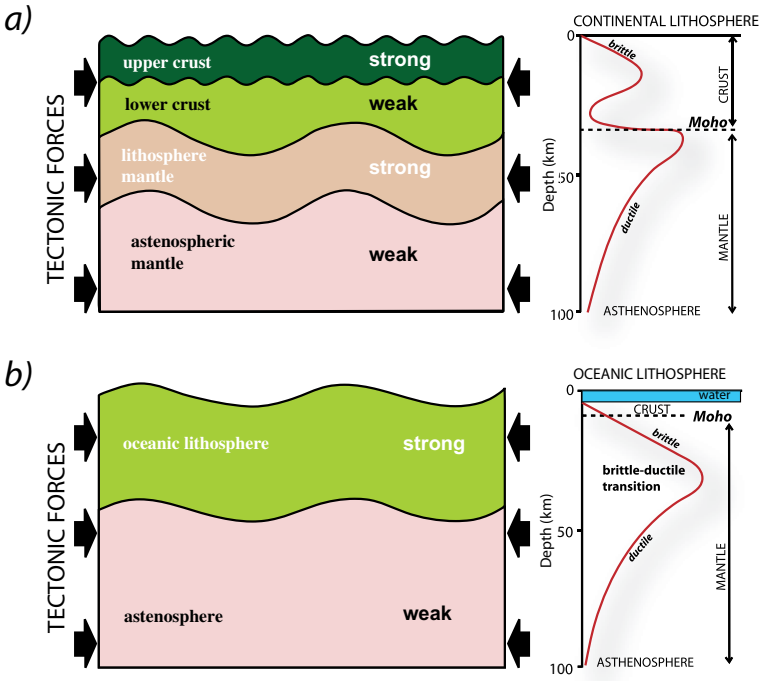

Figure 2.6 *Conceptual model for lithospheric folding development and strength profiles for continental (a), and oceanic (b) lithospheres under horizontal tectonic stress. Modified after Muñoz-Martín et al. (2010).*

lithosphere [Fig 2.5d,e and f].

In addition, recent studies carried out by *Burov and Cloetingh* (2009), suggest the interaction between mantle-plume activity and lithospheric folding in continental lithosphere. Their results demonstrate that the interaction between both processes may lead to a strong amplification, attenuation or modification of folding surface expression.

All the above mentioned mechanisms could provide a similar surface expression in terms of topography for a different lithosphere mechanism or interaction of two simultaneous episodes, e.g. folding vs mantle anomaly (*Burov and Cloetingh,* 2009). Therefore, careful interpretation of geophysical and geological information should be made in order to distinguish the possible mechanism involved in intra-plate mountain building. In this context, the focus of this thesis states on intra-plate deformation related to buckling of the lithosphere in convergence settings. The next section displays the localisation of lithosphere folds both, in oceanic and continental lithosphere worldwide.

2.4.1 Global distribution

Lithosphere folds have been recognised all over the world [Fig.2.7]. The combined analyses of gravity and topography signals allow the identification of periodic undulations which are believed to correspond with large-scale folding (*Stephenson and Cloetingh,* 1991). So far, these undulations may affect the oceanic and continental lithosphere. Figure 2.7 and Table 2.1 summarise the main proposed areas where large-scale folding has been identified.

In the following subsections, I briefly discuss the parameters controlling folding under

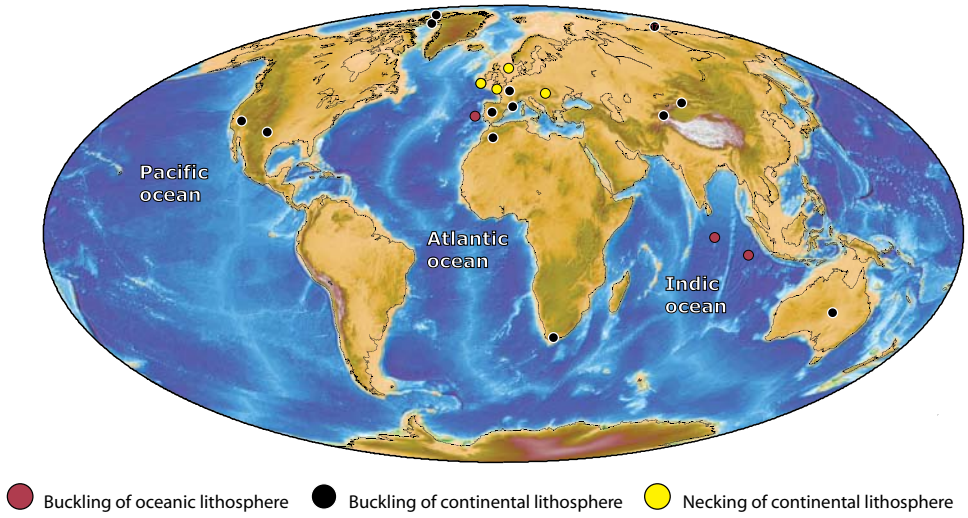

Figure 2.7 *Summary of the places where lithosphere folding has been recognized worldwide. Coloured circles correspond with a classification followed in this thesis taking into account "passive" buckling and buckling of continental and oceanic lithosphere.*

different tectonic regimes affecting continental and oceanic lithospheres.

2.4.2 Continental lithosphere

Buckling of continental lithosphere has been identified all over the world. However, most of the suggested areas are located in the Northern hemisphere. A reason for this peculiar distribution is the thermo-mechanical state of the lithosphere. According to *Cloetingh et al.* (1999), the life-span for lithosphere folds is around 20 My in absence of sufficient compression.

Such a time-controlled relationship is related to the thermal age, and in turn, the rheology of the lithosphere, which is intrinsically independent from any previous heterogeneity, such as tectonic structures. However, numerical and analogue experiments have demonstrated the importance of pre-existing structures on the nature and initation of folding (*Cobbold,* 1975; *Smith,* 1975; *Williams and Jiang,* 2001). Therefore, only strong and old lithospheres may be able to maintain the up-warping of the Moho for My [Fig 2.8]. That would explain why only areas such as South Africa, Siberia, central Australia or the Arctic Canada still maintain large-scale folds. In the rest of the Northern hemisphere the recent Alpine orogenic phase led to a series of areas subjected to periodic (active) buckling (Iberia, Moroccan Atlas, Central Asia or the Alpine foreland) or non-periodic (under vertical forces or passive) buckling like the Viking graben or the Pannonian Basin (*Stephenson and Lambeck,* 1985; *Stephenson et al.,* 1990; *Burov et al.,* 1993; *Horváth and Cloetingh,* 1996; *Van Wees and Cloetingh,* 1996; *Cloetingh et al.,* 1999; *Cloetingh and Burov,* 1996; *Teixell et al.,* 2003; *Ziegler and Dèzes,* 2007; *Cloetingh and Burov,* 2011a).

In fact, folding of the European lithosphere is determined by the presence of young lithosphere and sedimentary loads which influence and control the shape and wavelength of the folds. Despite of the strain rate history, driving forces from plate boundaries or rheological influence on large-scale folding, areas characterised by cold and strong lithosphere could be deformed by a process of folding (i.e. Iberia). In addition, numerical models carried out by *Cloetingh et al.* (1999) suggest the importance of lithosphere strength on the symmetry or

Area	λ (km)	Thermal Age (My)	Lithosphere	Tectonic regime	Present day state	Type	Reference
Central Asia	200-250	175	Continental	Compression	preserved	B	Burov et al., (1993)
Central-Western Europe	100-200	>100	Continental	Compression	preserved	B/N	Ziegler et al., (1995)
Iberia	250-300	45	Continental	Compression	active deformation	B/N	Cloetingh et al., (2002)
Atlas Mountains	250-300	45	Continental	Compression	active deformation	B/N	Teixell et al., (2003)
Arctic Canada	200	200	Continental	Compression	preserved	B/N	Stephenson and Cloetingh, (1991)
Siberian platform	500-600	400-600	Continental	Compression	preserved	B	Cloetingh et al., (1999)
Central Australia	400-500	>700	Continental	Compression	preserved	B	Stephenson and Lambeck, (1985)
Indian Ocean	200-250	60	Oceanic	Compression	active deformation	B	McAdoo and Sandwell, (1985)
South Africa	300	>300	Continental	Transpression	preserved	-	Cobbold et al., (1992)
Pannonian Basin	350-400	>20	Continental	Compression	active deformation	N	Horváth and Cloetingh, (1996)
Brittany	250-300	>100	Continental	Extension	preserved	-	Lefort and Agarwal, (2000)
Viking graben	60	300	Continental	-	active subsidence	N	Van Wees and Cloetingh, (1996)
Apennine Mountains	-	65	Continental	Transpression	preserved	B/N	Doglioni et al., (1994)
Western USA	200	>65	Continental	Transpression	-	-	Tikoff and Maxson, (2001)

Table 2.1 *Compilation of regions where lithospheric folding has been suggested. The type of lithosphere involved and also the tectonic regime are shown. "B" stands for regular folding style, whereas "N", stands for irregular folding, and "B/N" stands for those cases displaying folding interference of styles.*

asymmetry of folding. Hence, a weak and young lithosphere yields shorter wavelengths than strong and old lithospheres (for instance Iberia). Nevertheless, the pre-crustal configuration of inverted basins may imply a multi-wavelength mode of deformation which involves larger wavelengths than predicted, such as inferred in the Pannonian Basin (*Cloetingh et al.,* 2005).

Another good example of folding of the continental lithosphere has been provided by *Tikoff and Maxon* (2001). These authors have attributed the Rocky Mountain uplift to large-scale deformation of the foreland and continental interior of the western edge of North America. The observed wavelength of the arches is ca. 190 km, compatible with a mechanism of lithosphere buckling. In addition, differences on the style of deformation (i.e. Thin-skinned or thick-skinned tectonics) might account for coupling-decoupling processes involving the North-American lithosphere. More recently, *Gao et al.* (2011) have suggested the presence of a series of periodic undulations on the Moho surface that maybe interpreted as lithosphere folds, based on a tomographic survey carried out in north-western North America.

2.4.3 Oceanic lithosphere

Oceanic domains have been extensively studied during the last century (*Meinesz,* 1934; *Heiskanen and Meinesz,* 1958). Currently, comparison of gravity and bathymetry studies have been used in order to explain substantial differences observed from one ocean to another (i.e. differences between Atlantic and Indic ocean arise from different tectonics settings along plate boundaries). The first studies carried out by *Watts and Ryan* (1976) and *Watts* (1978), have shown that the observed bathymetry in most of the oceans cannot account for the state of isostasy of the submarine mountain chains. Consequently, the differences observed in the calculated elastic properties of the oceanic lithosphere should be influenced by the thermal age of the lithosphere.

In this frame, seismic profiles and borehole drilling information have been analysed to identify the presence of lineaments which may be related to large-scale folds affecting oceanic

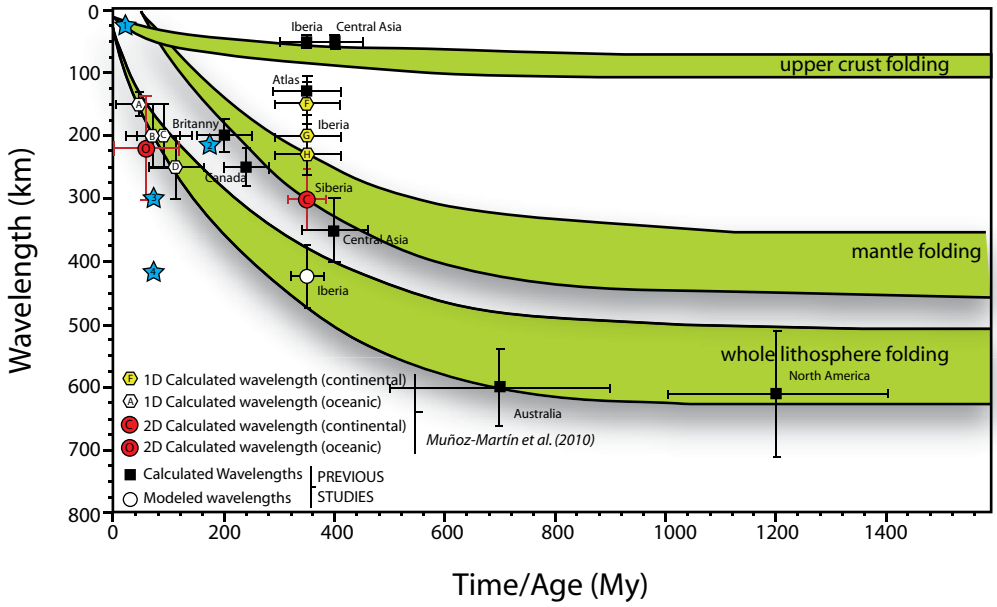

Figure 2.8 *Wavelengths of folding as a function of thermal age based on previous studies in Iberia (Cloetingh et al., 1999): circles and hexagons from Muñoz-Martín et al. (2010). Numbers correspond to regions: (1) North America; (2) Paris Basin; (3) Iberia; (4) Pannonian Basin.*

lithosphere (*Weissel et al.,* 1980). These folds could account for the isostatic compensation of the chains. *McAddo and Sandwell* (1985) and *Beekman et al.* (1996), based on the comparison of free-air gravity anomalies and topographic data together with seismic reflection profiles, suggest that the observed lineaments along the Indian Ocean were probably related to large-scale folds. They carried out a series of numerical models that confirmed observed wavelengths of 100 and 300 km. However, the process of buckling is aided by the presence of faults that in some cases were reactivated during subsequent episodes of tectonic deformation. These results suggest that the key factors controlling folding of oceanic lithosphere are basically dominated by the thermal age of the lithosphere, despite previous heterogeneities affecting the crust may also play an important role, as numerical models carried out by *Gerbault et al.* (1999) have shown.

2.5 Folding of the Ibero-African lithosphere

First attempts for correlating overall deformation with large-scale folding of the lithosphere were made by numerical modelling carried out by *Cloetingh et al.* (2002). These authors linked the actual distribution of topography to the coupling of both, Atlantic ridge pushing and Betic NW-SE convergence during late Miocene times (*Andeweg et al.,* 1999). In addition, *De Vicente and Vegas* (2009a) emphasised the importance of the Pyrenean phase of the Alpine cycle (N-S compression) rather than the late Betic episode for mountain building in Iberia. Analyses of fission track (FT) data and sedimentary facies at several places in northern and central Spain have pointed out towards early Tertiary development of topography and subsequent block tilting.

Previous studies carried out in the Atlas Cordillera have shown the relationship between

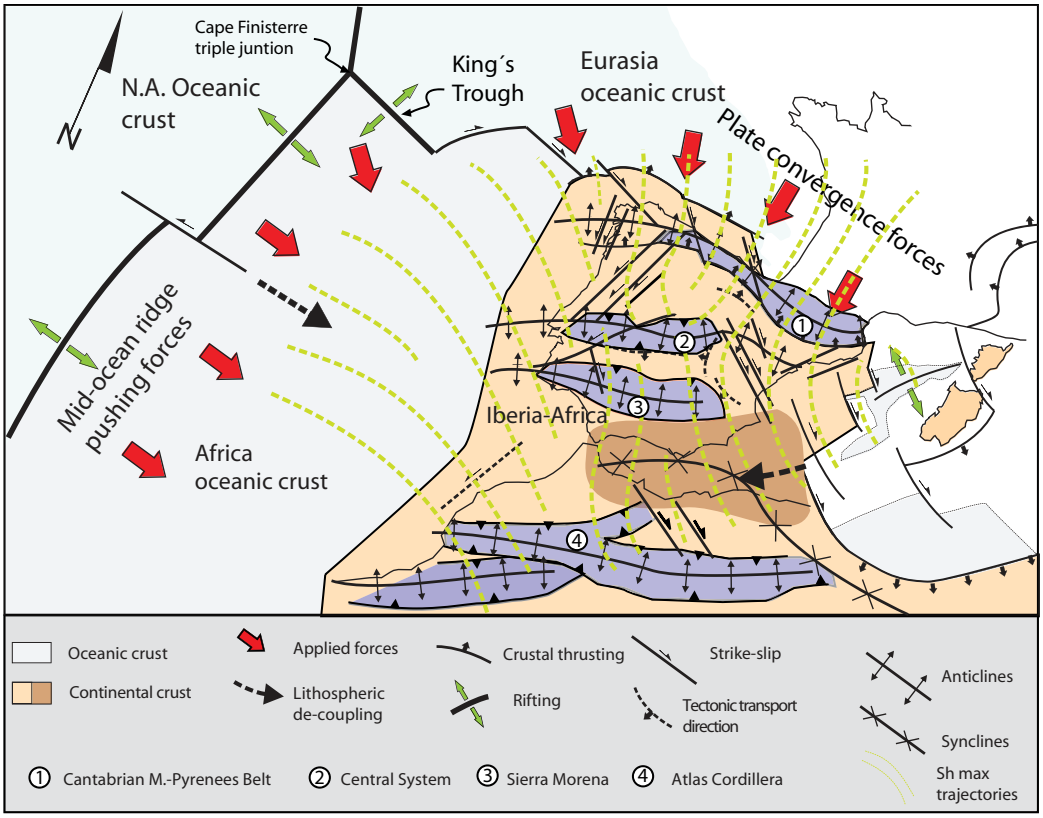

Figure 2.9 *Tectonic sketch map of late Oligocene-early Miocene Ibero-African margin illustrating main forces and major features related to folding. Circles correspond to intra-plate topographic uplifts. Sh. Max trajectories show a neutral point in central Iberia and the N-S trend during main Pyrenean phase of the Alpine cycle. Modified after De Vicente and Vegas (2009).*

non-compensated isostatic load and high topography (*Teixell et al.,* 2003). Several hypothesis explain these differences as a result of lithosphere folding and high thermal anomalies created by mantelic-plume channels, the so called "Moroccan Hot Line" in De *Lamotte et al.* (2009); *Teixell et al.* (2003) and *Zeyen et al.* (2005), extending across northern Africa towards western and central Europe, or a combination of both (*Burov and Cloetingh,* 2009). However, the recognition of certain similarities concerning same tectonic phases in Iberia and the Atlas Cordillera together with the timing of deformation and uplift based on FT data analyses, structural analyses and sedimentary record carried out by *Ghorbal et al.* (2008), led *De Vicente and Vegas* (2009a) to consider a series of folds extending from the Pyrenean-Cantabrian Mountains Belt towards northern Africa [Fig 2.9]. The greatest wavelengths are in the order of 500 km with intermediate ones are about 150-250 km and the smallest reach 80-40 km (*Cloetingh et al.,* 2002; *Tejero et al.,* 2006; *Muñoz-Martín et al.,* 2010).

Consequently, the whole system extending from Europe to Africa has been related to large-scale folds, with possible interaction of thermal anomalies related to mantle channels in northern Africa, and Mediterranean back-arc extension along the eastern part of the Iberian realm.

Chapter 3

Cainozoic deformation of Iberia: a model for intra-plate mountain building and basin development based on analogue modelling

Inferences from analogue models support lithospheric folding as the primary response to large-scale shortening manifested in the present-day topography of Iberia. This process was active from the late Oligocene-early Miocene during the Alpine orogeny and was probably enhanced by the reactivation of inherited Variscan faults. The modelling results confirm the dependence of fold wavelength on convergence rate and hence the strength of the layers of the lithosphere such that fold wavelength is longest for fast convergence rates favouring whole lithosphere folding. Folding is associated with the formation of dominantly pop-up type mountain ranges in the brittle crust and thickening of the ductile layers in the synforms of the buckle folds by flow. The mountain ranges are represented by upper crustal pop-ups forming the main topographic relief. The wavelengths of the topographic uplifts, both, in model and nature suggest mechanical decoupling between crust and mantle. The presence of an indenter, representing the opening of the King´s Trough in the north western corner of the Atlantic Iberian margin controls the spacing and obliquity of structures. This leads to the transfer of the deformation from the moving walls towards the inner part of the model, creating oblique structures in both brittle and ductile layers. The effect of the indenter, together with an increase in convergence rate produced more complex brittle structures. These results show close similarities to observations on the general shape and distribution of mountain ranges and basins in Iberia, including the Spanish Central System and Toledo Mountains.

3.1 Introduction

The Iberian Peninsula represents the westernmost edge of the continental part of the Eurasian plate. The actual distribution of mountain ranges has been linked to the convergence between the African and European plates during the Cainozoic as documented along its plate boundary (i.e. Pyrenean stage), and the plate interior. Convergence during the late Oligocene give rise to mountain uplift and deformation of the Cantabrian-Pyrenean belt.

This chapter is based on Fernández-Lozano, J., Sokoutis, D., Willingshofer, E., Cloetingh, S., and De Vicente, G., (2011). Cenozoic deformation of Iberia: a model for intra-plate mountain building and basin development based on analogue modelling. Tectonics, Vol. 30, TC1001, 26 PP., doi:10.1029/2010TC002719

The oldest un-deformed rocks in the Pyrenees are Pliocene and late Miocene in age on the north and southern margin, respectively (*Mattauer and Henry*, 1974). In addition, high topography is present in the Peninsula interior and the Betics, which at the same time can be seen as the last increment (last 11 Ma) of mountain building in Iberia [see Fig.3.1].

Models attempting to explain the reoccurrence of significant topography over distances of several hundreds of kilometres in Iberia invoke buckling of the lithosphere (*Cloetingh et al.,* 2002) or isostatic response to crustal thickening (*Casas-Sainz* and De Vicente, 2009b); block rotation and uplift (*Vegas et al.,* 1990), or the interaction of several processes regarding thickening and uplift during the main episode of convergence and subsequent stretching by back-arc extension in the Mediterranean (*Vergés and Fernández*, 2006).

Among the above mentioned processes folding of the continental lithosphere has been suggested to be an efficient mechanism that leads to mountain building and general uplift and subsidence (*Stephenson et al.,* 1990; *Burov et al.,* 1993; *Doglioni et al.,* 1994). The stability of such structures has been estimated to be in the order of 20 Ma maintaining the Moho isotherms relatively stable during most of the life span of such folds (*Cloetingh et al.,* 1999). Subsequently, the folded lithosphere may be subject to gravity driven deformation like collapse or lateral extrusion of lower crustal material as proposed by *Bird* (1991); *Rey et al.* (2001); *Cloetingh et al.* (1999); *Burg et al.* (1997) and *Burov and Watts* (2006).

In order to gain insight into the feasible processes that lead to the present-day distribution of topography and uplift in intra-continental lithosphere, a series of analogue models have been conducted. This chapter shows the modelling results which complement previous existing numerical experiments (*Cloetingh et al.,* 2002). Several parameters are tested in order to understand the mechanism that control the wavelength of the folding but also the style of deformation distributed along the upper crust. Furthermore, in this chapter I include a number of topics concerning rheological stratification of the lithosphere and geometry of the deformed lithosphere. Consequently, these models aim to understand the effect of rheological and geometrical heterogeneities affecting the Iberian lithosphere during most part of the Cainozoic Era.

3.2 Cainozoic deformation and plate reorganisation

From Permian to Triassic period the tectonic setting of Iberia has changed to mainly extensional leading to widespread rifting along the northern Iberian continental margin [Fig.3.2a and b]. NE-SW to NW-SE wrench faults related to late Permian unroofing-stage of the Variscan orogen along the western margin of the Gondwana continent, were reactivated (*Arthaud and Matte,* 1977). As a result a series of early Triassic depocentres were established along the present-day Iberian and Atlas regions subjected to active subsidence. This episode of tectonic subsidence was followed by thermal re-adjustment of upper mantle isotherms during the early Jurassic (*Van Wees and Stephenson,* 1995).

A second episode of Mesozoic extension took place between the late Jurassic-early Cretaceous period (*Álvarez-Marrón,* 1996) [Fig.3.3a and b]. During this time, the Cape Finisterre triple point was active leading to an opening along the Palmer ridge, which was created 60 My ago in the NE Atlantic. The Palmer ridge opening led to uplift and spreading along the "King´s Trough" about 27 million years ago (Cann and Funnell, 1967). Paleomagnetic data from sediments of the Lusitanian basin and the Algarve (*Márton et al.,* 2004), indicate a 26° counter clockwise rotation of Iberia produced by the opening of the Bay of Biscay during the late Creta-

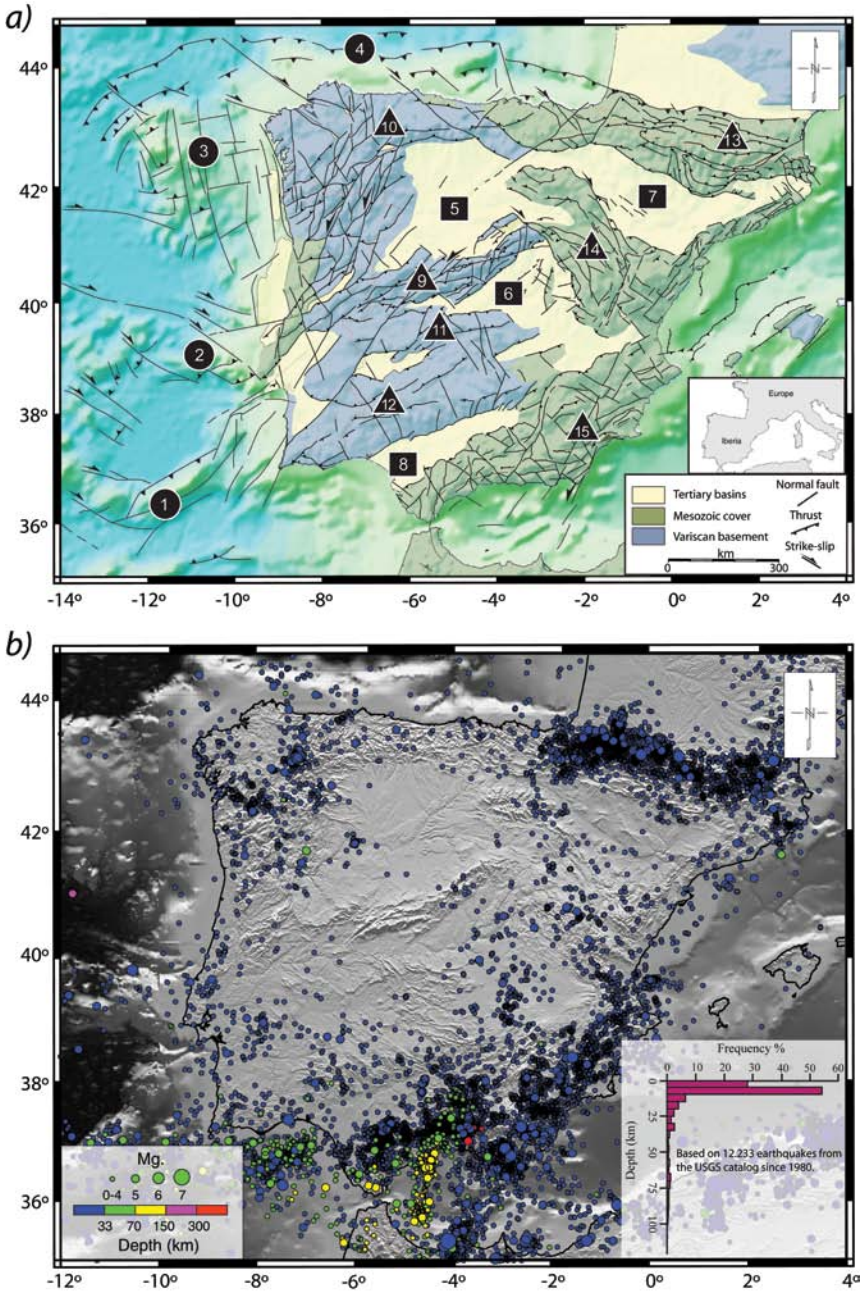

Figure 3.1 *a) Simplified geological and structural sketch map of Iberia showing the main tectonic fabric. Tectonic structures inland after De Vicente (2005). Circles: main features off-shore; 1) Gorringe Bank, 2) Extremadura Spur, 3) Galicia Bank, 4) Gulf of Biscay. Squares: main basins 5) Duero Basin, 6) Tagus Basin, 7) Ebro Basin, 8) Guadalquivir Basin. Triangles: main mountain ranges; 9) Spanish Central System, 10) Cantabrian Mountains, 11) Guadalupe-Montanchez Sierras and Toledo Mountains, 12) Sierra Morena, 13) Pyrenees, 14) Iberian Chain, 15) Betics. (b) Seismicity map of Iberia illustrating earthquake epicentres between 1980 and 2010. Data from USGS. Frequency plot indicates the distribution of seismic activity in depth. Markedly interesting is that most of the seismicity is located at 10 km depth within the plate interior.*

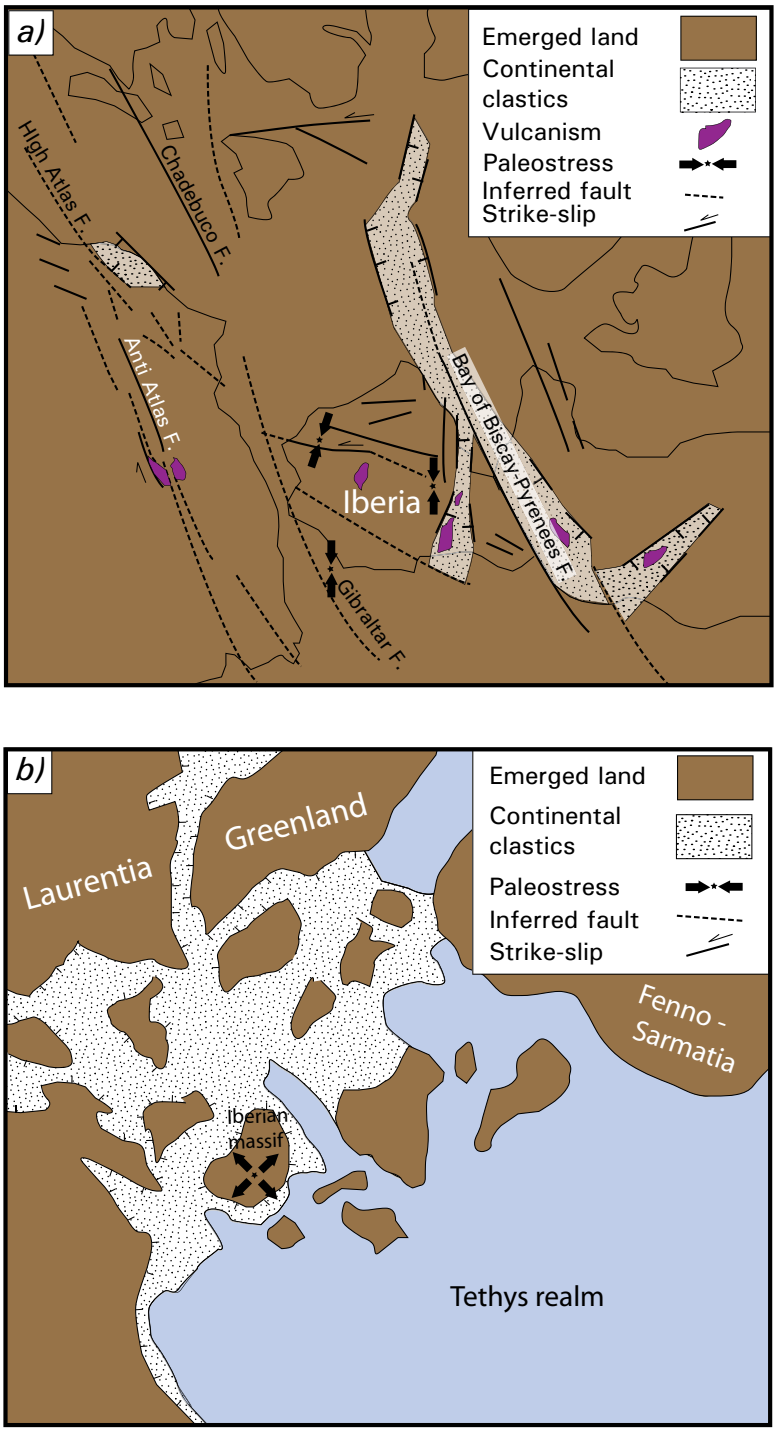

Figure 3.2 *Paleogeographic reconstruction of the Iberian Microplate. (a) Permian. (b) Triassic, modified from Arche and López-Gómez (1996). Paleostress data after Jabaloy et al. (2002).*

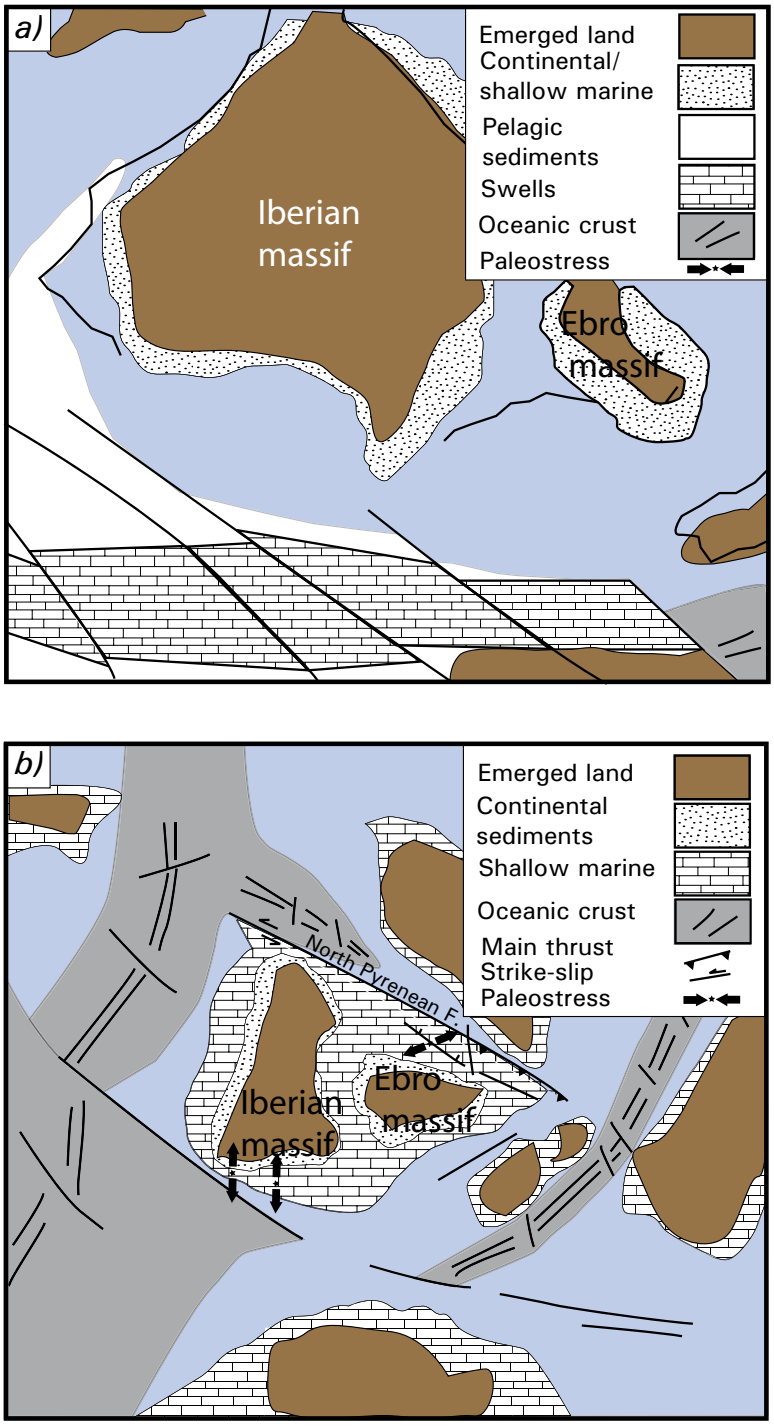

Figure 3.3 *Paleogeographic maps of the Iberian Microplate. (a) Jurassic (Oxfordian); (b) Cretaceous (Cenomanian), modified from Gibbons and Moreno (2002) after Vera (1998). Paleostress data after Jabaloy et al. (2002).*

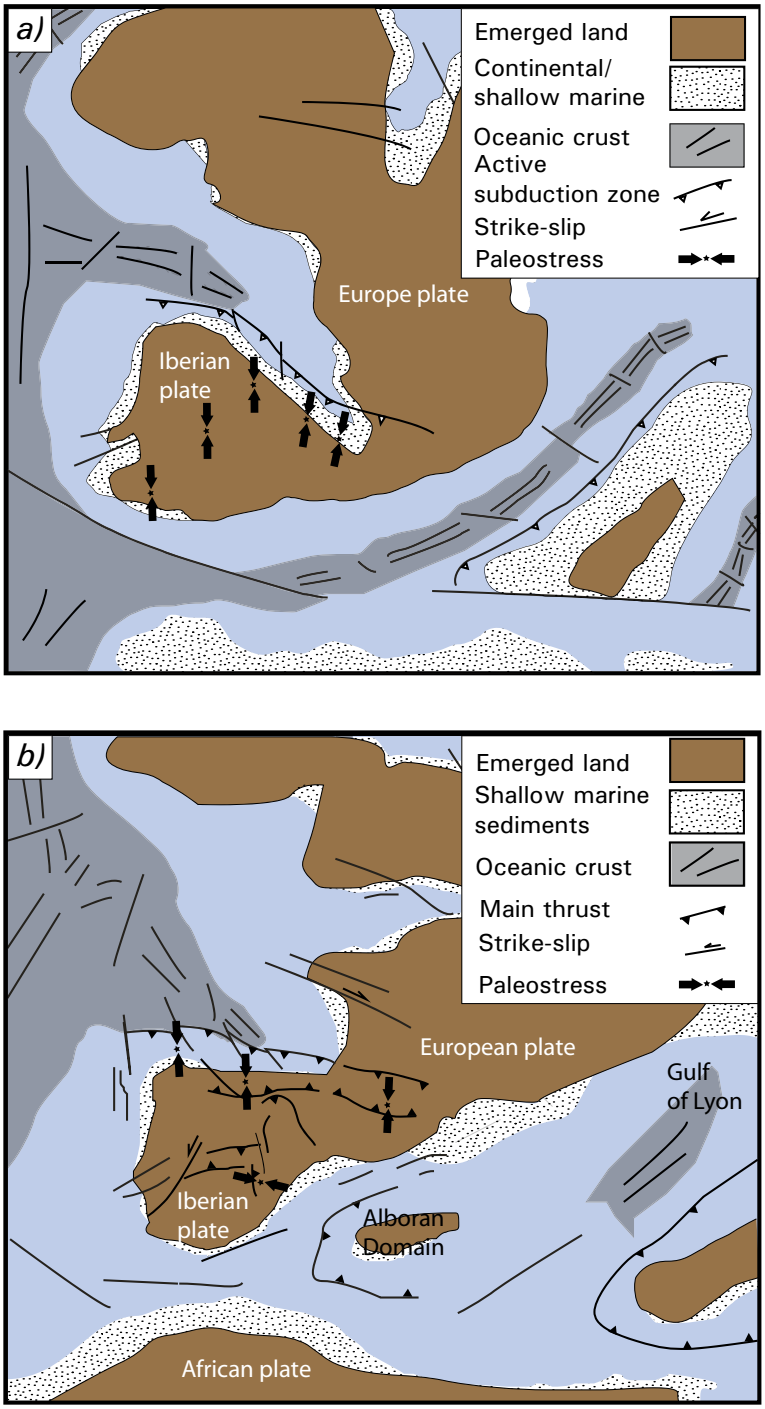

Figure 3.4 *Paleogeographic reconstruction of the Iberian Microplate. (a) Late Cretaceous (Campanian). (b) Oligocene-Miocene, modified from Andeweg (2002). Paleostress data after Jabaloy et al. (2002) and De Vicente and Vegas (2009a).*

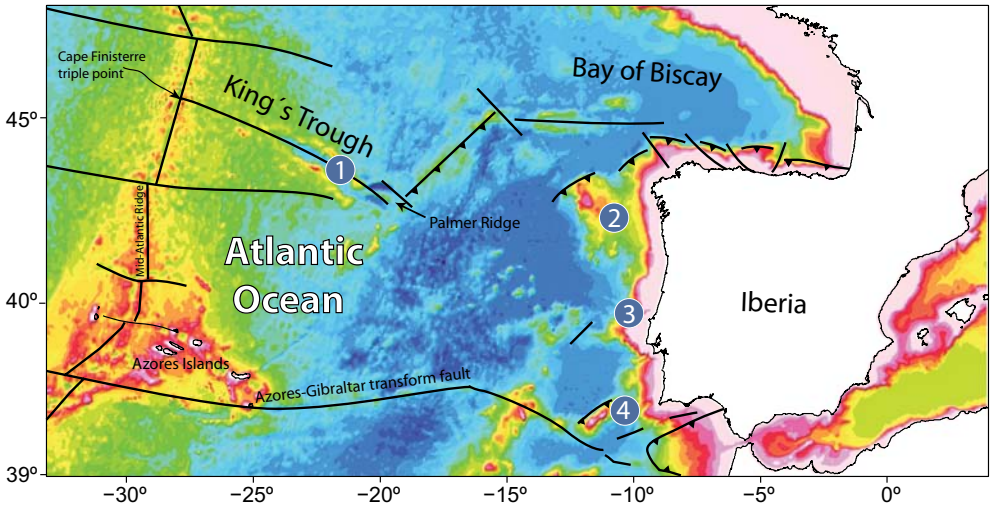

Figure 3.5 *Bathimetric map of the Atlantic margin of Iberia showing the most relevant features refered in the text. (1) King´s Trough; (2) Galicia Bank; (3) Extremadura Spur and (4) Gorringe Bank.*

ceous [Fig.3.4b]. Rotation was accommodated along major left-lateral strike-slip faults without any evidence of earlier and additional counter clockwise rotation during the Cretaceous. After late Cretaceous, Iberia remained attached (mechanically coupled) to the African Plate until the late Eocene (*Vegas et al.,* 2005a).

From Eocene to late Oligocene Epoch, main phases of under-thrusting took place along the Cantabrian margin as well as subduction of Iberia under the European plate leading to the formation of the Pyrenean Mountain Belt towards the east, an asymmetric double verging orogenic wedge, which is more developed on its southern side (*Muñoz,* 1991).

Apatite fission track data (AFT) and facies analysis of sedimentary sequences in basins next to the main mountain chains have shown that since the late Eocene to late Oligocene, the Cantabrian Mountains-Pyrenees border was uplifted (*Martín-González et al.,* 2006). At the same time the asymmetric Spanish Central System was activated, in the beginning, along its western sector (Eocene) and finally through the Guadarrama sector during the early Miocene (*De Bruijne and Andriessen,* 2002).

Meanwhile Mesozoic sedimentary basins of the present-day Iberian Chain underwent an oblique inversion from late Eocene to early Miocene (*Del Rio et al.,* 2009; *De Vicente and Vegas,* 2009a) which is compatible with the N-S convergence during the Pyrenean Stage.

During late Oligocene, the opening of the King´s Trough in the Atlantic margin together with the opening of the Valencia Trough influenced the orientation of the Sh_{max} trajectories, which turn into E-W orientation in the King´s Trough, NNE orientation at the eastern end of the Pyrenees and NE orientation in the Valencia Trough as constrained by paleo-stress data (*Vegas et al.,* 2005b; *De Vicente and Vegas,* 2009a) [Fig.3.5].

From late Oligocene onward Iberia has been part of the Eurasian plate. Kinematic models for present-day plate motions by *Minster and Jordan* (1978) and distribution of earthquakes show that Iberia is actively deforming as part of Eurasia (*Roest and Srivastava,* 1991) [Fig.3.6]. The extrusion of the Alboran block towards the southwest was followed by collision of this micro-

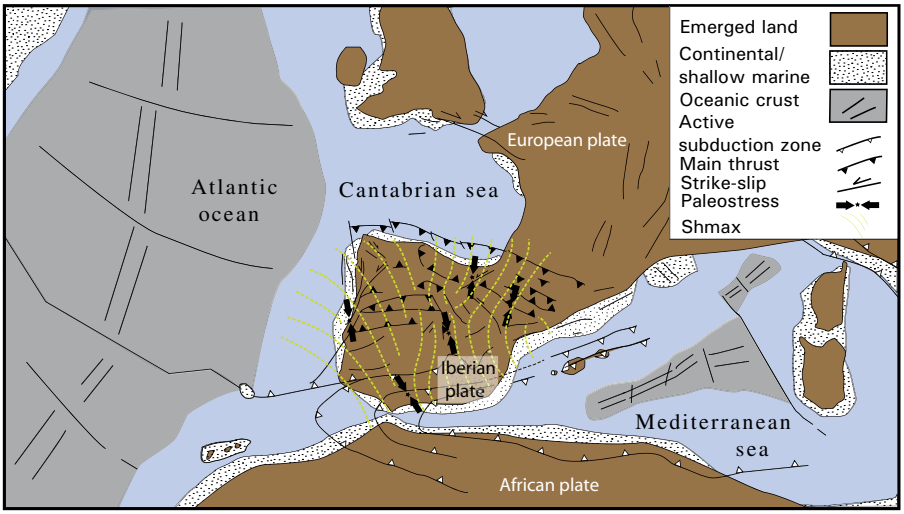

Figure 3.6 *Paleo-reconstruction of plate configuration during Oligocene-Lower Miocene Times. Main active acting forces and SH_{max} trajectories modified after De Vicente and Vegas (2009a).*

terrane during the early Miocene giving rise to the Betics (second stage of Alpine Orogeny).

The distributed deformation model proposed by *Vegas et al.* (1990), based on paleomagnetism and plate kinematic models shows how the deformation is dispersed along the Gulf of Cadiz. The strong plate-coupling may explain the efficient stress transmission towards the plate interior (*Ziegler et al.,* 1995; *Tikoff et al.,* 2002; *Ziegler et al.,* 2002), and the presence of seismically active regions in western Spain through the reactivation of pre-existent fault corridors (*De Vicente and Vegas,* 2009a).

In the area of Alboran, however, weak coupling between Africa and Iberia has been proposed based on present-day stress field data and numerical models (*Jiménez-Munt et al.,* 2001; *Vegas et al.,* 2008).

3.3 The role of late-Variscan tectonic structures

It has long been recognised in Iberia that pre-existing late-Variscan faults (mainly strike-slip and normal faults) are of importance during Alpine compression (*Arthaud,* 1975; *Vegas,* 1975; *Arthaud and Matte,* 1977; *Rosales-Calvo et al.,* 1977; *Ubanell,* 1981; *Doblas,* 1994; *Ziegler and Dezes,* 2006). Despite not all of these faults were reactivated during Alpine times. Those situated in the Iberian foreland were prone to reactivation as they were properly oriented to the main alpine stress-field [Fig.3.7]. Recently, *De Vicente and Vegas* (2009a) have classified some of the late-Variscan structures that may have played an important role during Alpine N-S shortening. Under this N-S stress field, faults trending NW-SE and NE-SW could have been reactivated (*Marques et al.,* 2002; *De Vicente and Vegas,* 2009a). The latter are mostly represented in the western part of Iberia, affecting the Variscan basement. These structures form part of a well-defined sinestral strike-slip fault system where compressional step-overs situated at fault tips favoured mountain uplift and basin formation (Vilariça-Bragança and Regua-Verin Fault Systems, Farias, 1987 and Moreira, 1985). Although the timing of fault activity is not well constrained during the Cenozoic (Oligocene-Miocene activity), recent Plio-Quaternary movement has been

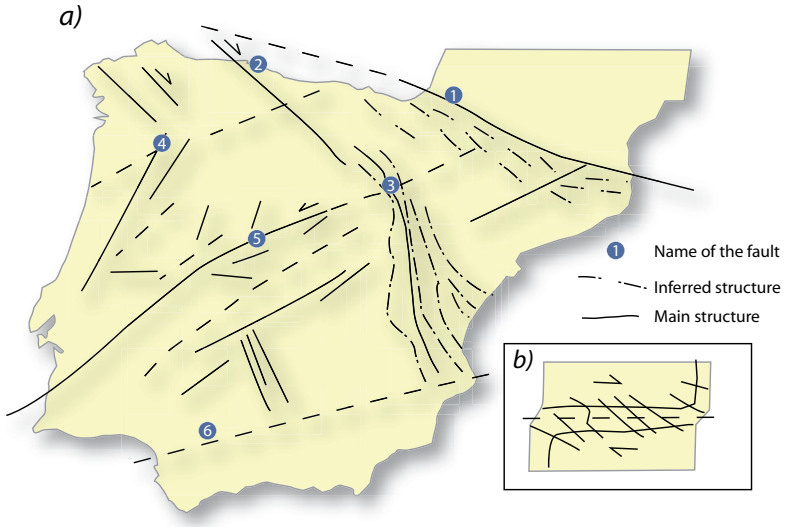

Figure 3.7 *(a) Illustrates major late-Variscan Wrench fault systems in Iberia. Numbers: 1) North Pyrenean Fault; 2) Ventaniella Fault; 3) Somolinos Fault; 4) Vilariça-Branç a Fault System; 5) Messejana-Plasencia Fault, and 6) Guadalquivir Fault (modified after and Vegas, 1975) (b) Stress field interpretation within the context of a large-scale wrench system from Arthaud and Matte (1977) .*

recorded with movement rates up to 0.3-0.5 mm/y (*Cabral,* 1989). Moreover, historical and present-day seismicity portray the tectonic activity of the fault system during NW-SE tectonic shortening (*Moreira,* 1985).

Farther east, reactivation of NE-SW to NW-SE oriented late-Variscan faults as normal faults during Mesozoic times led to thick sequences of Triassic to Cretaceous sediments all over the Iberian Chain (*Hernando-Costa,* 1973; *Alvaro et al.,* 1979; *Sopeña et al.,* 1988). The early episodes of the Pyrenean Orogeny led to partial inversion of the basin during the Eocene (*Mata et al.,* 2001) and subsequent uplift during the Oligocene-Miocene (*Guimerá et al.,* 1996; *Guimerá and González,* 1998; *Casas-Sainz and Faccenna,* 2001; *De Vicente et al.,* 2009b). For instance, the NW-SE Somolinos Fault, considered a dextral strike-slip with a thrust component during the Cainozoic, was reactivated as a normal fault during the Permo-Triassic and strike-slip afterwards in the Cretaceous. Present-day seismicity occurs along the fault indicating a strike-slip component under NW-SE directed stresses (the latest earthquake was recorded in 2011, IGN earthquake database). More extended details concerning late-Variscan pre-existent structures can be found in Chapters 5 and 6.

Unlike the aforementioned examples, the classification of pre-existent late-Variscan structures in central Spain remains controversial. Several authors have pointed out the importance of these faults on the final evolution and uplift of the Spanish Central System (*Ubanell,* 1981; *Portero and Aznar,* 1984; *Ribeiro et al.,* 1990; *Vegas et al.,* 1990; *De Vicente et al.,* 1992; *De Bruijne and Andriessen,* 2000; *Tejero et al.,* 2006; *De Vicente et al.,* 2007). However, recent data based on numerical models suggest that the formation of the Spanish Central System might be related to thermo-mechanical differences between the granitic crust of the range and the adjacent metamorphic Duero and Tagus mesetas (*Martín-Velázquez and De Vicente,* 2011). This hypothesis, underlies the importance of rheological differences instead of the reactivation of pre-existent structures as fundamental factors influencing the evolution of the ranges. Hence, it is likely that areas in Spain with significant rheological differences may have localized deformation

during the transmission of stresses through the plate interior. Therefore, rheological differences may explain recent seismicity observed in Galicia (NW Spain) when compared with the lack of earthquakes in the surrounding area of the Cantabrian Mountains. This area represents and igneous basement bordered to the east by the metasedimentary basement rocks of the Cantabrian Mountains. This configuration suggests that differences in rock-mechanics may have favoured the reactivation of structures which in turn caused the recorded seismicity (1995 seismic crisis, *López-Fernández et al.,* 2008).

In fact, despite pre-existent structures located in the main internal part of the Iberian foreland have been widely studied, their presence in the main basins is not well documented yet. Recent seismic reflection profiles and well-logs obtained along the northern border of the Duero basin have shown the continuation of dominantly E-W trending faults (*Herrero et al.,* 2010). These structures run parallel to the Mountain front and may have controlled the evolution of the Duero basin and adjacent uplifts (Galaico-Leoneses Mountains), leading to a rather irregular basin relief. The presence of E-W trending hills and depression within the Duero Basin suggest that reactivation of pre-existing structures affecting the Paleozoic basement beneath, may have influenced the observed irregular patterns observed. Some similarities are also seen in the Tagus Basin, where the Tertiary sediments conceal important basement structures interpreted as Pre-Mesozoic faults and lineaments (*Rodriguez-Aranda et al.,* 1995; *Muñoz-Martín and De Vicente Muñoz,* 1999). It is important to remark that the occurrence of pre-existent structures and their influence on strain localisation has also been described with certain similarities to what we can observe in Spain in other areas of recent intra-plate tectonic activity like the Colombian Cordillera (*Cortés et al.,* 2006), the Atlas system or the US Rocky Mountains, in North America (*Tikoff and Maxson,* 2001 and *Teixell et al.,* 2003).

Broadly speaking, three late-Variscan fault systems have been considered of major interest to have significantly contributed to the final configuration of topography in Iberia during the Pyrenean episode of N-S compression. Although these tectonic structures are described in this section, they will also be addressed in chapters 4 and 5 where they have been included in the analogue experiments.

» *Vilariça-Bragança Fault System (VBFS)*

The Vilariça-Bragança Fault System and close related structures represent a more than 350 km long fault zone trending NE-SW with a notable geomorphic expression [Fig.3.7]. It is part of a rather linear structure giving rise to elevated areas (positive step-overs associated with thrusting) and depressions (i.e. Vilariça Basin). Moreover, the main faults are segmented along strike by E-W and NW-SE secondary structures. Nowadays, the VBFS with more than 150 m of vertical offset is considered seismically active as it has been shown by the historical and present-day earthquake records (*Ribeiro et al.,* 1990; *Pinheiro et al.,* 1996; *Miranda et al.,* 2009). The main structures strike NE-SW and are reactivated as sinistral strike-slip faults, although upthrusting of the eastern block towards WNW has been described in some areas (*Cabral,* 1989).

Despite the complex evolution of the fault system, it is generally agreed that is of late-Variscan age, related to the latest episodes of the Orogen (*Vegas,* 1975; *Arthaud and Matte,* 1977; *Ribeiro et al.,* 1990; *Vegas et al.,* 2004). However, little is known about its Mesozoic tectonics history. During most of Jurassic and Cretaceous mid-Atlantic rifting, these fault system could have been active as extensional features (*Pinheiro et al.,* 1996). The Tertiary evolution, conversely, marks a transition into a transpressive regime (*Cabral,* 1989; *Marques et al.,* 2002). It is not well known whether the fault system was active during the entire Cainozoic, however, *De Vicente and Vegas* (2009a), suggest that this system could have transferred the deformation towards the central part of Iberia during Oligocene-Miocene times, playing an important role on

the tectonic evolution and the continuation of the Pyrenean-Cantabrian Orogenic front towards NW Iberia (*Vegas et al.,* 2004). Until now, there is only evidence of Neogene-Quaternary activity recorded by field data and seismic epicentres. During these Epochs, the rates of movement are about 0.2 to 0.5 mm/y (*Cabral,* 1989).

Recent studies carried out by *Tesauro et al.* (2008) and *Tesauro et al.* (2010), portrays a mean Moho depth between 30 km and 32 km along the fault trace [Fig.3.23c]. In addition, it is important to mention the broad heat flow anomaly (up to 120 mWm^{-2}), indicating the existence of a thermal anomaly (*Fernández et al.,* 1998) in the uppermost crust [Fig.3.23b]. Recently, it has been suggested that such a thermal anomaly could influence the depth of the brittle-ductile transition zone, which in turn would have controlled the focal depth of earthquakes in western Iberia (between 5 and 22 km, IGN seismic database).

» *The Somolinos Fault and the main Iberian Basin depocenters*

The Somolinos Fault involves more than 34 km of accumulated displacement cutting important structures like the Spanish Central System Southern Border Fault (*Bergamin et al.,* 1996). The approximated length of the fault roughly exceeds 150 km of apparent movement. Towards the NW it is covered by the sediments of the Duero Basin, although it could continue along NW-SE trending Quaternary valleys. It has been active during the Mesozoic (under strike-slip and extensional regime (*Hernando-Costa,* 1973; *De Vicente et al.,* 2009b) and Tertiary (under transpression), causing vertical movements until today (a recent earthquake took place in July 2011, Mb1.6). Originally, this fault has been categorized as late-Variscan (*Vegas,* 1975; *Arthaud and Matte,* 1977; *Álvaro et al.,* 1979; *De Vicente et al.,* 2009b), although an older age cannot be ruled out (*Hernando*, per.comm.). During the first stages of the Iberian rifting, the Somolinos Fault might have represented part of the master fault system (Somolinos-Ventaniella Master Faults) that controlled Mesozoic sedimentation during extension (*Sopeña et al.,* 1988; *Arche and López-Gómez,* 1996). This type of listric structures has been described in a pure-shear model, where hot lithosphere mantle becomes involved in deformation (*McKenzie,* 1978; *Arche and López-Gómez,* 1996). Therefore, these structures played two important roles. On the one hand they formed part of the Mesozoic Iberian Rift, and on the other hand they constituded the boundary between a cold and stable Variscan lithosphere to the west and a hot Mesozoic lithosphere that represents the present day Iberian Range. This limit, therefore, could be considered to be markedly heterogenous (both thermally and rheologically) represented by a transition lithosphere.

In addition, in the configuration of the Iberian Range during Alpine tectonic inversion a series of E-W structures, which confined the main Mesozoic depocentres during the stage of basin formation were crucial. These depocentres have been defined as the Cameros and Maestrazgo sub-basins characterised by more than 8.000 and 5.000 m of marine sediments, respectively. Seismic reflection profiles indicate that these structures, inherited from the Variscan times (involving paleozoic basement), developed as listric faults, leading to the formation of broad roll-over anticlines where thickness variations were controlled by basement heterogeneities such as tectonic structures, basin highs, etc (*Casas-Sainz,* 1993; *Casas-Sainz and Gil-Imaz,* 1994; *Guimerá et al.,* 1995; *Rivero et al.,* 1996; *Casas-Sainz et al.,* 2009a). Something similar occurred associated to the Maestrazgo sub-basin, which represents a late Jurassic-early Cretaceous depocentres (*Guimerá et al.,* 1996; *Salas and Guimerá*, 1996). This depression is governed by a series of E-W structures, which divided it into several sub-basins. These sub-basins formed part of a series of semi-grabens that have been considered as the syntaxes between the two main branches of the Iberian rift (Iberian and Catalan-Coastal ranges). By the beginning of the Tertiary episode of shortening, both depocentres were inverted leading to mountain reliefs (*Casas-Sainz,* 1993; *Guimerá et al.,* 1996; *Cortés-Gracia and Casas-Sainz,* 1997; *Guimerá and González,*

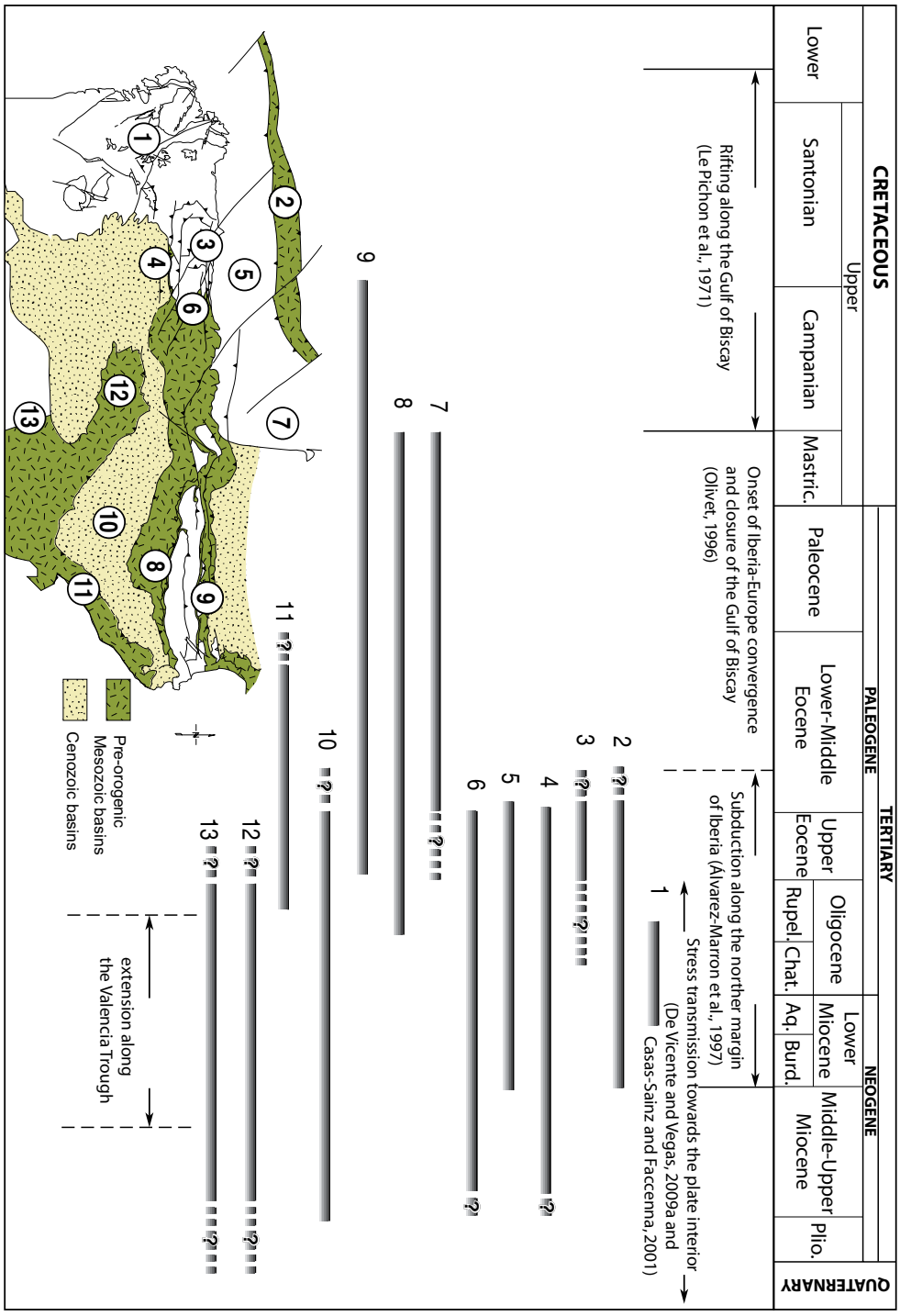

Figure 3.8 *Diagram showing the temporal evolution and onset of deformation events during the late Cretaceous and Tertiary in northern and central Iberia.*

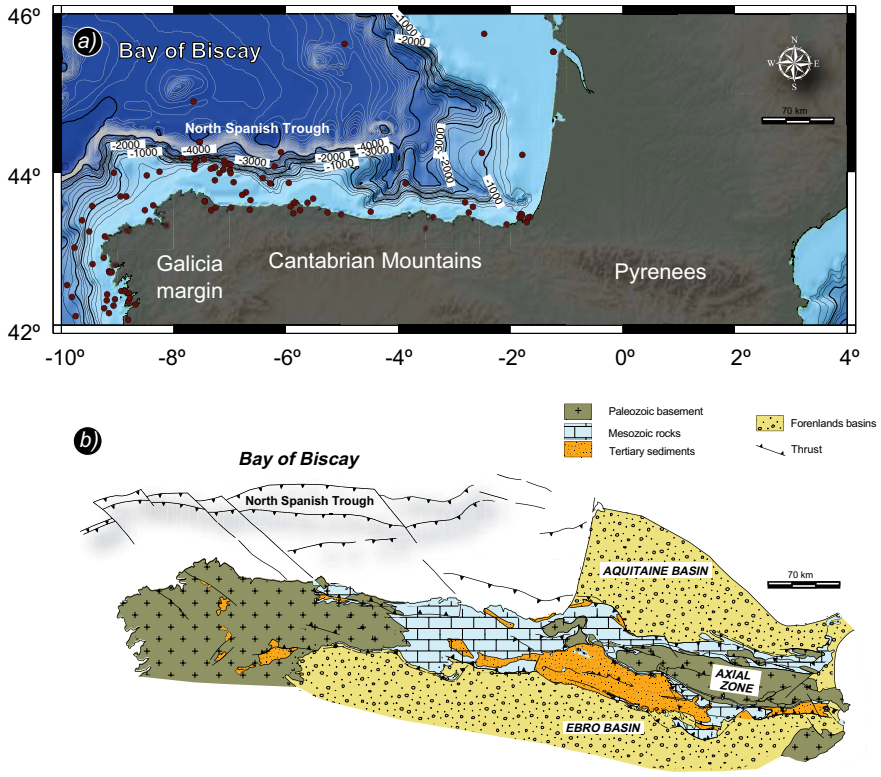

Figure 3.9 *(a) Contour map of the Bay of Biscay oceanic margin portraying seismic epicentre locations. Present-day shallow seismicity along the margin indicates active crustal deformation along a series of north-verging thrust shown in the geological sketch map based on Teixell (2000) (b).*

1998; *Guimerá et al.,* 2004; *De Vicente et al.,* 2009b).

» *Messejana-Plasencia Fault*

Considered probably one of the most outstanding structures in Iberia, its trace can be followed along more than 500 km from central Spain towards the Atlantic platform. Its geomorphic expression results in a series of valleys that configure pull-apart basins filled with Tertiary sediments, whereas segmented topographic highs represent compressive step-overs. The fault, trending NE-SW has been described as a late-Variscan sinistral strike-slip intruded by a mafic dike (*Feio,* 1952; *Vegas,* 1975; *Arthaud and Matte,* 1977). The dike, Jurassic in age, has yield a similar age than other mafic dikes found along the Atlas Mountains and the Newfoundland margin (*Vegas,* 2000; *Palencia-Ortas et al.,* 2006). The Mesozoic evolution of the fault system has been related to the opening of the Mid-Atlantic. N-S extension of the Iberian margin (*Pinheiro et al.,* 1996) led to widespread extension and intrusion of the mafic dike. Cretaceous to Quaternary activity of the fault is reported under a sinistral strike-slip and transpressive regime respectively (*Villamor,* 2002; *Araújo,* 2004). During the Tertiary times, it has been suggested that the fault may have influenced the reactivation and evolution of crustal-scale tectonic structures that have contributed to the uplift of the Spanish Central System (*Vegas et al.,* 1990). Although the fault records less than 3 km of overall displacement, structural and sedimentary analysis indicates recent movement rates below 0.1 mm/y, which may be considered as a seismic hazard every 10.000 years. The seismic activity along the Plasencia fault has been suggested as a possible source for

the 1755 Lisbon earthquake (Moreira, 1968).

The earthquake provoked a Tsunami destroying the city and finally reached the British Island in a few hours, causing more than 20.000 fatalities.

Tertiary to Quaternary fault activity has been linked to the Africa-Iberia collision. Within this tectonic framework, the Messejana fault may have played a very important role for the effective transmission of stresses from the southern plate boundary, where a mechanism of strong plate-coupling has been invoked to explain present-day seismicity in Central Spain (*Vegas,* 2005b).

3.4 Distribution of mountain ranges and related basins

In the following sub-sections the main geological units of the Iberian Plate are described paying special attention to the age of tectonic uplift and basin formation through geological and structural information, fission track (FT) and stratigraphic data.

3.4.1 Alpine evolution of intra-plate mountain ranges

The opening of the Bay of Biscay during the late Cretaceous led to the first pulses of compression along the Cantabrian Margin. Ongoing deformation caused the closure of a series of E-W trending transtensional basins, and the raising of the Pyrenean orogen in the early Eocene. Uplift along the Pyrenees was followed by the tectonic inversion of the present-day Catalan-Coastal and the Iberian Ranges (east and west, respectively) thereby forcing the retreat of the Cantabrian Sea to the northwest. During the late Eocene, the first vertical movements are recorded along the Spanish Central System causing the exhumation of the range during most of the Tertiary (*De Bruijne and Andriessen,* 2002). The intra-plate Cainozoic uplift is recorded by the deposition of continental sediments filling the main basins (Duero, Ebro and Tagus Basins). A chronological description of Cainozoic deformation and uplift is shown in Figure 3.8 In the following section I describe the tectonic evolution of mountain ranges and the subsequent formation of associated basins during the Pyrenean Orogeny in Iberia.

3.4.1.1 Northern Spain

» Cantabrian Mountains-Pyrenees border

The Cantabrian Mountains are the western prolongation of the Pyrenean belt in Iberia extending along 700 km from E to W. Together they form a mountain system with mean altitudes that reach 1.000 and 2.000 m, respectively. This high topography resulted from the oblique convergence between the Iberian and European plates and the tectonic inversion of Mesozoic transtensional basins during most of the Cainozoic times. Recent seismic activity along the margin portrays present-day crustal deformation along a series of north-verging thrusts that uplift the Bay of Biscay marine platform [Fig.3.9]. Geophysical data show double polarity of the subduction with major amounts of shortening decreasing from east to west (135 km and 85 km, respectively) (*Muñoz,* 1991) [Fig.3.10]. The Iberian plate subducts under Europe in the Pyrenees, whereas below the Cantabrian mountains, the Iberian lower crust is underthrust by possibly thinned continental crust of Iberian affinity, indicating partial subduction below Europe (*Boillot,* 1988; *Pulgar et al.,* 1996; *Fernández-Viejo,* 1998; *Pedreira et al.,* 2007).

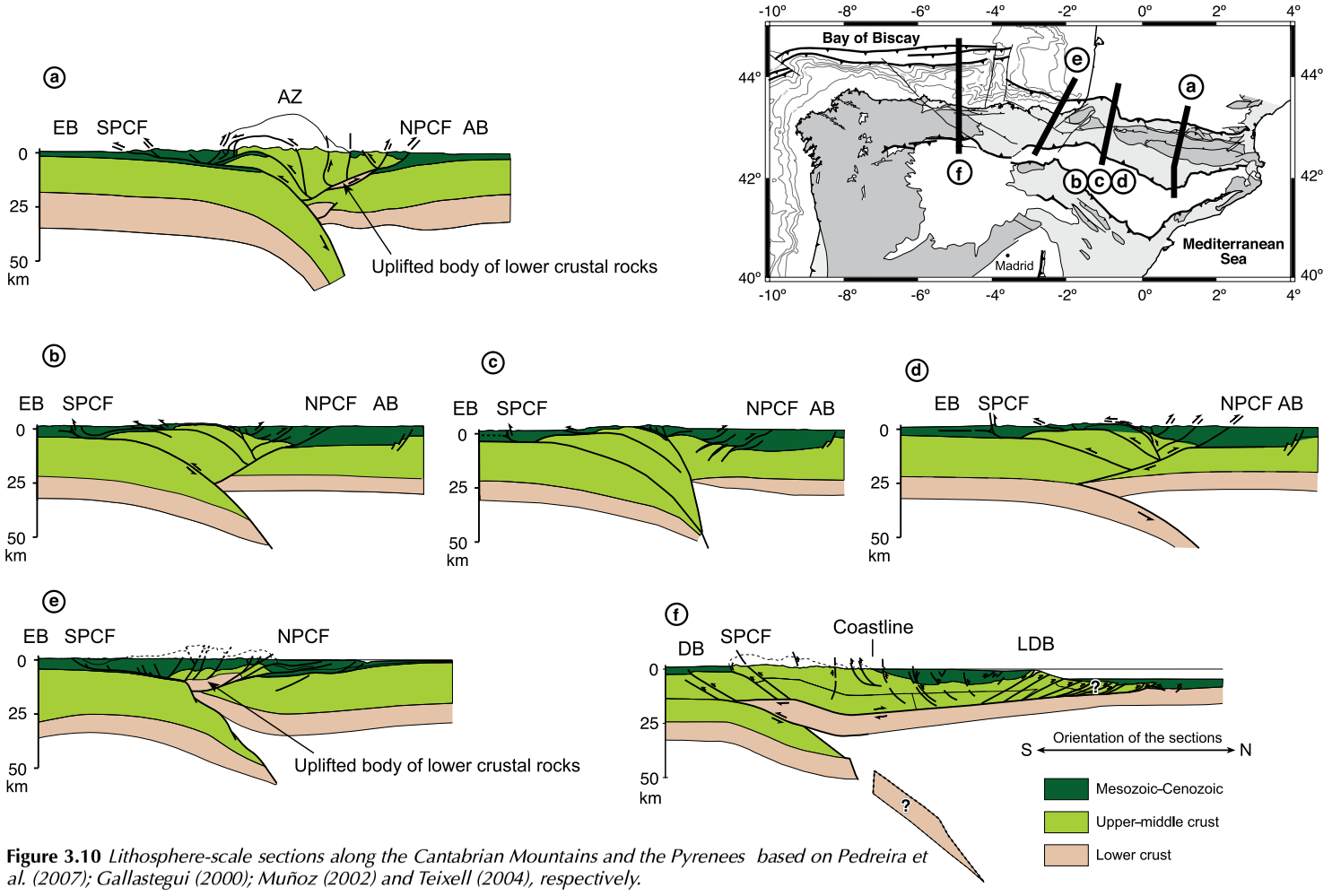

Figure 3.10 *Lithosphere-scale sections along the Cantabrian Mountains and the Pyrenees based on Pedreira et al. (2007); Gallastegui (2000); Muñoz (2002) and Teixell (2004), respectively.*

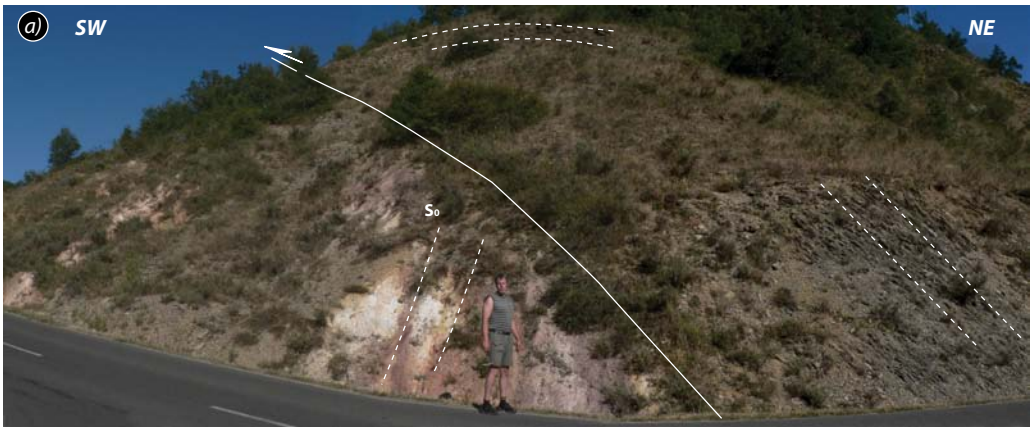

Figure 3.11 *(a) Unconformably lying Cretaceous and Tertiary sediments of the Duero basin at the contact with a southern border thrust of the Cantabrian Mountains (Cistierna, León). (b) Panoramic view of the Bierzo Basin. (c) Southern border thrust of the Bierzo basin and (d) Northern border thrust of the Bierzo basin.*

Continental collision along the northern margins resulted in thickening of the Iberian crust. Moho depths reach more than 50 km under the Pyrenees; 40 to 48 km underneath the Cantabrian Mountains and 30-32 km towards Galicia (*Fernández-Viejo,* 1998; *Gallastegui,* 2000; *Pedreira et al.,* 2003; *Díaz and Gallart,* 2009) [Fg.3.23a]. The Cantabrian Mountains are characterised by a basal detachment, dipping towards the north between 15° and 18° and involve several thrust faults that place Palaeozoic rocks on top of Cretaceous to Tertiary rocks and sediments of the Duero foreland basin (*Gallastegui,* 2000). The result of a simultaneous interference of sedimentation, erosion, and tectonic uplift is represented by a progressive unconformity that can be observed along the northern border of the Duero [Fig.3.11a].

Towards the west, the Cantabrian mountain front ends into a series of thrusts verging north and south that constitute the pop-down of the Bierzo Basin [Fig.3.11b, c and d]. However, along the east, the southern Pyrenean front is characterised by a series of antiformal stacks of thrusts that overlie Tertiary sediments of the Ebro foreland basin.

Recent studies based on geological mapping and geomorphologic markers like drainage networks or erosion surfaces carried out by *Martín-González* (2009) has provided new insight into the disappearance of E-W Pyrenean relief towards the south and the N-S to E-W distribution of Tertiary basins together with their connection with Alpine structures. However, *De Vicente and Vegas* (2009a) have proposed a mechanism of strain partitioning through a series of left-lateral deformation belts related to the Vilariça Fault System which end at compressive step-overs that compensate the total amount of shortening. In addition, fission track data show a complex cooling history from the Cretaceous Period to Tertiary (Eocene-Oligocene, Miocene-Pliocene) related to mountain building in that part of Iberia (*Martín-González et al.,* 2006).

3.4.1.2 Central Iberia

Due to the lack of deep seismic data (wide angle reflection and refraction profiles) little is known about the lithosphere structure in central Spain. Despite the large amount of geological/structural data and gravity surveys, only the areas of the Central System and Iberian Range have been extensively studied (*Surinach and Vegas,* 1988; *Salas and Casas,* 1993; *Casas-Sainz and Gil-Imaz,* 1994; Cortés-Gracia and *Casas-Sainz,* 1997).

N
S
Bierzo Basin
c
N
S
Cantabrian Mountains
Bárcena
Dam
b
S_0
a

» The Spanish Central System and Toledo Mountains

The Spanish Central System (SCS) constitutes a more than 700 km-long mountain range extending from Portugal to Central Spain. It is defined as an asymmetric pop-up structure bordered to the north and south by the Duero and Tagus Basins (*De Vicente et al.,* 2007) [Fig.3.12a, c and d]. Deep seismic profiling carried out by *Banda et al.* (1983) and *Surinach and Vegas* (1988) show a crustal thickness of 32-35 km with thickening of the lower crust by up to 4-5 km [Fig.3.23a]. Gravity modelling also supports this crustal architecture (*De Vicente et al.,* 2007)[Fig.3.12b]. The total amount of calculated shortening by *De Vicente et al.* (1996) reaches 20% of bulk shortening across the central part of the Range. Shortening is taken up by segmented border faults (a northern and southern border fault), facing N and S, respectively. The northern border is mostly covered by Tertiary sediments of the Duero basin. The southern thrust is more segmented involving Palaeozoic, Mesozoic and Tertiary sediments. These faults juxtapose Variscan basement over Miocene fluvial sediments consisting of sandstones and conglomerates. Within the whole mountain system, a series of pop-ups and pop-downs create space for intra-mountain basins filled with Tertiary sediments (Lozoya Basin, Amblés basin) [see Fig.3.12a]. Seismicity is scarce along the Range, mainly localised along NE-SW and N-S striking faults, whereas most of the activity is distributed within the Madrid Basin portraying the presence of normal faults.

Asymmetric uplift of the chain has been recorded by FT data starting in the early Eocene in its western sector (Gredos Sierra) and late Miocene in the eastern part (Guadarrama sector) (*Andeweg et al.,* 1999; *De Bruijne and Andriessen,* 2000; *De Bruijne and Andriessen,* 2002). These episodes of exhumation have been related to reactivation of properly oriented late-Variscan faults under N-S oriented alpine stress. The total amount of exhumation calculated by these authors varies between 3,8 km and 3 km. However, this data seems to contradict field evidence. Recently, a Permo-Triassic palaeo-surface has been found in some areas of the Spanish Central System which would imply a smaller amount of exhumation (*Christine Franke* pers. comm.).

Further south, separated by the Tertiary depression of the western part of the Madrid Basin raises the Toledo Mountains. This mountain system shows close structural similarities with the occidental part of the Central Range. It is mostly represented by Hercynian granites affected by a north and south border, thrusted over Cretaceous rocks and Tertiary sediments of the Madrid Basin. In addition, paleo-stress analyses carried out by *Muñoz-Martín and De Vicente* (1994) has shown a N-S alpine orientation of the maximum stress at least, Late Miocene in age. This data is in agreement with the age of uplift provided by AFT-data (*Barbero et al.,* 2005) where AFT traces suggest a cooling episode at 20 Ma. However, compared with the nearby Spanish Central System, the tectonic uplift seems to be relatively irrelevant (km).

» The Iberian Range

The Iberian Range is characterised by a complex sedimentary and structural history developed within an intra-cratonic area. It has been often divided into several units: Castillian and Aragonese branch and the linking unit which connects the Iberian Chain with the Catalan-Coastal Ranges to the east. The general structure shows two differentiated areas: the eastern part evolves into two antiforms (push-ups) separated by a broad synforms (Almazán Basin) and the western part underlain the trend of a fold system (*Casas-Sainz and Gil-Imaz,* 1997; *Casas-Sainz et al.,* 2009a) [Fig.3.13].

The borders of the Chain are thrusts with offsets up to 4 km (Cameros thrust). The estimated amount of Tertiary shortening is close to 80 km taken up by crustal thickening (thrusting) and

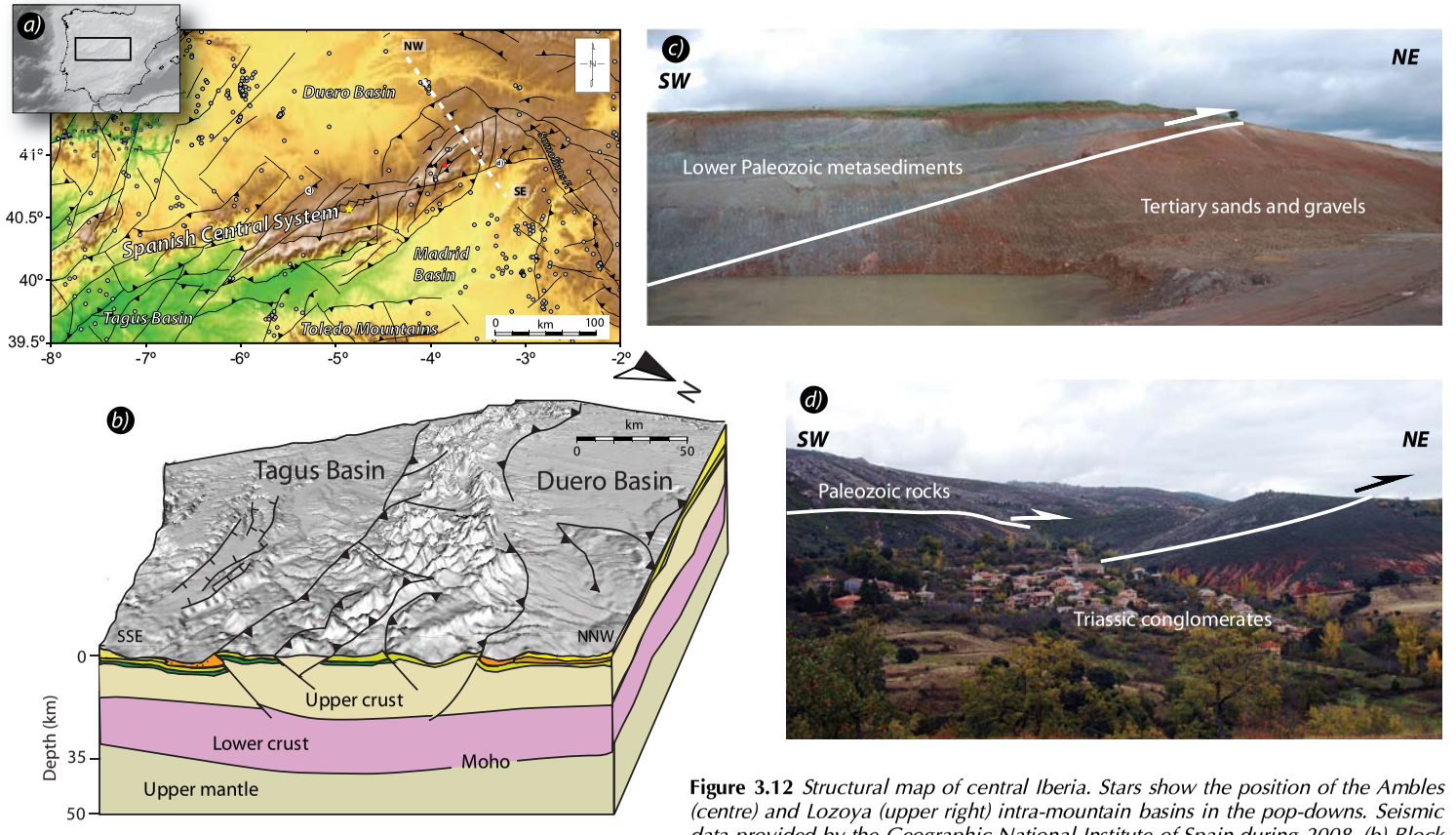

Figure 3.12 *Structural map of central Iberia. Stars show the position of the Ambles (centre) and Lozoya (upper right) intra-mountain basins in the pop-downs. Seismic data provided by the Geographic National Institute of Spain during 2008. (b) Block diagram based on seismic profiles carried out by Suriñach and Vegas (1988), illustrating the deep structure underneath the Spanish Central System showing the pop-up-like structure affecting the upper crust, and the apparent thickening of the lower crust by 4 km. Main border thrusts that comprise the Central Range pop-up: (c) northern border fault and (d) southern border fault (see (a) for location).*

folding [Fig.3.14a and b]. Despite the high crustal thickness, which is supported by gravity anomalies [Fig. 3.23a and Fig. 3.22b], a controversial view of the Chain maintains the scientific community divided (*Salas and Casas,* 1993; *De Vicente et al.,* 2009b). The scarce deep seismic profiles available in the area hamper the estimation of accurate crustal thicknesses underneath the Iberian Range. Although gravity surveys have provided an estimation of the crustal-mantle transition depth (*Salas and Casas,* 1993; *Guimerá et al.,* 1996; *Guimerá and González,* 1998; *De Vicente et al.,* 2009b), it remains unclear whether the upper most crust may have been detached along mid-crustal levels (thin-skin tectonics) or on the contrary, thrusting may cross-cut the entire crust (thick-skin tectonics) (*Salas and Casas,* 1993; *Guimerá et al.,* 1995; *Guimerá et al.,* 2004)

The tectonic evolution of the Range started in the late Permian-Triassic period and was extended through most of Mesozoic times as a result of the Atlantic and Tethys oceanic opening, which opened a gateway for sea flooding. These episodes of rifting formed a broad extensional basin called Celtiberian Basin, where a series of fault-related minor sub-basins controlled sedimentation [Fig.3.14c]. Somehow, its location, situated between two Alpine chains (Pyrenees and Betics); the double vergence geometry of the range and its location within the Iberian plate interior led several authors to consider the Iberian Chain as an incomplete aulacogene (*Álvaro et al.,* 1979).

The origin of the Celtiberian aulacogen starts in the lower Triassic. A triple-junction caused by a mantelic plume originated the aulacogen and another two branches to the south (the Betic-Balear system). During this episode of rifting, deformation appeared localised along inherited Variscan to late-Permian faults. However, during the early Jurassic and late Cretaceous (190–180 Ma 155–150 Ma, 97–88,5 Ma) stretching was distributed resulting in local extension along the chain. These episodes of rifting were followed by active thermal subsidence which allowed accommodation of thick sedimentary sequences (*Van Wees and Stephenson,* 1995; *De Vicente et al.,* 2009b). Altogether, the Iberian Basin represents a rhomboid-shape trans-tensional basin represented by a series of NW-SE to NE-SW master faults and an E-W to NW-SE transfer faults which compartmented the basin (*Arche and López-Gómez,* 1996; *Van Wees et al.,* 1998; *Vargas,* 2009). During the Tertiary episode of plate convergence between Iberia and Europe the oblique Mesozoic rift basin was tectonically inverted giving rise to a series of NW-SE trending mountains (*Casas-Sainz eta al.,* 1998; *Casas-Sainz and Gil-Imaz,* 1997; *Guimerá et al.,* 2004; *De Vicente et al.,* 2009b). As a result, the main extensional depocentres (Sierra de Cameros and Montalbán) linked by strike-slip systems were uplifted and thrusted into the present-day configuration.

A more detailed tectonic and sedimentary description of the Iberian Range is given in Chapter 6.

3.4.1.3 Atlantic margin

The evolution and opening of the Northern-Atlantic margin has been conditioned by the ongoing rifting started during early Triassic -period. Drifting of the Iberian plate since Mesozoic times to the east led to the development of new plate boundaries with non-coeval activity. During the early Cretaceous, the establishment of the Azores-Palmer Ridge triple junction to the north led to the counter-clockwise rotation of Iberia and opening of trans-tensional basins along the Cantabrian Border. In addition, the uplift of the ocean floor along the Palmer ridge (60 Ma.) subsequently led to the opening of the King´s Trough (27 Ma.) [see Figure 3.5 for location]. As a result vertical movements took place alongside the Galicia Bank (Cann and Funnell, 1967). This episode of ocean floor spreading and crustal detachment led to the exhumation of mantelic rocks and incipient volcanism along the Atlantic off-shore of Iberia. The present-day tectonic activity of the margin is marked by a series of E-W trending seismic corridors that highlight the presence of basement uplifts [Fig.3.1b]. The main uplifted features are described below:

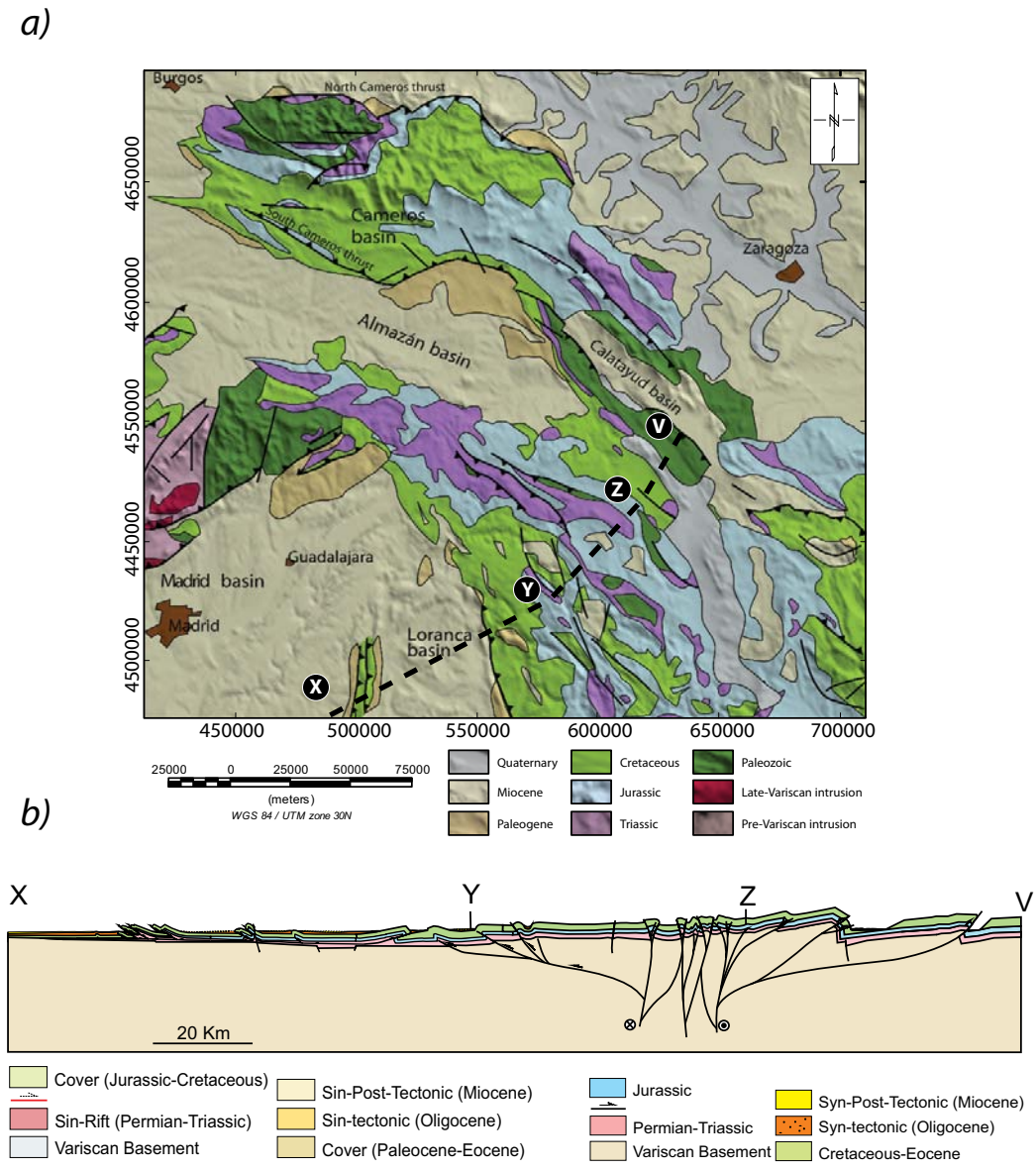

Figure 3.13 *(a) Geological map of the Iberian Range showing the main features. (b) Geological cross-section shown in (a), after de Vicente et al. (2009b).*

» Palmer Ridge-King´s Trough

Situated in the north-western part of the Atlantic margin of Iberia is perhaps one of the most recent off-shore features [Fig.3.5]. Considered as a short-lived plate boundary; a compressional boundary or a re-oreintated former bend in the Mid-Atlantic ridge, it has been widely studied by *Searle and Whitmarsh* (1978); *Kidd et al.* (1982); *Cann and Funnell* (1967) and *Ramsay* (1970). The opening of the North Atlantic led to basement uplift (igneous and metamorphic) about 60 My ago along the Palmer ridge, an asymmetric ridge on the seafloor

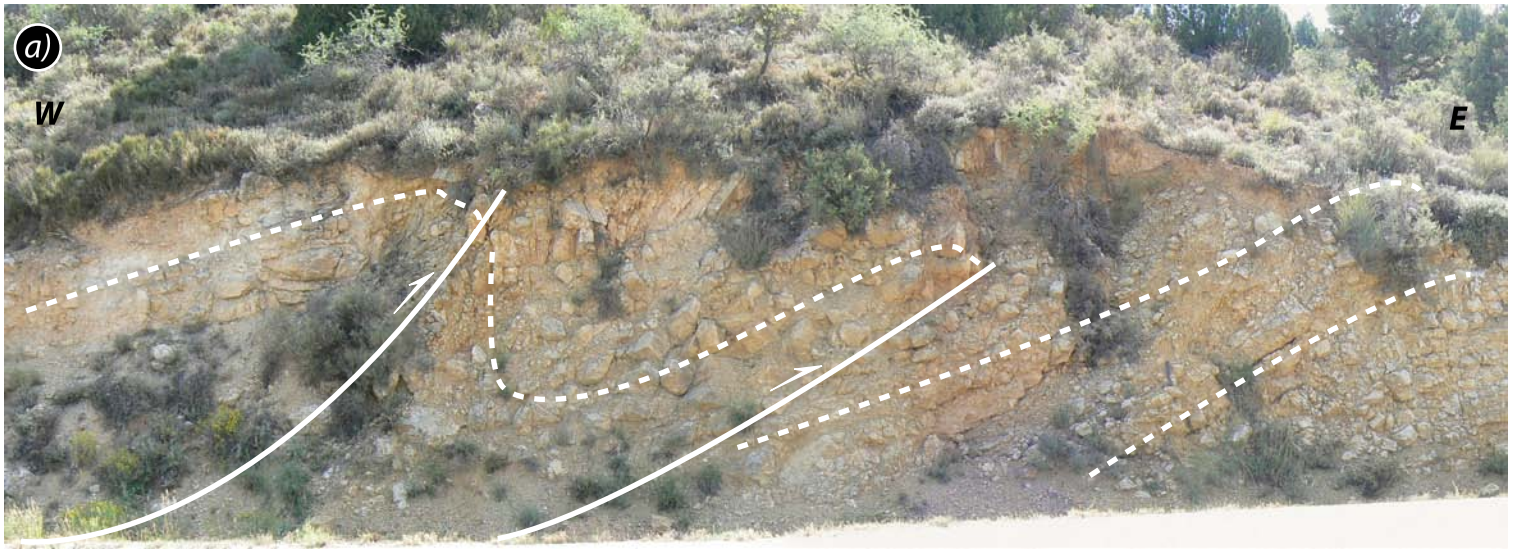

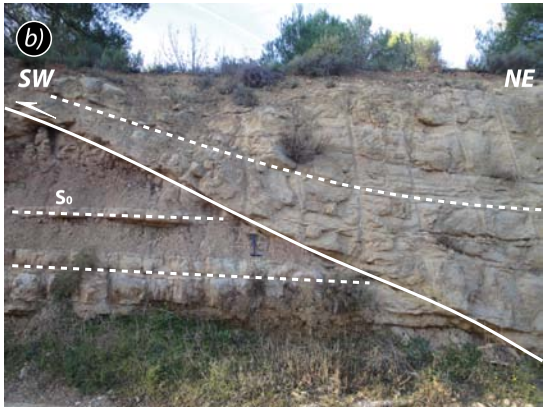

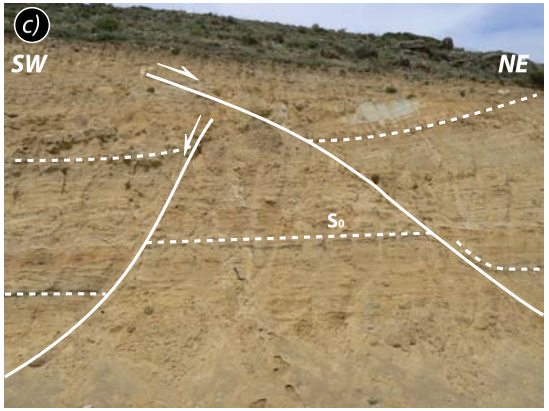

Figure 3.14 *(a) Imbricated thrust affecting Cretaceous rocks near Albarracín (Iberian Range). (b) Cretaceous rocks overthrusted (Montalbán). (c) Remnant Cretaceous sub-basin affected by a set of conjugated normal faults that may have controlled sedimentation during the Mesozoic.*

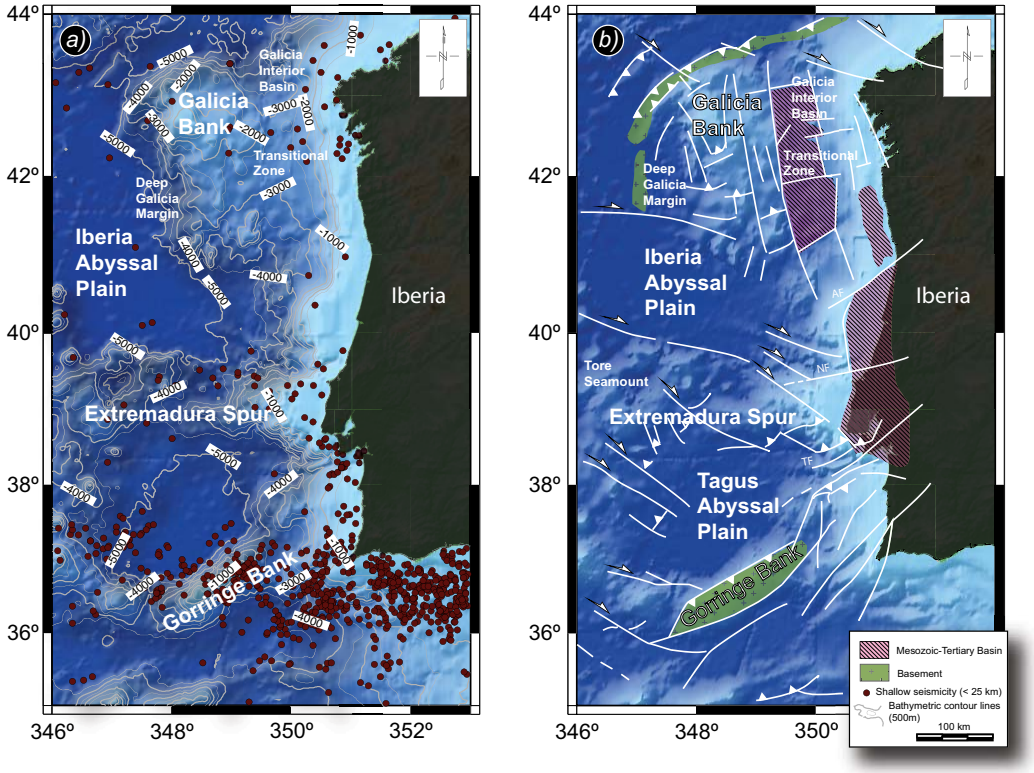

Figure 3.15: *(a) Contour map of the Atlantic margin bathymetry. Superimposed seismicity reveals a series of E-W trending seismic corridors along the Galicia Bank, Extremadura Spur and Gorringe Bank. (b) Principal tectonic structures affecting the basement and location of Mesozoic-Tertiary basins situated in the margin.*

moving from the mid ocean-ridge to its actual position (650 km far from the spreading centre). The ridge forms part of the NW-SE trending bathymetric feature called King´s Trough that started opening at 27 My ago, which is probably related to the NW-SE oriented convergence between Eurasia and Iberia that gave rise to the Azores-Biscay Rise. Furthermore, the ridge is the result of two different episodes of seafloor spreading and may influence the counter-clockwise rotation of the Iberian Plate during most of the Cretaceous (*De Vicente and Vegas,* 2009a).

» Galicia Bank

Despite its complex structural configuration, four morphostructural provinces are clearly recognisable: the Galicia Interior Basin, the Transitional Zone, the Galicia Bank and the Deep Galicia Margin [Fig.3.15a]. The area is surrounded to the north by the Biscay Abyssal Plain, and to the south-west by the Iberian Abyssal Plain. The seafloor morphology is the result of two successive Mesozoic extensional phases represented by consecutive pre-rift, syn-rift and post-rift episodes (*Mauffret and Montadert,* 1987).

The first phase is related to the breaking-up of Pangea prior to the opening of the central Atlantic during the Triassic (characterised by N-S and NNW-SSE normal faults and NE-SW strike-slip systems). The second phase associated with the Upper Jurassic to Early Cretaceous opening of the north Atlantic. However, recently it has been proposed that extensional faulting occurred during overall spreading of the oceanic margin (*Vázquez et al.,* 2008). The westward

migration of extension led to new fault activity and reactivation of previous structures until the beginning of the Paleogene. The onset of the Pyrenean convergence led to the reactivation of Mesozoic structures and thrusting on the northern border of the margin. The general structure of the Galicia Bank region is characterised by basement tilted blocks along normal faults giving rise to horst and graben morphology. Most of the post-rift section is affected by neotectonic normal faults disconnected from the basement. However, seismic profiles show locally reactivation of basement structures (anticlines and synclines affects the sedimentary cover). The northern part of the margin displays an arc-shaped morphology as a result of a NE-SW trending reverse fault. The fault is segmented into two well-differentiated branches linked by a NW-SE strike-slip fault and connecting the NW Iberian continental margin with the Bay of Biscay. Towards the western part of the Iberian Abyssal Plain, the end of the reverse fault tip involves deformation and uplift of a peridotite ridge. In addition, *Vázquez et al.* (2008), have proposed that the overall morphology of the Galicia Bank is the result of a broad antiform related to crustal thrusting during the Pyrenean orogeny. This crustal structure would form part of a series of E-W trending lithosphere-scale folds that extends towards the Iberian onshore (*Cloetingh et al.,* 2002; *De Vicente and Vegas,* 2009a; and *Fernández-Lozano et al.,* 2011).

» Extremadura Spur

Besides its E-W direction, the Extremadura Spur has been considered to be connected with the on-shore Iberian relief (i.e. Central Range). Much of its bathymetry rises between 1.000 m and more than 5.000 m [see Fig.3.15a]. Located between the Iberia Abyssal plain to the north and the Tagus Abyssal plain to the south, it represents the border between submarine canyons at both sides. Despite little is known about its physiography, the western part constitute an important volcanic area (Tore Seamount) followed by the uplifted block of the sensu stricto Extremadura Spur to the east. The origin is linked to the opening of the central Atlantic and it is characterised by broad Mesozoic extension and basin formation. Magnetic anomalies (Jurassic in age) extends towards the Tagus Abyssal plain which confirm a late Tithonian age (147 Ma.) for continental break-up (*Srivastava et al.,* 2000) followed by subsequent alpine inversion. Seismic profiles close to the Iberian margin show the presence of Miocene sediments affected by reverse faulting while to the west normal faulting cross-cut the Mesozoic series (*Alves et al.,* 2003). The Extremadura Spur is bordered by two big fault-zones represented by the Nazaret fault to the north and the Tagus fault to the south. Both structures are considered important Mesozoic transfer-faults and are connected with the Iberia on-shore (*Alves,* 2009). Moreover, the southern border is dominated by NW-SE reverse faulting which accommodate the uplift. Shallow seismicity (<25 km depth) extends E-W along the whole ridge defining the physiography of the area.

» Gorringe Bank

It is a NE-SW trending ridge, 80 km wide and more than 200 km long slightly tilted towards the northeast. The bathymetry ranges between 100 m the shallower part, and more than 5.000 m in the abyssal plains. Deep seismic reflection and refraction profiles carried out across the Gorringe Bank provides structural and timing constrains on the nature and evolution of the ridge. Prior to the Alpine movements, the area was subjected to the Atlantic opening related-extension (Barremian-Aptian). As a result, emplacement of oceanic crust and upper mantle rocks took place. Subsequent thrusting led to serpentinization and uplift of mantle peridotites up to 10 km, leading in turn to mantle rocks exposure at the sea floor. However, the ridge origins remain unclear. Somehow, the distribution of deep seismicity and earthquake fault-plane solutions add controversy into the possibility of a subduction zone in the area (*Souriau,* 1984; *Maldonado et al.,* 1999). In addition, new bathymetric data and stress analyses support the idea of an un-clear and more complex plate boundary between Iberia and Africa (*Stich et al.,* 2005; *De Vicente,* 2008; *Zitellini,* 2009). *Pinheiro et al.* (1996) argued about the presence of a reverse fault along

the northern border. However, *Soriau* (1984), based on geoid anomalies, deduced from Seasat altymetric data, states that the ridge is far from isostatic equilibrium or compensated at great depth through a couple of border reverse faults (*Gall et al.,* 1997) at both sides of the ridge. Finally, a recent study carried out by *Jiménez-Munt et al.* (2010), explains the state of isostatic equilibrium observed, as a direct consequence of mantle serpentinization along with flexural isostasy and thrusting at lithospheric scale, questioning the role of broken plate or crustal scale thrusting.

3.4.2 Cainozoic intra-plate basins

The formation and uplift of mountain ranges in Iberia has been associated with the latest episode of convergence between the Eurasian and Iberian plates. Consequently, a series of related foreland basins were developed along the Pyrenean-Cantabrian Orogen. The advance of the orogenic front towards the south led to mountain uplift and deposition of thick sedimentary sequences causing the retreating of the marine realm towards the north and west. Therefore, the Duero and Ebro basins evolved as foreland basins. Moreover, the effective transmission of stresses from the Pyrenean border to the plate interior led to general uplift through the reactivation and inversion of pre-existent Variscan faults (Central Range) and Mesozoic extensional basins (Iberian Chain). As a result, a new group of intra-plate basins were developed. The most important of them is the Tagus Basin in Central Spain, which is considered as the foreland basin of the Spanish Central System (De Vicente et al., 2007), whereas the Almazan Basin has been linked to the uplift of the Demanda-Cameros Unit (*Casas-Sainz et al.,* 2000) [Fig.3.16].

In general the Iberian basins differ from one to another on geometry, size and origin. Several attempts for a basin classification have been made. Among others that stand out are *Friend and Dabrio* (1996) and *Civis* (2004). The first authors classified the Iberian basins based on tectono-stratigraphy, distinguishing between foreland basins, interior basins and rift-type basins. However, the latter author distinguishes between two different groups of basins concerning the tectonic setting. Those developed during Tertiary compression, mainly dispersed along the Betics and Pyrenees and another group related to Oligo-Neogene extension, basically linked to the opening and evolution of the Valencia Trough. Since both established classification converge into the same tectonic processes, this terminology has been widely extended. In addition, *Martín-González and Heredia* (2011) suggested the presence of a broad basin probably connecting with the Duero and Ebro Basin in the NW Iberian Peninsula. This basin became segmented into several small intra-montane basins during the uplift of the westernmost corner of Iberia.

The following sub-chapter outlines the most important tecto-stratigraphic relations to constrain the timing and evolution of the main intra-plate basins in Iberia which will contribute to the understanding of vertical motions across the plate interior. Distribution of depocentres as well as sedimentary thickness have been analysed in order to gain insight into the onset of intra-plate deformation and evolution of mountain fronts.

3.4.2.1 Ebro Basin

The Ebro Basin is situated along the southern border of the Pyrenean belt and covers more than 85.000 km^2 [Fig. 3.16]. It is surrounded to the North by the Pyrenees and the eastern termination of the Cantabrian Mountains, the Catalan Coastal Ranges to the east and the Iberian Chain to the south. The main Tertiary sedimentary depocentres are located to the East (>3.000 m), the central northern basin border (3.000 m) and the western area (east of the Bureba Corridor, 4.000 m) [Fig.3.17].

The Ebro basin is considered the relative foreland basin of the Pyrenees and its infilling

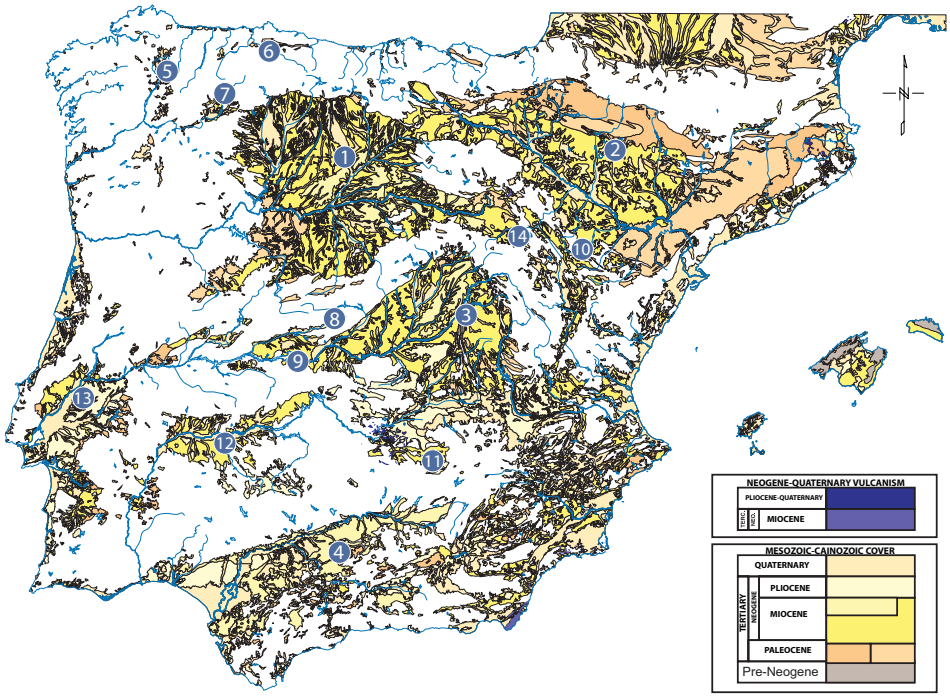

Figure 3.16 *Cainozoic basins of Iberia. Circles: 1) Duero; 2) Ebro; 3) Tagus (Madrid Basin); 4) Guadalquivir; 5) As Pontes; 6) Oviedo; 7) El Bierzo; 8) Amblés; 9) Coria; 10) Teruel and Jiloca; 11) Ciudad-Real; 12) Guadiana; 13) Lower Tagus; 14) Almazán. After De Vicente et al. (2011).*

history has been controlled by the Alpine uplift of the mountain belt during Eocene-early Miocene. Thermal modelling studies carried out by *Gaspar-Escribano et al.* (2003) show the control exerted by the flexure of the basement underlying the Ebro Basin on the basin infill history. These results suggest a major influence of lithospheric processes on the subsidence of the basin. Nevertheless, the emplacement of the Iberian Range to the south (Oligocene-Miocene) and the inversion of the Mesozoic rift basin of the Catalan Coastal Ranges (Oligocene-early Miocene) led to the actual configuration and establishment of the present-day drainage system.

Despite the triangular shape of the basin, the Tertiary filling history follows an asymmetric pattern to the east and a relative symmetric one to the west, controlled by the almost synchronous uplift of the western segment of the Pyrenean-Cantabrian Mountain belt and the Demanda-Cameros Unit (north and south respectively). The age of the sediments has been constrained by magnetostratigraphic studies and fossil sites (marine and mainly continental fauna). In addition, the climatic conditions that have governed the evolution of the basin since the Late Cretaceous have been established by stable isotopic signatures of lake sediments. Therefore, the Ebro basin represents a natural laboratory for studying the relations between tectonics, climate and sedimentation and has been extensively studied during the last decades (*Riba et al.,* 1983; *Anadón et al.,* 1985; *Oberhänsli and Allen,* 1987; *Vergés,* 1995; *Garcia-Castellanos et al.,* 2003).

During the Palaeocene-early Eocene, the sedimentary record is characterised by alluvial plains, fluvial sequences and lacustrine systems to the SE and deltaic systems towards the NE [Fig.3.18]. These sedimentary sequences rest unconformable on Palaeozoic and Mesozoic rocks and mark the tectonic activity recorded along the southern border of the Pyrenees (Boixols and Cotiella submarine thrust sheet emplacement). As a result of tectonic load, markedly increased

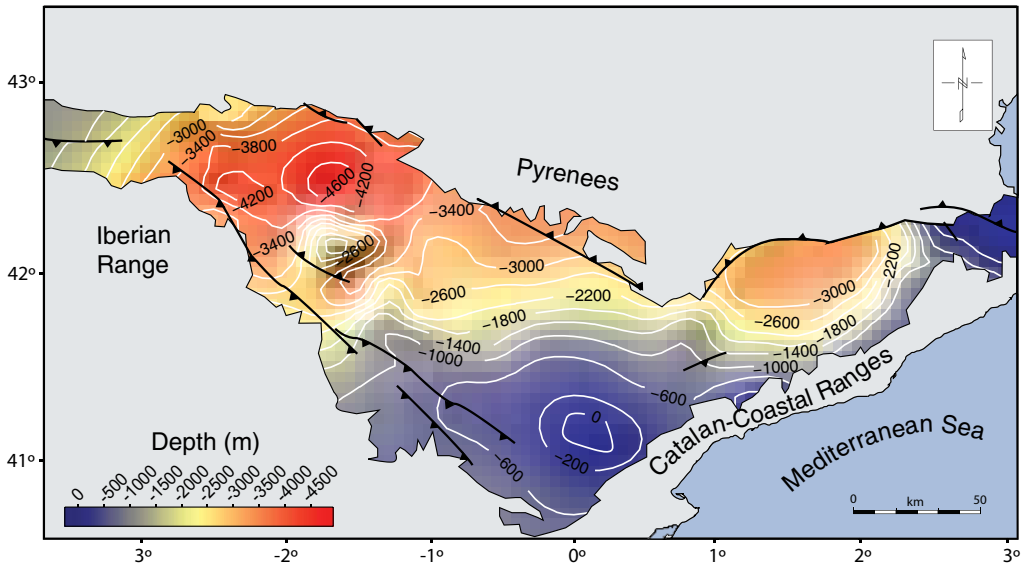

Figure 3.17 *Isobaths contour map of the Ebro basin illustrating the main sedimentary depocentres (bottom of the Tertiary >4.500 m in the W and about 2.500 m to the E). Data from ITGE (1990).*

on subsidence and accommodation space led to east-west oriented turbiditic troughs (*Gibbons and Moreno,* 2002). The final emplacement of thrust sheets (nappes and antiformal stack thrusts from Cotiella and Freser) led to the widely development of wide deltaic platforms to the north.

The Eocene Epoch shows a sedimentary break (i.e. hiatus) and local unconformities as a result of tectonic activity (inital stage of the Cadi nappe and isolation of small basins that led to restricted evaporitic environments, for instance the very well known Cardona salt deposits). Tectonic activity along the Cameros-Demanda thrust (*Casas-Sainz,* 1993), and the External Sierras and Gavernie thrust sheets led to expansion of alluvial fan deposits (*Puigdefábregas et al.,* 1992; *Vergés,* 1995) towards the western and central part of the basin (S and E provenance). In addition, a lacustrine system developed in the central part of the basin showing the retreating of the seas to the NE (carbonate platforms and siliciclastic coastal deposits together with fan-delta deposits).

Throughout the Oligocene, continental environments disconnected from the sea prevailed. Alluvial fans became gradded into central evaporitic and carbonate lacustrine systems. Several syntectonic unconformities as well as sedimentary breaks are recorded along the southern border of the Pyrenees. The growing of the Cadi nappe and the External Sierras to the east and west respectively led to isolation and tectonic transport of basins (Jaca piggy-back basins) establishing coalescent alluvial fans and increasing the subsidence. Westward flowing rivers developed lacustrine systems to the west (mainly evaporitic). A new tectonic pulse during the late Oligocene reactivated basement thrust activity to the northern and southern parts of the basin. As a result, the Ebro basin became finally disconnected from the sea and a period of closed intra-mountain drainage was established (*García-Castellanos et al.,* 2003). Consequently, alluvial fan systems developed along the basin margins increasing the sediment supply. Finally, in the late Oligocene the opening of the Valencia Trough (NW Mediterranean) led to subsequent extension along the Catalan Coastal Range which in turn may have aimed to enlarge the endorheic drainage system of the Ebro Basin until the end of the Miocene (*García-Castellanos et al.,* 2003).

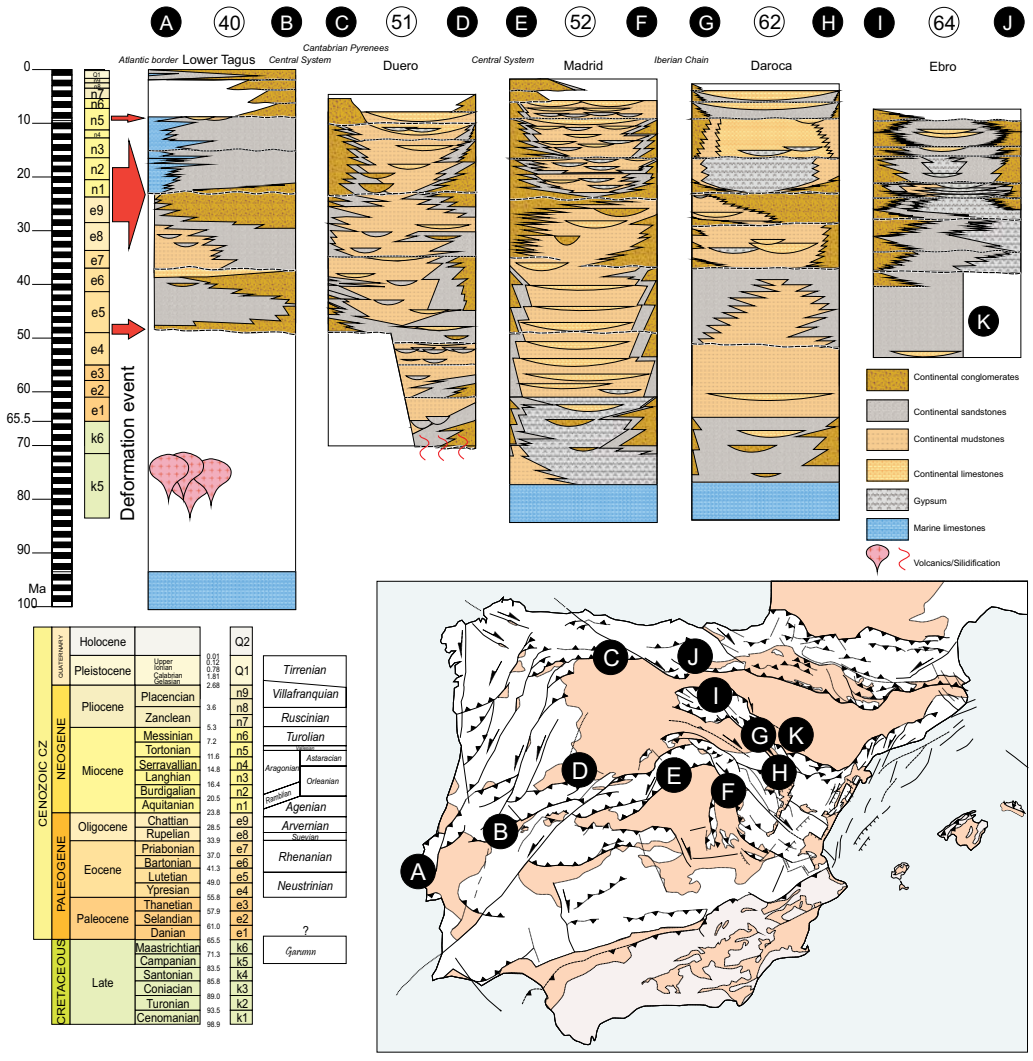

Figure 3.18 *Tectono-stratigraphic columns for the Tagus, Duero, and Ebro Basins. After De Vicente et al. (2011). See general map for location.*

The Neogene infilling history of the basin was marked by a series of syn-tectonic unconformities along the basin margins and the opening of the drainage system of the basin into the Mediterranean Sea. Alluvial fan deposits from the northern and southern margins interfered with saline and lacustrine systems. Wide alluvial plains and fluvial systems developed towards the west (during the Agenian-middle Aragonian). From middle Aragonian onwards, evaporitic lakes became isolated from marine influence and were replaced by carbonate lacustrine systems occupying the central and western part of the basin. These lacustrine systems appear to onlap on the stable eastern margin of the Iberian Range indicating the end of tectonic activity in the southern border of the basin. However, further west, along the Pyrenean and Iberian Range margins activity continued (*Gibbons and Moreno,* 2002).

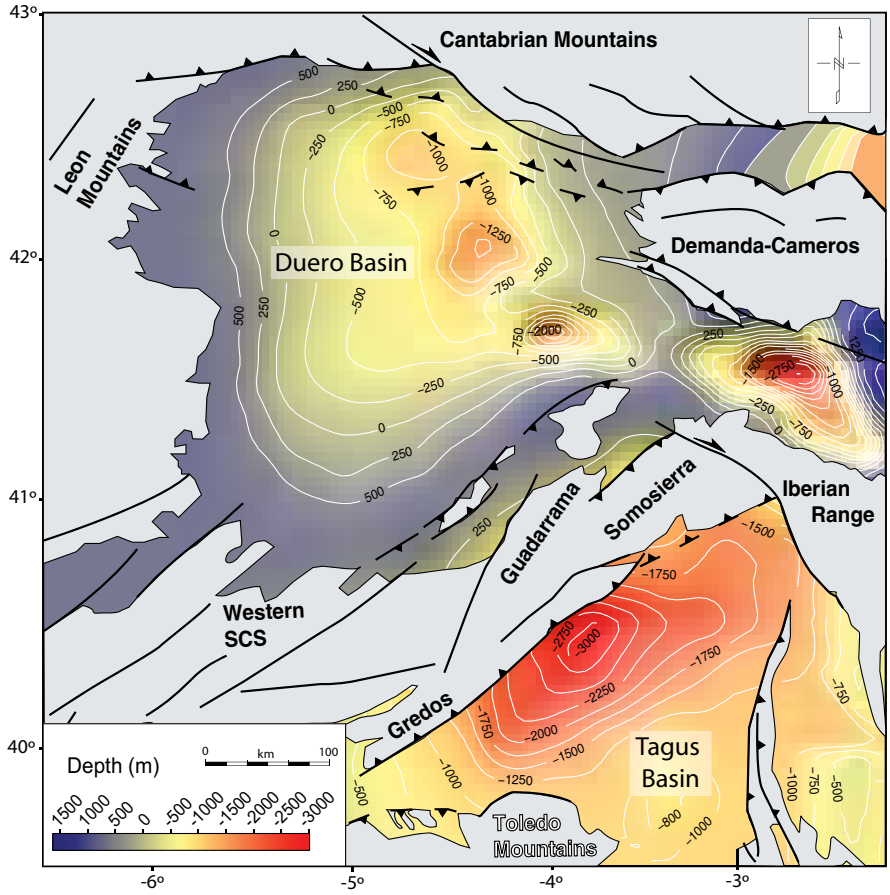

Figure 3.19 *Depth to the basement contour map of the Duero-Almazán and Tagus Basin illustrating the main sedimentary depocentres (>2.500 m bottom of the Tertiary in the Duero basin, 2.700 m in the Almazán sub-basin and >3.000 m in the Madrid basin). Data from Corrochano (1989); Rey-Moral et al. (2004) and De Vicente et al. (2007).*

3.4.2.2 Duero Basin

The Duero Basin is the largest Cainozoic basin in Spain comprising a total surface area of nearly 50.000 km^2 [Fig.3.16]. It is filled with more than 2.500 m of sediments in its deepest part [Fig.3.19]. In some places the sediments can be found over altitudes of 800 m. The Cainozoic fluvio-lacustrine sediments (Paleocene in age?) that fill the basin, rest conformable on upper Cretaceous sub-tidal sediments that occupy the northern and eastern areas [Fig.3.18]. Towards the west they lie unconformably on Variscan basement. In general these Cainozoic sediments represent advancing fan-delta systems (*Corrochano and Armenteros*, 1989). In the eastern sector several folds have been mapped, explaining the differences in altitude and the incision produced by rivers, where different erosion surfaces have been preserved from upper Oligocene epoch (*Benito-Calvo and Pérez-González,* 2007).

Four erosion surfaces have been described in the NE part of the Duero basin related to different episodes of uplift recorded along the Cantabrian Mountains and Sierra de la Demanda-Cameros borders. The exhumation of the Iberian Range has been associated to the first erosion

surface that affects upper Cretaceous sediments and is defined by these authors as being late Oligocene-early Miocene in age, which coincides with the data provided by *Alonso-Gavilán and Armenteros* (2004) based on evaporitic facies.

Fault activity in the western and northern borders of the basin have been recognised during the middle Eocene marked by the propagation of alluvial fans towards the inner parts of the basin (*De Vicente et al.,* 2007 and references therein).

Towards the south, at the border with the Spanish Central System, the first sediments are Eocene leading to the accumulation of thick alluvial fan sequences.

3.4.2.3 Tagus Basin

The Tagus Basin is an intracratonic basin with an overall surface extension of more than 20.000 km^2. It is bordered to the north by the Spanish Central System range and the Castilian Range and to the south by the Toledo Mountains [Fig.3.12]. However, the basin has been segmented into the Madrid and Loranca basins caused by the tectonic extrusion of the Altomira Range to the west (a Mesozoic fold-thrust belt considered a piggy-back thrust).

During the Tertiary filling history of the basin, sedimentation was controlled by the interaction between the Alpine tectonic uplift of the Spanish Central System and the transpressive regime experienced along the Iberian Chain. Pre-existing tectonic structures and the isostatic compensation of topography supported by the Spanish Central System may have influenced the accommodation of thick Tertiary sedimentary sequences (*Van Wees et al.,* 1996). As a result, more than 3.500 m of sediments were deposited along a narrow trough situated in the western part of the basin, based on seismic profiles and well logs (*Junco and Calvo,* 1983). However, the progressive increase in basement depth towards the E led to more than 3.000 m of sedimentary thickness along a NE-SW striking trough, extending from the Toledo Mountains to the east [Fig.3.19]. This is inferred from the different infilling geometry between middle Miocene units and the underlying sediments (*De Vicente et al.,* 2007).

The Tertiary sedimentary sequence ranges from late Cretaceous-Eocene to upper Miocene [Fig.3.18]. They represent the retreating of marine conditions to the north east (from shallow marine to continental). Paleogene units correspond to alluvial fan deposits presumably of pre-tectonic origin (lutites, gypsum and conglomerates with minor amount of limestones, during the Eocene). Overlying this unit, lacustrine sediments with sand and conglomerate levels to the top records a coarsening-upwards sequence (Oligocene), showing progressive unconformities at mountain fronts [Fig.3.20 a and c]. Well logs in the eastern part of the basin show an intra-Paleogene unconformity. Upper Paleogene sediments onlap truncated lower Paleogene sediments indicating tectonic activity (*De Vicente et al.,* 2007). The Miocene rests unconformable on the underlying Paleogene. Relative stable areas of the basin were covered by palaeosoils and were influenced by pedogenetic processes under relative arid conditions. Close to the mountain front (Spanish Central System) the reduction of soil development in alluvial fans indicates an increase on sediment supply. Unlike the Paleogene sediments, exposure of Neogene sediments indicates the presence of proximal facies portraying the propagation of the mountain front (Central Range) towards the relative foreland of the Madrid Basin. Consequently, this episode may represent an increase of tectonic activity in the area (*Alonso-Zarza et al.,* 1992). The Miocene sediments of the Tagus basin have been subdivided into three units (lower, intermediate and upper Miocene units).

The lower Miocene unit rests unconformably on the Paleogene sediments (erosive angular unconformity). It is compound of lacustrine evaporates and limestones prograding

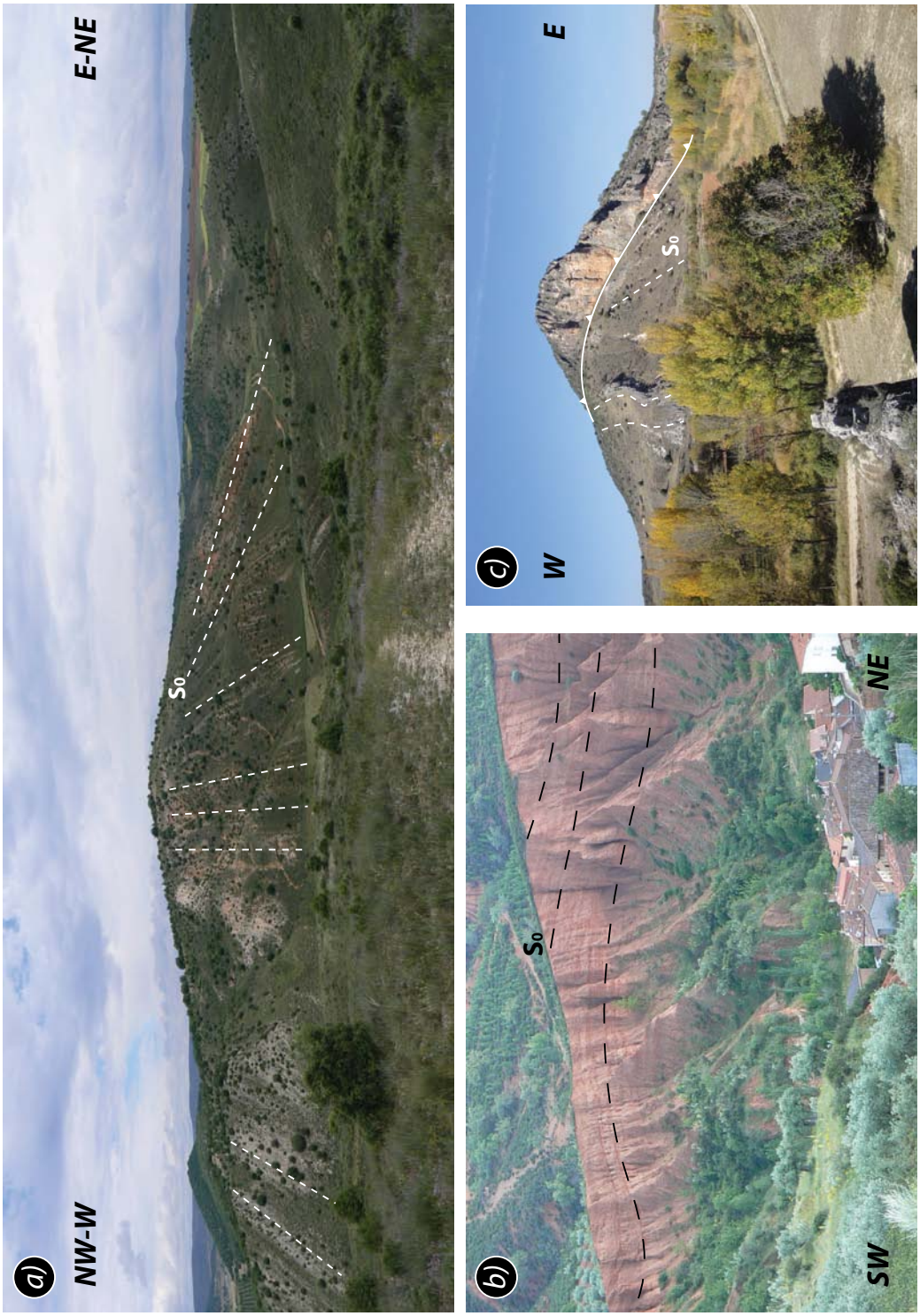
a
NW-W
E-NE
S0
c
W
E
S0
b
SW
NE
S0

towards the central part of the basin, while towards the basin borders they turn into siliciclastic deposits from fluvial (NE) and alluvial fan origin (W). The tectonic activity along the surrounding Spanish Central System and the Iberian Range would increase the amount of sediments carried by intermittent rivers and mass flows (*Capote et al.,* 1990). The presence of Iron rich well cemented conglomerates and calcretes would also indicate arid to semiarid conditions during the tectonic pulses that uplift the main mountain borders.

The Intermediate unit (Aragonian-Vallesian) shows a retrogradation of alluvial fan deposits (restricted to the basin margins N and NE, where tectonic uplift was taking place) leading to the expansion of lacustrine series (mostly carbonates) and development of soils. Finally, the upper Miocene unit consists of fluvio-lacustrine N-S oriented systems (mostly carbonates). This unit rests unconformable over the underlying unit and it is only observed towards the centre of the basin (well developed karstic surface). This unconformity has been linked to changes on the stress regime from compression to extension associated with lithosphere flexure of the Spanish Central System (*Andeweg et al.,* 1999). So far, the transition from closed systems of evaporitic affinity would lead progressively to the deposition of more carbonated equivalents (Paramo units), which indicates, on the one hand a change of the climatic conditions and on the other hand the decrease of evaporitic solutions provided by the Mesozoic rocks of the surrounding areas (*Calvo,* 1989).

Vertical movements triggered by collapse of evaporitic materials in the intermediate and lower Miocene units above the regional base level led to river incision and arrangement of the drainage system (*Alonso-Gavilán,* 2004).

The transition towards the establishment of exoreic basin behaviour of the Tagus River, led to basin infill and pediment surface formation. The latter was probably enhanced by the final stage of uplift and tilting towards the SW of the surrounding mountain fronts (*De Bruijne and Andriessen,* 2000). As a result, a series of iron rich quartzite-bearing conglomerates and lutites were finally deposited onlaping the borders with the mountain systems to the north and east (Raña deposits, Turolian-Pliocene based on correlation with the sediments of the same age on near basins, since these sediments don´t contain fossils). In some areas in central Spain, these conglomerates appear folded indicating tectonic origin [Fig.3.20b] either by final compressive pulses related to the Betics or flexural load of the Spanish Central System, (*Andeweg et al.,* 1999).

3.4.2.4 Minor intra-plate basins

The structural complexity and architecture of the mountain belts in Iberia have conditioned the position and evolution of intra-mountain basins. Such small basins spread all over the plate interior. The tectonic evolution of these basins is related to strike-slip fault corridors striking NE-SW to NW-SE like the As Pontes, Pedroso, Moeche basins in Galicia; El Bierzo, Oviedo in western Iberia and Amblés, Coria in Central Spain related to E-W oriented thrusting, as well as normal faults, generally N-S oriented like Moiñonovo basin in Galicia or Jiloca and Teruel grabens in Eastern Spain. Recently, *De Vicente et al.* (2011) have examined the type of basins regarding their sizes and tectonic history in order to deduce a common overall evolution linked to lithospheric folding. As a result, a series of basement uplifts would have isolated small intra-mountain basins from the main foreland basins (Duero-Ebro-Tagus Basins). These episodes of isolation would be defined by a series of sedimentary brakes that were extensively common

◀ **Figure 3.20** *Field example of sedimentary sequences along the southern border of the Spanish Central System. (a) Progressive unconformity at the southern hinge of the Baides anticline. (b) Folded Plio-Quaternary conglomerates (Raña deposits); and (c) Progressive unconformity at the contact with the Huérmeces thrust.*

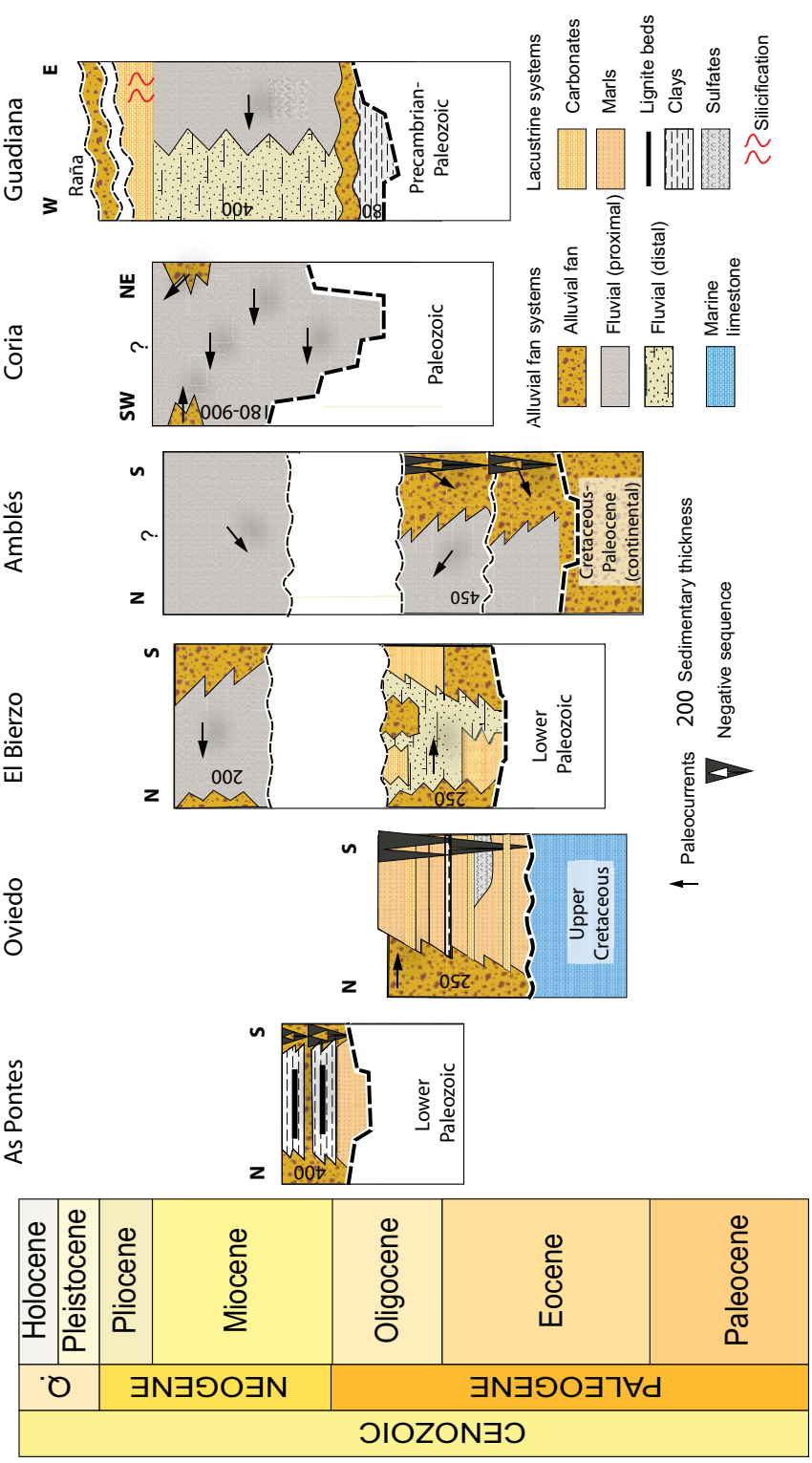

Figure 3.21 *Tectono-stratigraphic columns for minor intra-plate basins distributed along western Iberia. Modified from Alonso-Gavilán et al. (2004). See location in Figure 3.16.*

over the 30 to 15 My time span with a maximum about the Oligocene-Miocene.

The most important of those Intra-mountain basins in northern Spain are the Oviedo, El Bierzo and As Pontes basins and show in general, a clear pattern of evolution from older sedimentary sequences to much younger ones, respectively. This timing relationship implies different stages of uplift that shift towards the west during the Pyrenean Orogeny (*De Vicente et al.,* 2011; *Martín-González and Heredia,* 2011). The first continental sediments were deposited during the Eocene in the Oviedo Basin that became isolated from the sea prior to the formation of the Duero Basin (*Truyols et al.,* 1991). Major tectonic activity has been recorded during the Oligocene towards the west coeval with the latest episodes of sedimentation in the Oviedo Basin [Fig.3.21]. Meanwhile, sedimentation continued till the early Miocene in the As Pontes and El Bierzo basin. Two episodes of uplift are recorded in El Bierzo Basin, characterised by differences in source areas (Paleocurrents indicate western and eastern provenance of continental deposits during the Oligocene and early Miocene, respectively, *Martín-González,* 2009; *Martín-González and Heredia,* 2011).

In central Spain, the basins of the Amblés, Coria and Guadiana record simultaneously episodes of continental sedimentation from the early Palaeocene and Eocene. It was at the beginning of the Cainozoic when the uplift of the Central System led to isolation of these intramountain basins. The main depocentres are found close to the central part of the basins reaching sedimentary thicknesses between 180 and 900 m. Basins situated in the north show several unconformities affecting the Eocene sediments (Amblés Basin), whereas they become younger towards the south (Coria and Guadiana Basins, respectively) [Fig.3.21].

3.5 The Iberian lithosphere

In recent years, studies addressing the Alpine tectonics in Iberia have demonstrated the contribution of intra-plate deformation to creation and distribution of mountain ranges. In order to better understand the recent and ongoing lithospheric processes in Iberia, integration of seismic and gravity data, analysis of topography and stresses is vital. In the next section I provide a wide list of geophysical data from different sources available in Spain (*Banda,* 1983; *Surinach and Vegas,* 1988; *Choukroune and Team,* 1989; *Roure,* 1989; *Choukroune et al.,* 1990; *Pedreira et al.,* 2003; *Simancas et al.,* 2003; *Ruiz et al.,* 2006b; *Palomeras et al.,* 2009; *Díaz and Gallart,* 2009 and *Ayarza et al.,* 2010).

3.5.1 Crustal structure and topography

The most striking feature observed from satellite images and topographic maps is the regular distribution of E-W to NE-SW trending mountain ranges and Tertiary basins in Iberia and their relative high mean altitude of more than 650 m, which is one of the highest topographic averages in Europe [Fig.3.22a].

The comparison between the spectrum obtained from the Bouguer gravity anomalies and the signal provided by the undulations produced by the topography show different wavelengths; the smaller ones around 50-80 km and the largest ones (250-500 km) related to crustal and mantle deformation, respectively (*Cloetingh et al.,* 2002 and *Muñoz-Martín et al.,* 2010). Recently, *Tesauro et al.* (2007, 2008) provided an integrated study of the lithospheric properties of the European lithosphere based on seismic tomography, seismic reflection and refraction and receiver functions data. Their results show large crustal thickness variations in Iberia with maximum values in the Pyrenees-Cantabrian Mountains, Central Iberia and the Betic Cordil-

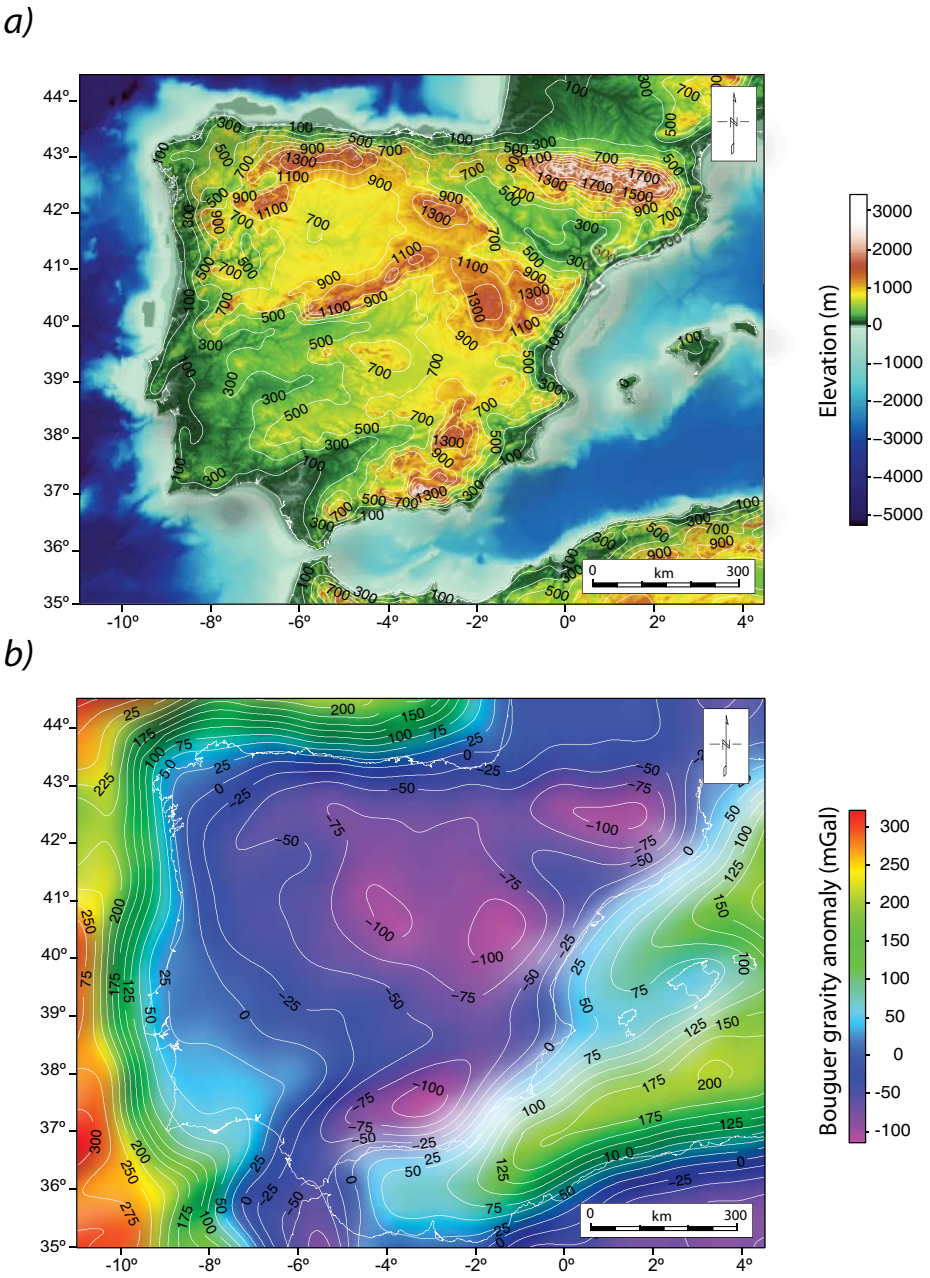

Figure 3.22 *Smoothed iso-contour maps of topography in meters (a). Bouguer gravity anomalies. Data obtained from Mézcua et al. (1996).*

lera (50-35-40 km respectively) [Fig. 3.23a], which are also portrayed by distinct negative gravity anomalies [Fig. 3.22b]. The residual isostatic gravity anomalies obtained by *Álvarez-García* (2002) considering the Airy-Heiskanen model for a 30 km crustal root, reveal broad differences on isostatic equilibrium across Iberia caused by a density deficit under elevated areas (crustal roots) [Fig.3.24]. The southern border of the Duero Basin, Galicia margin, Spanish Central Sys-

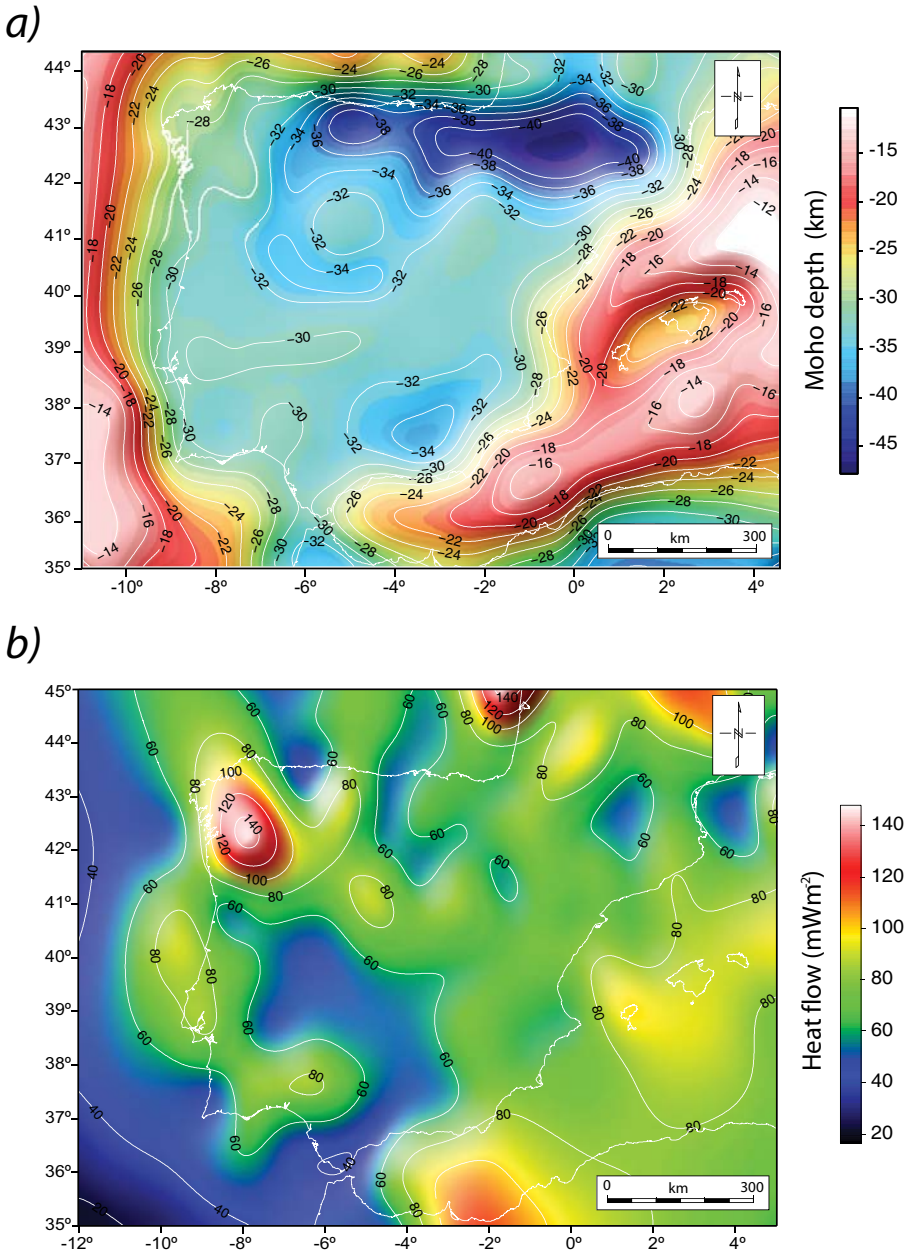

Figure 3.23 *(a) Moho depth map (see explanation in the text). Data from Tesauro et al. (2008).(b) Smoothed contour maps of heat flow. Data from Fernández et al. (1998) and Hurter and Schellschmidt (2003).*

tem and the Iberian Range show slightly positive values (between 20 and 40 mGal) indicating unexpectedly a lack of isostatic equilibrium. A possible explanation for such isostatic anomalies stands on the presence of elevated basement, probably related to the flexure of the lithosphere or a deeper Moho than expected (*Andeweg,* 2002; *Gaspar-Escribano et al.,* 2004). However, the area of the Eastern Cantabrian Mountains-Pyrenees-Ebro basin seem to be close to a state of iso-

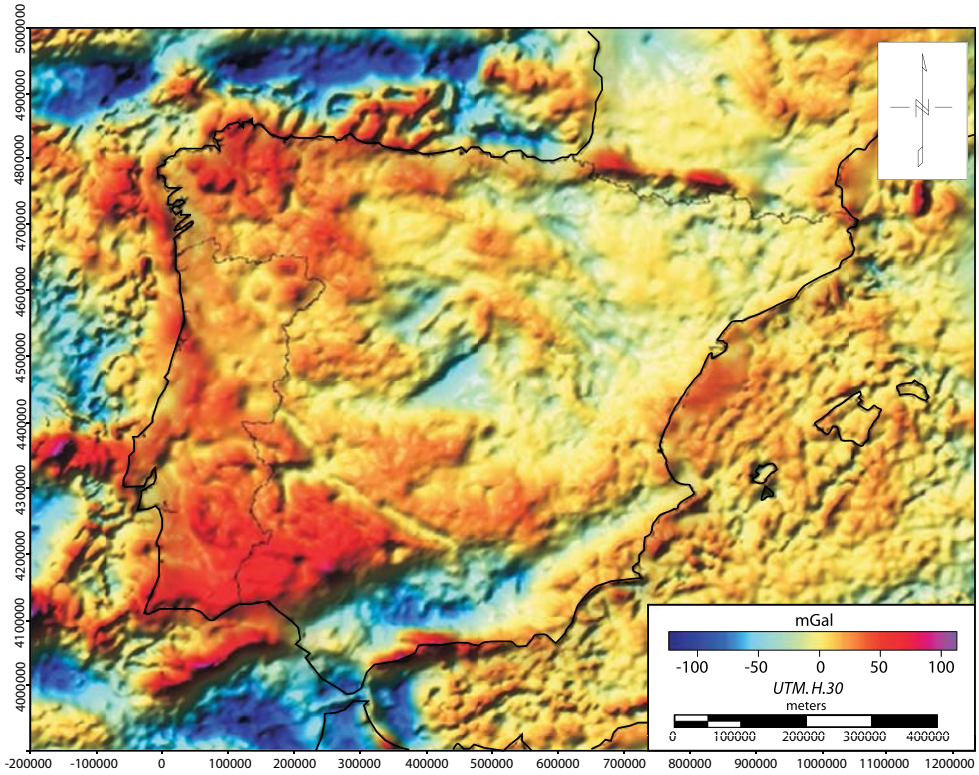

Figure 3.24 *Isostatic regional gravity anomaly displaying the areas close to isostatic equilibrium in Iberia. Modified from Álvarez-García (2002).*

static equilibrium (~0 mGal), whereas the maximum observed in the central part of the Pyrenees (local isostatic anomaly >50 mGal) has been related to the presence of a high density body situated in the crust. Reflection and refraction profiles along the Cantabrian Mountains (*Gallastegui,* 2000) and Sierra Morena (*Simancas et al.,* 2003) recognise the presence of a reflective middle crust which appears not to be continuous for the whole Peninsula, but areally restricted. The above mentioned regions contrast with the less negative Bouguer anomalies of the main basins, which are correlated with a relative shallow position of the Moho (ca. 29-30 km). In addition, the north western most corner of Galicia, the crust is thinner as a result of the opening of the Atlantic Ocean and passive margin formation.

3.5.2 Thermal structure and rheology

The thermal structure of the Iberian lithosphere has been linked to the combined effect of the latest tectonic events and inherited crustal-mantle heterogeneities. As a result, the thermal state of the lithosphere has been modified leading to large differences between thermal conditions close to the surface and in great depth. These differences are the final expression of the Mesozoic rifting and later Alpine compression during the Tertiary times.

Recent surface heat flow data compiled by *Fernández et al.* (1998), show high values along the eastern part of Iberia, close to 100 $mWm^{-2,}$ and in the south western area of the Portuguese Algarve with an average of 60-80 mWm^{-2}. Moreover, a maximum has been identified in northwestern Spain reaching values over 120 mWm^{-2}, although it has been considered

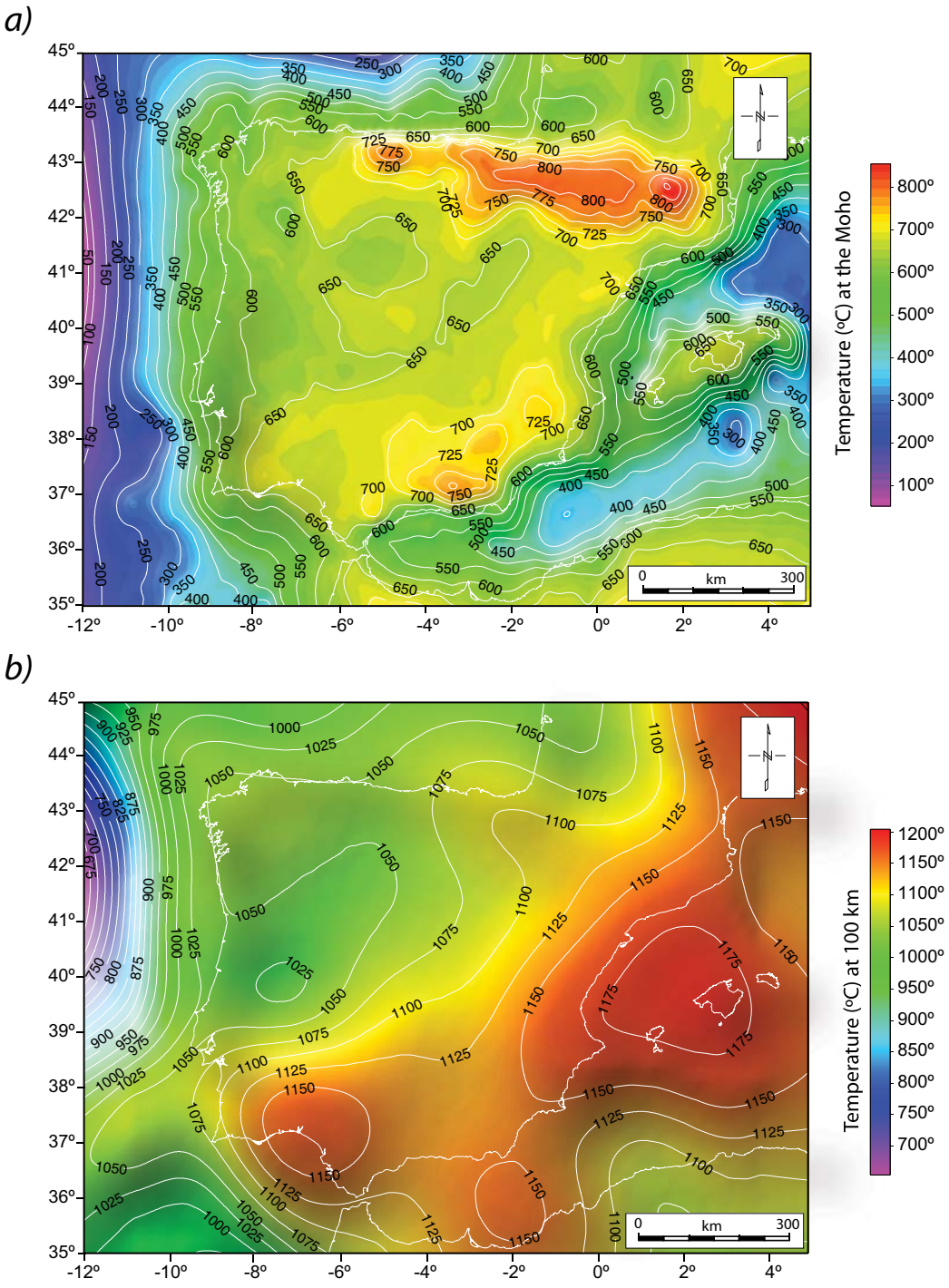

Figure 3.25 *(a) Iso-contour map of Moho temperature (b) and temperatures at 100 km depth, showing the main lithosphere thermal anomalies. Data from Tesauro et al. (2010).*

Table 3.1

Layer	Analogue Material	Density ρ (kg/m^3)	Coefficient of friction μ	Viscosity η (Pa s)	Power n
Normal lithosphere					
Upper crust	Feldspar sand	1300	0.7 35 Pa (Cohesion)		
Lower crust	Silicon mix 1 (PDMS)	1486		$4.80 \cdot 10^4$	1.8
Mantle lithosphere	Silicon mix 2 (PDMS)	1606		$1.23 \cdot 10^5$	1.7
Inverted lithosphere					
Upper crust	Feldspar sand	1300	0.7 35 Pa (Cohesion)		
Lower crust	Silicon mix 1 (PDMS)	1400		$1.87 \cdot 10^5$	1.8
Mantle lithosphere	Silicon mix 2	1510		$2.08 \cdot 10^4$	1.9
Asthenosphere	Sodium polytungstate	1610		1.2	

Table 3.1 *Material properties*

remarkably local by the authors (few km^2). In addition, the high values observed in the Alboran Sea have been related to a thermal anomaly that causes long weavelengths and amplitudes of the heat flow signal (>100 mWm^{-2}, *Soto et al.,* 2008) [Fig.3.23b]. These temperature differences would, therefore, explain focal depth variations recorded in different areas of Spain (northwest, central and eastern Spain [see also Fig.3.1]). Additionally, *Tejero and Ruíz* (2002), calculated values about 60-70 mWm^{-2} for the main plate interior, showing that the mantle heat flow increases with diminishing surface heat flow. Based on these results, the authors calculated strength profiles from the Iberian lithosphere that predict a brittle mantle below the Duero and Tagus Basins and a relatively weak mantle under the Spanish Central System [Fig.3.26], which might be related to the thickening of the lower crust as suggested from seismic refraction profiles by *Suriñach and Vegas* (1988).

In addition, Moho temperatures calculated by *Tesauro et al.* (2007), show maximum values under the Pyrenees and the Betics, which are probably related to the deep root of each orogen. Predicted lateral temperature variations at 100 km depth along a NE-SW belt in south-eastern Iberia could be the result of different processes occurring since the early Miocene, such as the opening of the Valencia Through, extension in the Catalan-Coastal Ranges, and over-thrusting of the Alboran block [see Fig.3.25a and b].

All the above mentioned data were used by *Van Wees et al.* (1996) and *Ruíz et al.* (2006a) to estimate the elastic properties of the Iberian lithosphere. The seismogenic thickness

Table 3.2

Layer	Density ρ(kg/m^3)	Viscosity η (Pa · s)	Layer thickness h (m)	Velocity v (m · s^{-1}) Exp-I-III-V-VII	Velocity Exp-II and -IV	R_m
Normal lithosphere						
Upper crust *nature*	2670	-	$1.5 \cdot 10^4$	$7 \cdot 10^{-3}$	$14 \cdot 10^{-3}$	-
Upper crust *model*	1300	-	$1 \cdot 10^{-2}$	$5 \cdot 10^{-3}$	$1 \cdot 10^{-2}$	-
Lower crust *nature*	2900	$1.0 \cdot 10^{21}$	$1.5 \cdot 10^4$	$7 \cdot 10^{-3}$	$14 \cdot 10^{-3}$	28
Lower crust *model*	1486	$4.08 \cdot 10^4$	$1 \cdot 10^{-2}$	$5 \cdot 10^{-3}$	$1 \cdot 10^{-2}$	21
Mantle lithosphere *nature*	3400	$4 \cdot 10^{21}$	$3.0 \cdot 10^4$	$7 \cdot 10^{-3}$	$14 \cdot 10^{-3}$	33
Mantle lithosphere *model*	1606	$1.87 \cdot 10^5$	$2 \cdot 10^{-2}$	$5 \cdot 10^{-3}$	$1 \cdot 10^{-2}$	36
Inverted lithosphere				Exp-III, VI and VIII		
Upper crust *nature*	2670	-	$1.5 \cdot 10^4$	$7 \cdot 10^{-3}$		-
Upper crust *model*	1300	-	$1 \cdot 10^{-2}$	$5 \cdot 10^{-3}$		-
Lower crust *nature*	2950	$1.0 \cdot 10^{22}$	$1.5 \cdot 10^4$	$7 \cdot 10^{-3}$		2.93
Lower crust *model*	1400	$1.87 \cdot 10^5$	$1 \cdot 10^{-2}$	$5 \cdot 10^{-3}$		5.28
Mantle lithosphere *nature*	3400	$1 \cdot 10^{21}$	$3.0 \cdot 10^4$	$7 \cdot 10^{-3}$		139.21
Mantle lithosphere *model*	1510	$2.3 \cdot 10^4$	$2 \cdot 10^{-2}$	$5 \cdot 10^{-3}$		183.86

Table 3.2 *Scaling parameters. Rm, refers to Ramberg Number for ductile layers.*

(Ts) is close to 10-17 km [compare with figure 3.1b] while the value obtained for the effective elastic thickness (Te) reaches 24 km which is compatible with the seismic activity in the intra-plate domain restricted to the upper crust (*Martín-Velázquez et al.,* 2009). The lower crust and upper mantle of Iberia are essentially devoid of seismicity. Based on these data, the Iberian lithosphere is probably composed of a brittle upper crust, a ductile weak lower crust and a relatively strong upper mantle.

3.6 Analogue modelling set-up

3.6.1 Geometry, rheology and scaling

The experiments were performed in a rectangular Plexiglas box with transparent vertical sidewalls. One of them was mobile and acted as an indenter. The moving wall was connected

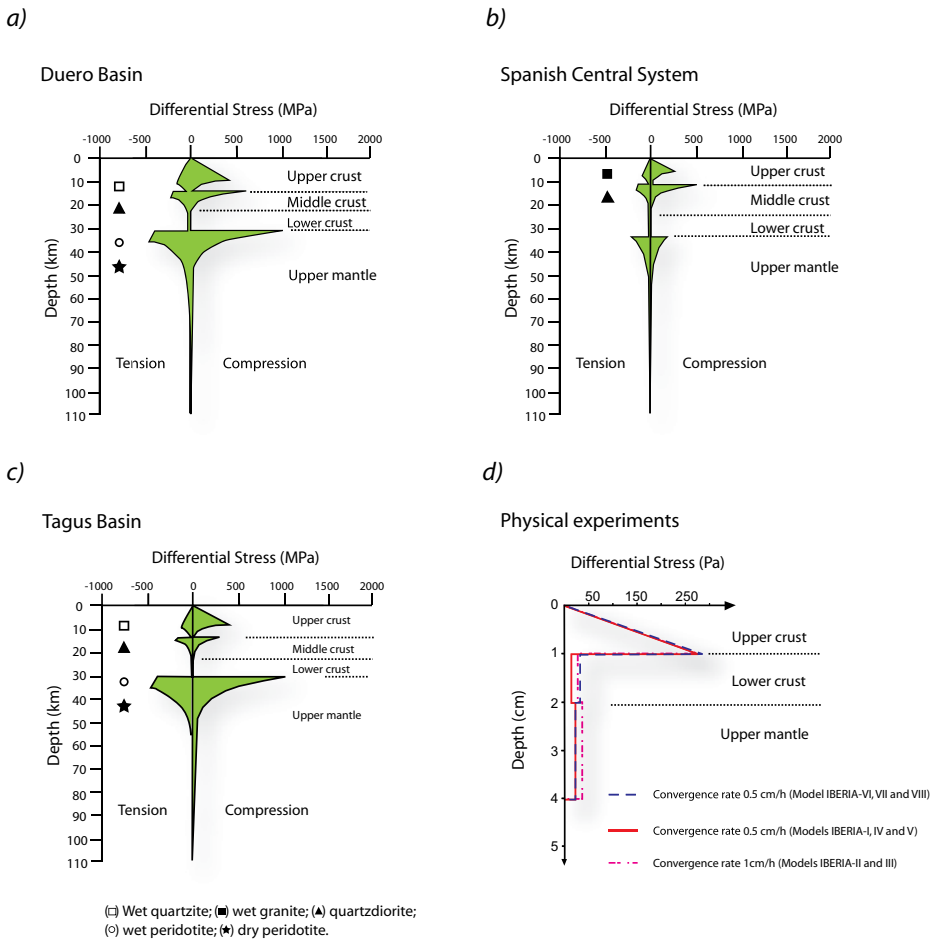

Figure 3.26 *Lithosphere strength profiles from the Duero Basin (a); Spanish Central System (b) and Tagus Basin (c) at 60, 70 and 65 mWm^{-2} respectively calculated by Tejero and Ruíz (2002). (d) Strength profiles before deformation from experiment with inverted lithosphere (IBERIA-VI); normal lithosphere at a convergence rate of 0.5 cm/h (IBERIA-I, IV and V) and normal lithosphere at 1cm/h (IBERIA-II and III).*

to a low frequency electric engine through a screw-jack. Velocities adopted for this study are 0.5 cm/h and 1cm/h.

The 3-layer models [Fig.3.26] consist of ductile, slightly non-Newtonian silicone (PDMS or Rodorshil Gomme mixtures) layers representing the upper mantle and lower crust, respectively. A K-Feldspar sand layer represents the brittle upper crust. These layers, which are characterised by the properties listed in Table 3.1 rest on an asthenospheric material made of a mixture of polytungstene and glycerol to ensure isostatic equilibrium. The experiments have been performed under normal gravity conditions. A laser-scan has been used to obtain the digital elevation model combined with top-view pictures taken with a digital camera at constant time rate during evolution of the model.

The main variables investigated in this study comprise of: (a) convergence rate changes and

hence the degree of crust-mantle decoupling, (b) the strength of the lower crust and upper mantle, and (c) the geometry and length of the experiments to ensure that the resulting wavelengths of deformation were not biased by the model dimensions [see Tables 3.1 and 3.2, Fig. 3.27].

Following *Weijermars and Schmeling* (1986), scaling of the experiments was based on geometric, kinematic and dynamic similarity between model and natural prototype, Iberia. Scaling parameters are displayed in table 1 and are constrained by geophysical and geological data from Iberia (see section 3). The total surface of the models represent the main plate interior as shown in Figure 3.28. Dynamic similarity obtained through dimensional analysis is based on the Ramberg Number (R_m) and Smoluchowsky Number (S_m) for the viscous and brittle behaviour, respectively (*Ramberg,* 1967; *Weijermars and Schmeling,* 1986):

$$Rm = \frac{\rho g l^2}{\eta V} \qquad [3.1]$$

$$Sm = \rho_b g h b c + \mu \rho_b g h_b \qquad [3.2]$$

where ρ and ρ_b are the density of the ductile and brittle materials respectively, g is the gravity acceleration, l and h_b the thicknesses of the ductile and brittle layers, c the cohesion, η the viscosity, V the velocity and μ the friction coefficient.

For the brittle part of the lithosphere under compression, differential stresses were calculated following the equation (*Weijermars and Schmeling,* 1986):

$$\tau = \frac{2[c_0 \mu \rho z(1-\lambda)]}{(\mu^2+1)^{1/2} - \mu} \qquad [3.3]$$

where τ is the differential stress, c_0, cohesion, μ, the coefficient of friction, ρ the density, z the layer thickness and λ, the pore pressure (assumed to be non significant in the models).

For the ductile layers, the differential stress is resolved by the equation (*Brun,* 1999):

$$\tau = \eta v \qquad [3.4]$$

where τ is the differential stress; η refers to viscosity and ν to convergence rate respectively.

3.6.2 Simplifications and general assumptions

In this study we assume an initially homogeneous lithosphere, which is devoid of lateral changes in composition, temperature and/or rheology or inherited structures. It has been shown by *Sokoutis et al.* (2005) and *Willingshofer and Sokoutis* (2009) that weak zones in the lithosphere are important for governing wavelength and amplitude of deformation, but do not necessarily influence its style or dominant deformation mechanism. Moreover, since the influence of pre-existent late-Variscan faults seems to have played an important role during latter alpine deformation they will be dealt in detail in Chapters 5 and 6.

Erosion/sedimentation is controlled by tectonic and climatic processes. The models presented here assume the onset of mountain building during the Africa-Iberia convergence when morpho-climatic processes would develop slowly across the entire Peninsula without significant changes in basin configuration. In experiments IBERIA-IV, V and VI, a rigid indenter was implemented, which represents the opening of the King´s Trough in the north western corner of the Atlantic margin of Iberia [see Fig.3.5 for location]. The effect of this feature led to the establishment of constrictional deformation conditions within the Iberian Plate during the

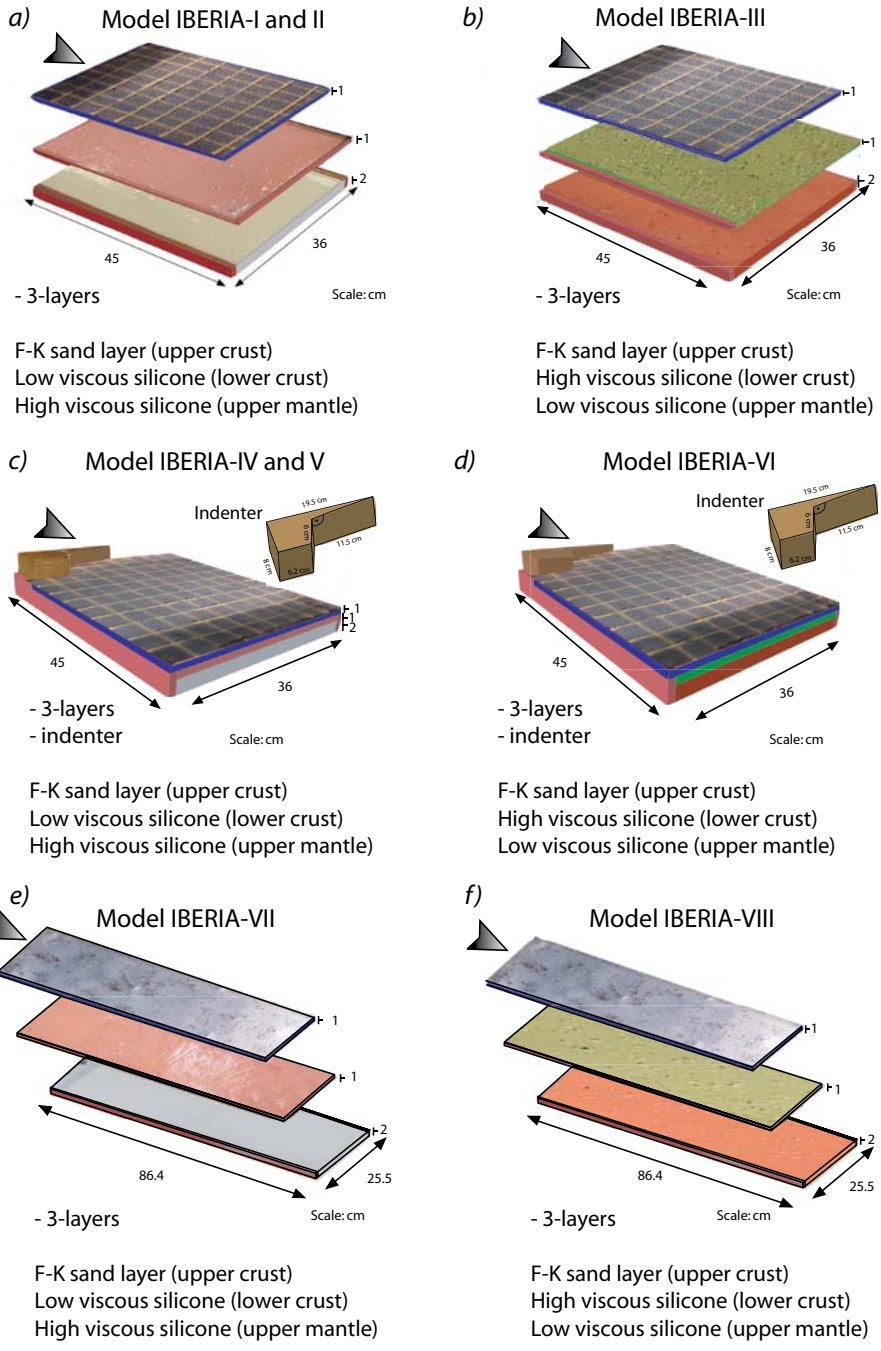

Figure 3.27 *Model Set-up for experiments for normal lithosphere (a) IBERIA-I and II, (convergence rate equivalent to 0.5 cm/h and 1 cm/h, respectively). (b) Inverted lithosphere: strong lower crust and weak lithosphere mantle, IBERIA-III. See Table 3.1 for material properties and natural equivalent. Grid spacing is 4 cm. (c) Normal lithosphere with an indenter, IBERIA-IV and V (convergence rate 0.5 cm/h and 1 cm/h, respectively). (d) Inverted lithosphere and indenter, model IBERIA-VI (convergence rate 0.5 cm/h). (e) Large-scale models: normal lithosphere (model IBERIA-VII, 0.5 cm/h) and (f) inverted lithosphere (model IBERIA-VIII).*

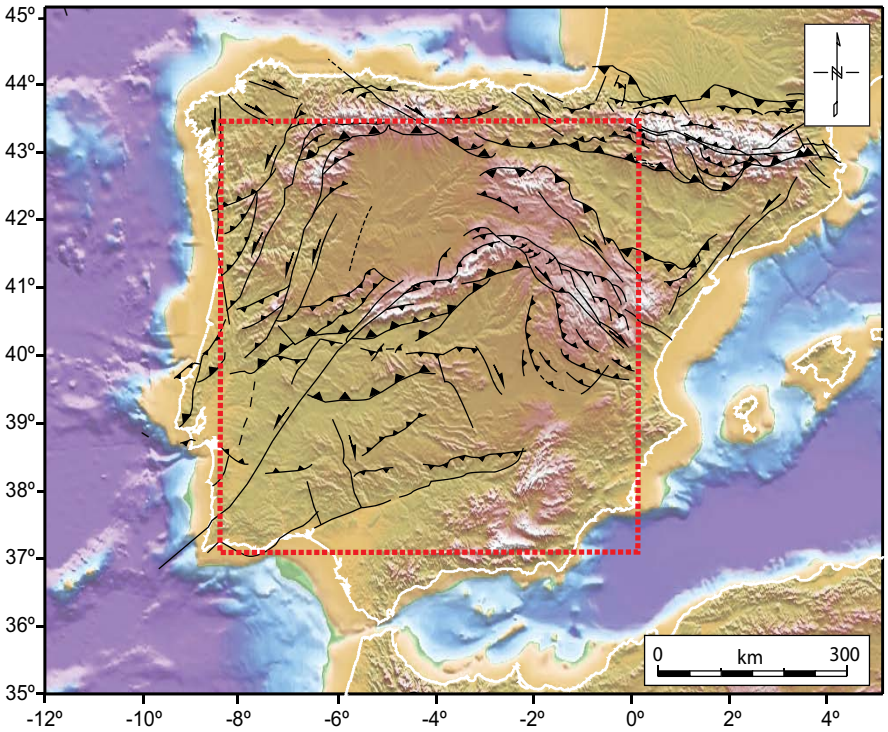

Figure 3.28 *Tectonic map of Iberia and location of the study area shown in the final interpretation of the analogue models (red-dashed inset). Main tectonic structures after De Vicente and Vegas (2009a)*

early Tertiary (opening in opposite directions to the main N pushing of Iberia), as well as the transfer of the stresses along a series of fault corridors in the western part of the microplate. The opening of the King´s Trough forced in part the locking of Iberia, facilitating the subsequent stress transmission (*De Vicente and Vegas,* 2009a).

The analogue experiments were shortened by 20% of their initial size at a constant rate, representing the bulk shortening affecting central Iberia during the Pyrenean stage of the Alpine Orogeny (*De Vicente et al.,* 1996). The collision rate in Iberia, however, fluctuated through time from periods of high to low convergence from late Cretaceous to middle Miocene.

3.7 Modelling Results

3.7.1 Crust-mantle coupling

Variations of convergence rates are used to investigate the influence of crust-mantle coupling on the deformation of the model lithosphere.

3.7.1.1 Model IBERIA-I: weak crust-mantle coupling (convergence rate 0.5 cm/h)

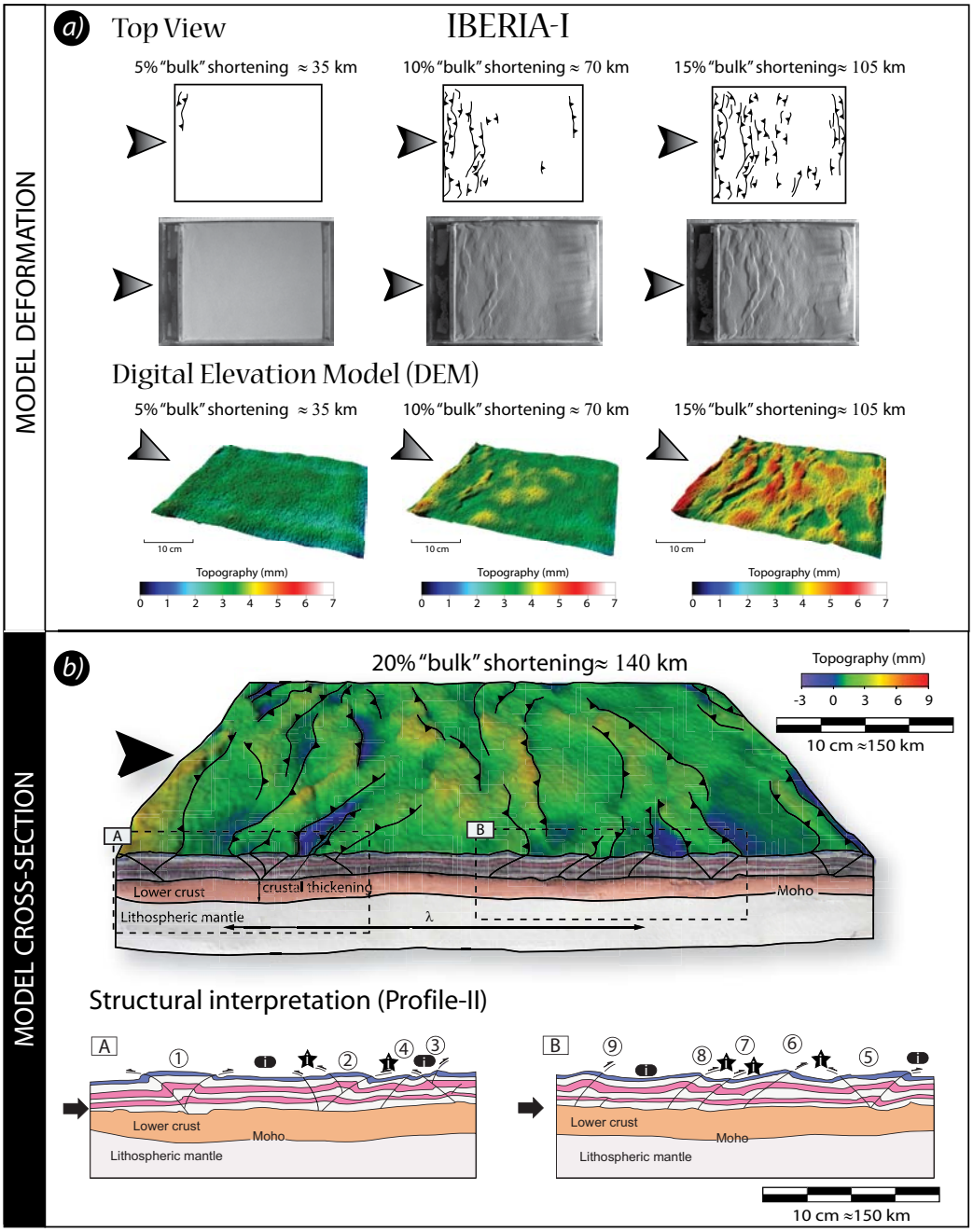

Figure 3.29 *(a) Structural interpretation of top-view images and digital elevation model (DEM) from model IBERIA-I. See text for further explanation. Arrows show the direction of convergence. (b) 3-D model Iberia-I showing profile-I. The ductile lithosphere is slightly folded (lower crust and upper mantle) whereas the upper crust is thrusted by pop-ups and single thrusts. Arrows show the direction of shortening. Profiles A and B: labelled circles indicate thrust evolution during shortening; ellipsoids: Inter-mountain basin and stars: intra-mountain basins.*

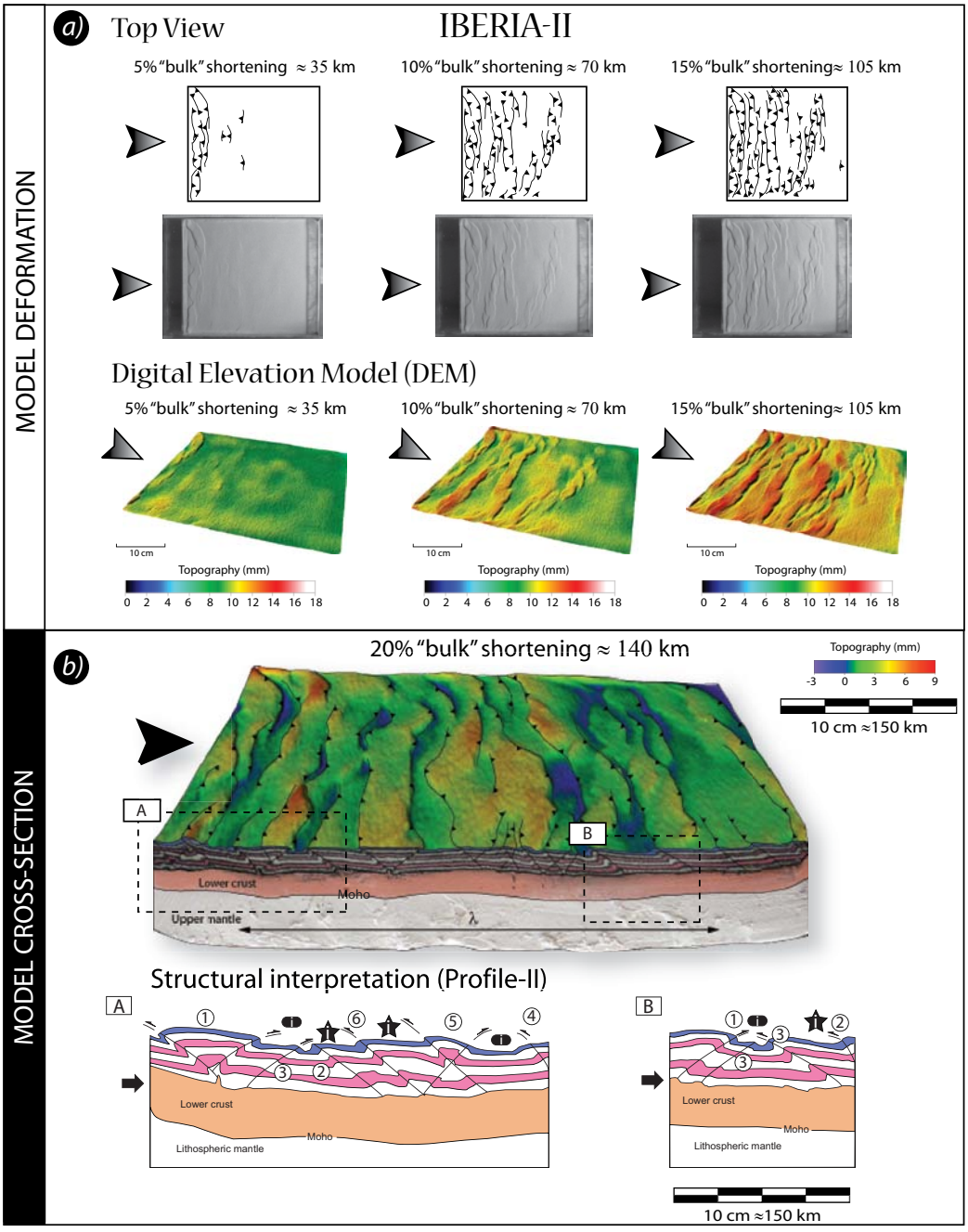

Figure 3.30 *(a) Structural interpretation of top-view images (top) and digital elevation model (DEM) (bottom) from model IBERIA-II. See text for further explanation. Arrows show the direction of convergence. (b) Cross-section along profile-I (model IBERIA-II) showing more complex structures than previous model developed in the brittle part of the crust. Inset box A and B from profile. Arrows show the direction of shortening. Numbers refer to temporal evolution of thrusting. Ellipsoids represents intra-mountain basin and stars inter-mountain basins without taking into account temporal evolution. Profiles A and B: labelled circles indicate thrust evolution during shortening; ellipsoids: Inter-mountain basins and stars: intra-mountain basins.*

Experiment IBERIA-I serves as a reference for the other models. After 5% of bulk shortening a pop-up structure developed close to the moving wall. With increasing shortening, these thrusts propagate laterally while newly formed thrusts do not develop immediately in front of the older ones as often observed in fold and thrust belts (imbricated thrusts), but at a distance, which is larger than the width of the first pop-ups [Fig. 3.29a]. At 15% of bulk shortening (BS) the deformation reached the opposite wall.

Small curved fore-thrusts and back-thrusts developed and the distance in between clusters of thrusts is reduced (cross section, [Fig.3.29b]. At the end of the experiment, deformation was distributed over the entire length of the model as new small pop-ups developed in between the former structures and small basins formed in between relatively wide pop-ups and thrusts, suggesting that shortening was taken up by many structures with limited amount of displacement.

Digital elevation models [Fig.3.29a, lower panel] show that the relief is structurally controlled and hence evolves through time as the thrusts and pop-ups propagate. By the end of the experiment the finite topography reflects general uplift with narrow intervening depressions.

In cross-section the geometry of the brittle crust is controlled by thrusts, pop-ups and pop-downs [e.g. between thrusts 3 and 4 in sub-section A of Figure 3.29b]. Slight thickness variations in the ductile crust correlate with the location of the pop-ups and thrusts in the upper crust such that thickening occurred at the locations of the upper crust structures, which also coincide with the locations of syn-forms of gentle, long wavelength folds of the upper mantle layer.

3.7.1.2 Model IBERIA-II: strong crust-mantle coupling (convergence rate 1cm/h)

Deformation in experiment IBERIA-II is concentrated close to the moving wall during the first 10% BS. Different to model IBERIA-I, thrusts and pop-ups occupied most of the model space already after 10% BS. Moreover, thrusts were arranged in an en-echelon fashion [Fig. 3.30a]. Small intervening basins dominantly have elongate shapes. In the later stage the deformation appears more distributed and there is no relative advance towards the static wall. New small thrusts appear in areas that were not deformed before. After 20% BS numerous thrusts cut most of the model surface separating depressions in between them [Fig.3.30].

Unlike the previous model, general uplift occurs since the beginning of shortening; at 15% BS highest elevations are reached. However elevations seem to be areally distributed at later stages of deformation through the entire model [compare digital elevation models from Fig.3.29a and Fig.3.30a lower panels]. Faulting in model IBERIA-II is more distributed along the surface. Most of the brittle structures appear to have nucleated on the ductile lower crust which accommodates deformation by flowing over the mantle, causing vertical uplift. The spacing of thrusting is shorter compared to experiment IBERIA-I.

The upper crustal architecture as displayed in Fig.3.29 is dominantly characterised by pop-up (inset A) and pop-down (inset B) structures imbricate thrusts mainly occur between the main pop-ups. During an episode of forward thrusting (up to 10% BS) inter-mountain basins developed, which have subsequently been deformed by back–thrusting. The viscous upper mantle displays gentle long wavelength low amplitude folding and the geometry of the ductile lower crust is governed by the upper crust and upper mantle geometries, respectively.

3.7.2 Rheology of the lower crust and upper mantle

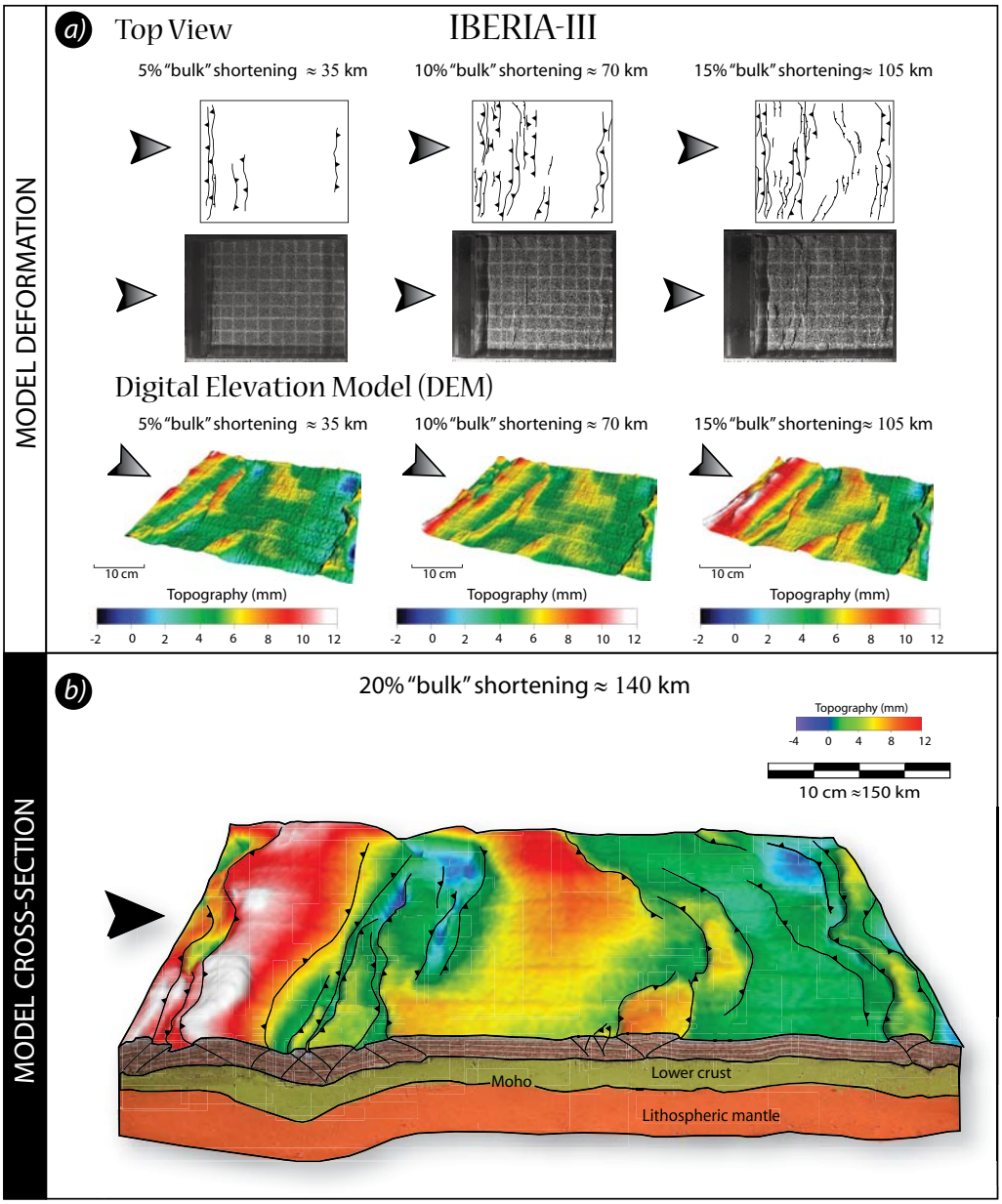

Figure 3.31 *(a) Structural interpretation of top-view images and digital elevation model (DEM) from model IBERIA-III (weak mantle under convergence rate of 0.5 cm/h). See text for further explanation. Arrows show the direction of convergence. (b) 3D model after 20 % of bulk shortening shows two broad antiforms (white arrow indicates direction of shortening).*

3.7.2.1 Model IBERIA-III: strong lower crust, weak upper mantle

In experiment IBERIA-III the viscous lower crust is stronger than the upper mantle resembling a crème-brûlée-type rheology of the lithosphere (*Jackson*, 2002a). Soon after the

onset of shortening thrusts appear close to the moving wall [Fig. 3.31a]. After 10% of deformation, thrusting jumped to the inner part of the model. The first intermountain basins (referred here as a relative foreland basin between two mountain chains) developed at this stage [digital elevation models Fig.3.31a]. Surface uplift is concentrated close to the moving wall, where it can be linked to the development of thrusts and pop-ups, as well as in the middle part of the model, where controlling structures are largely missing at the surface. With the advance of shortening, the inner part of the model started to deform by pop-ups, which are arranged in an en-echelon fashion. At the same time earlier formed basins became shortened and partly consumed under the mountain ranges pop-ups. New basins appear in the forefront of the thrust [Fig.3.31b].

The cross section along profile-II [Fig. 3.31b] resembles the geometry of a folded lithosphere with well developed synforms and antiforms. The amplitude of folding is a function of the distance to the advancing wall. Furthermore, the cross-section reveals that the broad, uplifted zone in the centre of the model is controlled by folding of the viscous layers rather than upper crustal basins.

3.7.3 Influence of an indenter

3.7.3.1 Model IBERIA-IV

This experiment aimed at testing the effect of constriction produced by the opening of the King´s Trough in the north western part of the Iberian Atlantic platform (*Cann and Funnell,* 1967; *De Vicente and Vegas,* 2009a) and its results on the pattern of intraplate deformation in Iberia.

Accordingly, we use a rigid indenter to observe if there is effective transmission of deformation from the moving wall towards the inner part of the model. In contrast to the previous models, we observed deformation being concentrated within zones of finite width [Fig. 3.32a], which are separated from nearly undeformed parts of the model.

This general pattern of deformation was already established after 10% BS. Thereafter shortening led to the lateral propagation of thrusts and to a minor extent to the generation of new structures. Strongly deformed regions dominantly correlate with topographic lows suggesting that deformation of the upper crust is incapable of explaining the monitored topography.

The wavelength of the deformation is highlighted by the indenter geometry as the same amount of shortening is applied over different initial lengths of the model. Topographic uplift is clearly defined along two central antiforms followed by two broad basins at both sides [blue areas in the digital elevation models at 20% of bulk shortening, Fig.3.32b, lower panel]. Cross sections show that the upper mantle and lower crust are folded and thickened. The lower crust is thickened in areas where the Moho is depressed and main mountain ranges are localised. A stage of basin development is rapidly followed by uplift influenced by the down warping of viscous layers and in some cases with crustal structures (i.e. blind thrust).

3.7.3.2 Model IBERIA-V

The setup of experiment IBERIA-V is similar to the previous except that the convergence rate has been doubled to 1cm/h (representing ~14 mm/y). In the first stages of shortening, the deformation localised close to the moving wall and ahead of the indenter [Fig. 3.33a]. Close to the moving wall, brittle structures develop oblique to the shortening direction as a result of the indenter geometry. Thrusting advanced forward leading to overall deformation of the model

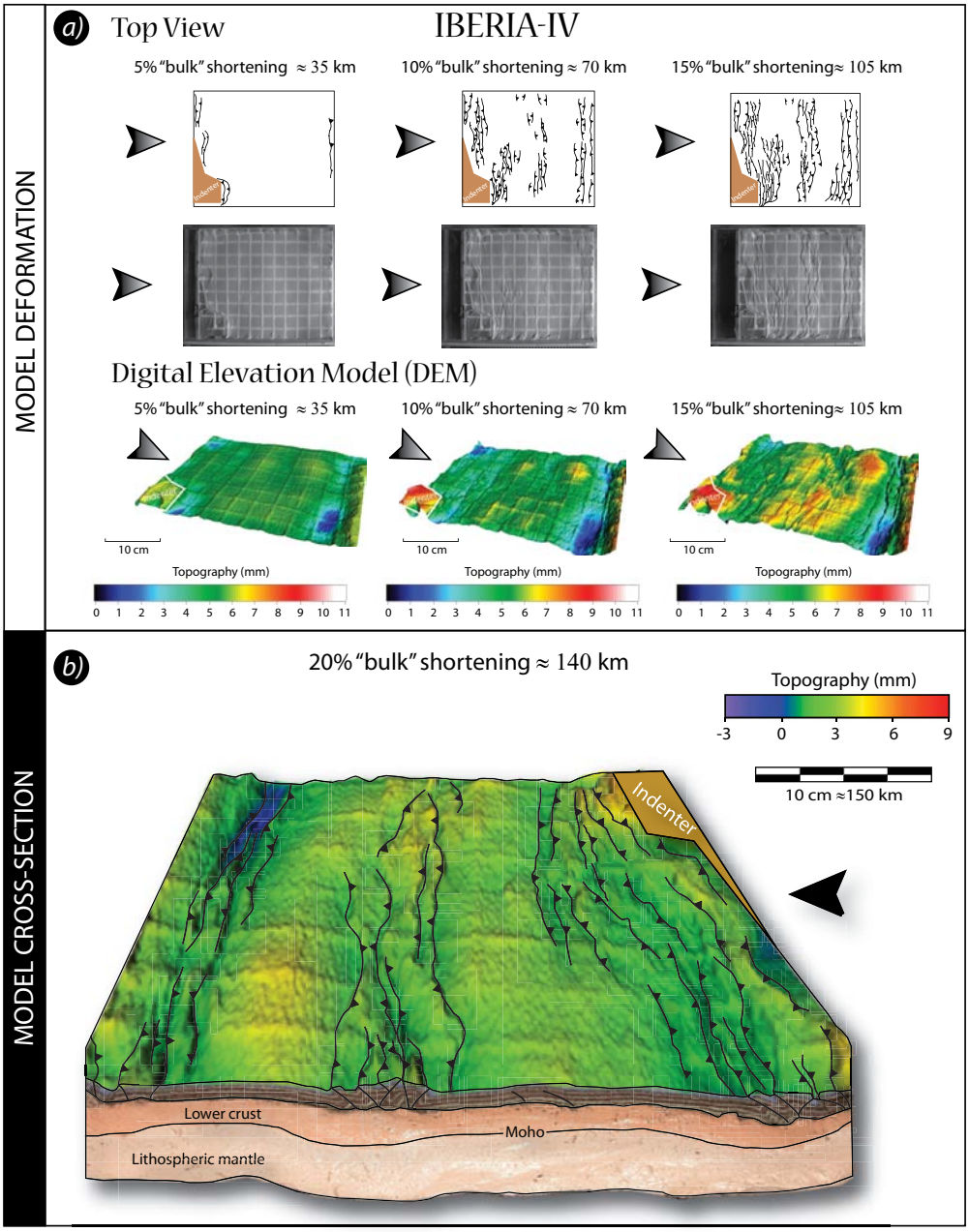

Figure 3.32 *(a) Structural interpretation of top-view images and digital elevation model (DEM) from model IBERIA-IV. See text for further explanation. Arrows show the direction of convergence. (b) 3D box, representing model IBERIA-IV from profile-I. Ductile layers are folded and heterogeneously thickened along the main synclines where mountain ranges developed. The model shows two wide uplifted basins developed in between thrust systems. Some blind thrusts within the basins produce uplift in later stages of deformation. This process may lead to high altitudes in areas like the Duero Basin in Iberia.*

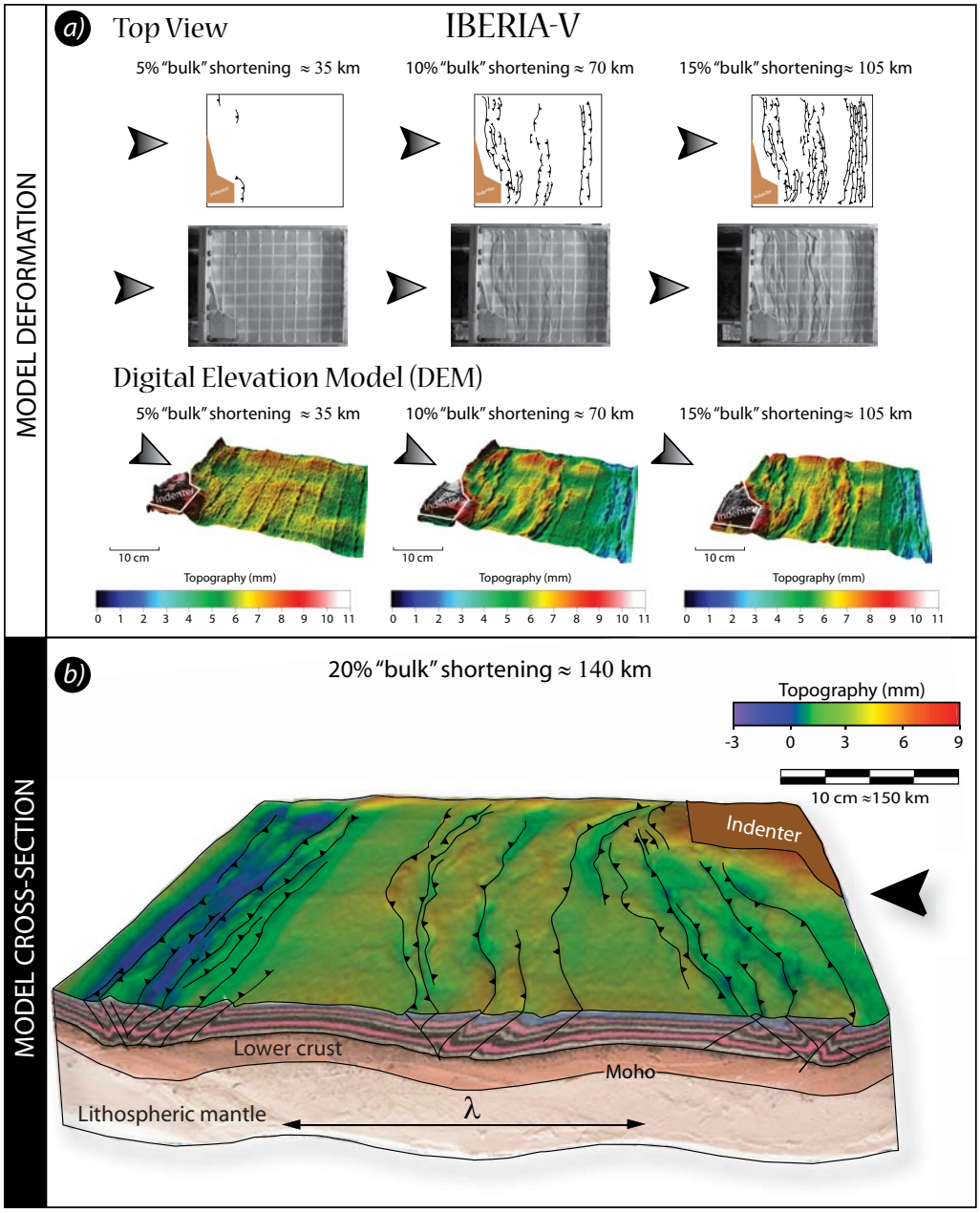

Figure 3.33 *(a) Structural interpretation of top-view images and digital elevation model (DEM) from model IBERIA-V. See text for further explanation. Arrows show the direction of convergence. (b) Cross-section along profile-I (model IBERIA-V). The arrows show the direction of convergence. Ductile layers are folded. The lower crust presents thickening below the synclines where main mountain ranges are localised. The basins are uplifted and appear on top of the lithosphere anticlines.*

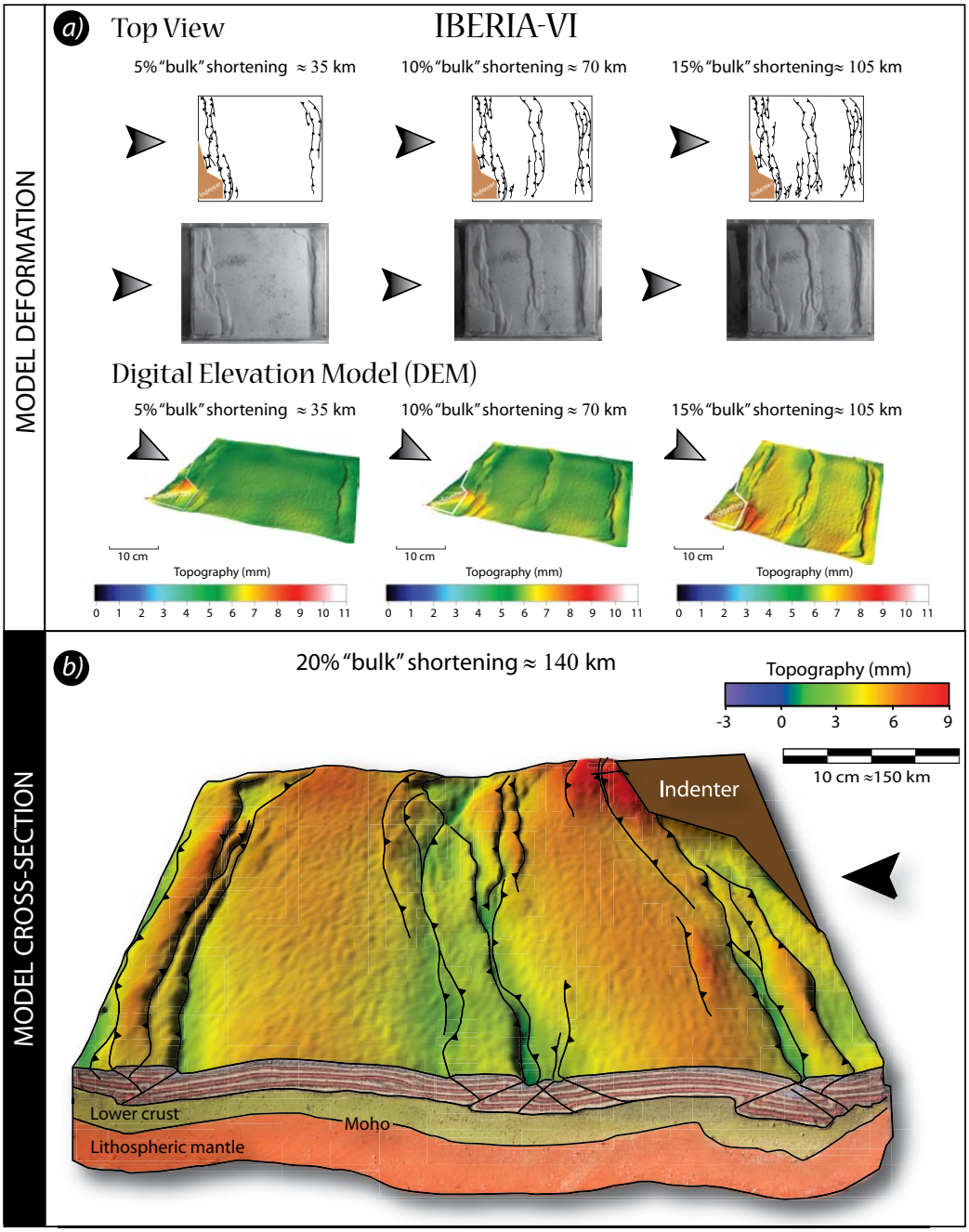

Figure 3.34 *(a) Top view images from model IBERIA-VI. Digital elevation models show the evolution of topography (see explanation on the test). (b) Digital elevation model shows general uplift of the model with two broad antiforms separating the main topographic features.*

surface. Similar to experiment IBERIA-III, localisation of structures occurred in regularly spaced zones, which are separated by largely undeformed regions. The cross section portrays large-scale folding of the model lithosphere [Fig. 3.33b], which seems to control the distribution of brittle structures such that they mainly coincide with the synforms of the folds. Compared to model IBERIA-IV, the amplitude of the folds is higher but thickness variations of the ductile layers are subdued, suggesting that more shortening was taken up by folding than concurrent thickening of the layers.

3.7.3.3 Model IBERIA-VI

Experiment IBERIA-VI is characterised by a strong lower crust and a weak upper mantle and the presence of an indenter (see Figure 3.27 for details). The first thrusts appear close to the advancing as well as the rigid walls [Fig. 3.34a]. Further shortening led to the development of the first pop-up in the central part of the model at about 10% BS. Similar to experiment IBERIA-III shortening has been accommodated by fewer regularly spaced structures. These structures in the brittle crust are pop-ups in the centre of the model or pop-downs close to the moving wall [Fig. 3.34b]. The location of these structures coincides with the position of synforms of the folded ductile layers. Two big antiforms without internal deformation, which developed between narrow synforms, correspond to regions of high elevation and a shallow experimental Moho.

In places where the displacement along a single structure was significant (e.g. the backthrust confining the pup-down close to the advancing wall), the ductile crust and upper mantle are advected upward leading to pronounced lateral thickness variations in the weak upper mantle.

3.7.4 Role of model size

3.7.4.1 Model IBERIA-VII

Model IBERIA-VII, which is distinctly twice longer than the previous ones, serves to ensure that the results described above are of significance and not influenced by the length of the box. Buckling of the lithosphere became evident during the first phase of shortening.

Three pronounced uplifted regions developed close to the advancing wall prior to the formation of thrusts [see 5% BS digital elevation model from Fig.3.35a]. Wavelength and amplitude of folds was similar to the models performed in a shorter box suggesting their independence to the chosen model length. Further shortening localised uplift along the previous structures giving rise to well developed antiforms. Mountain ranges are the result of single thrusts and pop-ups which rolled over from elevated areas to the position of lithosphere synforms probably pushed by flow of the ductile crust. However, the initial position of basins remains unchanged. The final stage of deformation shows an important reduction of spacing between pop-ups close to the moving wall [Fig.3.35b structural interpretation inset A].

Towards the central part of the model, wider pop-ups are formed [inset B Fig.3.35b]. Differences in pop-up spacing support the idea of strain localisation along the margin which is also apparent on the thickening of the lower crust and geometry of folding surfaces.

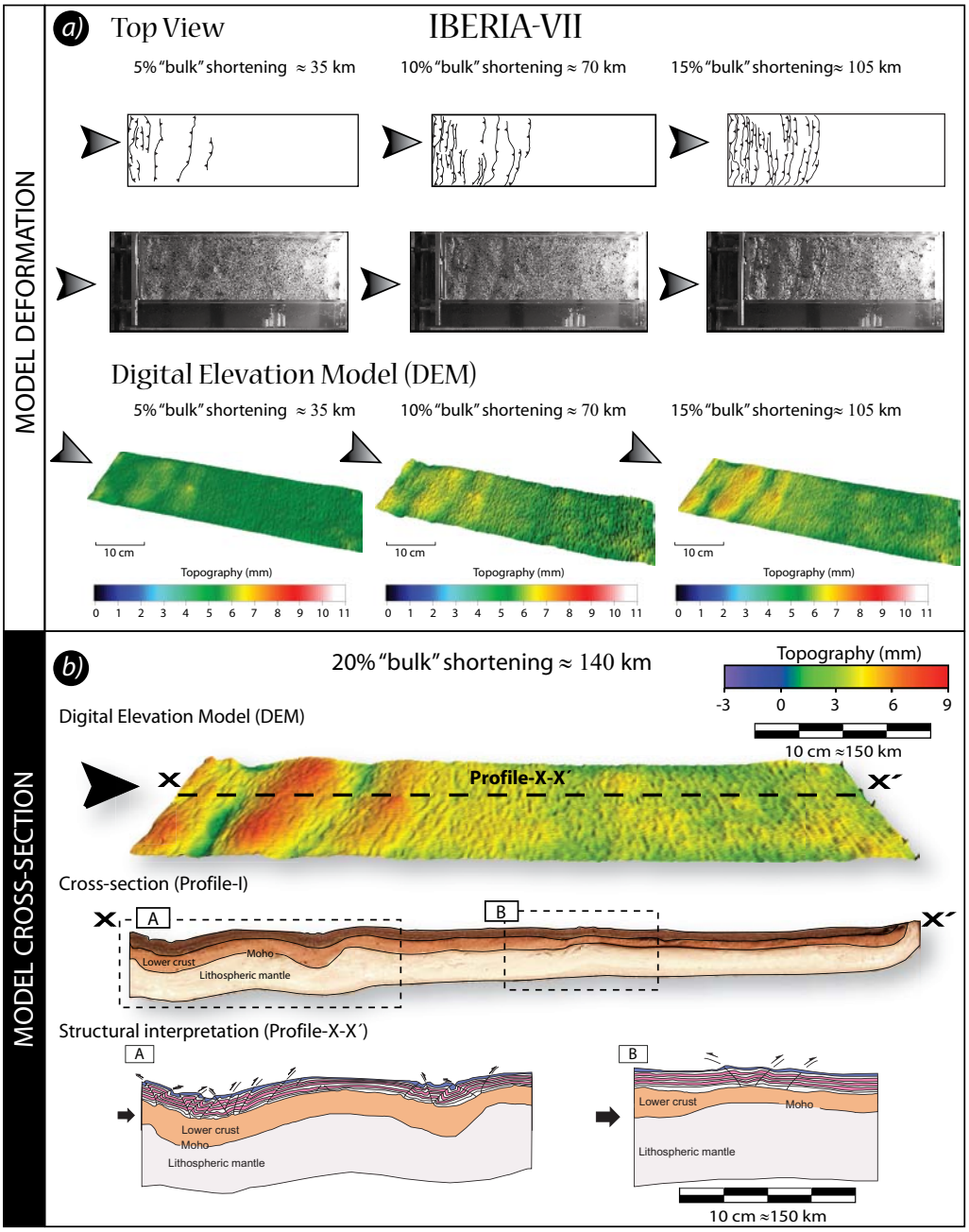

Figure 3.35 *(a) Structural interpretation of top-view images and digital elevation model (DEM) from model IBERIA-VII (normal lithosphere under convergence rate of 0.5 cm/h). See text for further explanation. Arrows show the direction of convergence. (b) Digital elevation model shows general uplift of the model with three antiforms localised close to the moving wall (white arrow indicates direction of shortening). Profile along X-X´and cross-sections from insets A) and B) providing the structural interpretation.*

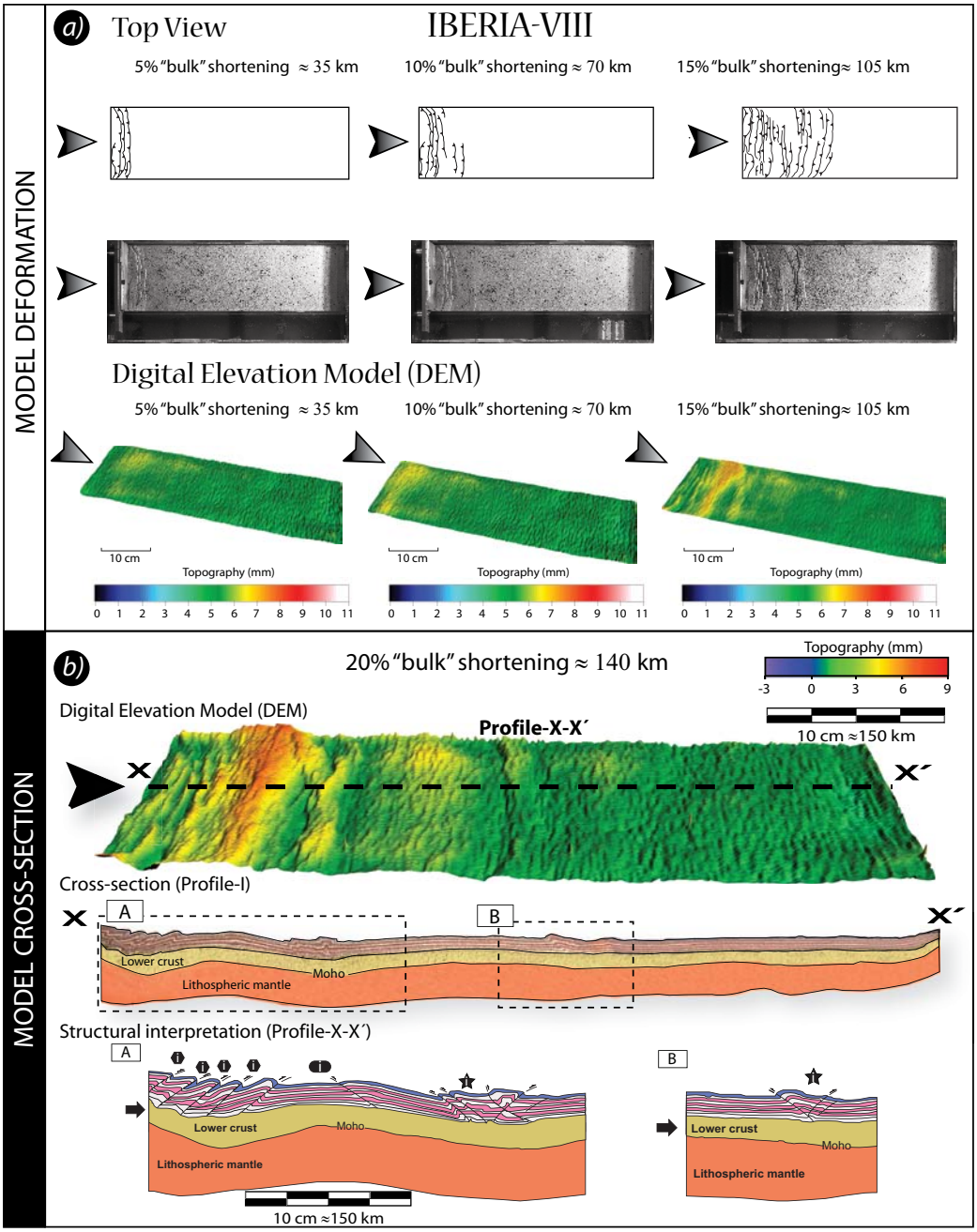

Figure 3.36 *Top-view image and structural interpretation of surface deformation (model IBERIA-VIII, strong lower crust and weak lithosphere mantle). Digital elevation models at 5, 10 and 15% of bulk shortening. (b) 3-D model and cross-section along profile X-X´. Profiles A and B: Polygons mark imbricated thrust; ellipsoids: Inter-mountain basin and stars: intra-mountain basins.*

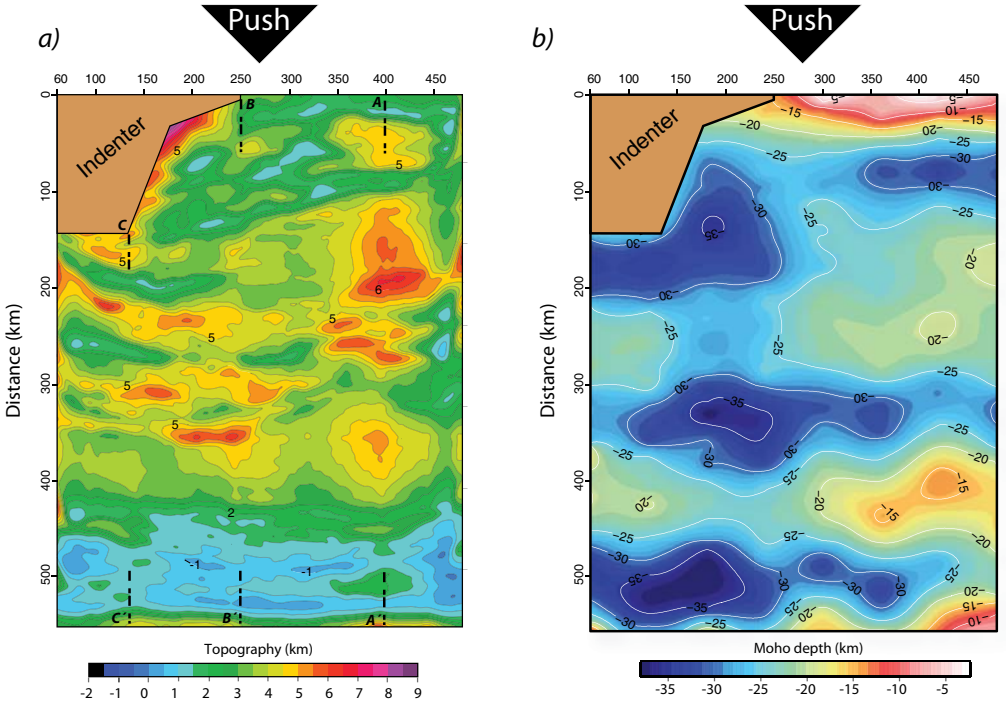

Figure 3.37 *(a) Contour map of topography from model IBERIA-V re-scaled to km and b) Iso-surface of the Moho, showing active folding at the crust-mantle interface.*

3.7.4.2 Model IBERIA-VIII

The comparison with the previous model show differences concerning wavelength and upper crustal tectonic deformation highlighting the changes in strength (strong lower crust and weak upper mantle). During the entire process of shortening, deformation was localised close to the advancing wall through a series of thrust crossing the upper most crust. Final stages of deformation (15% to 20% BS) indicate moderated uplift along an antiform situated orthogonal to the strain direction. Deformation at upper crustal levels is characterised by the presence of a series of duplexes situated close to the moving wall and a series of pop-ups and single thrust developed towards the central part of the model. A single uplift observed in the Moho appears close to the moving wall, where the highest values of elevation are reached [Fig.3.36a and b]. Distinctly to what it is observed in the last model (IBERIA-VII), deformation and uplift are basically restricted to the proximity with the moving wall indicating that deformation did not propagated forward [compare digital elevation models from Fig. 3.35a and Fig.3.36a].

Three different kinds of basins were developed during ongoing deformation by upper crustal thrusting. Duplexes led to a series of piggy-back basins in the proximity of the advancing wall while intra-mountain basins where specifically located within groups of pop-ups or at the intersection between a pop-up and a single thrust. Moreover, the presence of broad inter-mountain ranges is controlled by the wavelength of the deformation, resulting in their distribution between two separated groups of pop-ups or single thrust.

3.8. Discussion of Modelling Results

3.8.1 Relationship of folding and faulting

The results of the analogue models suggest that the first response to shortening of a rheologically stratified lithosphere with uniform mechanical properties of each layer is buckling (with exception of hot and weak lithospheres, e.g. Pannonian). Thrusting is developed at the very beginning of deformation along the inflexion points of the antiforms (*Davy and Cobbold,* 1991; *Martinod and Davy,* 1994). As the buckling instability amplifies the formation of newly formed structures such as pop-ups and pop-downs predominantly occurs at the sides of the synforms, whereas little deformation is observable at the position of the antiforms. On the other hand, folding and faulting could happen simultaneously, and folding may be accommodated by faulting as proposed by *Cloetingh et al.* (1999) and *Gerbault et al.* (1999).

In the beginning of deformation, faulting in the upper crust occurred as a consequence of weakening of the system, during increasing strain-rate along the vertical lithosphere segment. The vertical distribution of strain towards the mantle led to thickening of the ductile crust. These results are in agreement with numerical modelling performed by *Jarosinsky et al.* (2009), where the highest strain-rates are localised along the lithosphere synclines. Consequently, lithosphere folding is enhanced by active de-coupling between upper crust and mantle.

3.8.2 Experimental Moho depth and surface topography

The constructed map of the Moho aimed to infer the crustal/mantle interface variations produced by folding of the entire lithosphere. Figure 3.37b shows the depth of the Moho surface in model IBERIA-V scaled to nature [see Table 3.1 for nature/model scaling thicknesses]. Abnormally shallow Moho close to the moving wall reflects boundary effects and shall not be discussed here. According to the map shown in Figure 3.37, a shallow Moho occurred in regions coinciding with antiforms of the mantle folds, suggesting that flow of the lower crust took place leading to thickening in the synforms (Moho deepens) and thinning in the antiforms. Meanwhile, the deepest part is localised near the indenter appearing oblique to the main shortening direction. This is related to the effect caused by the constraining geometry. In addition, topography shown in Figure 3.37a is located in those areas where the Moho reaches deepest depths. Furthermore, the highest values of elevation are localised close to the moving wall and indenter. However, major amplitude of the synforms seems to modify the mountain range elevation.

The above mentioned results, point out the presence of two different wavelengths affecting the topography (short wavelength) and surface of the Moho (long wavelengths). Consequently the topography wavelength is smaller than the mantle folds [represented by ups and downs on the surface of the Moho in Fig.3.37]. Cross-sections of model IBERIA-V show in Figure 3.38 the position of deepest Moho below the main uplifted areas. Profile A-A´ shows a relative flat Moho close to the moving wall. Close similarities are also pointed out on profile B-B´. However section C-C´, situated close to the indenter indicates a strong periodic pattern which allows comparison with a folded structure. It is important to remark that the profiles maintain similar Moho depths with clear variations between 10 km depth at the model borders and >30 km in the deepest areas.

The increasing velocity enhances the coupling between the lithosphere layers amplifying the wavelengths of the folding [compare Fig.3.30 and 3.33]. Long distance between thrusts during the early stages of the model deformation suggests that their spacing is controlled by folding of the mantle lithosphere. Subsequently stages of shortening might allow the lower crust to become an active body on the deformation mechanism. That may decrease the wavelength of

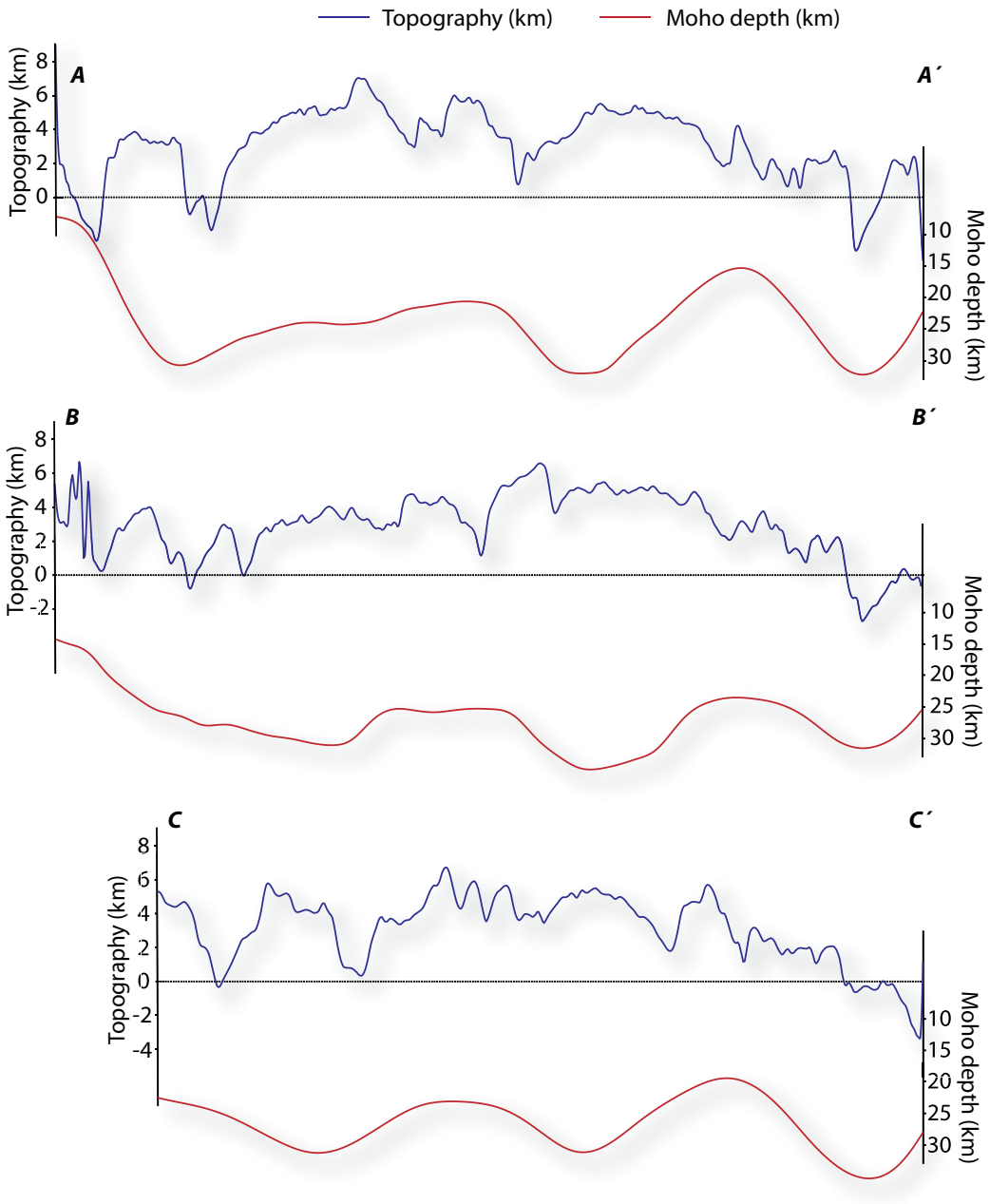

Figure 3.37 *Cross-sections of deformed model IBERIA-V along profiles A-A´, B-B´and C-C´shown in Figure 3.36a. See further explanation in the text.*

the lower crust folding, different from the mantle wavelength.

Numerical models carried out by *Burov et al.* (1993), show the strong control on wavelength and model deformation exerted by rheological stratification of the lithosphere. This

fact has been highlighted by analogue experimentation, involving a brittle-ductile layer system (*Martinod and Davy,* 1992) and field observations (*Bonnet et al.,* 2000). The analogue models are in full-agreement with these results, showing an increase of wavelength on those models with stronger upper lithosphere mantle [wavelength in model shown in Figure 3.29 is 250 to 300 km while for a weaker upper lithosphere mantle in Figure 3.31, is around 150- 225 km]. Conversely, the change in the amplitude of the folding with the increase of velocity seems to be related to the distribution and localisation of the deformation in the model. Distributed deformation promotes low amplitude whereas if it is more localised higher amplitudes are observed [see figures 3.29, 3.30, 3.33 and 3.34].

Despite the fact that the analogue models do not deal with tectonic inversion neither reactivation of pre-existing crustal heterogeneities, it is worth to mention the close similarities of the modelling results with certain areas of tectonic activity in nature. In such context, the Eastern Cordillera in Colombia shortened by more than 70 km is the result of basement structure reactivation and foreland propagation overriding the Nazca Plate. Balanced cross-sections show the strong localisation along old faults, and the style of deformation defined by imbricated thrust and positive flower structures (*Cortés et al.,* 2006). Another good example is presented by Teixell *et al.* (2003) in the Moroccan Atlas. The uplift of the Atlas along an asymmetric thrust system gives rise to an intraplate mountain chain where most probably, inherited late-Variscan faults are involved. Gravity data shows a good correlation in the position of the anomalies between the areas of strain localisation (topographic uplifts) at the surface and crustal thickening (Moho depth variations). This is clearly observed in the majority of the models, where the main mountain system appears located where the Moho is deepest (crustal root). Moreover, these regions in general show a relative thickening of the lower crust and upper mantle [Fig 3.29, 3.33 and 3.35]. Additionally, strong similarities with the intraplate mode of deformation in the US Rockies exist, where foreland deformation occurs in form of arches affected by blind thrusts and pop-ups as a result of reactivation and neo-formed thrust during the Laramid Orogeny (75-50 Ma) leading to lithosphere buckling (*Tikoff and Maxson,* 2001).

Another important fact brought by the modelling result is the relevant position of the main mountain ranges within broad synforms where the crust thickened. A field example in Iberia is the inverted Cameros Basin, situated in the northern part of the Iberian Chain, which was transported 25 km toward the north during the Iberia-Europe convergence (*Casas-Sainz and Gil Imaz,* 1998) The actual relief is situated over a relative thickened crust (~40 km) (*Guimerá and González,* 1998). This situation seems to be controlled by the wavelength of the folding affecting the ductile part of the lithosphere together with brittle deformation involving the uppermost part of the crust.

3.8.3 Implications for mountain building and basin development in Iberia

3.8.3.1 Basement uplift controlled by lithosphere folding amplification

Analogue models provide a lithospheric section consisting of a faulted upper crust that is uplifted by single thrust and pop-ups, a thickened ductile lower crust, and a folded lithospheric mantle. These relationship between crustal and mantle deformation and thickness variations along intraplate belts can explain the observed geometries within plate interiors. A remarkable example is constituted by the Spanish Central System (SCS) in central Spain. Figure 3.39a and b illustrates the comparison between the lithosphere below the Central System and part of the section provided by the model IBERIA-V. The mountain ranges coincide with the loci of Moho depressions of the buckle folds. Intra-mountain basins are developed in between pop-ups.

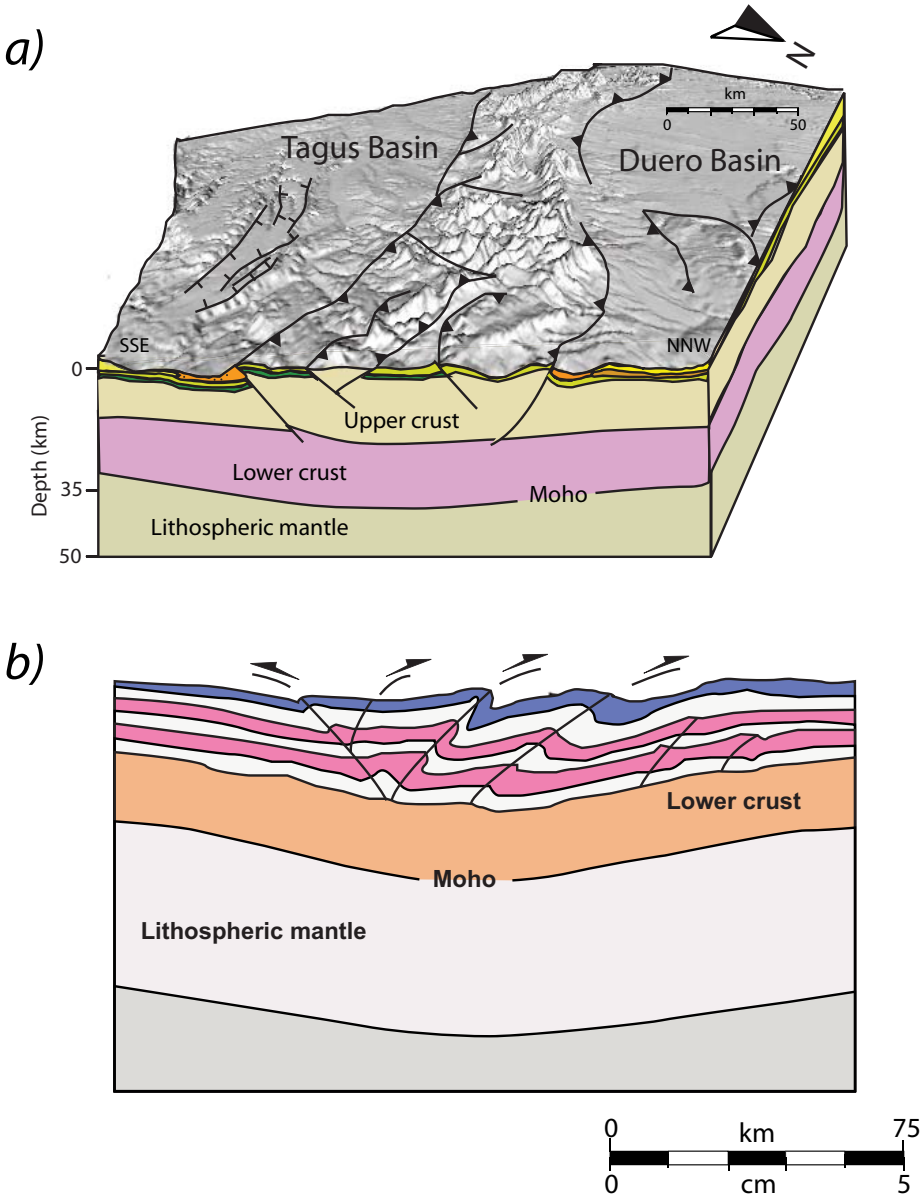

Figure 3.39 *(a) Cross-section along the profile NNW-SSE based on seismic data compiled by Díaz and Gallart (2009). (b) Lithospheric scale cross-section of profile-I (model IBERIA-V).*

Inferences from modelling support the idea of relatively strong crust-mantle decoupling favouring SCS-type structures. Pop-up structures nucleate at the brittle-ductile transition and propagate upward. Meanwhile ductile thickening becomes evident in the lower crust. The time span between the first observable thrust at the surface and the beginning of deformation in the central part leads to the conclusion that folding is involved in the mechanism that transfers deformation from the front towards the inner part of the model. Subsequently, intraplate deformation and thickening are related to both, thrusting and folding of brittle and ductile layers that com-

pose the Iberian lithosphere. Unlikely, those models where crustal-mantle coupling is strong, the lower crust thickened slightly. Moreover, the pop-ups do not appear as common structures turning into imbricate thrust or single thrust. Differences in style of thrusting may be considered as the result of crustal-mantle coupling.

Observed similarities between models and nature led to the conclusion that higher convergence rates spread deformation faster. This would be in accordance with the observed relative time-scale evolution of the models. Model IBERIA-II [convergence rate of 1cm/h, see Table 3.1] shows a lag time of 5 My between the beginning of shortening structures in the border close to the moving wall and the structures developed in the inner part of the model. At 10% BS (which nearly corresponds to Eocene times) the middle part of the model starts to deform by thrusting, giving rise to mountain system development [Fig.3.29]. These results might explain the observed temporal evolution proposed by *De Bruijne and Adriessen* (2002) based on fission track analysis in the Spanish Central System and Toledo Mountains (*Barbero et al.,* 2005). Consequently, models IBERIA-I and IBERIA-V are probably the most plausible scenarios for a relatively stable lithosphere affected by shortening. Thickening of the lower crust is accompanied by thrusting on the upper most part of the crust [compare Fig. 3.29 and 3.33]. These close similarities explain deformation and basement uplift in the intra-plate setting of Iberia, providing a useful lithospheric section which aids in the interpretation of gravity and seismic data available in Central Spain.

3.8.3.2 Intra-mountain evolution, migration and subsequent basin disconnection: a broken foreland basin model

Analogue experiments show two different types of basins. Inter-mountain basins are in general wider and longer than intra-mountain basins and are situated in between mountain ranges. As shortening progresses these basins are uplifted and can become internally deformed, because they coincide with the location of the antiforms of the folded mantle.

The Duero Basin is an example of such an inter-mountain basin that is flanked by two mountain ranges and which is on remarkable high altitude (~900 m).

On the contrary, intra-mountain basins appear to be associated with pop-downs, they are narrow and located in-between faults affecting the same mountain range. These basins were formed by internal deformation and uplift of much broader basins that were finally disconnected during ongoing deformation. According to *Martín-González and Heredia* (2011), a similar evolution has been proposed for the Duero basin, suggesting a "broken foreland basin" model based on previous studies by *Jordan* (1995) [Fig.3.40]. In this model, foreland basins become disconnected during the advance of thrusting towards the plate interior leading to the interruption of flood plain sedimentation and the development of proximal fan deposits close to the new mountain fronts. Furthermore, the early Duero foreland basin would form part of the active Cantabrian orogenic front as a foreland related-basin during the Paleogene. However, during the early Miocene, it became segmented in several small intra-mountain basins as a result of tectonic uplift of adjacent reliefs (like the Bierzo basin and other small basins situated in the Galicia Massif). Consequently, this model may explain the differences observed in the sedimentary record of small basins in the west, related to the Duero foreland basin (since the Oligocene).

A similar basin evolution is also observed in central Spain, where basins like the Ambles or Lozoya Basin are developed within the main Spanish Central System as pop-downs. [compare Figure 3.12a and 3.29a]. Consequently, the evolution of these basins follows two different evolutionary steps. Firstly, convergence results in the development of a restricted sedimentary sequence disconnected from the main foreland sedimentary sequence, associated with thrusting. Secondly, the latter basin is internally deformed by single thrusts and blind reverse faults that

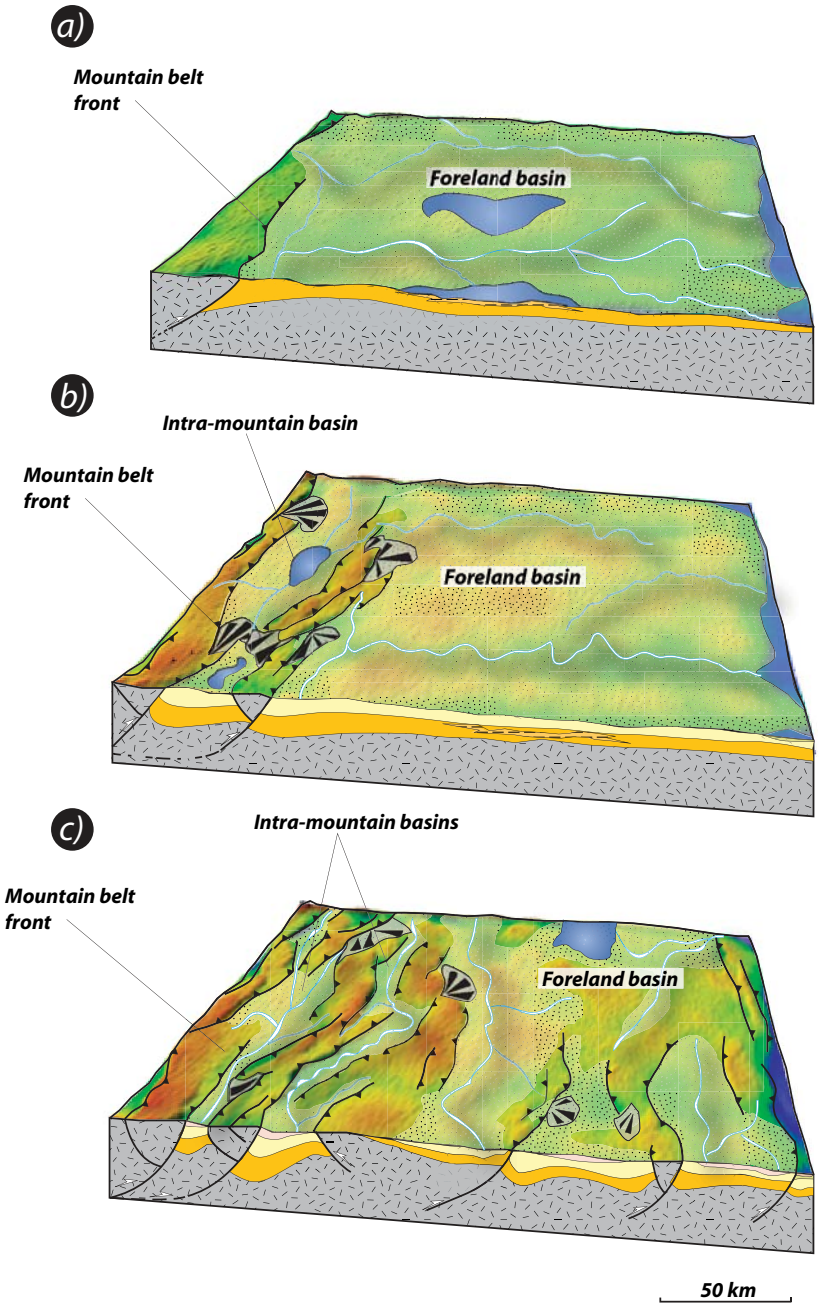

Figure 3.40 *A broken foreland basin model proposed by Martín-González and Heredia (2011), and based on the results from analogue experiment IBERIA-I. (a) Initial stage represented by a broad foreland basin developed close to the mountain front. (b) Subsequent stress transmission towards the interior leads to uplift and partial disconnection between a small basin and the foreland basin. Basin individualisation is favoured by thrusting (pop-ups and single thrusts) developed in front of former thrusts that involved basin sediments within pop-downs. (c) Final stage: total disconnection between foreland basin and intra-mountain basins related to thrusting and deposition of sedimentary sequences leading to intra-mountain basin formation.*

appear behind the main thrust-front, starting the disconnection from the main basin and resulting, in turn, in the deposition of an intra-mountain sedimentary sequence differentiated from the sedimentary sequence deposited in the foreland basin [see temporal evolution in Figure 3.40 producing internal uplift of the basins].

3.9 Conclusions

This chapter dealt with the conditions which can explain the actual configuration of mountain ranges and basins in Iberia as a result of Cainozoic deformation. The convergence between Iberia and Europe that led to the formation of the Pyrenees caused the effective transmission of stress towards the plate interior of Iberia during the Paleogene reaching a relative maximum around the Oligocene-Miocene boundary (22 My). Comparison of analogue modelling results has shown close similarities to mode of deformation found in nature, suggesting that the first response to shortening is buckling of the entire lithosphere. Therefore, lithospheric buckling is a viable mechanism controlling the E-W to NE-SW striking regular distribution of mountain ranges in Iberia. These results are compatible with geological and geophysical data from the Spanish Central System, Toledo Mountains and Sierra Morena. Moreover, the buckling of the lithosphere is associated with thickening of the ductile layers, particularly when the layers are weak. Strong decoupling, therefore, favours flow of the ductile lower crust from the antiforms to the synforms resulting in significant thickness variations of the ductile lower crust.

The longest wavelengths of folding were developed where the mantle is strong, or when the crust-mantle coupling was high, whereas shorter wavelengths are present when the mantle is weak even though the lower crust is stronger than the mantle. As such the distribution of mountain ranges is related to the rheological stratification of the lithosphere. Furthermore, the strength of the lower crust also influences the style of deformation in the brittle crust such that strong lower crust leads to asymmetric pop-ups, and duplexes in areas of localised deformation while a relatively weak lower crust leads to imbricated single thrusts or symmetric pop-ups. It is also important to remark the influence of the opening of the Kings Trough, represented in the models by the presence of an indenter which seems to be limited to affect the orientation and spacing of thrusts within the upper crust. It could be, therefore, considered as a geometrical constraint, influencing the evolution and shape of structures in the western most margin of Iberia as well as the Cainozoic uplift of the area. These results support the idea of elevation along the Galicia Bank and northwestern corner of Iberia (*Martín-González and Heredia,* 2011).

The modelling results also emphasise that uplift and internal deformation of inter-mountain basins like the Ebro or Duero Basins may be related to broad folds situated close to the Orogenic belt of the Cantabrian Mountains-Pyrenees. Consequently, uplift of these basins potentially marks the position of lower crustal and/or upper mantle antiforms.

Chapter 4

Integration of gravity and topography analysis in analogue modelling: understanding lateral strength variations in Iberia and their influence on intra-plate mountain building

In the western part of the Iberian microplate the main topographic highs trend E-W to NE-SW and are periodically spaced with wavelengths of 250 km. In contrast, topography is irregularly spaced and dominantly trends NW-SE, E-W and NE-SW in the north-eastern part of Iberia, the region of the Iberian Chain. This contrasting feature can be explained as being the expression of shortening of continental lithosphere, which contains two well defined domains characterised by different tectono-thermal state of the lithosphere. The hypothesis is supported by analogue modelling for which a new processing routine has been developed, which combines spectral analysis of gravity and topography. In this way gravity data can be used to distinguish and correlate areas of folded crust, characterised by periodic gravity fluctuations and areas of dominantly thickened crust, which display localised gravity lows. Gravity modelling has been performed under full in-depth control of the lithosphere structure through slicing of the experiment. As such, gravity signals from the models serve a better understanding of gravity data from natural cases in terms of underlying deformation mechanism.

4.1 Introduction

Several mechanisms have been suggested to explain topographic uplift along relatively stable continental areas in Europe including lithosphere folding, plume activity, or tectonic inversion (*Cloetingh et al.,* 2002; *Vergés and Fernández,* 2006). A common method to investigate intra-plate tectonics is the comparison of topography and gravity (*Stephenson et al.,* 1990; *Burov and Molnar,* 1998). In particular these studies have permitted to infer mechanisms of lithospheric folding or thrusting by comparing periodic and non-periodic patterns of gravity and topography within intra-plate settings (*Stephenson and Cloetingh,* 1991; *Lefort and Agarwal,* 2002).

The topographic pattern in Iberia shows striking differences from east to west. The western part, Variscan in age, shows an E-W trending periodic pattern, while the eastern part with a Mesozoic tectono-thermal age is characterised by NE-SW, E-W and NW-SE topographic trends. Up to now, intra-plate topography in Iberia has been explained in terms of: lithospheric folding, block rotation or crustal thickening related to thrusting (*Vegas et al.,* 1990; *Cloetingh et al.,* 2002; *Guimerá et al.,* 2004; *De Vicente and Vegas,* 2009a; *Casas-Sainz and De Vicente,* 2009b; *Fernández-Lozano et al.,* 2011). However, none of these mechanisms separately can satisfactorily explain these observed topographic differences on the scale of Iberia. Furthermore,

in order to gain insight into the main process/s that may govern such topographic differences in Iberia, the different spectral characteristics in gravity and topography between eastern and western Spain have been studied. The results, can shed light on the processes involved in the final configuration of mountain belts. Consequently, if lithospheric folding has controlled the surface expression of topography, the spectral signals would show a periodic pattern. However, if these signals are not periodic, an additional mechanism may have been involved in the evolution of intra-plate reliefs. The application of spectral analysis on lithospheric scale models is a new and powerful methodology that aims to emphasize the role of lithospheric strength variations and pre-existent tectonic structures that may have controlled the final distribution of topography in Iberia.

Modelling results suggest that differences in orientations observed in Iberia may result from both, rheological differences and tectonic fabric during lithospheric folding. Reactivation of pre-existent tectonic structures under N-S shortening imposed a complex set of topographic trends as it has been previously claimed by *De Vicente and Vegas* (2009a). The analogue experiments highlight the importance of strain partitioning between folding and faulting (strike-slip and thrust) on the final configuration of topography under a single stress-field, contradicting, in turn, previous proposed models regarding rotating stress-fields under N-S and NW-SE tectonic shortening episodes (*Simón-Gómez,* 1986). More details concerning the present-day configuration of topography in Iberia are given in chapter 5, analysing the particle displacement field from the model surface to infer the role of late-Variscan structures and rheology.

4.2 Surface structure and lithospheric configuration of Iberia

The overall topography in Iberia is the result of the efficient transmission of stress from the Pyrenean border to the plate interior during Oligocene-early Miocene times. The Western part of Iberia is characterised by E-W to NE-SW oriented topographic highs, cross-cut by a series of Permian structures that have been reactivated during the Alpine contractional phases [i.e. Messejana Plasencia or Vilariça-Bragança among others, Fig.4.1]. The eastern part of the Peninsula, however, shows NW-SE to NE-SW and E-W trends, which seem to correlate with the orientation of the main Mesozoic rift (the rift-border Somolinos Fault NW-SE trending (*De Vicente et al.,* 2009b).

Geophysical data portray mean Moho depths of about 32 km for the plate interior, ~35 km along the Central System, 45 km under the Pyrenean-Cantabrian Mountains, 35-40 km under the Iberian Range and ca. 38 km at the site of the Betics [Fig.3.23a]. These depressions of the Moho are characterised by gravity lows indicating the presence of crustal roots underneath the main topographic highs (*Banda et al.,* 1981; *Díaz and Gallart,* 2009). In addition, new strength calculations carried out in Central Iberia predict strong mantle rheologies along the Duero Basin, and weak strengths along the Spanish Central System and Tagus basins (*Tejero and Ruiz,* 2002). Weak rheologies in the Iberian Range have been interpreted as a result of Mesozoic thermal weakening of the lithosphere due to widespread extension prior to the Alpine Orogeny (*Van Wees and Stephenson,* 1995). Although rheologically different, the lithospheric thickness of the Variscan and the Mesozoic domains were similar at the beginning of the Cainozoic orogenic episode, because thick piles of Mesozoic sediments along the Iberian Range (>5.000 m) compensate for the reduction of the lithosphere thickness due to extension (*Casas-Sainz and Gil-Imaz,* 1998) in eastern Iberia, and exhumation of the western part of Iberia has led to thinning of the Variscan crust (*Guimerá et al.,* 1996).

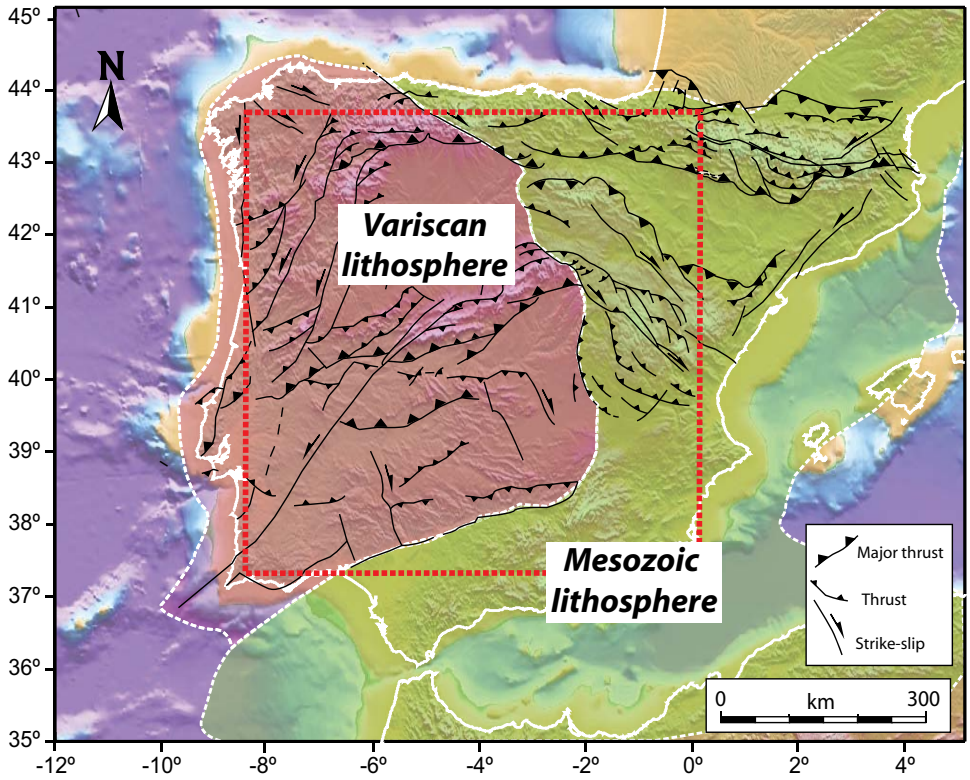

Figure 4.1 *Simplified sketch map of Iberia illustrating differences on lithosphere strength from an old and cold Varican lithosphere to the west and a weak and hot lithosphere towards the east (Mesozoic). Tectonic data from De Vicente and Vegas (2009a). Red inset marks the study area shown in the analogue experiments.*

4.3 Integrating analogue modelling with spectral analysis of gravity and topography

The following subsection is based on the comparison of analogue experiments with the obtained spectrums from calculated gravity and topography. Due to the fact that the analogue models scaling parameters have been fully described in Chapter 3, herewith I have provided a broad picture concerning the gravity interpretation and the spectral analysis carried out for the experimental results. Moreover, special attention is paid to the influence of late-Variscan structures as well as lateral strength variations on the final configuration of mountain ranges and its differences from west to east Iberia.

4.3.1 Analogue modelling

The physical analogue model lithosphere consists of three layers (brittle upper crust, ductile lower crust and ductile lithosphere mantle in agreement with geological and geophysical data (*Banda et al.,* 1981; *Tejero and Ruíz,* 2002). Two sets of experiments were carried out: with and without lateral strength variations, which aimed to infer the response of the lithosphere to these rheological differences between model domains (strong Variscan versus weak Mesozoic lithosphere) as well as inherited late-Variscan structures in terms of deformation mechanisms and topography development. Late-Variscan inherited structures were implemented, by

introducing a series of weak zones in model IBERIA-XIX. These zones correspond to the NW-SE trending Somolinos Fault in eastern Iberia and the NE-SW Messejana-Plasencia Fault across the strong lithosphere [Fig.4.1]. Despite model IBERIA-X maintains the same set-up than the previous model IBERIA-XIX, however, it has been implemented by adding the effect of the NE-SW trending Bilariça-Bragança Fault System situated in northwestern Spain. Moreover, the influence of the main E-W Mesozoic depocentres on mode of deformation has been tested for the Iberian Range (Cameros and Montalban sedimentary troughs, where 8.000 and >5.000 m of Mesozoic sediments were deposited, respectively). In order to complete the full set of models, I also decided to introduce a zone of weakness within the upper crust that represents the presence of granitoids in central Iberia to observe either, whether they controlled strain localization or they may have influenced the periodic pattern of gravity and topography observed across Spain.

Model properties and set-ups are shown in Figure 4.2 and Table 4.1, following previous studies by *Sokoutis et al.* (2005) and *Willingshofer and Sokoutis* (2009). The models were deformed by 20% bulk shortening (BS) according to the amount of crustal deformation in central Iberia calculated by *De Vicente et al.* (1996).

4.3.2 Gravity interpretation of physical experiments

4.3.2.1 Fundamentals of gravity

Variations in the Earth´s gravitational field are caused by differences in the density of rocks. Although, the variation of the acceleration due to gravity is in fact a measured value, it reflects variations in the crust and upper mantle (*Blakely,* 1996). Nowadays, gravity surveying has reached a large amount of applications within the field of geology (i.e. hydrocarbon exploration and mineral resources, monitoring volcanoes or military investigations). However, as we shall shortly see the combination of analogue modelling and the gravity survey has allowed to characterize crustal and upper mantle sources which permits to gain insight into the Earth deep processes. Furthermore, the effort to combine topography and gravity on analogue modelling for understanding intra-plate areas like Iberia, might help on the study of other extremely complex areas elsewhere in the world (Central Asia, Siberia).

The basis of the gravity method is mainly resumed on Newton´s Laws. The Universal Law of Gravity:

$$F = \frac{GxMxm}{R^2} \qquad [4.1]$$

where F is the force or attraction between two bodies with different mass, M and m that are inversely proportional to the square of the distance between their centres of mass (R). The gravitational constant (G) is $6{,}67 \times 10^{-11}$ $m^3\,kg^{-1}\,s^{-2}$.

The Newton´s second law of motion states:

$$F = mxg \qquad [4.2]$$

where m is the mass and g the acceleration of gravity. Furthermore, equations [4.1] and [4.2] provides the relationship:

$$g = \frac{GxM}{R^2} \qquad [4.3]$$

Table 4.1

Layer	Density ρ(kg/m^3)	Viscosity η (Pa · s)	Layer thickness h (m)	Velocity v (m · s^{-1}) Exp-IBERIA-I, IBERIA-XIX and IBERIA-X	R_m
Strong lithosphere					
Upper crust *nature*	2670	-	$1.5 \cdot 10^4$	$7 \cdot 10^{-3}$ - $14 \cdot 10^{-3}$	-
Upper crust *model*	1300	-	$1 \cdot 10^{-2}$	$5 \cdot 10^{-3}$ - $1 \cdot 10^{-2}$	-
Lower crust *nature*	2900	$1.0 \cdot 10^{22}$	$1.5 \cdot 10^4$	$7 \cdot 10^{-3}$ - $14 \cdot 10^{-3}$	29.03
Lower crust *model*	1486	$1.87 \cdot 10^5$	$1 \cdot 10^{-2}$	$5 \cdot 10^{-3}$ - $1 \cdot 10^{-2}$	22.23
Mantle lithosphere *nature*	3400	$4 \cdot 10^{21}$	$3.0 \cdot 10^4$	$7 \cdot 10^{-3}$ - $14 \cdot 10^{-3}$	33.80
Mantle lithosphere *model*	1606	$1.87 \cdot 10^5$	$2 \cdot 10^{-2}$	$5 \cdot 10^{-3}$ - $1 \cdot 10^{-2}$	36.86
Weak lithosphere				Exp-IBERIA-XIX and IBERIA-X	
Upper crust *nature*	2670	-	$1.5 \cdot 10^4$	$7 \cdot 10^{-3}$	-
Upper crust *model*	1300	-	$1 \cdot 10^{-2}$	$5 \cdot 10^{-3}$	-
Lower crust *nature*	2950	$2.0 \cdot 10^{20}$	$1.5 \cdot 10^4$	$7 \cdot 10^{-3}$	146
Lower crust *model*	1532	$9.75 \cdot 10^3$	$1 \cdot 10^{-2}$	$5 \cdot 10^{-3}$	110
Mantle lithosphere *nature*	3350	$1 \cdot 10^{21}$	$3.0 \cdot 10^4$	$7 \cdot 10^{-3}$	133
Mantle lithosphere *model*	1590	$2.3 \cdot 10^4$	$2 \cdot 10^{-2}$	$5 \cdot 10^{-3}$	194
Granite *nature*	1532	$1.0 \cdot 10^{21}$	$5 \cdot 10^{-3}$	$5 \cdot 10^{-3}$	-
Granite *model*	2950	$1.24 \cdot 10^4$	$5 \cdot 10^{-3}$	$5 \cdot 10^{-3}$	-

Table 4.1 *Scaling parameters. Rm, refers to Ramberg Number for ductile layers.*

Since gravity varies due to the flattened shape of the Earth and its surface topography is not completely regular (which means variable mass distribution), the value of the gravity field attraction is inversely proportional to the square of the Earth´s radius (R). Subsequently, the force of gravity is due both to the mass of the earth and to the centrifugal force caused by the Earth´s rotation. The average value of g at the Earth´s surface is 9,80 m/s^2, whereas the equivalence of 0,01 m/s^2 is 1 Gal in honour to Galileo. In general, modern instruments for gravity surveying provide high sensitivity, based on precise observations of the orbits of artificial satellites and gravity meters. The improvement of survey equipment enables accurate measurements from milli to micro-gals (10^{-3} to 10^{-6} Gals).

In the last century, artificial satellites also aim to measure the shape of the Earth. In 1930 an oblate ellipsoid was defined for the shape of the Earth, it was called the International

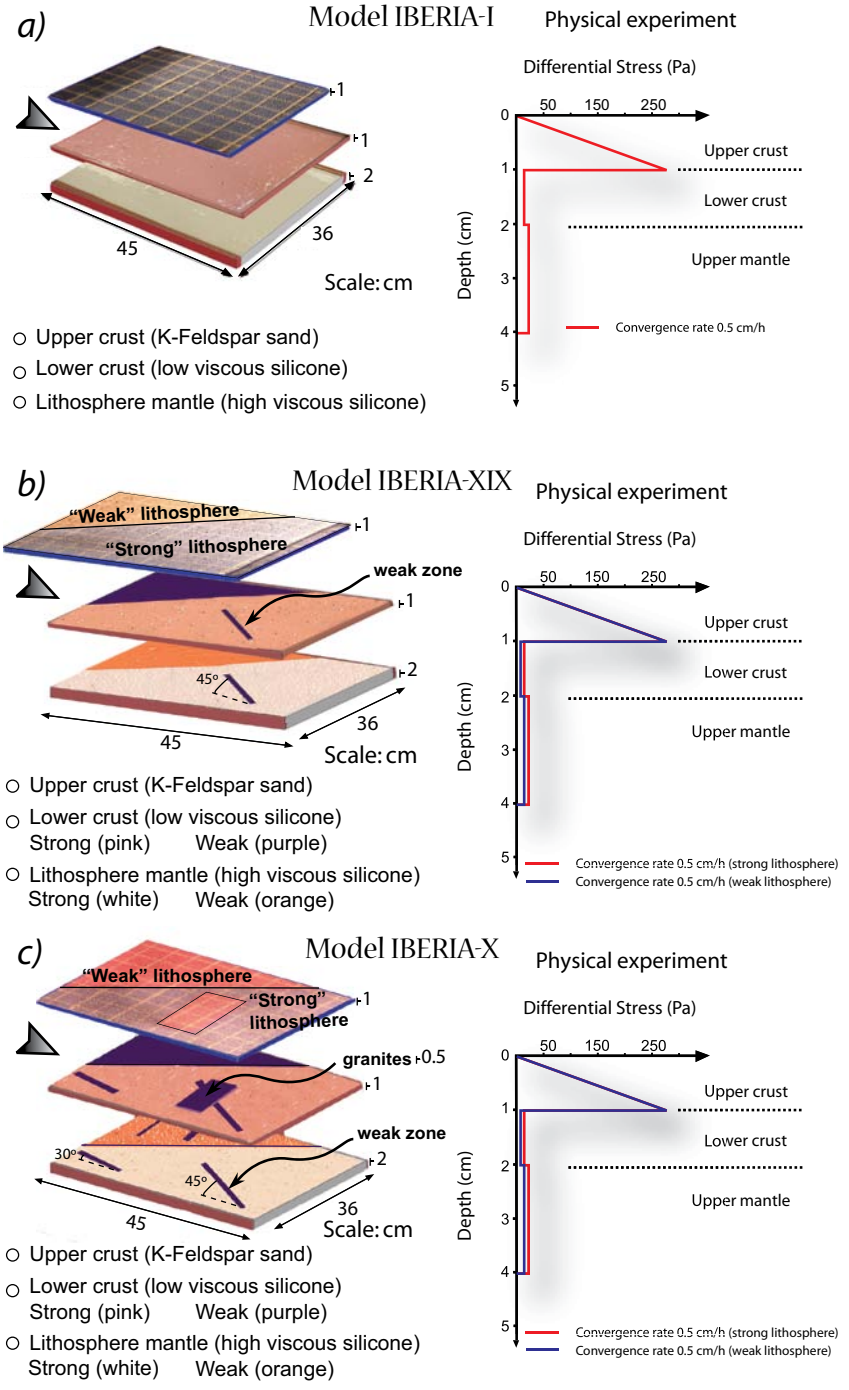

Figure 4.2 *Model set-up and strength profiles from analogue experiments. (a) Model IBERIA-I (homogeneous lithosphere). (b) Model IBERIA-XIX (heterogeneous lithosphere). (c) Model IBERIA-X with heterogeneous lithosphere and E-W weak zones affecting the weak lithosphere.*

Reference Ellipsoid. This ellipsoid is a close approximation to the equipotential surface of gravity at sea level, defined as the geoid. The later, reflects the distribution of mass inside the Earth, close to the free ocean surface off-shore. Whether or not the actual sea-surface coincides with the reference geoid will depend on the mass distribution below sea-surface. In general, the actual sea-surface shows large deviations from the reference geoid being the largest ones in Iceland and Indonesia (about 67 m and 100 m, respectively) and in South India (about -110 m). Nevertheless, in the continents it is affected by the mass of land above mean sea level, causing the downward or upward (if a hill or mountain whose centre of gravity is outside the ellipsoid) gravitational attraction toward the centre of the Earth. Therefore, the solid Earth rigidity, it is much more difficult to measure the deviations of the actual geoid with respect to the reference geoid. These differences, either onshore or offshore are called geoid anomalies or geoid undulations [Fig.4.3] (*Lowrie,* 1997; *Kearey et al.,* 2002).

The direction of gravity at a point is defined as perpendicular to the equipotential surface through the point, where the plumb line represents the tangent line to the direction of gravity at any specific point given (this value provides the orthometric height, which is the vertical distance between the Earth surface and the geoid). Therefore, this line is not straight, but slightly curved due to variations in the direction of gravity which in turn, depends on the characteristics of local density [Fig.4.3]. Eventually, the theoretical value of gravity about the above defined International Reference Ellipsoid can be obtained by differentiating the gravity potential. This let us to obtain the radial and transverse components of gravity which can be combined to give the formula for gravity normal to the ellipsoid in terms of latitude:

$$g_n = g_e(1 + \beta_1 \sin^2 \varphi + \beta_2 \sin^4 \varphi) \qquad [4.4]$$

where g_e is the acceleration at the equator, λ is the latitude and β_1 and β_2 are constants. From equation [4.4], we observe that the normal gravity is therefore, latitude dependent.

Finally, in 1980, the International Association of Geodesy (IAG) adopted a new Geodetic Reference System which eventually led to the World Geodetic System 1984, given by:

$$g_n = 978032.677\left[(1 + 0.0019\sin^2\varphi) \Big/ \sqrt{1 - 0.0066\sin^2\varphi}\right](mGal) \qquad [4.5]$$

4.3.2.2 Corrections to gravity observations

In general, gravity meter measurements must be translated to values of observed gravity by multiplying to an instrumental calibration factor. In order to describe the series of corrections it is worth noticing their contribution to observe gravity. In fact, the interior of the Earth is not uniform, and gravity varies with latitude due to both, the Earth´s rotation and deep density variations. There are several factors which may influence the values caused by perturbations related to influence of tides, large differences between mountains and close and deep valleys or the way the data are acquired (instrumental drift).

For such a reason, gravity must be corrected from the ellipsoid upward to the level where the measurement was made. In principle, this problem is solved by applying the necessary gravity corrections.

» Free-air correction

The free-air correction ignores the effects of mass between the measurement and

reference levels, providing the vertical gradient of the gravity field. Therefore, it depends on the distance between the station and the reference surface (the reference geoid). The correction becomes positive when the station is placed above sea-level and negative if it is below. Furthermore, it ignores the mass that may exist between the level of observation and sea level. Notice too that the application of the free-air correction provides the free-air anomaly (i.e. indicates whether surface topography such as a mountain is compensated or not by a crustal root):

$$g_{fa} = -0.3086x10^{-5}h \qquad [4.6]$$

$$\Delta g_{fa} = g_{obs} - g_{fa} - g_0 \qquad [4.7]$$

where h is height above sea level, g_{obs} is observed gravity and g_0 the theoretical gravity.

Figure 4.4, shows a topographic edifice supported by a crustal root under isostatic equilibrium. The free-air anomaly produces a short-wavelength, and large amplitude strongly influenced by mountain. The obtained anomaly tends to rise inland showing a strong correlation between topography and gravity. In general, the free-air anomaly is always of opposite sense to the Bouguer correction.

» Bouguer correction

The Bouguer gravity anomaly reflects anomalous mass bodies with density above or below 2.670 kgm^{-3}, also known as reduction density (notice that in some cases 2.400 kgm^{-3} or even 2.100 kgm^{-3} are employed as reference values of density). Consequently, the Bouguer anomaly considers that the space between station and reference level is occupied by an infinite layer with a density equal to the density reduction value.

$$g_{obs} = 0.4186x10^{-5}\rho h \qquad [4.8]$$

where ρ is the density and h the height of the station. The anomaly, therefore, becomes defined by the free-air correction, the Bouguer correction and the terrain correction. The Bouguer correction accounts for the effect produced by additional mass between the level of observation and sea level. However, the simple Bouguer anomaly ignores the shape of the topography, influencing the measurements made near topographic features. In addition to the simple correction, a complete Bouguer anomaly accounts for the terrain correction and compensates the effects of topography especially in areas of moderate to extreme topographic differences between mountains and valleys. The complete Bouguer correction is strictly necessary if the topographic difference within a sector is more than about 5% of its distance from the station (*Lowrie,* 1997). Application of the Bouguer correction provides the Bouguer anomaly given by the following relation:

$$g_{obs} = g_{obs} - g_{fa} - g_{sb} - g_t - g_0 \qquad [4.9]$$

where g_{obs} is the observed gravity, g_{fa} the free-air correction, g_{sb} the simple Bouguer correction, g_t the terrain correction and g_0 the theoretical gravity.

Figure 4.4b shows the effect of a mass deficit (crustal root) on the free-air and Bouguer anomalies. Differences between free-air (positive) and Bouguer (negative) anomalies arises from the Bouguer plate correction.

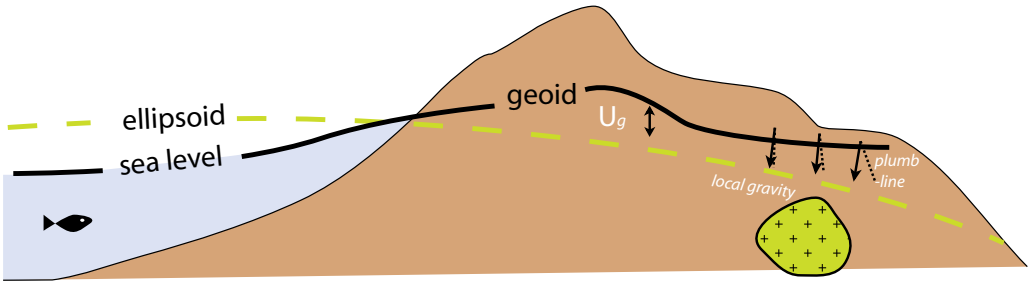

Figure 4.3 *Geoid variations caused by mass attraction within continental areas. A topographic edifice or a mass excess below the ellipsoide cause the elevation of the geoid above the ellipsoid. Ug refers to the geoid undulation. Modified after Blakely (1996).*

4.3.2.3 Geological factors and assumptions

Since the gravity value depends on rock density; changes in lithology (metamorphic, igneous or sedimentary rocks) as well as fracturation, weathering and porosity variations through the pile of rock decreasing in depth may provide broad differences in the value of measured gravity. Consequently, to fairly decrease the errors over a broad range of densities often considered for gravity estimations, approximate average of values is provided by laboratory rock analyses.

This thesis considers a simplified column of rock through the entire lithosphere based on previous studies carried out in central Spain by (*Stapel,* 1999; *Tejero and Ruíz,* 2000; *Tejero and Ruíz,* 2002). Therefore, following the initial model set-up, the lithosphere has been considered a laterally homogenous volume of rock represented by an upper crust (granitic composition), a lower crust (felsic-granulite composition) and upper lithosphere mantle (peridotitic composition) see Table 4.1 for further details on density values.

In order to obtain the gravity signal provided by the analogue modelling results, it is necessary to keep in mind certain assumptions. Among others, the most significant are as follows:

» There are no lateral density variations within each layer. It is assumed that rock did not suffer weathering nor porosity changes due to fracture or lithological changes.

» No presence of sedimentary cover or any other kind of basin sedimentary deposits which significantly allowed gravity changes.

» There are no igneous intrusions or volcanic rocks which would induce density changes across the crust of the model.

» Vertical homogeneity along the entire upper and lower crust as well as the modelled mantle.

Finally, all the above mentioned geological factors and simplifications allowed accomplishing the gravity analyses of the analogue modelling results. The main obtained results are shown in the following sub-section.

4.3.2.4 Gravity modelling

The analogue experiments were deformed by 20% BS. After deformation, a series of cross-sections were performed parallel to the convergence direction. Every cross-section

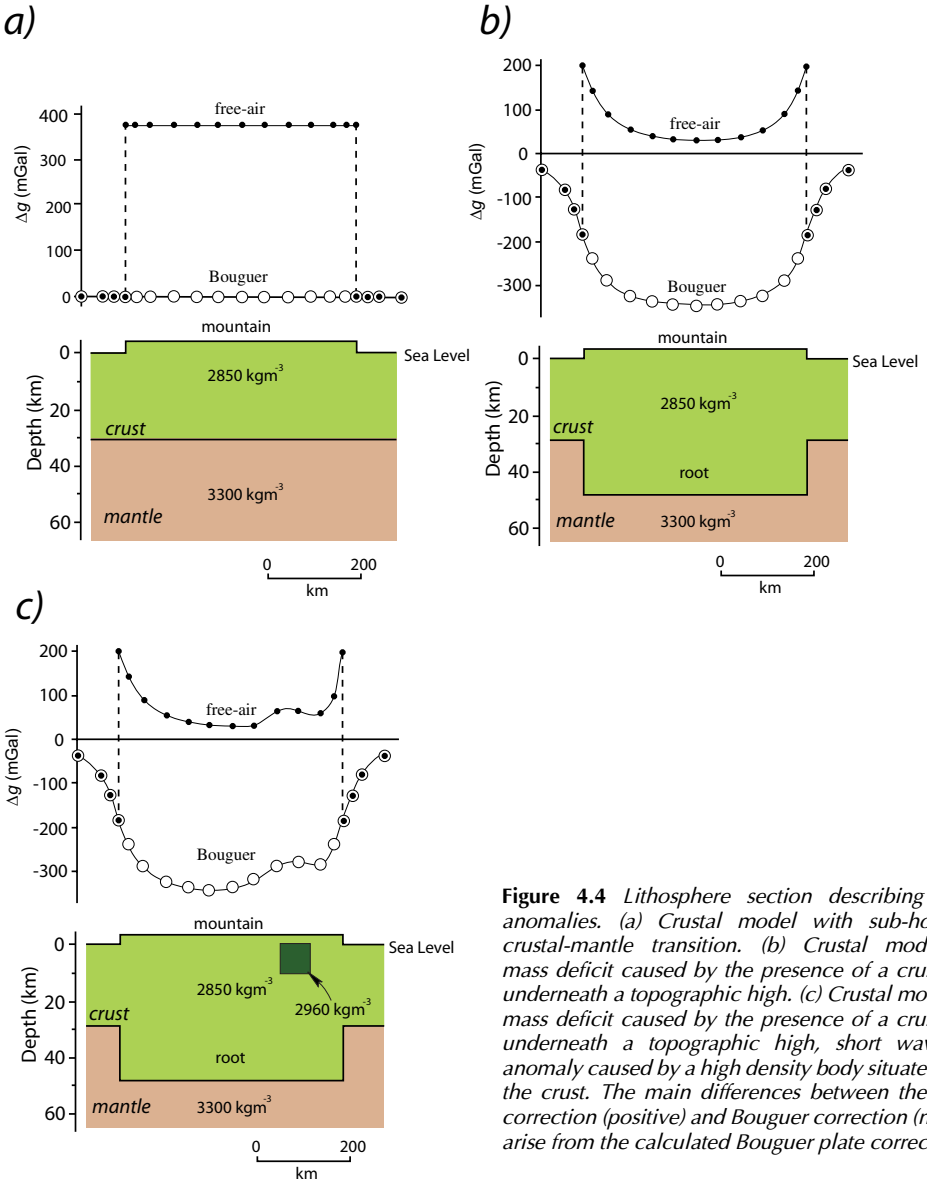

Figure 4.4 *Lithosphere section describing gravity anomalies. (a) Crustal model with sub-horizontal crustal-mantle transition. (b) Crustal model with mass deficit caused by the presence of a crustal root underneath a topographic high. (c) Crustal model with mass deficit caused by the presence of a crustal root underneath a topographic high, short wavelength anomaly caused by a high density body situated within the crust. The main differences between the free-air correction (positive) and Bouguer correction (negative) arise from the calculated Bouguer plate correction.*

was digitized and re-scaled to nature values (in km). Therefore, the depth to the Moho was interpolated from every digitized cross-sections. Moreover, Digital Elevation Models (DEMs) from the model surface were taken through a high resolution 3D laser-scan. The 2+1/2D gravity models have been performed after running the physical experiments, due to the fact that two datasets were necessary: on the one hand, the density values measured for each model layer; on the other hand, the layer thickness along the cross-sections after deformation [Fig.4.5b and c]. Density data were measured for each material using a regular picnometer [Table 4.1, material properties].

Cross-sections allowed the construction of 2+1/2D gravity models in order to calculate the gravitational anomaly caused by an irregular-shape layer body. The Bouguer gravity anomaly was, therefore, based on the obtained cross-sections from the physical experiments after model deformation. In general, in the 2+1/2D formulation, the bodies can be assigned finite strike-lengths in both directions (X and Y). That means that the polygons that comprise the model do not implicitly extend to infinity. Therefore, the computer algorithm allows definition of lateral borders in order to maintain the proper dimensions for a good estimation of the gravity anomaly.

The theoretical response was calculated along every cross-section by taking into account the density data and structure obtained from each cross-section. This kind of modeling assumes that the shape of the body is replaced by countless thin rods or line elements aligned parallel to the strike. Each rod makes a contribution to the vertical component of gravity at the origin [Fig.4.5a]. The gravity anomaly provided by the structure is calculated by adding-up the contributions of all the line elements; mathematically, this is the integration over the end surface of the body, and the gravity anomaly follows the equation:

$$\Delta g_z = 2G\Delta\rho \int z d\theta \qquad [4.10]$$

where Δg_z is the gravity anomaly, G is the gravity constant and $\Delta\rho$ the density contrast. The angle θ is defined to lie between the positive x-axis and the radius from the origin to a line element [Fig.4.5], and the integration over the end-surface has been changed to integration around its boundary. The computer algorithm for the calculation of this integral is greatly speeded-up by replacing the true cross-section shape with an N-sided polygon [Fig.4.5a]. In addition to the assumed density contrast, the only important parameters for the computation are the (x, z) coordinates from the polygon corners. Iteratively, the calculations were repeated for each successive point on the profile at every 1 km (re-scaled model to nature). Finally, the calculated gravity profile across the structure was compared to the observed anomaly and the residual differences were evaluated.

This forward modeling was performed using the **GMSYS®** software, that uses the methods defined by *Talwani et al.* (1959) and *Talwani and Heirtzler* (1964) and applies the algorithms described by *Won and Benis* (1987).

Certain noise on the gravity signal was produced along the model sides which required the use of a low-pass filter. Moreover, areas of extremely deep empty valleys below sea level (i.e. zero) led to estrange artefacts that have been filtered in order to smooth the signal provided by each body. This is important since the Bouguer anomaly is always calculated over sea level. Furthermore, the density reduction in such areas has been settled to the sediments density (~2.670 kgm^{-3}) to prevent strong peaks over the signal.

In addition, due to the fact that the upper crust represents a homogeneous layer without any local density variation (i.e. igneous intrusion, lateral rock changes, etc.) the terrain correction does not necessarily be applied, since the reduction density maintains constant along the Bouguer plate (2.670 kgm^{-3}). Actually, the gravity estimation accounts for the signal provided by deformed layers, in this case, density contrast between lower crust and upper lithospheric mantle. The anomaly, therefore, marks the deviations suffered by the Moho surface after deformation, allowing the comparison with the distribution of topography and position of Moho depressions.

4.3.3 Fourier analysis of periodic functions

Geophysical surveys focus on variations of physical quantities both to position or time. Good examples are provided by gravity or magnetic surveys (vector fields give scalar magnitudes,

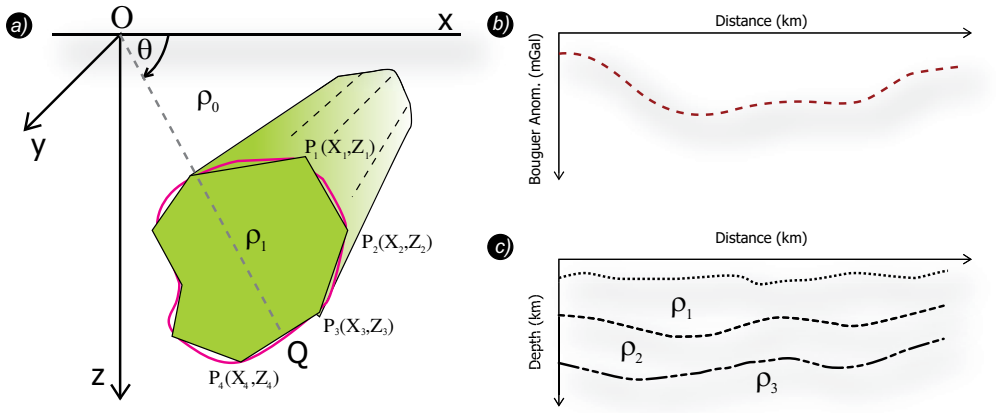

Figure 4.5 *Method of computing gravity anomalies of an irregular body: (a) A two-dimensional structure can be replaced with a multi-sided polygon. Modified after Lowrie (1997); (b) Theoretical Bouguer gravity anomaly given by density contrast between different layers of a model cross-section shown in (c)*

i.e. in gravity surveys mGal´s are obtained). However, the acquired signals need to be processed, converted and subsequently filtered in order to provide the values from the original waveforms (*Blakely,* 1996; *Kearey et al.,* 2002).

The reliability of the data depends not only on the amplitude of the measurement, but also on the selected intervals between measured samples. They both represent the sampling precision, often called dynamic range or sampling frequency. In addition, the sampling frequency, defined as the number of samples per unit of time or space represents an important parameter on data processing. In fact, the overall frequencies above an interval representing the half of the sampling frequency (the so-called Nyquist interval) results in to a serious distortion known as aliasing. Furthermore, the higher frequency components are folded-back. That implies the lost of information and subsequent lack of resolution. Therefore, in order to reduce such technical problems related to resolution, it is important to bear in mind what should be the most appropriated sampled frequency for the waveform, otherwise an antialiasing filter is needed to remove the frequency components above the Nyquist frecuency (*Kearey et al.,* 2002).

The analysis of signals provided by gravity, topography or magnetic field has been extensively studied to understand the mechanisms that shape the Earth (*McAdoo and Sandwell,* 1985; *Ricard et al.,* 1987; *Maus and Dimri,* 1995; *Rey-Moral et al.,* 2000). In general it is assumed that these signals represent periodic waveforms (i.e. they repeat themselves at a fixed time period). However, these waveforms are often referred to as functions of time (i.e. seismic waves) or space (i.e. gravity or magnetic waves). The first case, is represented in terms of frequency (the number of waves per time interval), whereas the latter frequency is replaced by the wavenumber or what is called spatial frequency, *K* (number of waveform cycles per unit distance). There is an intrinsic relationship between wavelength (λ) and wavenumber (*K*), following the expression:

$$K = \frac{2\pi}{\lambda} \qquad [4.11]$$

Periodic waveforms seem complex wave signals that need to be split and study separately (*Welch,* 1967). By means of the mathematical technique of Fourier analysis, any periodic waveform can be decomposed into a series of simple (sin or cosine) waves whose frequencies are integer multiples of the basic repetition frequency (fundamental frequency, 1/T). Moreover,

the method allows the representation of these waveforms over the time domain (by expressing amplitude as a function of time) or in the frequency domain (expressing amplitude and phase as frequency functions). For that reason, this method can provide insights into the relationship between potential fields (gravity) and topography.

The Fourier transformation is consequently given by the relation:

$$\Delta g(x) = \sum_{n=1}^{N} [(a_n \cos(nkx) + b_n \sin(nkx)] \qquad [4.12]$$

where g(x) is the composed function defined from N data equally spaced along the length kx and it is expressed as a function of sine and cosine. an and bn are the amplitudes of the sin and cosine respectively. The an value corresponds to twice the mean value of the function. Therefore, the first term of the equation g(x) represents the function within the space domain, while the second term represents the function in the frequency domain and it is called Discrete Fourier Transform (DFT).

The a_n and b_n terms are defined by the following equations from which the wavelength (λ) can be obtained:

$$a_n = \frac{2}{\lambda}\int_0^{\lambda} \Delta g(x)\cos(nkx)dx = \frac{1}{\pi}\int_0^{2\pi} \Delta g(x)\cos(n\theta)d\theta \qquad [4.13]$$

$$b_n = \frac{2}{\lambda}\int_0^{\lambda} \Delta g(x)\sin(nkx)dx = \frac{1}{\pi}\int_0^{2\pi} \Delta g(x)\sin(n\theta)d\theta \qquad [4.14]$$

Notice that the Fourier transform has a number of important properties like symmetries (components of a Fourier pair are interchangeable, i.e. in the short-term equation: g(t)=G(f) *G(f)=g(t)), linearity, scaling or differentiation, etc.

4.3.3.1 Data processing

The Fourier analysis may result arduous and difficult to accomplish by hand. An easy way to observe the fundamental wavelength is by means of the spectrum or graphical representation of the weightening functions. During the last decades the Fourier transformation has been programmed for computers, using the Fast Fourier Transform (FFT) algorithm following the Cooley-Tukey method (*Welch,* 1967; *Brigham,* 1974). This algorithm breaks the DFT into smaller DFTs making the Fourier analysis faster and efficient.

The DFT was accomplished by re-escaling the model sizes to nature. Six samples were studied (two per model and two more for the natural example Iberia). The cross-sections were obtained parallel to the main convergence direction. Subsequently the profiles were 545 km long profiles with a sampling pixel of 1 km for models and 2 km for Iberia (due to the grid resolution). Computer software able to accomplish the DFT allows amounts of observations about 512, 1024, 2048 or 4096. Finally, since the frequency range covered by the DFT depends on the amount of measurements and the sample frequency, the higher sample interval chosen must be 512 if a mean profile length of 545 km is taken into account.

4.4 Modelling results

4.4.1 Model with homogeneous strong lithosphere (IBERIA-I)

» *Topography*

During the first increments of shortening, deformation was distributed in front of the advancing wall leading to general uplift, which was controlled by closely spaced pop-ups and thrust [Fig.4.6a]. Later stages of deformation were characterised by advance of thrusting and associated uplift of the model surface. The lithospheric structure is characterised by folding and displays a regular wavelength of the ductile layers [compare 3D model in Figure 4.6b with spectrums from Figure 4.9a]. In addition, thickness variation within the lower crust amounts to about 40% of the initial layer thickness and depend on their position within the fold; i.e. thicker in the synforms and thinner in the antiforms.

» *Gravity anomalies*

The resulting gravity interpretation in Figure 4.9a shows two areas where gravity is anomalously low, which correlate with the deepest position of the Moho [compare Figure 4.6b with profile X-X´ in Figure 4.9a]. In contrast, profile Y-Y´ shows a broad anomaly, where gravity values are low, along most of the cross-section. This anomaly smoothes-out toward the less deformed area situated at distance to the moving wall. The Moho along this profile maintains a constant depth compared to section X-X´ [Fig.4.9a].

The spectral analysis carried out on topography and theoretical gravity shows two different wavelengths for the topographic data. Scaled to nature these show a short (40-50 km) and a long wavelength (250 km). However, the analyses carried out on profile Y-Y´ shows wavelengths for topography between 40-80 km and 150-250 km. The analyses of gravity indicate a dominant wavelength of about 150 km that correlates with the Moho geometry [Fig.4.9a].

4.4.2 Model with lateral strength variations (IBERIA-XIX)

» *Topography*

Localization of deformation is strongly controlled by the presence of pre-existent weak zones and the rheological difference between the two lithospheres [Fig.4.7a compare topo-view images with digital elevation models]. In model IBERIA-XIX strike-slip deformation, which was confined to areas where zones of weakness existed [Fig.4.7a] was followed by dominantly thrusting between 10% and 15% BS [Fig.4.7b]. The style of the latter is thrusts and pop-ups, which occur within a zone of limited width and are separated by seemingly undeformed and elevated regions. Different to model IBERIA-I, the amplitude and wavelength of the folding are bigger. Moreover, while thrusting was distributed throughout the model interior within the strong lithosphere, the weak lithosphere showed localised deformation. Interference patterns between E-W, NE-SW and NW-SE striking crustal structures developed during the same episode of shortening. Topographic profiles in Figure 4.9b show height differences from lithosphere to another [compare profiles in Fig.4.9b]. Accordingly, the Moho is at greater depth where the lithosphere is weak and where inherited zones of weakness were present at the onset of shortening.

» *Gravity anomalies*

Major differences in amplitude of predicted gravity anomalies are clearly seen from one cross-section to another. In cross-section X-X´, gravity anomalies hardly fluctuate between 0 mGal

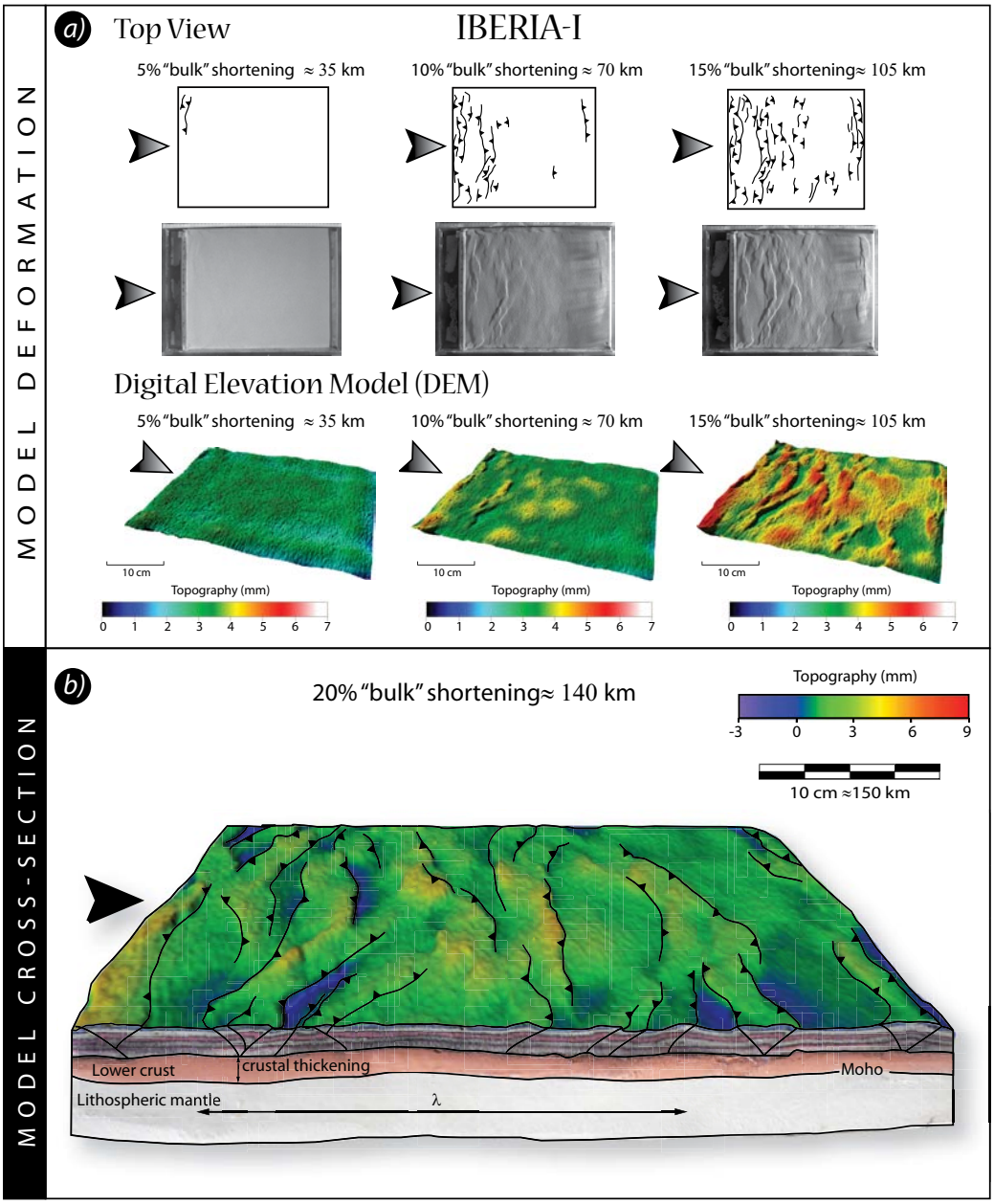

Figure 4.6 *(a) Model deformation consisting of structural interpretation of surface structures and digital elevation models showing episodes of uplift in model IBERIA-I. (b) 3D model after deformation and structural interpretation.*

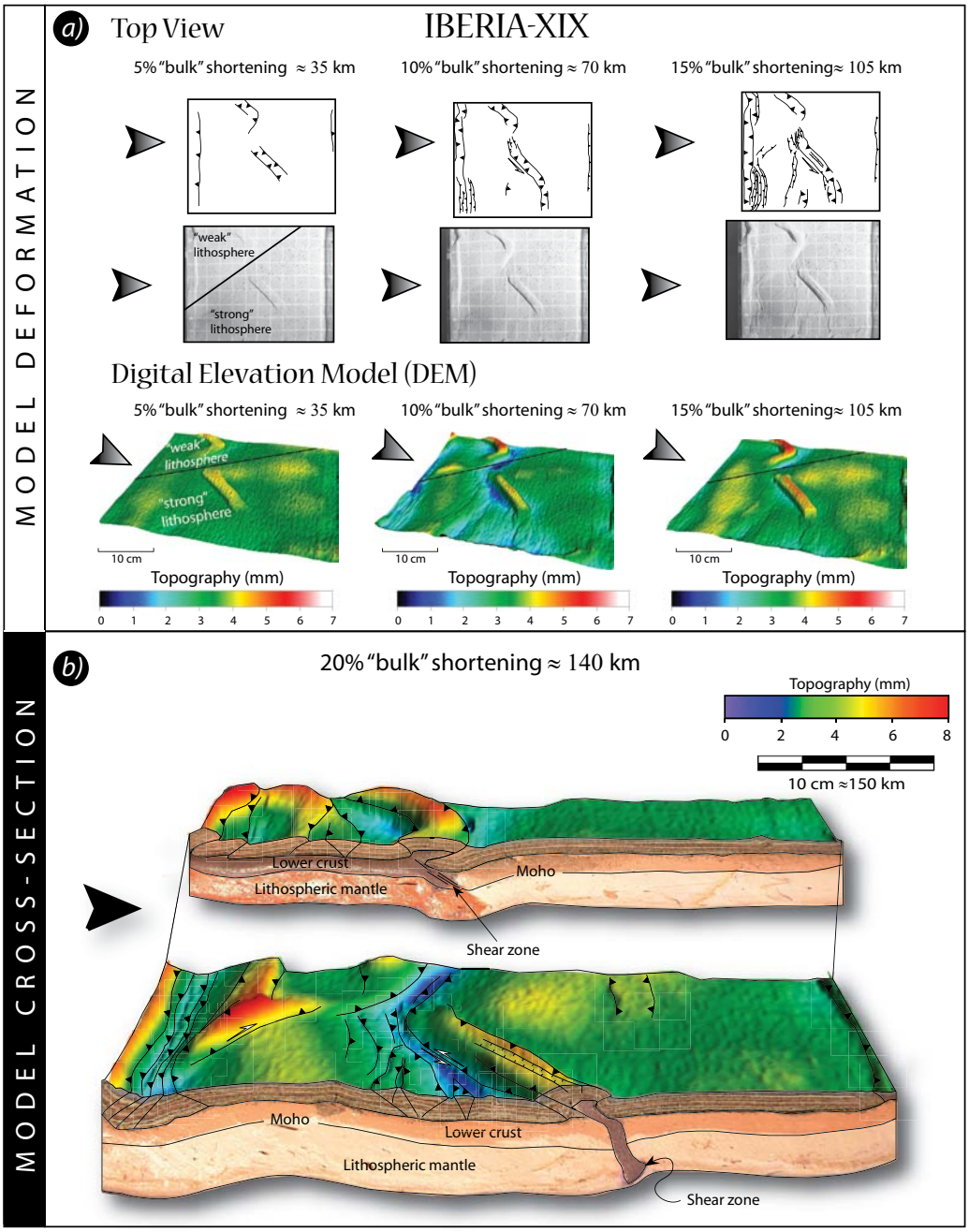

Figure 4.7 *(a) Several episodes of deformation from model IBERIA-XIX with heterogeneous lithosphere. (b) 3D model showing differences on mode of deformation (thickening vs. folding). See text for further details.*

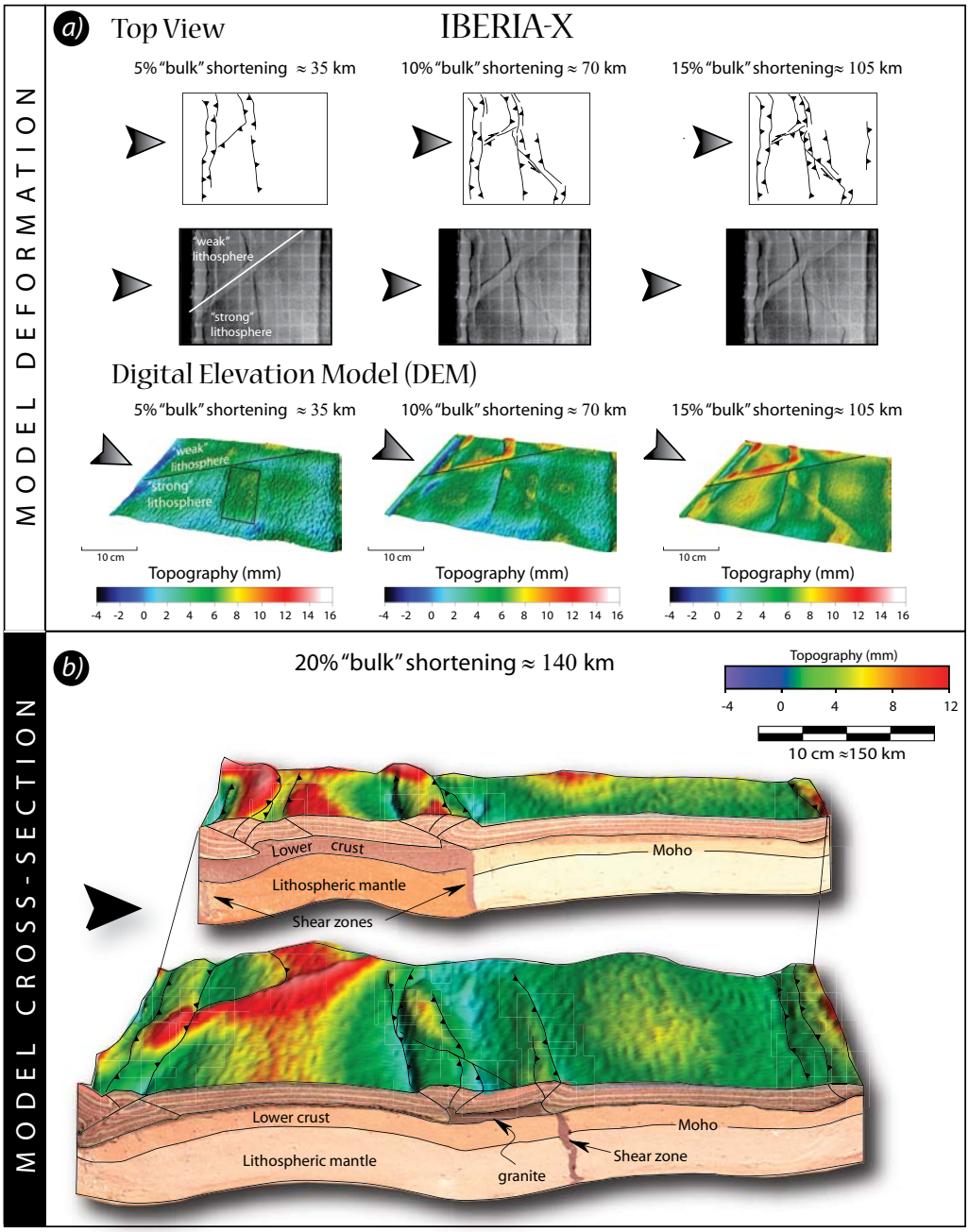

Figure 4.8 *Modelling results of IBERIA-X with heterogeneous lithosphere and E-W weak zones. Panel (a) shows structural interpretation and digital elevation models. (b) 3D model displaying the influence of weak zones on lithospheric folding localization and amplification.*

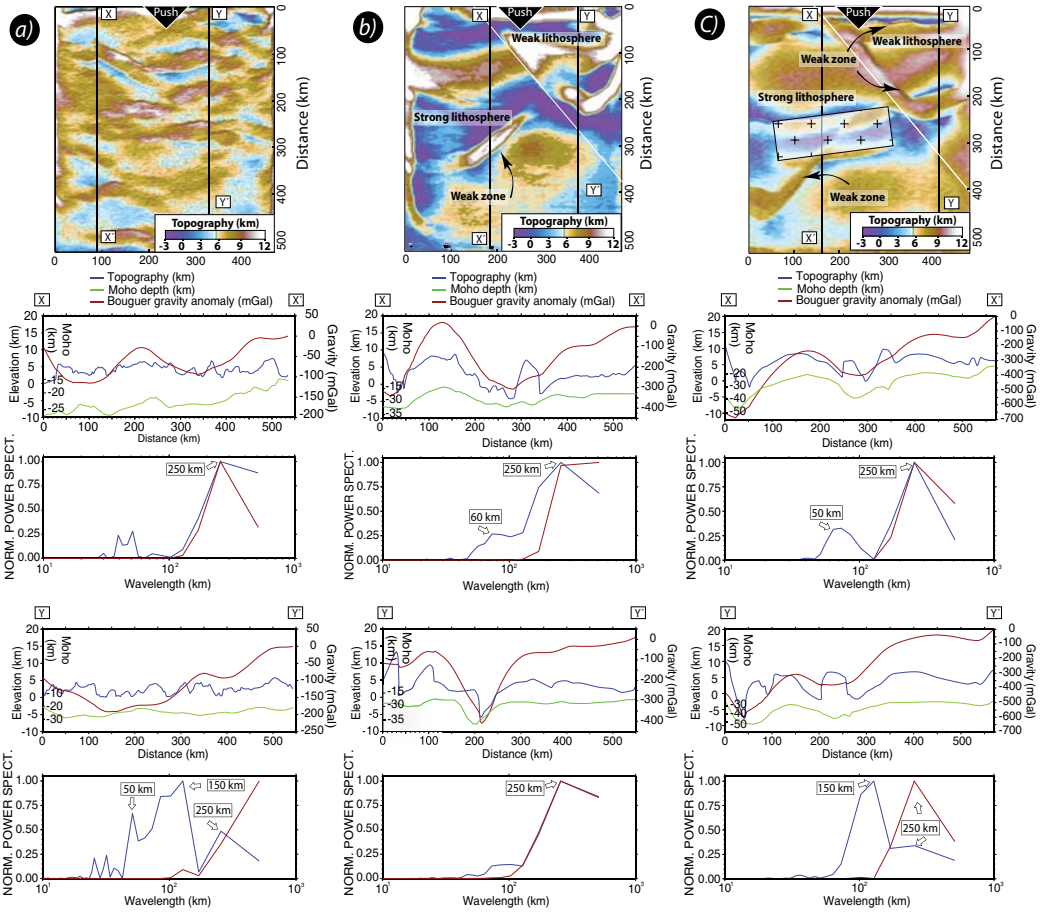

Figure 4.9 *Comparison between topography, Moho depth and Bouguer gravity anomaly and calculated spectrums for gravity and topography in experiment model IBERIA-I (a) along profiles X-X´ and Y-Y´. Digital elevation model from model IBERIA-XIX (b) profiles X-X´ across the strong lithosphere and Y-Y´ throughout the weak lithosphere. (c) Digital elevation model from model IBERIA-X and cross-section along profiles X-X´ (strong lithosphere) and Y-Y´(weak lithosphere).*

and -300, whereas along Y-Y´, amplitude varies between 0 and -420 mGal with a strong gravity minimum, highlighting the position of the deepest Moho [Fig.4.9b and 4.11]. The spectral analyses of topography and gravity shows wavelengths of 60-80 km and 150-250 km for topography and 250 km for the gravity signal along the cross-section X-X´ and 80 km and 250 km for the topography and gravity signals along cross-section Y-Y´ [see arrows in Fig.4.9b]. Additionally, when a linear filter is applied to the digital elevation model re-scaled to nature at 250 km, the wavelength of the mantle is reflected on the topography, indicating a series of uplifted areas from those subsiding following the pattern of folding [Fig.4.12].

Domains governed by crustal thickening are localised along the main synforms and near the contact with the weak zone [compare models in Figure 4.7 and 4.8]. The weak lithosphere shows a broad depression of the Moho in the central part of the model correlating with a strong gravity low [Fig.4.9b profile Y-Y´]. In contrast, the stronger lithosphere show a periodic pattern of the gravity and Moho signals related to the effect of folding [model IBERIA-XIX Fig.4.9b profile X-X´ and Fig4.12].

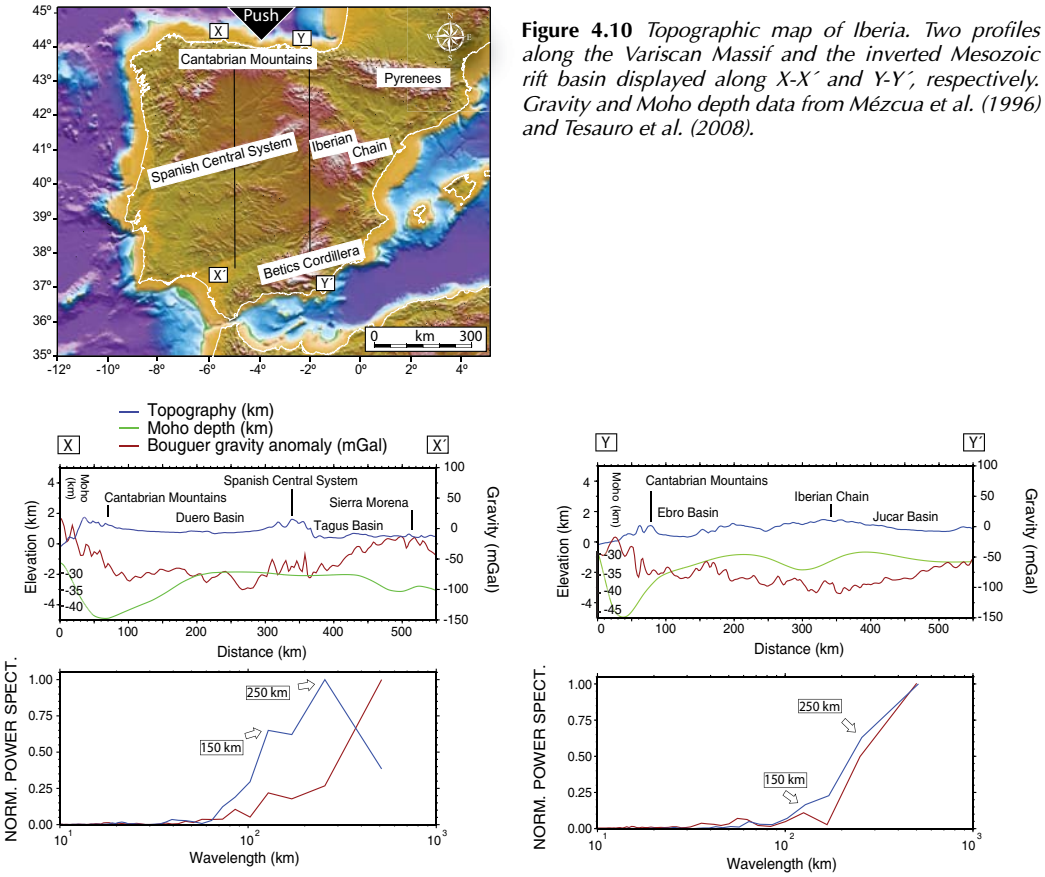

Figure 4.10 *Topographic map of Iberia. Two profiles along the Variscan Massif and the inverted Mesozoic rift basin displayed along X-X´ and Y-Y´, respectively. Gravity and Moho depth data from Mézcua et al. (1996) and Tesauro et al. (2008).*

4.4.3 Model with lateral strength variations and E-W Mesozoic depocentres (IBERIA-X)

» *Topography*

In model IBERIA-X with similar set-up as previous model IBERIA-XIX, but with the presence of zones of weakness representing granites, late-Variscan structures and E-W Mesozoic depocentres across the weak lithosphere, deformation by thrusting was confined to the area close to the backstop and along the central weak zone (granites) connected by an oblique thrust up to 10% BS [Fig.4.8a]. Uplift is restricted towards the weak lithosphere and the central part of the model. Thereafter, deformation propagated outward, localising along the central part of the model through a series of thrusts and leading to the reactivation of the oblique weak zone in terms of strike-slip movement. Elevated topography continued rising along the weak lithosphere and the central part of the model (area of granites emplacement). Between 15 and 20% BS, uplift was related to those areas previously active, leading to an increase of the final elevation. Granites localized deformation along a series of pop-ups situated at the borders causing an area of subsidence in between. It is worth noticing that depocentres situated in the weak lithosphere reactivated controlling the wavelength of lithosphere synclines that uplifted topography. Pre-existent weak zones oriented 20º with the shortening direction were not reactivated, whereas

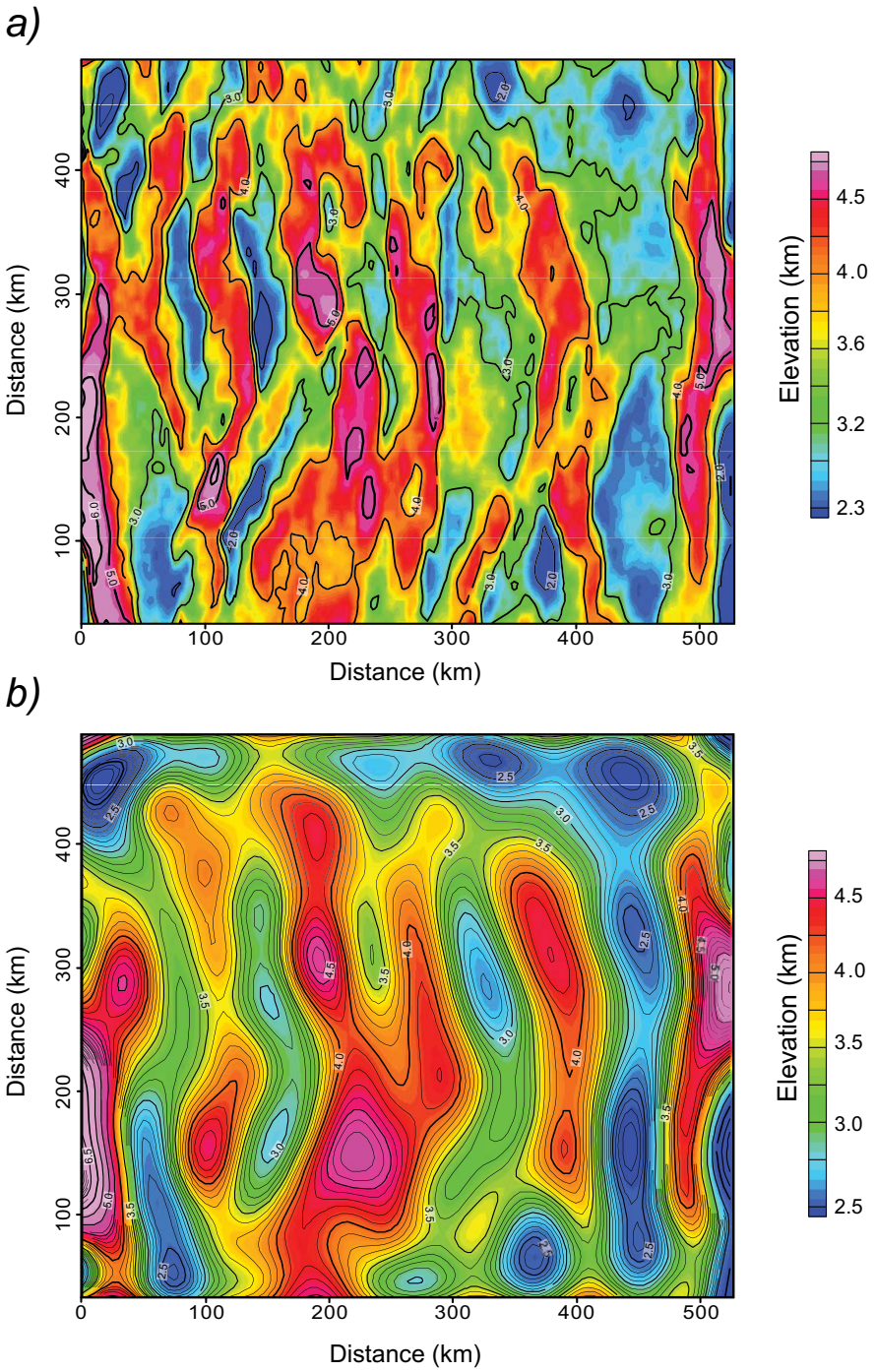

Figure 4.11 *(a) Digital elevation model and topography contour levels from model IBERIA-I (re-scaled to nature). B) Surface topography after applying a cosine roll-off filter at 150 km wavelength, showing the strong imprint of mantle deformation. Shortening from the left side.*

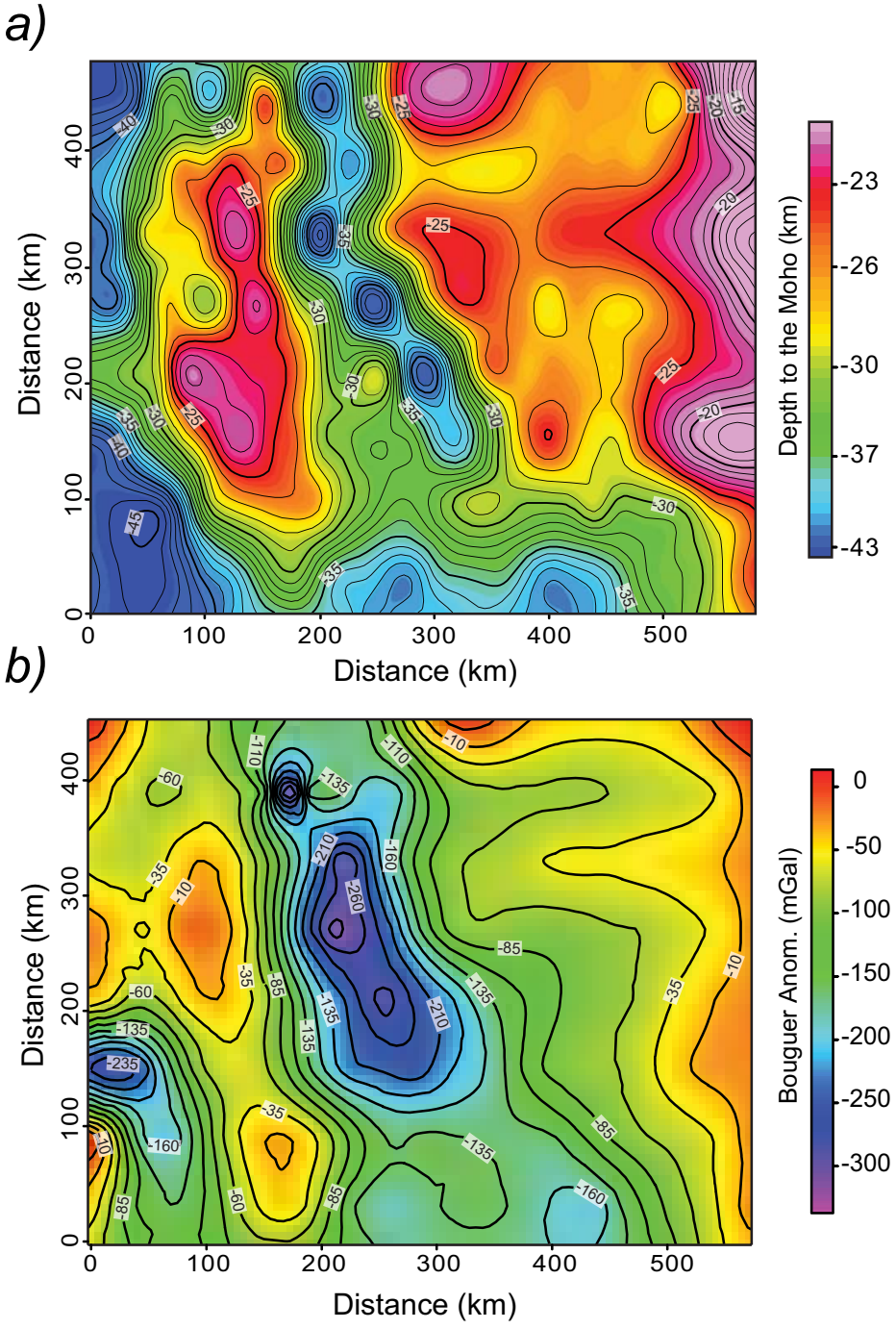

Figure 4.12 *(a) Moho depth map of model IBERIA-XIX. (b) Bouguer gravity anomaly.*

those comprising angles of 45º and 90º were all reactivated causing surface uplift.

» *Gravity anomalies*

The main difference with the previous models arises from the pronounced wavy surface of the Moho reaching deeper values along the weak and strong lithospheres. These major depressions are characterised by strong gravity lows (-500 to -300 mGal) [Fig. 4.9c, compare profiles X-X´ and Y-Y´]. Profile Y-Y´ shows two broad depressions of the Moho fairly correlated with theoretical gravity minimums, whereas these depressions are less pronounced along profile X-X´ [Fig. 4.9 and 4.14]. The observed differences with previous models reflect the influence of weak zones (both E-W depocentres and granites) and their contribution to fold localization.

Concerning the spectral analysis showed in profile X-X´ [Fig. 4.9c] displays wavelengths of topography about 50 km (short) and 250 km (long). However, gravity and topography signals match at 250 km wavelength. However, profile Y-Y´ shows a shift on topography wavelength to 150 km probably influenced by the position of the E-W trending weak zones that simulate the Mesozoic depocentres. Again, this profile indicates a match on topography and gravity at 250 km wavelength. Furthermore, a low-pass filter at 250 km was applied to the digital elevation model of the experiment surface. The result shown in Figure 4.15b reflects the effect of mantle deformation on surface topography indicating a series of elevated areas and subsiding domains extending periodically that are subsequently related to folding of the lithosphere.

4.5 Discussion

4.5.1 Lithosphere strength variations and topography

As a result of the Iberia-Eurasia collision, large-scale folding has been advocated to have shaped the early Cainozoic topography of Iberia (*De Vicente and Vegas,* 2009). This process is supported by periodically recurring variations of crustal thickness, topography and Bouguer gravity anomalies (*Stephenson et al.,* 1990; *Stephenson and Cloetingh,* 1991; *Burov et al.,* 1993; *Cloetingh et al.,* 2002). Analogue modelling results show that the strike (E-W, NW-SE and Ne-SW) and elevation (amplitude and wavelength, respectively) of topography are the response of the lithosphere to specified rheological boundary conditions including lateral strength variations and inherited structures. The spectral analysis of topography and gravity has been deployed to distinguish periodic from non-periodic signals over large areas. As such, presence/absence of periodicities can be used as a proxy to infer the dominant mode of deformation; i.e. folding versus thickening. Comparison of model profiles (topography, crustal thickness and gravity) and nature suggest that the observed periodicities are in phase as a result of large-scale folding within the strong lithosphere in the west, whereas the lack of regular signals (opposite phase) in the weak lithosphere to the east may indicate crustal thickness variations related to thrusting in the brittle and some kind of flow in the ductile crust.

The gravity and topographic profiles along western Iberia show long wavelengths around 150-300 km (*Muñoz-Martín et al.,* 2010), [Fig.4.10], most probably related to mantle deformation as also predicted by the analogue model results, while short wavelengths observed in topography (40-80 km) are related to crustal deformation (thrusting). However, such short signals appear attenuated by the influence of erosion processes and the presence of lateral density variations due to igneous intrusions within the crust which have not been incorporated in the analogue models.

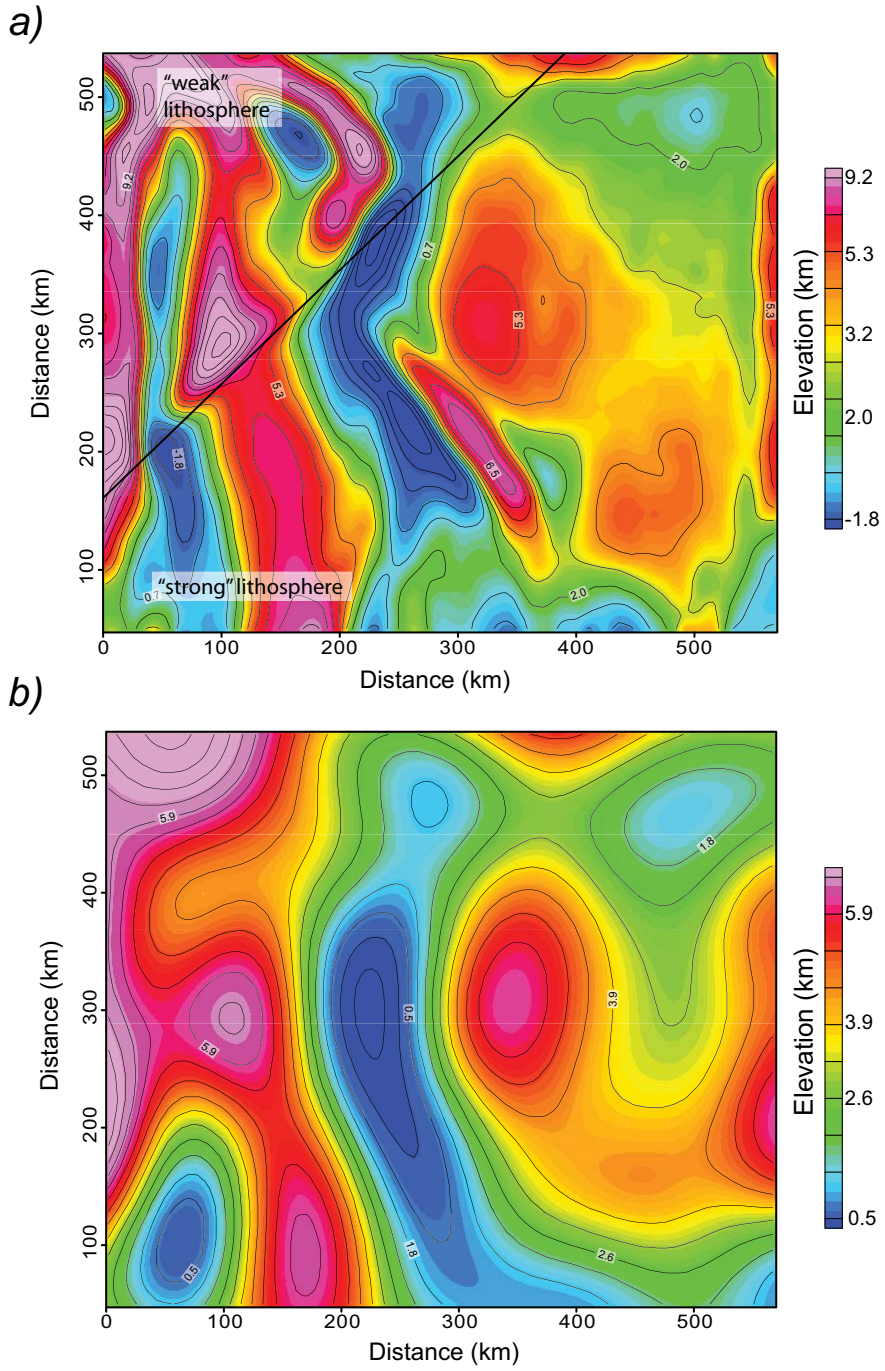

Figure 4.13 *(a) Digital elevation model and topography contour levels from model IBERIA-XIX (re-scaled to nature). Harmonic surface at 250 km wavelength, controlled by mantle deformation. Shortening from the left.*

The high topography associated with relative gravity maximums observed in the experiments [compare Figures 4.9 and 9.10] contrast with the lack of such features in nature where the main depressions are found. A feasible explanation stands for the presence of another mechanism that may have been involved in the Cainozoic evolution of topography in Iberia. This mechanism proposed by *Vergés and Fernández* (2006), invokes Neogene-Quaternary extension along the eastern margin of Iberia and it has been related to back-arch extension of the western Mediterranean. These authors suggest the possibility of a process of dynamic topography caused by isostatic reorganization due to a thermal anomaly located in eastern Iberia. In favour of this hypothesis, it is important to point out the presence of volcanism associated with this thermal anomaly along the Valencia Trough and the Catalan-Coastal Ranges (*Morgan and Fernández,* 1992; *Watts and Torné,* 1992; *Lewis et al.,* 2000). Another remarkable process that may explain such contrast in the topography and gravity signals can be related to Isostatic readjustment that occurred during the formation of the mountain ranges and subsequent vertical loads. This mechanism may explain high altitudes observed along the Duero basin related to the vertical load exerted by the Cantabrian Mountains and Spanish Central System during their uplift. This process can be influenced by the presence of erosion due to the fact that vertical movements and reactivation of mountain fronts is facilitated by erosion/sedimentation processes as it has been suggested by *Persson and Sokoutis* (2002) and *Bonnet et al.* (2007)

The Moho of the models deepens at synclines where topography is developed (through a series of pop-ups and thrusts) and shallows at antiforms. The Duero Basin is considered as a natural analogue that overlays upward deflected Moho related to buckling of the lithospheric mantle, because it maintains higher overall elevation than the Tagus and Guadiana Basins, respectively, demonstrating the tilting of the Iberian Meseta towards the southwest. This feature is also observed in model IBERIA-XIX along the strong (Variscan) lithosphere [Fig.4.9b]. The combined effect of flexural load caused by the Cantabrian-Pyrenean crustal wedge together with the lithosphere buckling mechanism can explain the pattern of basin uplift observed close to the convergence border along the strong lithosphere. However, this is not observed on the weak lithosphere where deformation is confined to a single syncline of thickened crust. Conversely, the relative homogeneous elevations observed along the eastern part of the Iberian Peninsula [compare Figure 4.9 b, c and 4.10] may be explained by the dominance of ductile thickening mechanism rather than folding.

4.5.2 The role of late-Variscan structures during Cainozoic deformation of Iberia: do they really influence folding?

Reactivation of pre-existent zones of weakness in the models led to strike-slip displacements during N-S shortening [compare models IBERIA-I and IBERIA-XIX in Figures 4.6 and 4.7]. Moreover, NE-SW striking faults accommodated left-lateral movements, whereas NW-SE striking faults were right-lateral. With the advance of deformation these faults became re-activated as thrusts leading to localised uplift. Natural examples of Iberian faults with similar behaviours are found along the Messejana-Plasencia and Somolinos Faults, respectively. The fact that these inherited late-Variscan faults have been reactivated during N-S Cainozoic compression showing different regimes (strike-slip and thrusting), indicates the importance of strain partitioning processes affecting indistinctly both the strong and weak lithospheres under a single phase of deformation.

The present-day topography in Iberia, therefore, is probably the result of a combination of deformation mechanisms. On the one hand, periodic large-scale folds extending along the westernmost part interfere with a series of inherited late-Variscan faults (i.e. Messejana-Plasencia Fault) giving rise to E-W to NE-SW trending mountain uplifts regularly spaced. On the other hand, topography in the eastern part follows NW-SE and E-W trends controlled by crustal thickening

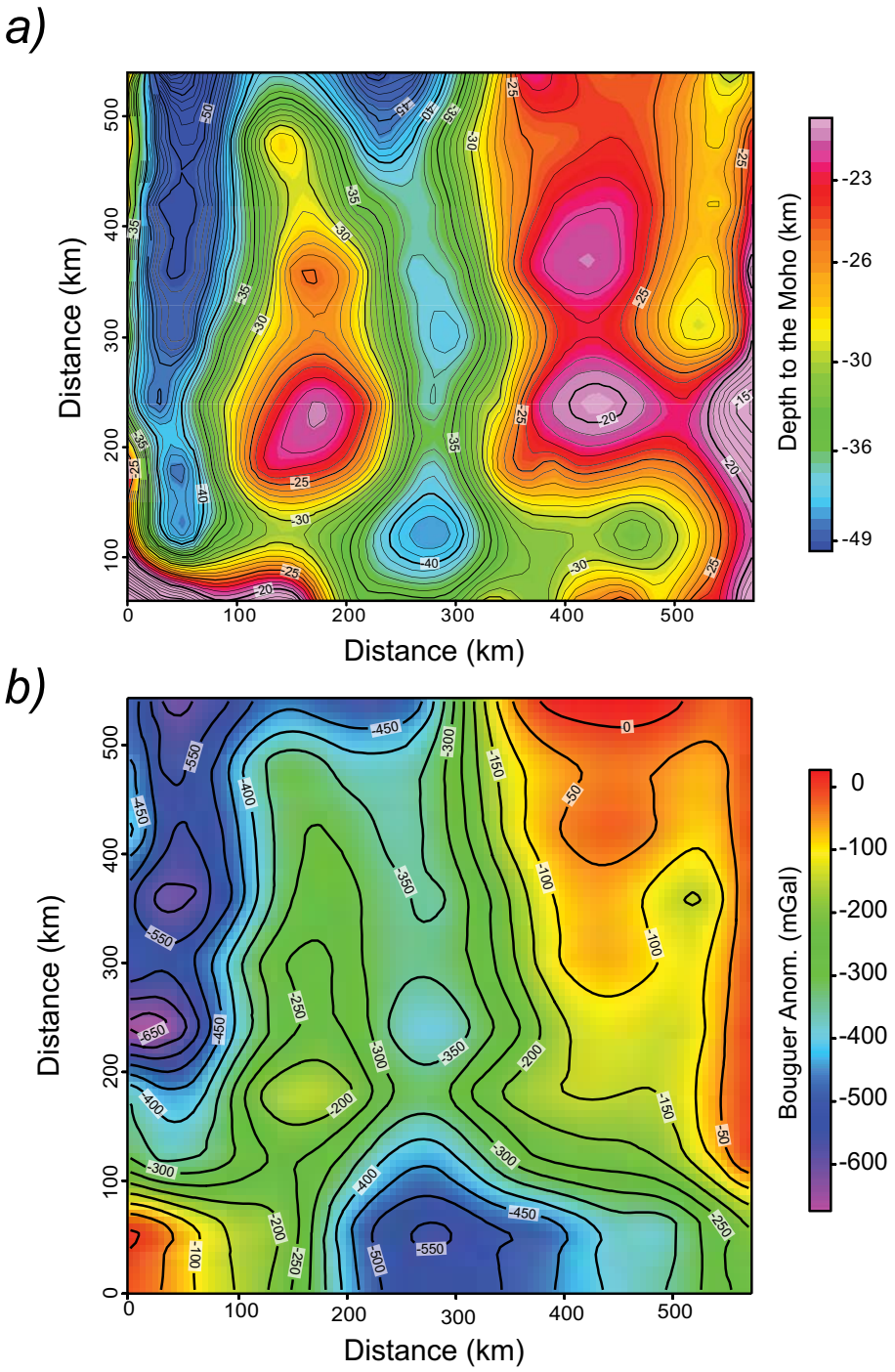

Figure 4.14 *(a) Moho depth contour levels of model IBERIA-X. (b) Bouguer gravity anomaly map.*

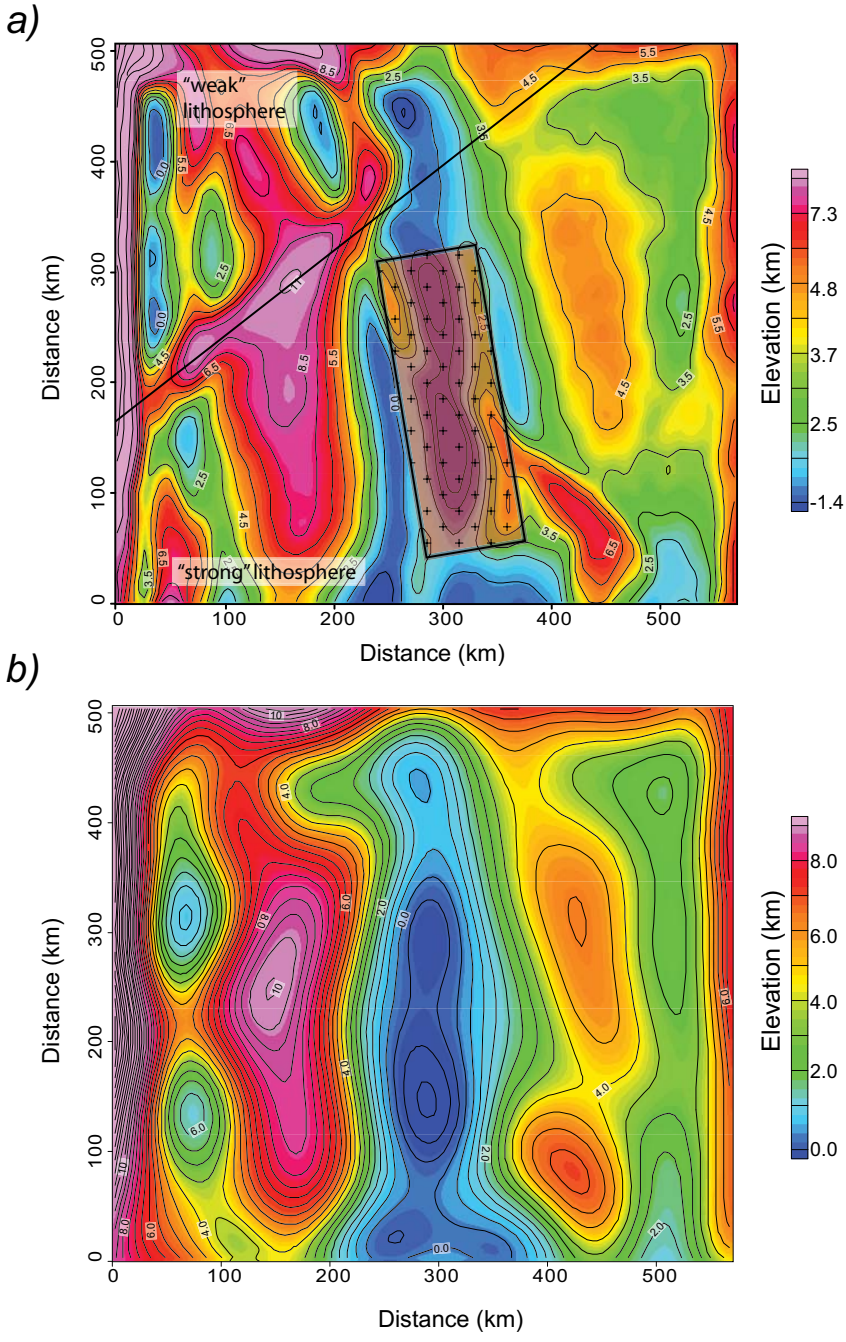

Figure 4.15 *Digital elevation model and topography contour levels from model IBERIA-X (re-scaled to nature). Surface topography after applying a low-pass filter at 250 km wavelength, showing the strong imprint of mantle deformation. Shortening from the left.*

related to reactivation of Mesozoic rift-related structures, which localised deformation during the Cainozoic (i.e. Somolinos Fault). However, hardly any topographic periodic pattern has been observed in this domain [Fig.4.10]. The methodology based on integration of gravity and topography analysis aimed to distinguish periodic from non-periodic patterns and observe the role of inherited structures on strain localization and topography build-up.

Particularly interesting is the fact that fold wavelengths are influenced by the presence of pre-existent structures in the models such as weak zones. The control exerted on fold wavelength has long been recognised in several studies (*Cobbold,* 1975; *Smith,* 1975; *Martinod and Davy,* 1992; *Martinod and Davy,* 1994; *Williams and Jiang,* 2001).

Paradoxically the models shown in this chapter preserve nicely folded lithospheres independently of both, rheological differences within the lithosphere and presence of pre-existent structures. However, the fold wavelength seems to be influenced by the position of such tectonic structures [compare Figures 4.6, 4.7and 4.8]. Inherited faults favoured strain localization and subsequent ductile thickening of the lower crust and mantle. This process of thickening was more efficient at those structures affecting a weak lithosphere. Moreover, after the fold growth has reached the crustal heterogeneity, the shape of the fold flattens out, decreasing the amplitude as well as the wavelength.

It is also important to remark the importance of the weak zone representing the granites of the Spanish Central System. This feature is reactivated immediately in the subsurface by thrusting, and led to fold growth and amplification of a broad synformal structure in the central part of the strong lithosphere. Apparently, these pre-existent structures affect the gravity signal, highlighting the differences of lithospheric strength by correlating areas of major crustal thickening with gravity lows. Models suggest that the different amplitudes and wavelengths observed from one lithosphere to another are indicative for lateral strength variations and the associated mode of deformation, influenced by the presence of pre-existing structures during compression. Therefore, these differences may have played an important role in nature during the final configuration of mountain ranges at the onset of the Cainozoic deformation.

4.6 Conclusions

Gravity undulations highlight differences of Moho topography in the models. Therefore, areas of thickened crust (synforms) are represented by low values of the Bouguer anomaly, unlike the thinned areas (antiforms). The newly developed methodology to perform spectral analyses of gravity and topography of analogue models also provides valuable information about the mechanism involving large-scale deformation in areas of intra-plate mountain building. Under this premise, the observed E-W trending periodic topography in western Iberia with wavelengths of about 250 km is representative of folding of the entire lithosphere, while the short wavelengths (50-80 km) involve crustal deformation. NW-SE and E-W topographic highs observed in the eastern part of Iberia are explained in terms of process of crustal thickening by the combined effect of ductile flow in the lower crust and thrusting. These differences arise from lateral thermo-mechanical variations across Iberia that efficiently controls the mode of lithosphere deformation.

Chapter 5

Strain partitioning and intra-plate deformation: the role of lateral strength variations in Central Iberia.

The boundary between the Spanish Central System and the Iberian Range in central Spain represents two well differentiated structural domains characterised by changes of fault orientation, deformation style and fold interference patterns. Present-day topography of the Iberian Range follows the tectonic trend of major Mesozoic rift-related structures, which have been inverted during Tertiary times (NW-SE, E-W and NE-SW). However, the mechanism that governs the observed topographic patterns remains unclear. In this chapter, I present a series of analogue models implemented with lateral lithosphere strength variations that aim to clarify the role of thermo-mechanical changes on mode of lithosphere deformation between central and eastern Iberia. Moreover, the analysis of the particle displacement field carried out over the surface of the models allowed to constrain the effect of inherited late-Variscan structures distinguishing among re-activated and neo-formed structures during N-S directed shortening related to the episode of Alpine deformation. The modelling results suggest that most of the pre-existing tectonic structures were reactivated with different kinematic regimes. Furthermore, strain has been partitioned into strike-slip faulting along NE-SW and NW-SE trending faults as well as thrusting along E-W trending structures. Although, inherited structures in general led to strain localisation in the models, the presence of a weak zone representing the Central System favours deformation in that region indicating that the late-Variscan faults may have little or no influence on the Cainozoic evolution, reactivation and uplift of the Central range.

5.1 Introduction

Regions of intra-plate deformation result from the effective transmission of tectonic stresses developed at active plate boundaries. This mechanism of tectonic steady state is reached when continent-continent collision attains the condition of mechanical plate coupling (*Ziegler et al.,* 1995; *Van Wees et al.,* 1998; *Luth et al.,* 2009). As a result, driving forces cause basement deformation through faulting that in turn, involves the overlying sedimentary cover. Consequently, folding and thrusting have been defined as common processes for crustal thickening within intra-plate domains (*Ziegler et al.,* 1998). However, these mechanisms can be caused either by several

stages of deformation or a single episode. Besides both mechanisms may independently characterise highly deformed thrust-belts, differentiating among multiple tectonic stages in the field can result complicated. A good example is the Iberian Range, located in eastern Iberia, where several episodes of deformation have been suggested in order to explain faulting and folding interference patterns.

The Iberian Range formed part of the Permo-Cretaceous rift basin (Iberian Basin) governed by major listric faults that played a key role on the final configuration of the basin depocentres during the Jurassic and Cretaceous period.

Subsequent Cainozoic tectonic inversion of the Iberian Basin, led to the final NW-SE trend of the Range during the Pyrenean and Betic orogenesis, respectively. As a result, a complex stress-field has been deduced from paleostress analysis (*Simón-Gómez,* 1986; *Liesa and Simón-Gómez,* 2009). In fact, the paleostress results are based on superimposed patterns of folding probably influenced by pre-existing rift geometries (inherited from the Mesozoic), and subsequent stress-field changes driven along plate boundaries during the Tertiary. Recently, *De Vicente and Vegas* (2009a) and *Fernández-Lozano et al.* (2010) have suggested that the overall topography in Iberia developed under N-S compression as a result of lithospheric-scale folds based on previous numerical studies carried out by *Cloetingh et al.* (2002). The Cainozoic evolution of the Iberian Range has been explained in terms of strain partitioning by *De Vicente et al.* (2009b), whereas, *Fernández-Lozano et al.* (2011) have highlighted the importance of lateral lithospheric strength changes inherited from the Mesozoic extension as the underlying reason for the overall trend of intra-plate topography of the Iberian Range. In this chapter I focus on the combined effect of pre-existent faults and lithosphere strength variations on mode of deformation, in order to explain the present-day topography trends observed across Iberia. Furthermore the importance of granites and Mesozoic rifting-related fault geometries in central-eastern Spain might have played a key role on mode of crustal deformation emphasising the episodes of tectonic reactivation and uplift.

Analogue models have demonstrated to be a powerful tool to solve complex geological problems. They are suitable for modelling different tectonic regimes (*Brun,* 1999; *Willingshofer and Sokoutis,* 2009, *Leever et al.,* (2011b). Consequently, this chapter brings together analogue modelling and analysis of surface displacement field that aimed to distinguish between different proposed mechanisms of deformation (i.e. folding vs. thickening), and estimate the role that may have played during Cainozoic N-S shortening.

5.2 Geological framework

The Iberian Range located in the eastern part of Iberia represents a good example of an intra-plate basin inverted during Cainozoic compression (*Álvaro et al.,* 1979) [Fig.5.1]. Widespread extension took place during two main rifting stages (late Permian to Hettangian and late Jurassic to early Cretaceous) related to Tethys and Central Atlantic ocean-floor spreading followed by subsequent thermally induced episode of subsidence (*Salas and Casas,* 1993; *Van Wees and Stephenson,* 1995; *Arche and López-Gómez,* 1996). The general trend of the range follows an overall NW-SE orientation along the eastern part of Iberia. Despite this continuous orientation along strike, E-W to NE-SW tectonic structures interfere with each other. The Range is also characterised by a thick pile of Mesozoic sediments ranging from early Triassic to late Cretaceous in age overlying the Variscan basement. Major thicknesses of Mesozoic sediments (Cretaceous) are found N and S, along the depocentres of the Cameros and the Maestrazgo area (*Salas and Guimerá,* 1996; *Casas-Sainz and Gil-Imaz,* 1997) [Fig.5.1]. Moreover, thrusts trending E-W to NW-SE brought basement rocks to the surface and onto young Mesozoic and Tertiary sediments of the main Basins (Ebro, Duero and Tagus Basin). Intra-mountain basins also record the subsidence of the Range controlled by tectonic extension (Calatayud-Montalbán

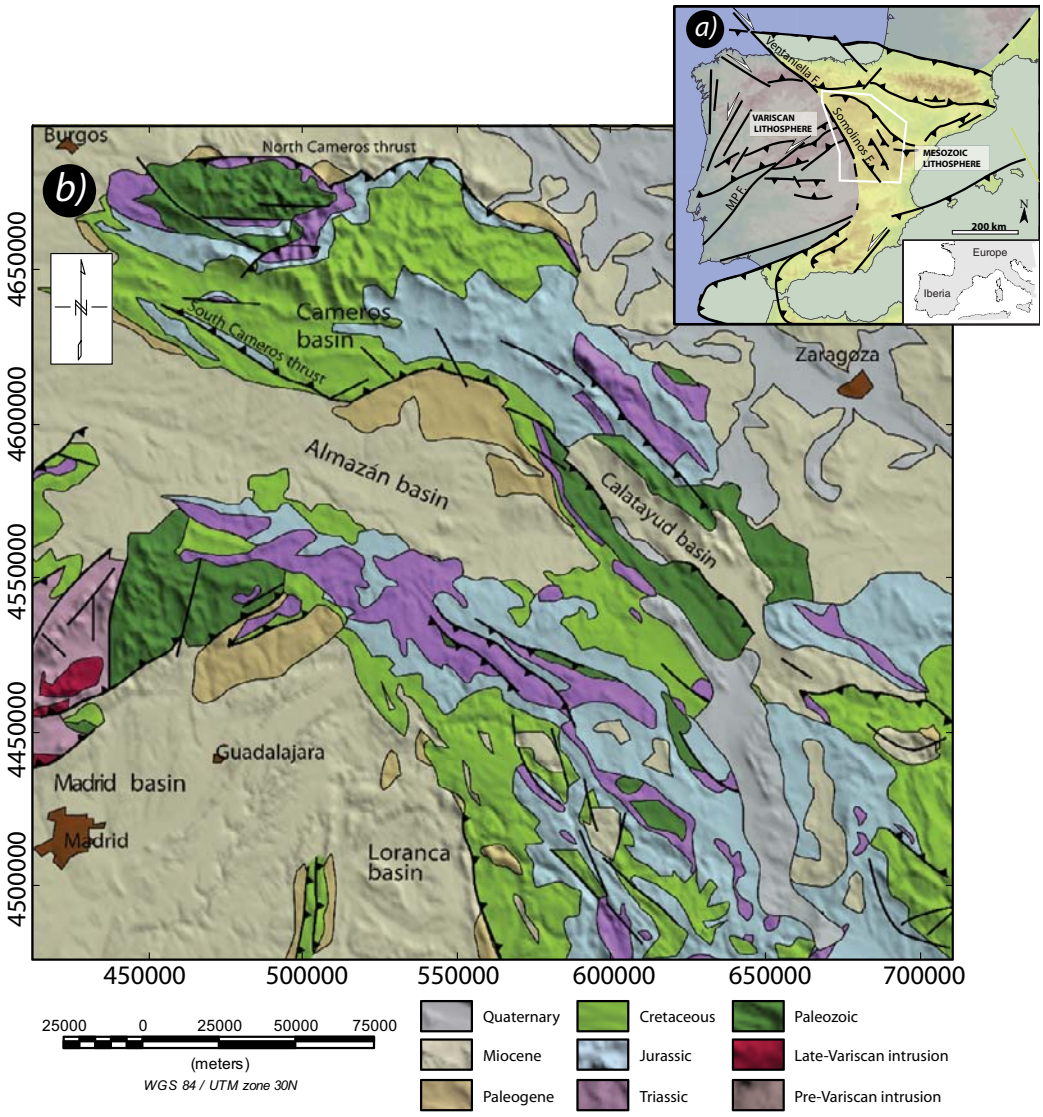

Figure 5.1 *(a) Tectonic sketch map of Iberia showing lateral strength changes from Variscan (to the west) and Mesozoic (to the east) domains referred to in this thesis. The area with the white outline denotes the location of the Iberian Range. (b) Simplified geological map of the Iberian Range.*

basin, separated by the Daroca High).

During the Mesozoic, the Iberian Range formed part of the intracratonic Iberian rift basin, controlled by widespread extensional features. However, the onset of Cainozoic compression, led to reactivation of former normal faults that turned into a complex pattern of fault systems with different orientations (mainly NW-SE, E-W and NE-SW) [Fig.5.1].

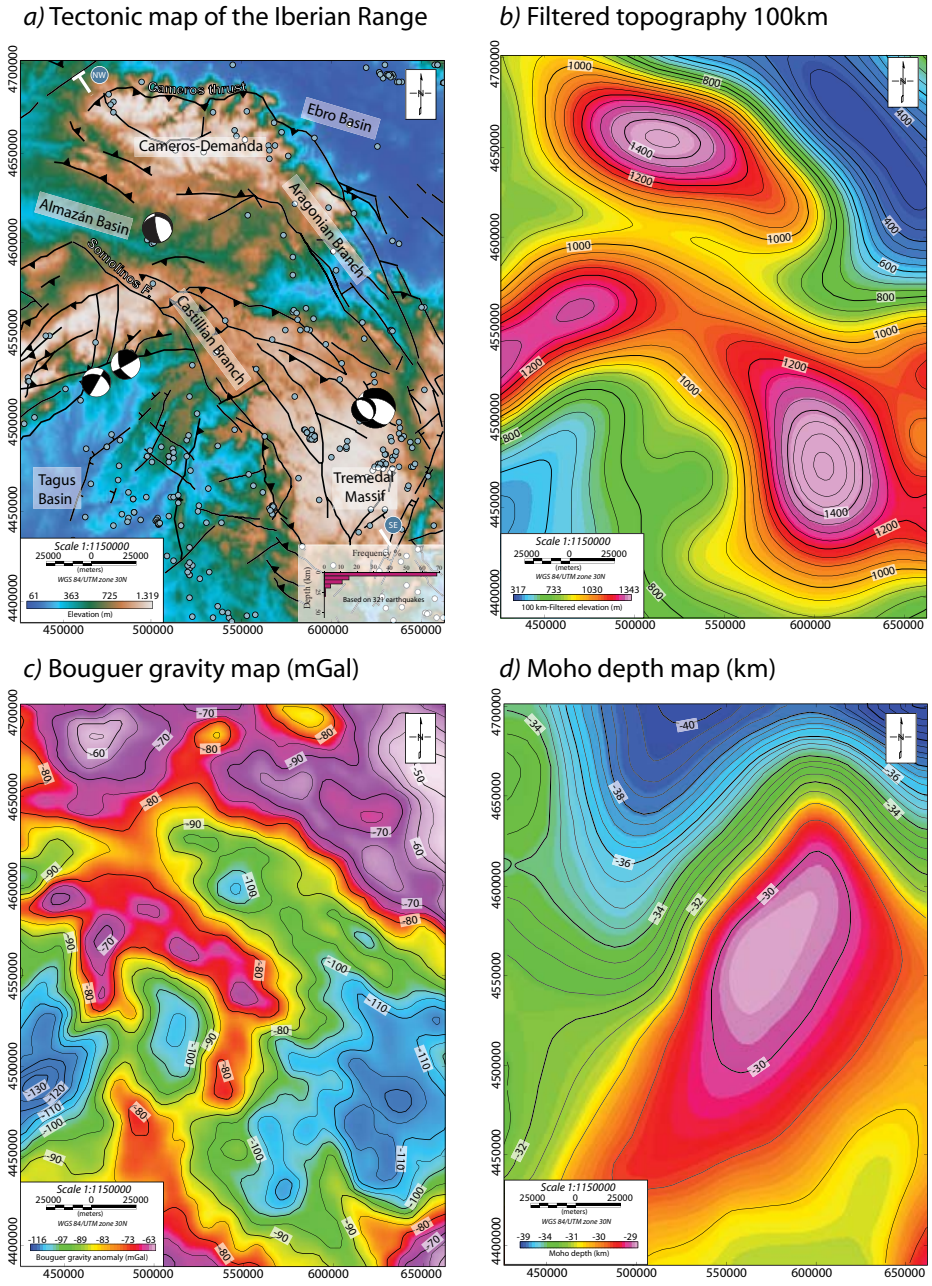

Figure 5.2 *(a) Tectonic map of the Iberian Range overlying the topography (90 m) in UTM coordinates. Focal mechanisms from Stich et al. (2003) and regional seismicity based on 321 seismic epicentres from the Spanish IGN database. Lower right inset shows the seismic distribution in depth. (b) Filtered topography showing the 100 km harmonic surfaces. Three major topographic highs become apparent related to the northeast Sierra de la Demanda-Cameros, the Spanish Central System to the west and the Albarracín Massif to the southeast. (c) Bouguer Gravity map illustrating the position of the main anomalies, data from Mézcua et al. (1996). (d) Moho map of the Iberian Range based on previous studies carried out by Tesauro et al. (2008) and Díaz and Gallart (2009).*

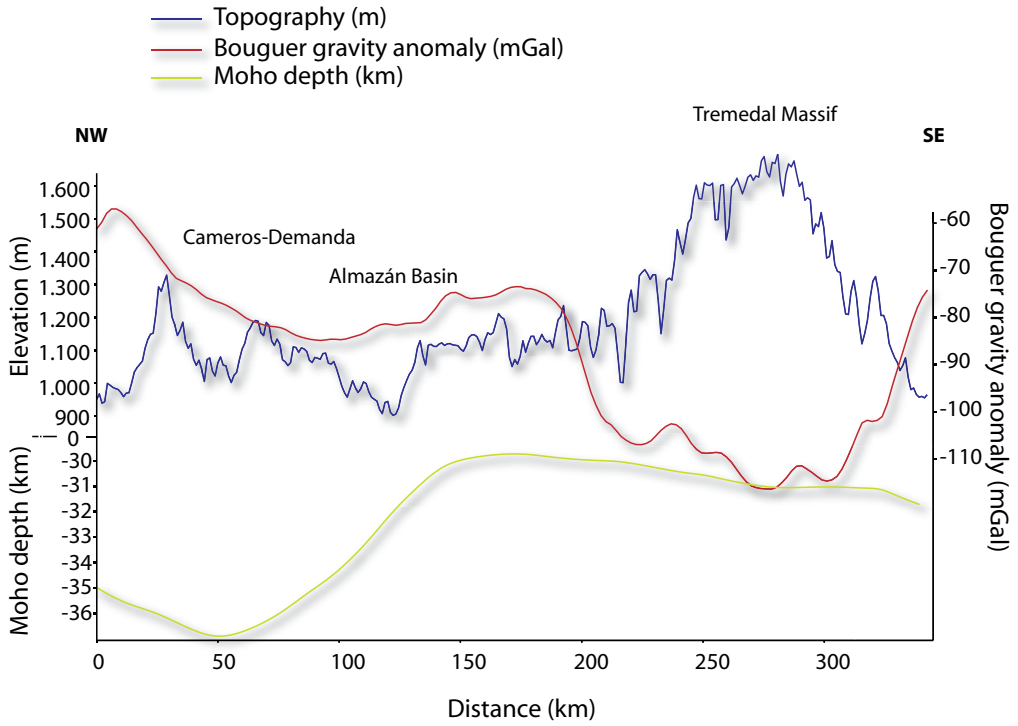

Figure 5.3 *Cross-section along a NW-SE profile displayed in Figure 5.2., portrays the strong correlation between topographic highs, regional gravity lows and deeper Moho (Moho depth and gravity data from Tesauro et al. (2008) and Mezcua et al. (1996), respectively). The increase in Moho depth is highlighted by a strong gravity low beneath the main mountain regions (Cameros-Demanda and Tremedal Massif).*

» Deep structure and regional seismicity of the Iberian Range

Seismic events are apparently scarce over the entire Iberian Range, and they are mainly distributed towards the southern part of the Chain. Despite focal depths are mostly shallower than 10 km [see Fig.5.2a], some seismic events occurred at depths of more than 20 km. In any case seismicity appears to be restricted to the upper most part of the continental crust and is often related to strike-slip and thrust faulting. However, towards the east, normal fault activity has also been recorded by fault-plane solutions related to the Neogene Teruel and Jiloca basins (*Herráiz et al.,* 2000; *Stich et al.,* 2003). These data clearly reflect the crustal and surface deformation; however, the deep structure of the chain, remains unclear well known.

Deep seismic lines (e.g. reflection) and the interpretation of gravity data have shown important differences between the lithospheric and crustal architecture of the Iberian Range (*Rivero et al.,* 1996; *Guimerá and González,* 1998; *Casas-Sainz et al.,* 2009a; *De Vicente et al.,* 2009b). Gravity data reveals a gravity minimum (-100 to -150 mGal) following NW-SE trends along the main topographic uplifts in the Iberian Range, corresponding to the Castillian and Aragonian Branches. Conversely, a NE-SW negative gravity trend defines the eastern border of the Central System [Fig.5.2c]. These regions of gravity minima are separated by NW-SE corridors with a gravity anomaly reaching -80 to -60 mGal. The effect of the sedimentary cover in the surrounding basins causes, in general, relative maxima (Ebro and Almazán Basins). However, the Tagus Basin represents a gravity minimum (-150 mGal). This local minimum has been related

to the vertical load caused during the uplift of the Central System along the southern border thrust. Consequently, gravity lows are located in areas of thickened crust, following the same trend than the main topographic highs [Fig.5.2b,c and d]. Moreover, these uplifted regions are associated with thrusting. The age of this uplift has been established to be Palaeogene to Middle Miocene based on fission track data, paleostress analysis and Tertiary sedimentary truncations (i.e. unconformities) along the borders of the Iberian Range (*Guimerá and González,* 1998; *Casas-Sainz et al.,* 2000; *Herráiz et al.,* 2000; *Mata et al.,* 2001; *Barrier,* 2002; *Guimerá et al.,* 2004; *Liesa and Simón-Gómez,* 2009).

Tertiary uplift of the Iberian Range has been associated with thrusting and folding involving basement rocks (thick-skinned tectonics), and the Mesozoic-Cainozoic sedimentary cover (thin-skinned tectonics, *Salas and Casas,* 1993). As a result the crust has been thickened, leading to significant variations on the Moho depth average (Guimerá and González, 1998). These differences are particularly important from north to south as it has been argued by *Tesauro et al.* (2008) and *Díaz and Gallart* (2009) based on the analysis of seismic receiver functions and tomographic data [Fig.5.3]. These data place the Moho depth at about 30 km in the interior of the Range and about 30 km to 32 km towards the Central System and Tagus Basin.The Moho deepens towards the northern part (Demanda-Cameros) (36-38 km) and connects with the Cantabrian-Pyerenean crustal roots (at 40 km), through the Ebro basin corridor (at 34 km). Apparently, the southern part of the Iberian Range is characterised by a relative thickening of the crust leading to Moho depths of about 35 km [Fig.5.2d]. However, *Salas and Casas* (1993) argued that the gravity low (-110 mGal) reached in the southern border of the Iberian Range might be related to a crustal thickening to about 43 km. These differences are correlated with topographic highs of the Demanda-Cameros Sierra, Spanish Central System and Tremedal Massif [Fig.5.2b], pointing towards their common origin related to basin inversion during the Cainozoic times.

5.3 Analogue modelling experiments

Two sets of analogue experiments are compared in order to understand the importance of the initial rift geometry prior to the onset of Alpine deformation, as well as, the influence of lateral changes on lithospheric strength between strong and weak lithospheres (Variscan to the west and Mesozoic to the east, respectively). The lithospheric scale models are based on geological and geophysical data from Iberia (*Surinach and Vegas,* 1988; *Guimerá et al.,* 1996; *Tejero and Ruíz,* 2002; *De Vicente and Vegas,* 2009a; *Díaz and Gallart,* 2009). The experiments consist of three layers from top to bottom: a brittle upper crust, a ductile lower crust and an upper lithosphere mantle [Fig.5.4]. These layers rest in isostatic equilibrium on a high-density fluid representing the asthenosphere within a Plexiglas tank, with a single moving wall. Different material properties were used to represent an extended lithosphere to the east (Iberian Basin) and a Variscan lithosphere to the west highlighting the boundary between both systems. Two weak E-W zones were implemented in the models representing the main Cretaceous depocentres (8.000 and 5.000 m of Cretaceous sediments in Cameros and Maestrazgo respectively). In addition, two more weak zones were deployed to model the N-S fault corridors extending over Portugal e.g. Bilariça-Bragança Fault System, (*De Vicente and Vegas,* 2009a) and the NE-SW Messejana-Plasencia Fault in central Spain. The effect of E-W trending granitic bodies was also introduced in the set-up as a weak silicone layer at the boundary between the lower and upper crust in order to infer the effect that may have played on strain localisation and uplift of the Spanish Central System in central Spain.

The analysis of fault kinematics carried out on the model surface follows the methodology described in *Leever et al.* (2011a), based on the study of surface displacement field. The "Particle Image Velocimetry" or PIV method is based on the comparison of two images

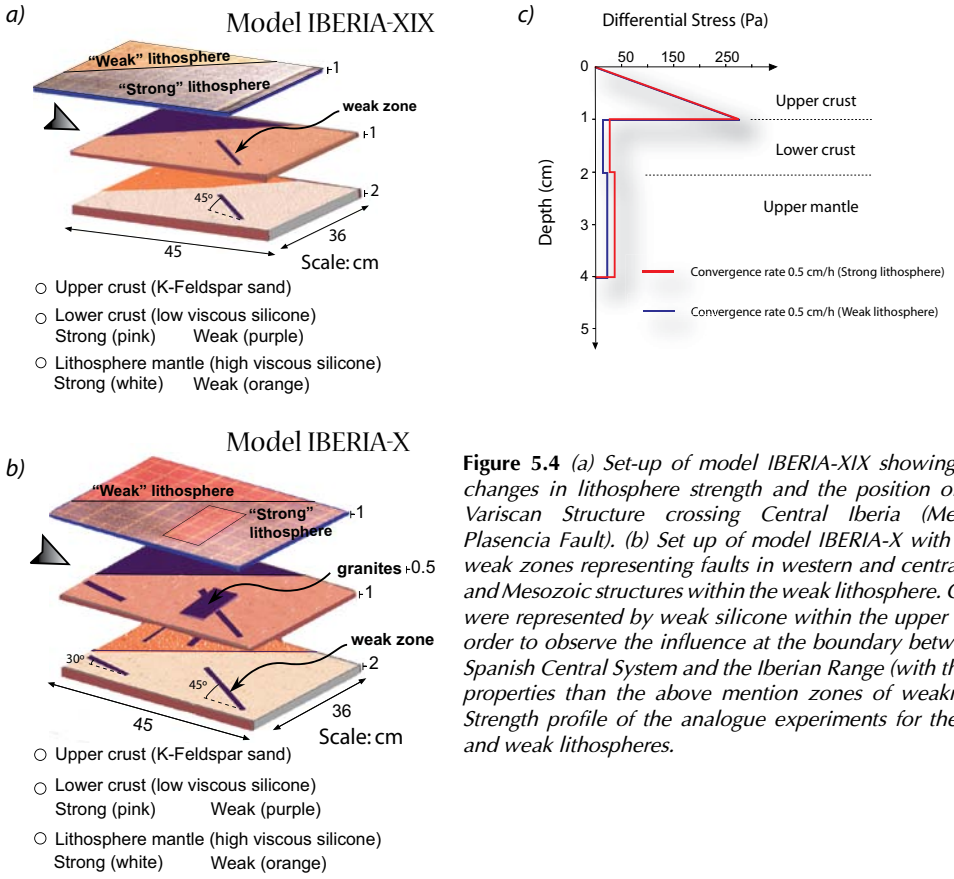

Figure 5.4 *(a) Set-up of model IBERIA-XIX showing lateral changes in lithosphere strength and the position of a late Variscan Structure crossing Central Iberia (Messejana Plasencia Fault). (b) Set up of model IBERIA-X with several weak zones representing faults in western and central Iberia and Mesozoic structures within the weak lithosphere. Granites were represented by weak silicone within the upper crust in order to observe the influence at the boundary between the Spanish Central System and the Iberian Range (with the same properties than the above mention zones of weakness).(c) Strength profile of the analogue experiments for the strong and weak lithospheres.*

within a fixed time interval. In order to carry out the image evaluation, a digital PIV recording must be divided in small subareas called "interrogation areas" (measured in picture elements or pixels). Therefore, if small-grain particles are scattered over the model surface, those particles within the interrogation areas will be correlated. Evaluation of PIV recordings is obtained by cross-correlation method, defined as a standard statistical method of estimating the degree to which two compared series of data are correlated (*Westerweel,* 1997; *Raffel,* 2007). The PIV method aims to investigate fault slip by correlation between the velocity field and slip orientation during model deformation. The method is based on the calculation of a directional derivative δv from the original velocity field by subtracting adjacent vectors with different orientations.

$$\partial\upsilon = \upsilon(x,y) - \upsilon(x+1,y) \qquad [5.1]$$

where υ is the initial vector field and δυ its directional derivative. Consequently, if the displacement field is constant the subtracting of adjacent vectors provides no resultant. However, if the magnitude and orientation of the vector field changes, it will provide a different vector ≠ 0. When the length of one of the vectors in dv exceeds a threshold value, its azimuth is plotted in a colour scale (0-360º). Therefore, high angles indicate convergence directions (~90º) while low angles (<45º) indicate dextral strike-slip. Therefore, we are able to identify different mechanism of fault slip (oblique or parallel to convergence direction) that took place during deformation. In this way, the method allows to study and distinguish between active, reactivated and non active faults, which implies that strain partitioning can be detected in the analogue experiments

Table 5.1

Layer	Density ρ(kg/m^3)	Viscosity η (Pa · s)	Layer thickness h (m)	Velocity v (m · s^{-1})	R_m
Strong lithosphere					
Upper crust *nature*	2670	-	$1.5 \cdot 10^4$	$7 \cdot 10^{-3}$ - $14 \cdot 10^{-3}$	-
Upper crust *model*	1300	-	$1 \cdot 10^{-2}$	$5 \cdot 10^{-3}$ - $1 \cdot 10^{-2}$	-
Lower crust *nature*	2900	$1.0 \cdot 10^{22}$	$1.5 \cdot 10^4$	$7 \cdot 10^{-3}$ - $14 \cdot 10^{-3}$	29.03
Lower crust *model*	1486	$1.87 \cdot 10^5$	$1 \cdot 10^{-2}$	$5 \cdot 10^{-3}$ - $1 \cdot 10^{-2}$	22.23
Mantle lithosphere *nature*	3400	$4 \cdot 10^{21}$	$3.0 \cdot 10^4$	$7 \cdot 10^{-3}$ - $14 \cdot 10^{-3}$	33.80
Mantle lithosphere *model*	1606	$1.87 \cdot 10^5$	$2 \cdot 10^{-2}$	$5 \cdot 10^{-3}$ - $1 \cdot 10^{-2}$	36.86
Weak lithosphere					
Upper crust *nature*	2670	-	$1.5 \cdot 10^4$	$7 \cdot 10^{-3}$	-
Upper crust *model*	1300	-	$1 \cdot 10^{-2}$	$5 \cdot 10^{-3}$	-
Lower crust *nature*	2950	$2.0 \cdot 10^{20}$	$1.5 \cdot 10^4$	$7 \cdot 10^{-3}$	146
Lower crust *model*	1532	$9.75 \cdot 10^3$	$1 \cdot 10^{-2}$	$5 \cdot 10^{-3}$	110
Mantle lithosphere *nature*	3350	$1 \cdot 10^{21}$	$3.0 \cdot 10^4$	$7 \cdot 10^{-3}$	133
Mantle lithosphere *model*	1590	$2.3 \cdot 10^4$	$2 \cdot 10^{-2}$	$5 \cdot 10^{-3}$	194
Granite *nature*	1532	$1.0 \cdot 10^{21}$	$5 \cdot 10^{-3}$	$5 \cdot 10^{-3}$	-
Granite *model*	2950	$1.24 \cdot 10^4$	$5 \cdot 10^{-3}$	$5 \cdot 10^{-3}$	-

Table 5.1 *Physical properties and layer thicknesses of the lithosphere and experimental layers. Velocity values correspond with convergence rate from nature and models. Ramberg number (Rm) of the model and the natural prototype.*

during deformation. These results imply that we can consistently identify a strain partitioning mechanism developed under a single phase of convergence.

5.4 Modelling results

Two sets of lithospheric scale models were performed with uni-directional convergence. Material properties are summarised in Table 5.1.

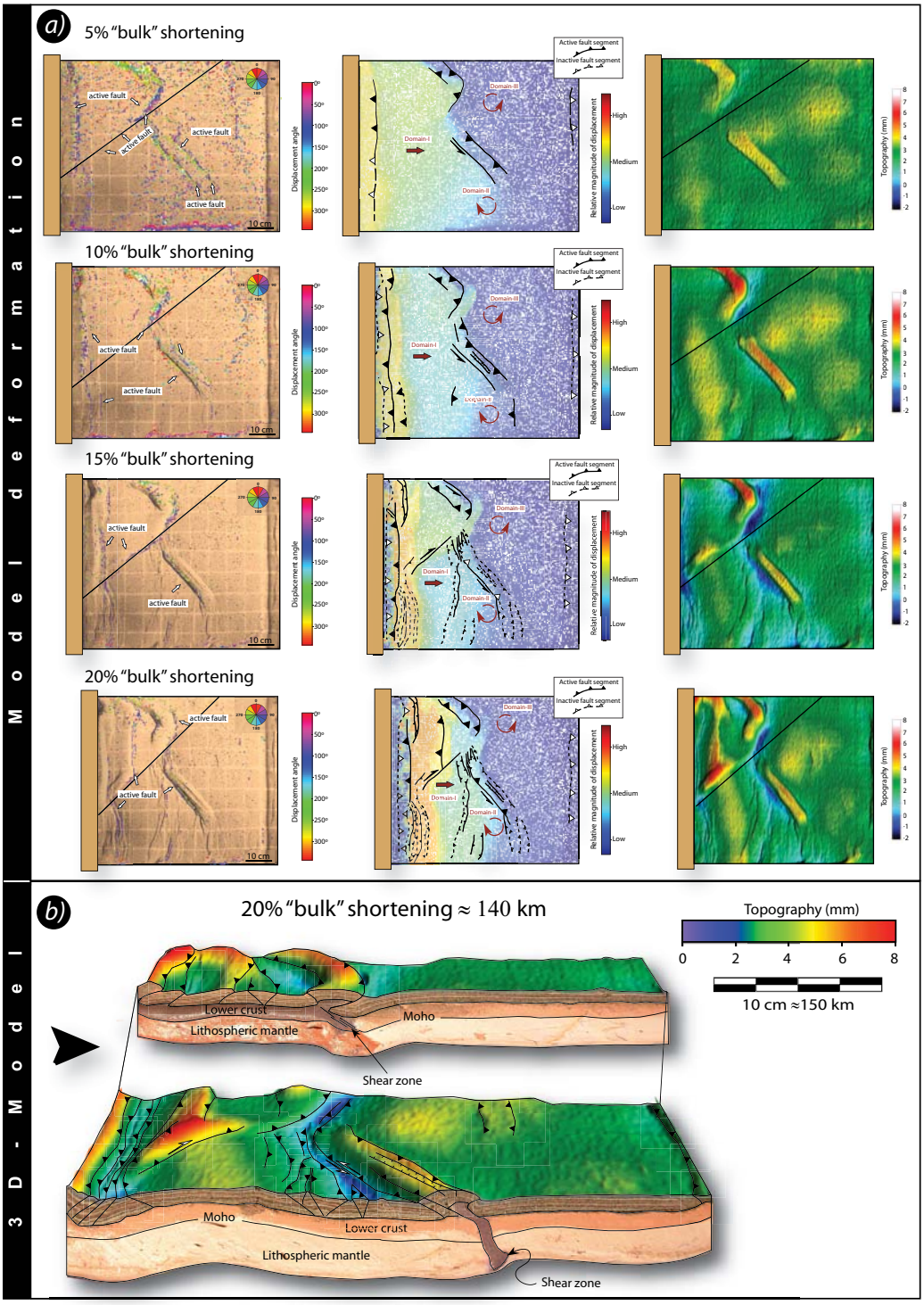
3 D - Model deformation
a)
5% "bulk" shortening
10% "bulk" shortening
15% "bulk" shortening
20% "bulk" shortening
active fault
10 cm
Displacement angle
Active fault segment
Inactive fault segment
Domain-I
Domain-II
Domain-III
Relative magnitude of displacement
High
Medium
Low
Topography (mm)
b)
20% "bulk" shortening ≈ 140 km
Topography (mm)
0 2 4 6 8
10 cm ≈150 km
Lower crust
Lithospheric mantle
Moho
Shear zone

5.4.1 Model without depocentres (IBERIA-XIX)

» Crustal structure and topography

The model shows localised deformation, controlled by the presence of pre-existent weak zones and the rheological discontinuity between the two lithospheres (weak and strong). Two stages of deformation related to strike-slip movements followed by pure thrusting were identified between 10% and 15% of bulk shortening (BS) [Fig.5.5a]. The velocity field of the surface reveals counter-clockwise rotation of the vectors caused by displacement along the main lithosphere boundary. Clock-wise rotation of slip vectors is also recorded within the strong lithosphere, through the weak zone representing the Messejana-Plasencia Fault. The change on vector distribution is induced by slip along the weak discontinuity (i.e. boundary) following a right-lateral displacement. Therefore, vector distribution support the idea of tectonic fault reactivation during compression, as it can be inferred from Figure 5.5a. During different stages of deformation, the fault displacement regime changes from pure strike-slip to thrust, leading to final uplift (5% to 20% BS). Back thrusting is reported to occur at 15 and 20% BS in the central part of the model. In addition, the non-coeval episodes of thrusting (fore- and back-thrust) were accommodated by extension through a series of graben situated on top of the main surface structures during episodes of tectonic quiescence. Moreover, strike-slip movement is apparently restricted to the main oblique discontinuities deformed under a regime of transpression [i.e. lithosphere boundaries and weak zones Fig.5.5a]. Consequently, a component of transpression, where thrust and strike-slip faults coeval with the same stress field, was always related to reactivated structures [Fig.5.5a compare top-view images with digital elevation models].

Faulting is mostly associated with imbricate thrusts and pop-ups that formed within wide lithosphere synclines while wide elevated areas are located between the main thrust families. Brittle structures were distributed through the model interior within the strong lithosphere, whereas in the weak lithosphere deformation localised along closely spaced thrust families. Interference patterns between E-W, NE-SW and NW-SE crustal structures developed under uni-directional shortening [strike-slip and thrusting coexisted during deformation, Fig.5.5a]. The interference patterns observed, therefore, suggests a mechanism of strain partitioning favoured by slip along pre-existent weak zones. These weak zones seem also to define the boundary for strain transmission as folding of the lithosphere is attenuated inside the strong lithosphere after having reached the weak zone. In addition, digital elevation models [Fig.5.5a] show clear differences in elevation between areas of strong and weak lithosphere. Topography over the weak lithosphere becomes higher while depressions reach deeper values [compare profiles in Fig.4.9b].

» Deep lithospheric structure

The strong lithosphere in the model is folded while the weak lithosphere becomes to some extent thickened several kilometres. The vector field highlights these differences by showing higher vector magnitudes along the strong lithosphere, whereas low displacement rates were distributed along the weak lithosphere [Fig.5.5a]. These magnitude variations resulted from differences on the mode of deformation within the different subparts of the lithosphere.

◀ **Figure 5.5** *(a) Model IBERIA-XIX depicting several stages of deformation showing inferred active structures interpreted following the PIV technique, structural interpretation showing the rotation and magnitude of the main slip vectors obtained from PIV, and digital elevation models showing the evolution of topography at 5%, 10%, 15% and 20% of bulk shortening respectively. (b) 3D model showing the correlation between the deep structure and the surface topography (black line marks the transition from a strong into a weak lithosphere). Folding affects the strong lithosphere, whereas the weak lithosphere is characterised by thickening of the lower crust and upper lithosphere mantle.*

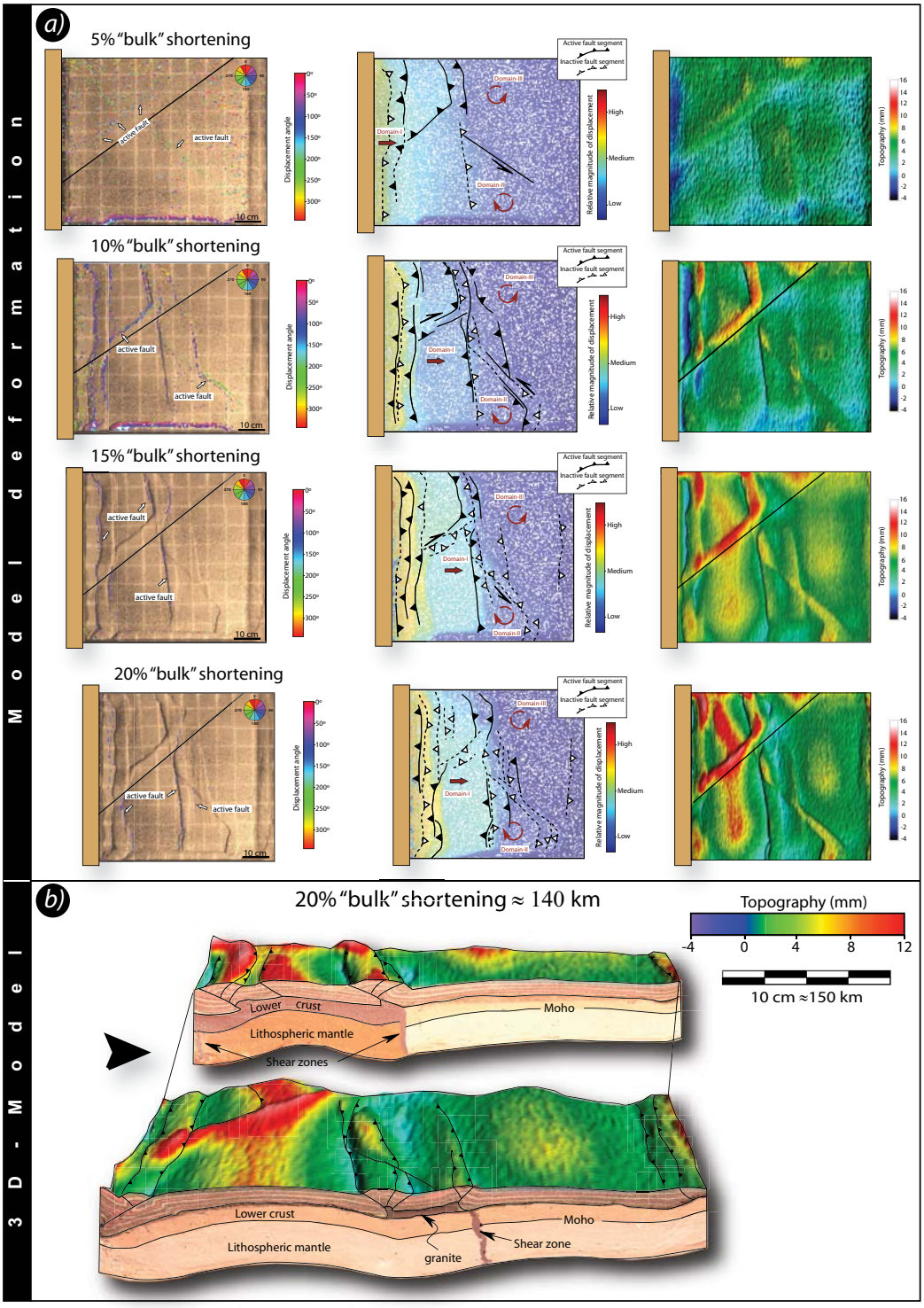
a)
Model deformation
5% "bulk" shortening
10% "bulk" shortening
15% "bulk" shortening
20% "bulk" shortening
active fault
10 cm
Displacement angle
Active fault segment
Inactive fault segment
Domain-I
Domain-II
Domain-III
Relative magnitude of displacement
High
Medium
Low
Topography (mm)
b)
3 D - Model
20% "bulk" shortening ≈ 140 km
Topography (mm)
-4
0
4
8
12
10 cm ≈150 km
Lower crust
Moho
Lithospheric mantle
Shear zones
granite
Shear zone

These variations correlate with the fluctuation of Moho depths. Therefore, for low magnitudes of displacement, the position of the Moho is in general deeper (weak lithosphere). That implies that vertical forces overcome the horizontal ones, localizing deformation, and therefore, facilitating crustal thickening. As a result, a relative maximum on the Moho depth is reached close to the moving wall [Fig.4.9b]. On the contrary, high rates of displacement are reached within the strong lithosphere. However, the presence of inherited faults plays a key role, controlling the depth of the Moho within the strong lithosphere, leading to important depth differences from one side of the fault to the other.

5.4.2 Model with E-W Mesozoic depocentres (IBERIA-X)

» Crustal structure and topography

Unlike the previous model, four weak zones have been introduced [Fig.5.4b]. Inside the weak experimental lithosphere, these weak zones represent the main Cretaceous depocentres that defined the geometry of the Iberian basins during the Mesozoic (E-W corridors). The two weak zones placed within the strong lithosphere correspond to inherited tectonic structures NNE-SSW and NE-SW oriented in the western and central part of Iberia, respectively (i.e. Vilariça-Bragança Fault System, *De Vicente and Vegas,* 2009). Moreover, the model contains a weak zone representing the granitic belt that entirely crosses the Spanish Central System within the upper crust (oriented around 80º with the direction of convergence).

The evolution of topography is linked to the development of thrust faults along with folds that elevate the surface at successive steps [Fig.5.6a, digital elevation models]. Rapid uplift of the model surface occurs first over the weak lithosphere following the orientation of the main depocentres (E-W) and the boundary between both lithospheres (NW-SE) at about 10% BS [Fig.5.6a]. Uplift along depocentres was favoured by thrusting, whereas dextral strike-slip faulting across the lithosphere boundary i.e. a tectonic, rheological and thermal boundary involved a component of transpression. The analysis of displaced particles indicates the counter clock-wise rotation of the vectors at the southern tip of the lithosphere boundary fault and the presence of oblique velocity vectors around the fault segment. Moreover, the PIV analysis also recorded movement along the pre-existent weak zones within the strong lithosphere that were reactivated several times, leading to sinistral strike-slip movements combined with thrusting that caused general uplift (5-10% BS). Similarly, the weak zone representing the Central Range granitoids inside the upper crust led to abrupt uplift along two pop-ups facing north and south respectively that were also reactivated at 10%, 15% and 20% BS [see vectors in Fig.5.6a]. The fault vergence changes such that the weak lithosphere is characterised by north verging thrust (i.e. facing the moving wall), whereas in the strong lithosphere mainly south verging thrusts and pop-ups as it has been revealed from displacement vectors [see 15% BS from Fig.5.6a].

» Deep lithospheric structure

The first response to shortening is folding of the entire model lithosphere. This is a striking difference with the previous model because the weak lithosphere was also folded.

◀ **Figure 5.6** *(a) Model IBERIA-X showing several stages of deformation at 5%, 10%, 15% and 20% of bulk shortening respectively. Inferred active structures interpreted following the PIV technique at each interval, structural interpretation showing the rotation and magnitude of the main slip vectors obtained from PIV. Reactivation of structures and strain partitioning are clearly depicted by coeval strike-slip faults and thrust under a single uni-directional compression. Digital elevation models show the evolution of topography. (b) 3D model showing the correlation between the deep structure and the surface topography. Unlike the previous model, folding affects both lithospheres. However, the observed wavelengths are higher for the strong lithosphere than or the weak lithosphere.*

Therefore, the position of E-W oriented weak zones might have influenced the weak lithosphere to fold by increasing strain localisation along narrow corridors. However, the wavelength varies from one lithosphere to another. This difference is also related to the presence of pre-existent structures that control fault localization. These faults may influence the amplitude and shape of the outer arch of the fold surfaces; for example, as it can be seen to occur within the strong lithosphere [Fig.5.6b]. These structures were originally vertical, cross-cutting through the lower crust and lithosphere mantle, indicating partial (de)-coupling between both layers. Likewise to the observed behaviour of the lower crust in the previous model, thickening is recorded along synclines whereas anticlines have been thinned. Consequently, as a result of lower crustal flow, the position of the Moho surface changed, following the fold shapes [Fig.5.6b].

5.5 Discussion

5.5.1 Influence of lateral lithospheric strength changes on mode of deformation

The existence of changes of thermo-mechanical properties of the lithosphere influences the way tectonic inversion takes place. Under this premise, large differences may result in geometry and style of deformation (including both folding and faulting), strain localisation or partitioning mechanisms (*Lankreijer et al.,* 1997; *Bonini,* 2007b; *Willingshofer and Sokoutis,* 2009; *Tesauro et al.,* 2010; *Sokoutis and Willingshofer,* 2011).

In strong lithospheres, deformation is efficiently transferred from plate boundaries to the interior. As a result, strain becomes distributed over wide areas. Weak lithospheres are characterised by strain localisation leading to narrow deformed belts (*Ziegler et al.,* 1995). There are many intra-plate areas on Earth where lateral variations of lithosphere strength have been inferred, among others: Pannonian Basin (*Cloetingh et al.,* 2005), Moroccan Atlas (*Teixell et al.,* 2003) and Iberian Range (*Van Wees and Stephenson,* 1995). Although their tectonic history and evolution are different, they present close similarities related to rheology contrast between weak and stiff lithospheric domains. They typically are characterized by a first episode of lithospheric extension followed by tectonic compression and subsequent basin inversion. These stress changes induced different thermo-mechanical behaviour with the adjacent areas, leading to broad diversity of tectonic styles and geometries related to the basin configuration prior to inversion. Consequently, at surface scale, the strong lithospheres seem to be affected by wide deformed areas where faulting involves the entire basement (thick-skinned tectonics proposed by *De Vicente et al.* (2007), along the Spanish Central System), whereas weak lithosphere results in narrow domains of deformation characterised by shallow detachment levels eventually rooted at syn-rift sequences like in the Iberian Range or the Moroccan Atlas (*Salas and Casas,* 1993; *De Lamotte et al.,* 2000; *Teixell et al.,* 2003; *De Lamotte,* 2009). It is also important to remark that changes on fault vergence and fault-style might be influenced by lithosphere rheology as it has been pointed out by *Bonini* (2007a) and *Fernández-Lozano et al.* (2011) for crustal and lithospheric scale models, respectively.

Comparison between field observations at the boundary between the Central System and the Iberian Range (*De Vicente et al.,* 2009) with analogue experiments suggest that differences in deformation style are correlated with lateral variations of lithosphere strength with a major influence of pre-existent tectonic structures that controlled the basin geometry during the Mesozoic. Balanced cross-sections and palinspastic reconstruction point to the importance of detachment levels on shallow thrusting as well as boundary faults that controlled the Mesozoic sedimentary basin infill during rifting (*Casas-Sainz et al.,* 1998; *Guimerá et al.,* 2004; *Casas-*

Saínz et al., 2009a; *Simón-Gómez and Liesa,* 2011). These inherited structures played a key role on the crustal thinning and thermal weakening of the Iberian Range lithosphere. Likewise, during the stage of tectonic inversion, such structures would have been reactivated as reverse faults, thrusts and strike-slip fault segments following the rift orientations prior to convergence. Close similarities are therefore found in model IBERIA-XIX, showing imbricate thrusts, closely spaced pop-ups and duplexes in the weak lithosphere, whereas wide pop-ups were widely distributed through the strong lithosphere. In addition, the importance of pre-existent crustal structures also influenced the final surface geometry as it has been depicted in Figure 5.5a (model IBERIA-X, where E-W depocentres within the weak lithosphere controlled the position of broad lithosphere synclines).

5.5.2 Strain partitioning within intra-plate domains

Strain partitioning processes have been often related to oblique convergence between plates, both in continent-continent and in oblique subduction systems (*Fitch,* 1972; *Woodcock and Daly,* 1986; *Koons,* 1994; *Tikoff and Teyssier,* 1994; *Mazzotti et al.,* 1999). However, little is reported from intra-plate domains where partitioning might have played a key role on the mode of deformation. Particularly, superposed deformation within plate interiors may be favoured by different geometries and rotation between basement blocks (*Peltzer and Tapponnier,* 1988; *R. Jones and Geoff Tanner,* 1995). Distinct lateral changes of lithospheric strength caused by crustal thickness and geothermal gradient variations may also occur (*Vauchez et al.,* 1998; *Storti et al.,* 2003). In the western United States, intra-plate strain is partitioned along the boundary between Sierra Nevada Mountains and the Basin and Range area. There, *Cashman and Fountain* (2000), argued that accommodation through a dextral strike-slip zone is split into domains dominated by translation, rotation and extension. Consequently, fault offset is accommodated by slip changes through individual faults as well as the geometry of the rotating blocks.

Recently, *Beauchamp* (2004), has discussed the influence of inherited structures and obliquity as important factors for strain partitioning during tectonic inversion along the margin of the High Atlas Mountains. Similarly, *De Vicente et al.* (2009b), have reported the tectonic inversion of syn-rift sequences over a pre-existing accommodation zone i.e. normal fault ramp geometry, controlled by the rifting geometry inherited from the Triassic-Cretaceous extensional episode that gave rise to the Iberian Basin. It is therefore widely accepted that the previous geometry of a rift basin influences the final configuration of the deformed belt during the stage of tectonic inversion (*Ziegler et al.,* 1998; *Guimerá et al.,* 2004; *Cloetingh et al.,* 2008). Moreover, recent crustal-scale models carried out by Ter Borgh et al. (2010), confirmed the importance of inherited basement ramps formed during extension that affected the Betics, prior to the Alpine convergence phase. Likewise, upper Jurassic-lower Cretaceous extension would have been accommodated through major extensional listric faults leading to thinning of the crust and followed by thermal weakening of the entire lithosphere (*Álvaro,* 1987; *Guimerá et al.,* 1996; *Casas-Sainz and Gil Imaz,* 1998; *Casas et al.,* 2009; *De Vicente et al.,* 2009b). Subsequently, the thinned lithosphere was prone to tectonic inversion during compression in the early Tertiary (*Salas and Casas,* 1993). As a result, rift structures (i.e. listric normal faults, roll-over anticlines etc.) were inverted following the main trend that controlled basin configuration during the Mesozoic. As such tectonic structures trending NW-SE, E-W and NE-SW correspond now to reverse faults that have led to subsequent mountain uplift during the Alpine Orogeny.

Analogue modelling results show that the initial structure related to the basin configuration governs: i) strain localisation along the main Mesozoic depocentres; ii) strain partitioning between master faults (lithosphere boundary), and minor inverted structures [compare Figure 5.5a and 5.6a].

Analysis of particle displacement carried out over the model surface, shows those oblique structures trending NW-SE and NE-SW were characterised by deformation under transpression, whereas E-W structures were reactivated as reverse faults. In addition, structures trending NNE-SSW were not active under uni-directional compression. A possible explanation for the non-reactivation of inherited faults might be due to the fact that oblique structures oriented at angles below (45º) with the convergence direction were not properly oriented to move under such stress field. Therefore, the model suggests reactivation of inherited faults >45º independently of the fault vergence. In addition, the analogue modelling results suggest that the boundary fault moved as a strike-slip fault that transferred deformation though a series of horsetail-secondary structures with E-W orientation. This is also compatible with field observation in the Iberian Range, where the main boundary fault (Somolinos Fault), is a strike-slip fault with a reverse component and local compressive step-overs that uplift the Range [for instance, the Huermeces thrust in Figure 3.20c]. Therefore, the observed structural trends match the fault kinematics as proposed by *De Vicente et al.* (2009b), suggesting that an uni-directed stress field can successfully explain the superposition of different tectonic orientations, making strain partitioning a reasonable mechanism for explaining the present-day configuration of the Iberian Range.

5.6 Conclusions

This chapter integrates lithospheric-scale analogue models along with analysis of displacement vector fields to constrain the effect of pre-existing faults and lateral lithosphere strength heterogeneities on present-day topography.

Lateral variations on lithosphere strength led to differences on vergence and style of deformation at crustal scale. The deep crust and mantle were folded or thickened during compression. Therefore, lithosphere strength changes are suggested to account for the high crustal thicknesses observed within the south-eastern most part of the Iberian Range. In addition, the presence of E-W striking depocentres in the Iberian Range (Cameros-Demanda and Maestrazgo) may also have strongly influenced the present-day crustal structure of the range, facilitating strain localisation and folding. These structural patterns ranging from NW-SE, E-W to NW-SE strikes seems to be the result of previous Mesozoic rift-related structures that were reactivated during Alpine compression. Furthermore, they would have facilitated the conditions for reactivation under the same stress-field. This is the example of the Somolinos fault segment, characterised by a component of transpression. This fault is considered as a strike-slip fault with some segments accommodating shortening in thrust fault mode.

The above-described results emphasize the role of strain partitioning during tectonic inversion. This mechanism may have been facilitated by the presence of lateral strength variations influenced by crustal thinning and high geothermal gradients inherited from the Mesozoic rifting. Subsequently, a N-S oriented stress-field may have reactivated Mesozoic rifting related structures by thickening and folding of the lower crust and upper lithosphere mantle, leading to the present-day topographic expression.

Chapter 6

Discussion and conclusions

The present study provides new insights into the processes of mountain building that occur in plate interiors like Iberia. Laboratory experiments display the effect of boundary conditions represented by lateral variations of lithosphere strength and pre-existent tectonic structures in Iberia (cross-cutting the entire continental crust) on the mode of lithosphere deformation during N-S convergence. Under such a stress field, strain partitioning appears to influence the orientation of mountain ranges through the reactivation of pre-existent faults. Moreover, these faults also may have influenced the wavelength of folding. However, the observed differences in topography from west to east Iberia can also be related to the rheological stratification of the lithosphere and its thermo-mechanical state; i.e. vertical lithosphere de-coupling. The strength of the lithosphere, governed by variations in temperature and composition changes its mechanical properties and, therefore, controls the wavelength of deformation. These differences influenced the mode of strain transfer from plate boundaries to plate interiors and affect the mechanisms of deformation of the lithosphere (i.e. folding versus thickening). The thermal age of the Iberian lithosphere (between 300 Ma and 150 Ma) has predominantly controlled the present-day configuration of mountain ranges during the Cainozoic episode of continental convergence. As a result, periodic (50 km to 250 km wavelength) topographic highs evolved under the control of large-scale folds developed during N-S convergence. These folds may also have controlled the high elevation of the Duero basin (~900m) and the general tilting of Iberia towards the southwest. The spectral analysis carried out for other intra-plate domains like the Moroccan Atlas or Central Asia with similar lithosphere tectono-thermal ages show close similarities with the topographic wavelengths found in Iberia. Therefore, intra-plate mountain building process in Iberia entail folding of the entire lithosphere supported by analogue, and gravity models.

6.1 Introduction

The analogue experiments suggest the presence of large-scale folds affecting the Iberian lithosphere. Such folds occur under very specific rheological conditions (composition and temperature-related), influenced by the presence of pre-existing zones of weakness i.e. faults and weak zones sensu stricto. Current models based on folding of plate interiors describe the mechanism without clearly denoting the shape and position of these large-scale folds. This chapter provides a broad view on the distribution of such folds in Iberia, and other proposed areas of folded lithosphere like the Moroccan Atlas or Central Asia. Moreover, I describe the crustal structure that may have influenced the uplift and tilting of Iberia to the southwest linked to mantle deformation, describing similarities and differences with seismic observations. Summarizing the modelling results and field work, I propose a possible scenario for intra-plate mountain building in Iberia dominated by the presence of large-scale folds affecting a partially de-coupled lithosphere to the west, and a highly thickened crust, as a result of tectonic inversion of Mesozoic basins to the east.

6.2 Folding of de-coupled lithosphere

Rheology profiles represent the strength variations that occur along a vertical lithosphere column. Although they do not specifically reflect lithological changes, they provide useful indirect information about composition, heat and stress (*Ranalli,* 1995). These profiles provide a first-order idea at which depth, deformation mechanisms operating in the brittle field change into dominant ductile behaviour. Recent studies suggest significant differences on lithosphere strength around the world (*Cloetingh and Banda,* 1992; *Cloetingh and Burov,* 1996; *Jackson,* 2002a, 2002b; *Burov and Watts,* 2006; *Thatcher and Pollitz,* 2008). These differences point to the possibility of a substantial contribution of the upper mantle to the total strength of the lithosphere in areas of cold and thick lithosphere. However, this observation is only supported by the focal depth distribution of earthquakes. More specifically, *Afonso and Ranalli* (2004), suggest regions where the strength is distributed in the upper crust and mantle, characterised by low surface heat flow, moderate crustal thickness, and felsic or wet mafic lower crustal compositions, whereas areas represented by high surface heat flow, variable crustal thickness, and dry mafic lower crustal composition are characterised by maintaining the total strength in the seismogenic crust. In addition, new studies concerning lithosphere strength in Iberia performed by *Tejero and Ruíz* (2002); *Gaspar-Escribano et al.* (2003) and *Ruíz et al.* (2006) provided insight into the rheological stratification of the Iberian lithosphere. Their results suggest strong mantle rheologies along the main basins (Duero, Ebro and Tagus) and weak rheologies along the Spanish Central System and eastern Spain involving a ductile lower crust, indicating the partial de-coupling of the Iberian lithosphere. Similar results were also obtained for Western Europe and particularly in Iberia by *Tesauro et al.* (2008). Additionally, this view would be supported by the calculated elastic thickness that varies between 25-30 km in the Cantabrian Mountains-Pyrenees, 17-20 km in central Spain, 5-10 km along the Ebro basin and the Valencia Trough. On the contrary, the seismogenic thickness in Iberia is variable and ranges from 9 to 17 km (*Tejero and Ruíz,* 2000) and is probably related to heat flow variations, which are especially important in the Spanish Central System, Galicia and Portuguese Algarve areas [see Figure 3.23a and b].

An attempt to study the influence of rheological differences and their influence on the mode of deformation has been carried out through numerical modelling (*Burov et al.,* 1993; *Cloetingh et al.,* 1999; *Burov and Watts,* 2006). Their study concludes that the mode of deformation (brittle-ductile) is influenced by the thermo-mechanical stage of the lithosphere favoured by the presence of previous heterogeneities (i.e. faults) or temperature variations that

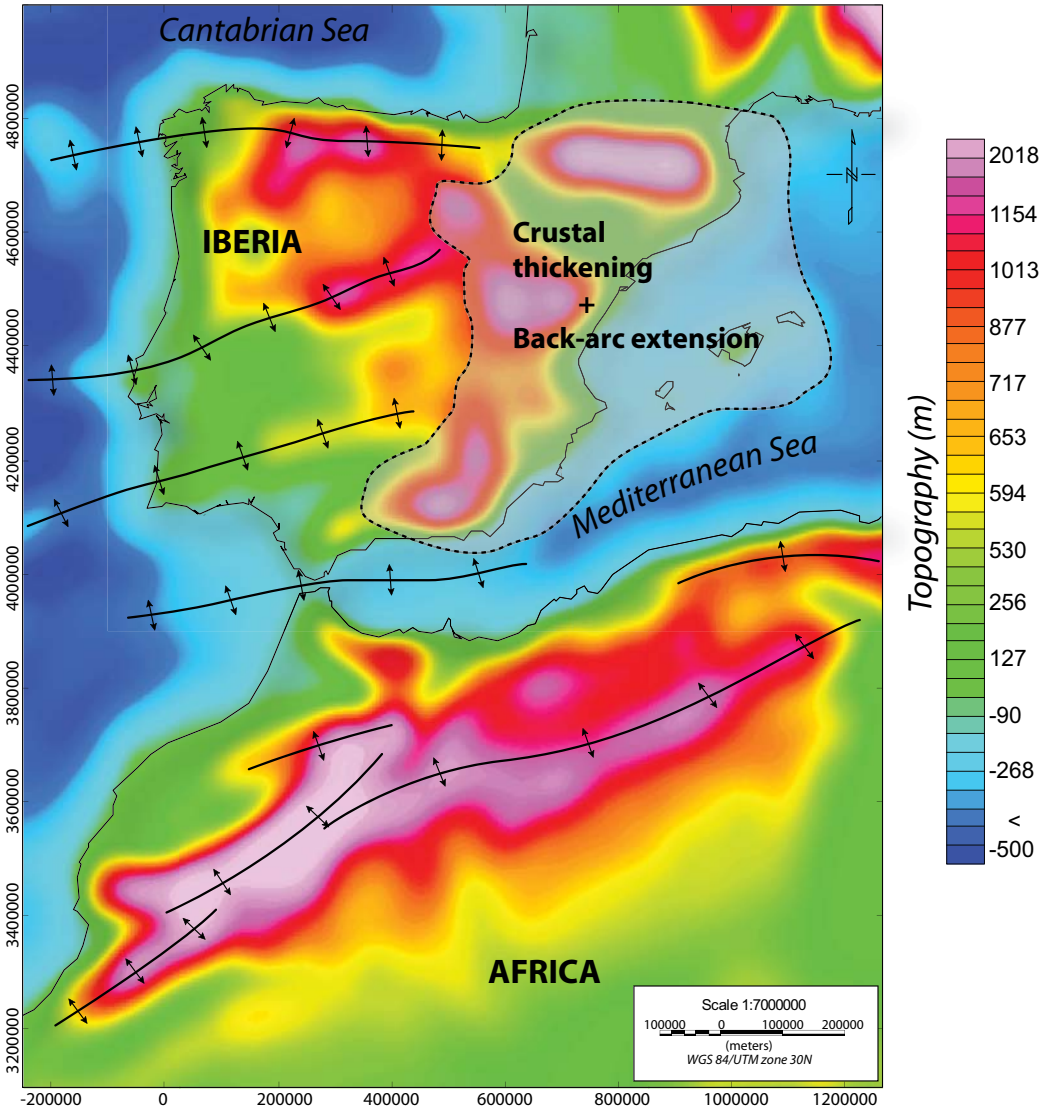

Figure 6.1 *Map showing the distribution of crustal antiforms in Iberia. Topography has been filtered at 250 km wavelength.*

may affect the rheological state of the crustal-mantle transition.

In Chapter 3, modelling results have been shown comprising a de-coupled lithosphere [Fig.3.27]. Models with a strong brittle upper crust, a weak lower crust and a relatively strong lithosphere mantle efficiently developed a trend of folds that controlled the position and formation of symmetric pop-ups and single thrust. These structures were oriented perpendicular to the convergence direction giving rise to a series of thrust controlled intra-mountain basins as well as inter-mountain basins between pop-ups. Lower crustal flow took place, leading to a slight thickening of crustal material under the main elevated areas (pop-ups and thrust). In the model with stronger lower crust than the lithospheric mantle, deformation was distributed

along the surface, leading to the effective transmission of stresses in the form of folding. This, in turn allowed higher elevation close to the moving wall by localization of crustal thickening and thrusting. A distinct difference can be identified on the mode of upper crustal deformation, characterised by certain asymmetry of the pop-ups, and the formation of piggy-back basins over duplex structures. Therefore, despite both lithospheres were initially de-coupled, the most probable scenario in Iberia can be represented by a strong upper crust, a weak lower crust and a relatively strong lithospheric mantle, which aids in distributing strain all over the model surface. This view would be supported by the presence of relatively shallow distribution of earthquakes (between 5 and 15 km in average) in the upper crust. Areas where the lower crust is thickened compared with the surroundings, like in the Spanish Central System or the Iberian Range (*Vegas and Suriñach,* 1987; *Surinach and Vegas,* 1988; *Guimerá et al.,* 1996) are in general, linked to Bouguer gravity lows. Lower crustal thickening would be linked to the presence of high values of heat flow as shown by *Fernández et al.* (1998), (favoured by the high radiogenic heat production of granitoids in Central Spain), which in turn may heat the basal part of the crust and favour lower crustal flow. Moreover, the presence of a relatively old Variscan lithosphere shown by the seismic profiles along western Iberia may also indicate an increase on mantle strength (*Banda et al.,* 1981; *Banda,* 1983; *Ayarza et al.,* 2010).

Taking all these observation together, it is probable that a strong mantle could transfer the stresses from the northern Pyrenean border to the plate interior controlling the position of mountain ranges through a mechanism of folding. In the following subsections I describe two well-known intra-plate scenarios where lithospheric folding has been proposed as a mechanism for mountain building and basin development.

6.2.1 Ibero-Atlas mountain belt

Even though geographically speaking both regions are set thousands of kilometres away from each other, the Ibero-Atlas domains share close geological and geophysical similarities. Both domains formed part of the Gondwana margin during most of the Palaeozoic Era. The onset of continental break-up led to a series of extensional basins filled up with typical Germanic Triassic facies (Buntsandstein, Muschelkalk and Keuper). A subsequent period of thermal subsidence continued with a new episode of tectonic-driven extension during the Jurassic-Cretaceous, where thick piles of marine sediments were deposited along E-W, NE-SW oriented basins (*Stapel et al.,* 1996; *Gouiza et al.,* 2010). The thermal relaxation of the geotherms led to partial melting and crustal magmatic assimilation, which in turn weakened the lithosphere by thinning of the crust.

During the early Tertiary, partial coupling of the Iberian and Europen plates lead to the formation of the Pyrenees and the intra-plate inversion of Mesozoic rift basins towards the southern foreland area. On a regional scale in the Moroccan Atlas, *De Lamotte et al.* (2000) argued for the presence of two phases of deformation, during the late Eocene and between Pleistocene to Quaternary. These deformation phases are contemporaneous with volcanic events at 35 Ma and between 15 and 6 Ma (*Harmand and Cantagrel,* 1984; *Missenard et al.,* 2006). Recent thermo-chronology data records the beginning of exhumation of the High Atlas during the eastward movement of Africa in the early Palaeocene (*Ghorbal et al.,* 2008). However, the first tectonic event comprised the time-span between the middle Palaeocene to middle Eocene. The axial zone of the High Atlas shows an important period of uplift from the early Miocene followed by the exhumation of the entire belt during the Middle Miocene (*Missenard et al.,* 2008; *Barbero et al.,* 2011). A major event of crustal shortening documented by more than 4.000 m of uplift along the axial region of the High Atlas is recorded as post-Miocene to late Pliocene in age and subsequently followed by roughly 1.000 m of uplift along the entire Atlas system (*Ghorbal et al.,* 2006; *Babault et al.,* 2008).

Geothermal and gravity modelling in agreement with deep seismic and magnetotelluric data indicate crustal thicknesses of about 38-39 km underneath the northern border of the High Atlas, thinning to the north and south reaching 35 km, e.g. Rif domain (*Makris et al.,* 1985; *Schwarz and Wigger,* 1988; *Wigger et al.,* 1992; *Zeyen et al.,* 2005; *Missenard et al.,* 2006). These data also points to the presence of a low velocity zone in the upper mantle (below 40-45 km) along the transition of the High to Middle Atlas. This zone is interpreted as a hot mantle, which intruded during the episode of tectonic calm (*Teixell et al.,* 2003; *Missenard et al.,* 2006; *Ledo et al.,* 2011). These variations in crustal thickness are highlighted by gravity (-120 mGal) and geoid (16-20 m) anomalies reaching maxima along the Middle and High Atlas and Anti-Atlas, respectively (*Mickus and Jallouli,* 1999; *Ayarza et al.,* 2005; *Fullea et al.,* 2007 and *Teixell et al.,* 2005).

The tectonic structure of the Atlas Mountains based on geological observations and geophysical data indicate the existence of a combination of thick- and thin-skin tectonics affecting indistinctly the basement and Mesozoic cover. The general structure of the Atlas Mountains is, therefore, interpreted as a broad pop-up with the main thrust facing south east, with maximum rates of shortening of about 15-24% (*Teixell et al.,* 2003; *Ayarza et al.,* 2005). Such an amount of shortening cannot account for the observed elevation (4.000 m), neither the crustal differences observed below the range. Consequently, a possible explanation related to the presence of a thermal anomaly or an anomalous shallow mantle (*Teixell et al.,* 2003; *Missenard et al.,* 2006).

Similarly, the Iberian micro-plate shares with the Atlas Mountains closely related tectonic stages from late Palaeozoic, Mesozoic and early Tertiary. The onset of the Cainozoic uplift started in the Pyrenees during the early Paleocene, leading to the tectonic inversion of the Mesozoic Catalan Coastal Ranges basin to the south east (*Gaspar-Escribano et al.,* 2003; *Gaspar-Escribano et al.,* 2004). Further south, thermo-chronology data from the Spanish Central System and the Iberian Range suggest an early (Eocene) episode of exhumation (*De Bruijne and Andriessen,* 2000; *Del Rio et al.,* 2009). A subsequent period of tectonic quiescence extended until the early Oligocene-Miocene when the maximum episode of uplift was reached along the Pyrenees, the Cantabrian Mountains and Central Spain (*Fitzgerald et al.,* 1999; *De Bruijne and Andriessen,* 2002; *Martín-González et al.,* 2006). Post-Miocene to Pliocene cooling ages have also been recorded in Central Spain (Guadarrama and Toledo Mountains) according to data from *Barbero et al.* (2005) and *De Bruijne and Andriessen* (2000).

Concerning the crustal architecture at the plate interior of Iberia, a series of pop-ups (Central System and Iberian Range) and thrusts (Cantabrian Mountains, Toledo Mountains or the Catalan-Coastal Intra-plate Mountains, etc) involving in some cases the Variscan basement, led to exhumation and uplift of the main ranges. Geophysical data suggest overall Moho depths of about 30-32 km, while major depths are reached underneath the main mountain ranges (35-37 km along the Central System and the Iberian Range, 40-50 km across the Cantabrian Mountains-Pyrenees).

Undoubtedly, a broad view of the entire system (Iberia-Atlas) allows the correlation between both mountain systems by comparing the distribution of mountain ranges and their geological history. The topography in western Iberia strikes E-W to NE-SW following the late-Variscan tectonic fabric (Cantabrian Mountains, Spanish Central System, Toledo Mountains and Sierra Nevada). These orientations are also observed along the Atlas chain, where the High Atlas follows NE-SW to E-W trends, while the Middle and Anti Atlas are NE-SW orientated. The presence of pre-existent structures that controlled the geometry of the Mesozoic rift basins (mainly Jurassic in the Atlas) has contributed to the present-day topography distribution (*Gouiza et al.,* 2010). Moreover, the amount of shortening in Central Iberia and the axial part of the Atlas are very similar (roughly 20% of total shortening). Additionally, geological observations

indicate that deformation in the Atlas was initiated within the external part of the system (axial Atlas chain); moreover, hardly any direct relation with the translations observed in the Tell-Rift area related to the Africa-Europe collision have been reported (shortening along the Rif System displays orthogonal patterns with the High Atlas). Therefore, the tectonic inversion of the Atlas Mountains cannot be linked to the collision of the Alboran block (*De Lamotte et al.,* 2000). Presumably, the early uplift recorded in the Atlas resulted, from the mechanical coupling between the Iberia-Europe plates that led to the building up of the Pyrenees Mountains and the subsequent effective stress transmission towards the southern foreland areas.

Based on these similarities, it has been suggested that Iberia and Africa are connected by a series of lithosphere folds that may have evolved in a similar way leading to a synchronous tectonic evolution and similar rates of uplift (*Teixell et al.,* 2003; *De Vicente and Vegas,* 2009a). These folds may have been active during the main episodes of exhumation in Africa (middle-late Eocene and Plio-Quaternary) and affected by mantle sources (i.e. thermal anomaly) during the episodes of tectonic quiescence in between (*De Lamotte et al.,* 2000; *De Lamotte,* 2009). Recent numerical experiments carried out by *Burov and Cloetingh* (2009) have successfully imaged these interactions, indicating major differences of the shape of topography in terms of their symmetry. Nonetheless, they argued that the interaction between lithosphere folds and mantle plumes might persist in time during several million of years depending on the thermal age of the lithosphere.

The search for a mechanism that could explain the origin of the periodic patterns observed in the Iberian-Atlas topography inspired *Muñoz-Martín et al.* (2010) to perform a spectral analysis of topography and gravity. These authors reported the presence of periodic patterns extending from the Cantabrian Mountains in Iberia to the Atlas in northern Africa. Their results showed long wavelengths of topography (between 250-300 km and 600 km). In addition, *Barbero et al.* (2011) have also documented wavelengths of 250-300 km in a local study across the Atlas Mountains. The harmonic surface of topography at 250 km shown in Figure 6.1 portrays a series of elevated areas periodically distributed along the Iberian-Africa continents. These uplifted areas correlate with the main mountain ranges from north to south (Cantabrian Mountains-Pyrenees, Spanish Central System, Sierra Morena, Gulf of Cadiz and High Atlas). These mountains define a series of basement uplifts or crustal folds that may also be continued towards the Atlantic Platform (Galicia Bank, Extremadura Spur and Gorringe Bank).

The spectral analysis carried out on the analogue modelling results shown in this thesis indicates wavelengths for gravity and topography of about 50 km and 250 km [Fig.6.1]. However, gravity and topography matches at harmonic surfaces of about 250 km, which reflect the effect of mantle deformation on topography, showing a series of periodically elevated domains followed by areas of subsidence [Fig.6.1]. The theoretical gravity and Moho depth maps from the experiment portray the existing good correlation between areas with a deep position of the Moho and the main gravity lows. The position of these anomalies is controlled by the influence of lateral strength variations and presence of pre-existent faults that correlates with the location of tectonic structures.

In view of the comparison between the analogue modelling results, geological and geophysical observations, as well as, the synchronous uplift documented by thermo-chronological data in Iberia mentioned above, this thesis concludes that the observed periodic pattern of intra-plate mountain ranges across western Iberian and northern Africa could be the result of large-scale folding of the lithosphere.

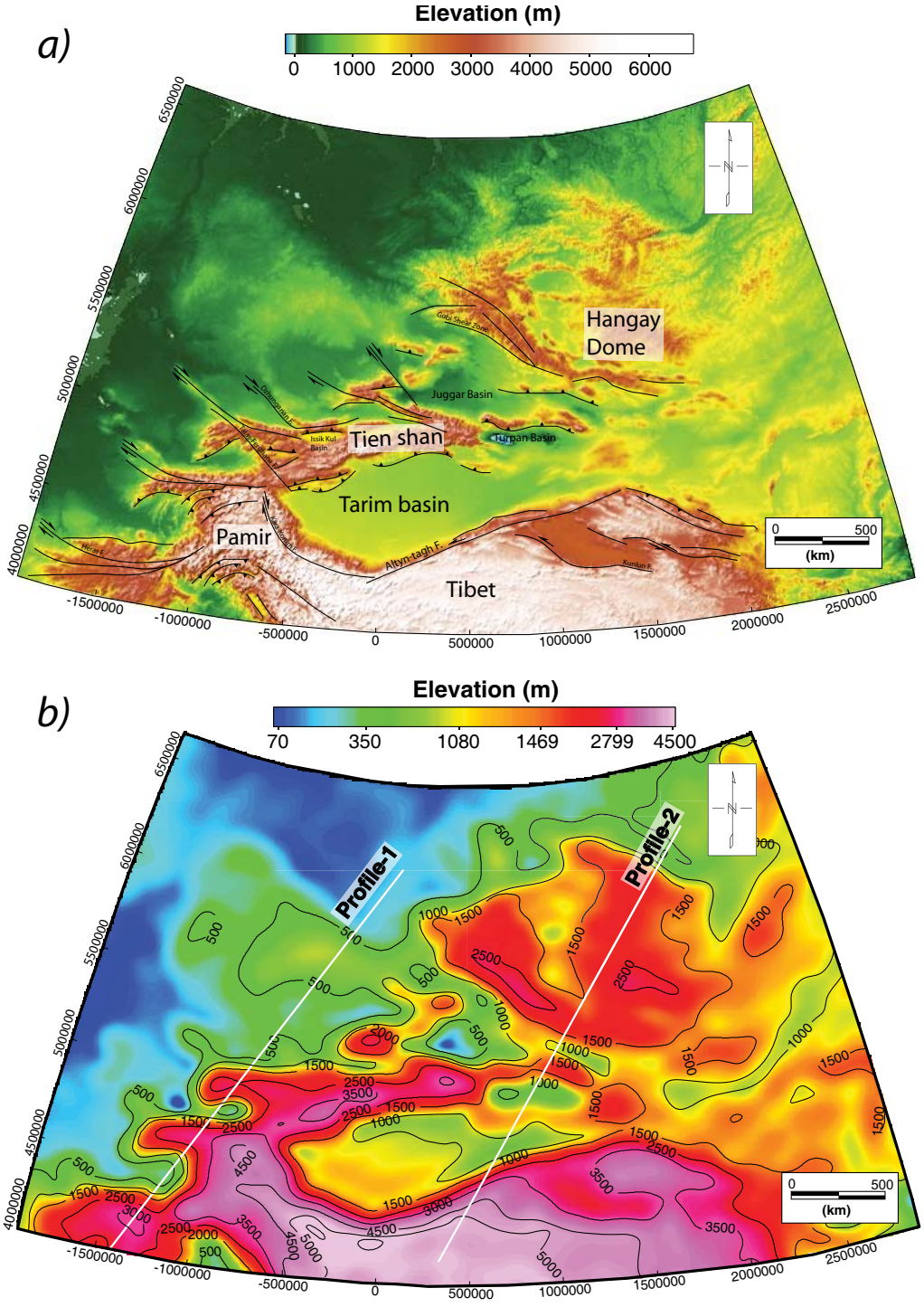

Figure 6.2 *(a) Structural map of Central Asia. (b) Filtered topography at 350 km and location of profiles shown in Figure 6.3.*

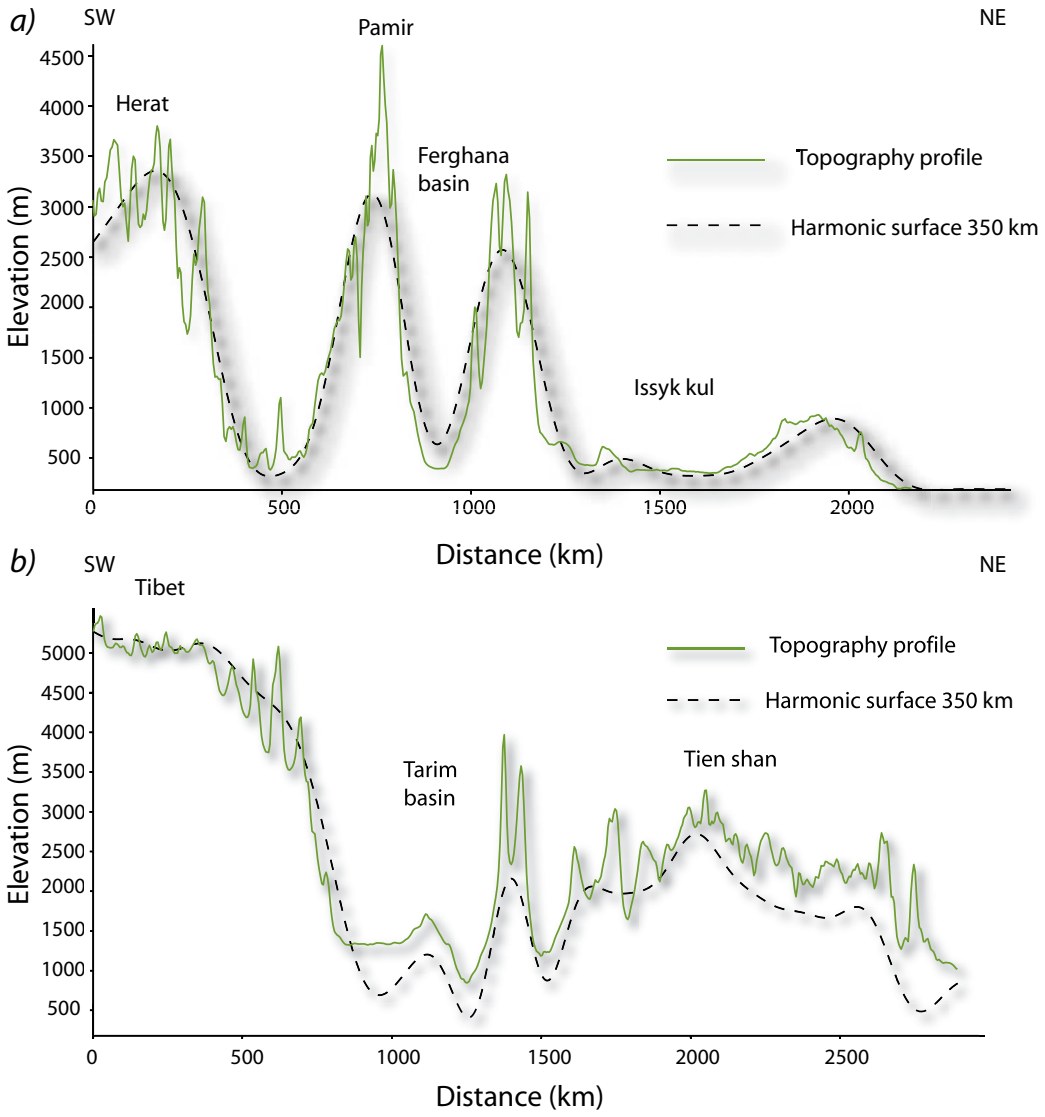

Figure 6.3 *Comparison between original topography and filtered topography (350 km harmonic surface) along profiles 1 (a) and 2 (b) shown in Figure 6.2b.*

6.2.2 Tien Shan Mountains in Central Asia

The Tien Shan fold-belt represents a highly deformed and seismically active intra-plate area, despite its far location from the Indo-Eurasian suture zone (more than 1.500 km). Moreover, it has been permanently active from the late Cretaceous. Its general structure is dominated by a series of E-W oriented, high elevation mountain ranges (over 7.000 m), alternating with parallel sedimentary basins, and separated by NW-SE right-lateral structures (i.e. Talas-Ferghana Fault, the Dzhungarian Fault, or the Gobi-Altai Shear Zone among the most important) [Figure 6.2a]. Almost 2.500 km long and ~400 km wide, the Tien Shan region shortened by more than 150 km at a rate of 20 mmy^{-1} according to GPS data (*Abdrakhmatov et al.,* 1996). Consequently, from

these data, it is possible to infer the total amount of shortening, which is ~35% for the entire Tien Shan range.

Apatite fission track thermo-chronology carried out in western and northern Issyk-Kul basin showed an episode of rock uplift and denudation starting between 20 and 10 Ma ago, and a second episode of exhumation 3 Ma ago. The northward propagation of the deformation from the Himalayan collisional border towards Central Asia suggests the northward tectonic rejuvenation of the mountain belt (*Dobretsov et al.,* 1996; *Jolivet et al.,* 2010).

The tectonic architecture of the Tien Shan ranges is governed by a series of Pre-Cainozoic terranes (i.e. Issyk Kul or Pamir terranes) that were attached to each other during the continental-convergence episode that gave rise to the Himalayas further south. The internal structure has been explained in terms of continental extrusion (*Molnar and Tapponnier,* 1975; *Tapponnier and Molnar,* 1979; *Avouac and Tapponnier,* 1993), strain partitioning mechanisms (*Cunningham et al.,* 1996) or lithospheric folding (*Burov et al.,* 1990; *Burov et al.,* 1993; *Nikishin et al.,* 1993; *Cloetingh et al.,* 1999). Recent seismic data, however, shows the complexity of the lithosphere structure portraying the underthrusting of the Tarim Basin underneath the southern front of the Tien Shan and the rotation of surrounding crustal fronts (*Buslov et al.*, 2007). As a result, a series of deformation belts were distributed and squeezed between relatively stiff blocks (like a piece of plasticine being squeezed between wooden indenters). It is also important to remark the influence of pre-existent structures oblique to the main E-W trending thrust that may have influenced the final reorganization and rotation of crustal blocks (*Jolivet et al.,* 2010).

Seismic reflection and refraction profiles indicate crustal thickness variations from roughly 40 km to 60 km across the northern part of the chain (*Ulomov,* 1974). Moreover, recent data from receiver functions show thickened crust of 55-70 km beneath most of the Tien Shan and 45 below the surrounding platforms, although under the Naryn basin the crust thins to about 45 km (*Oreshin et al.,* 2002; *Vinnik et al.,* 2004). These abnormally high crustal thickness values are correlated with major gravity anomalies found under the main Tien Shan, Pamir and northern edge of the Tibetan Plateau. Surprisingly, despite the presence of deep crustal roots, these gravity anomalies indicate that the range mostly is in isostatic equilibrium and, hence, only the southern border of the Tien Shan presents significant discrepancies between calculated and observed anomalies. These differences may in turn suggest the lack of isostatic equilibrium or the presence of a dynamic force of mantle source (*Burov et al.,* 1990; *Burov and Molnar,* 1998).

Additionally, a series of topography and gravity cross-sections were carried out across the mountain belt, parallel to the direction of convergence in order to study their periodic pattern (*Burov et al.,* 1993). The spectral analysis of these signals provided wavelengths of 30-50 km and 300-360 km. Short wavelengths have been related to topographic uplift controlled by thrusting along the borders of the range (southern fault of the Tien Shan and northern Pamir Mountains among others) (*Nikishin et al.,* 1993). Whereas the long wavelengths have been related to a mechanism of folding that may reconcile the general state of isostatic equilibrium observed across the region (*Burov et al.,* 1993). Figure 6.2b shows the filtered topography indicating periodicities of about 350 km along two profiles displayed in Figure 6.3. The comparison between the original topography successfully matches with the harmonic surface at 350 km indicating the presence of periodic patterns of topography.

The contribution of crustal to mantle deformation during folding of a relatively young lithosphere like Central Asia (Jurassic in age) has been investigated through a series of numerical models carried out by *Cloetingh et al.* (1999). The thermal weakening caused by the episode of Jurassic-Cretaceous extension, probably facilitated the de-coupling between the crust-mantle interface prior to the Cainozoic episode of convergence. Consequently, shortening of the entire

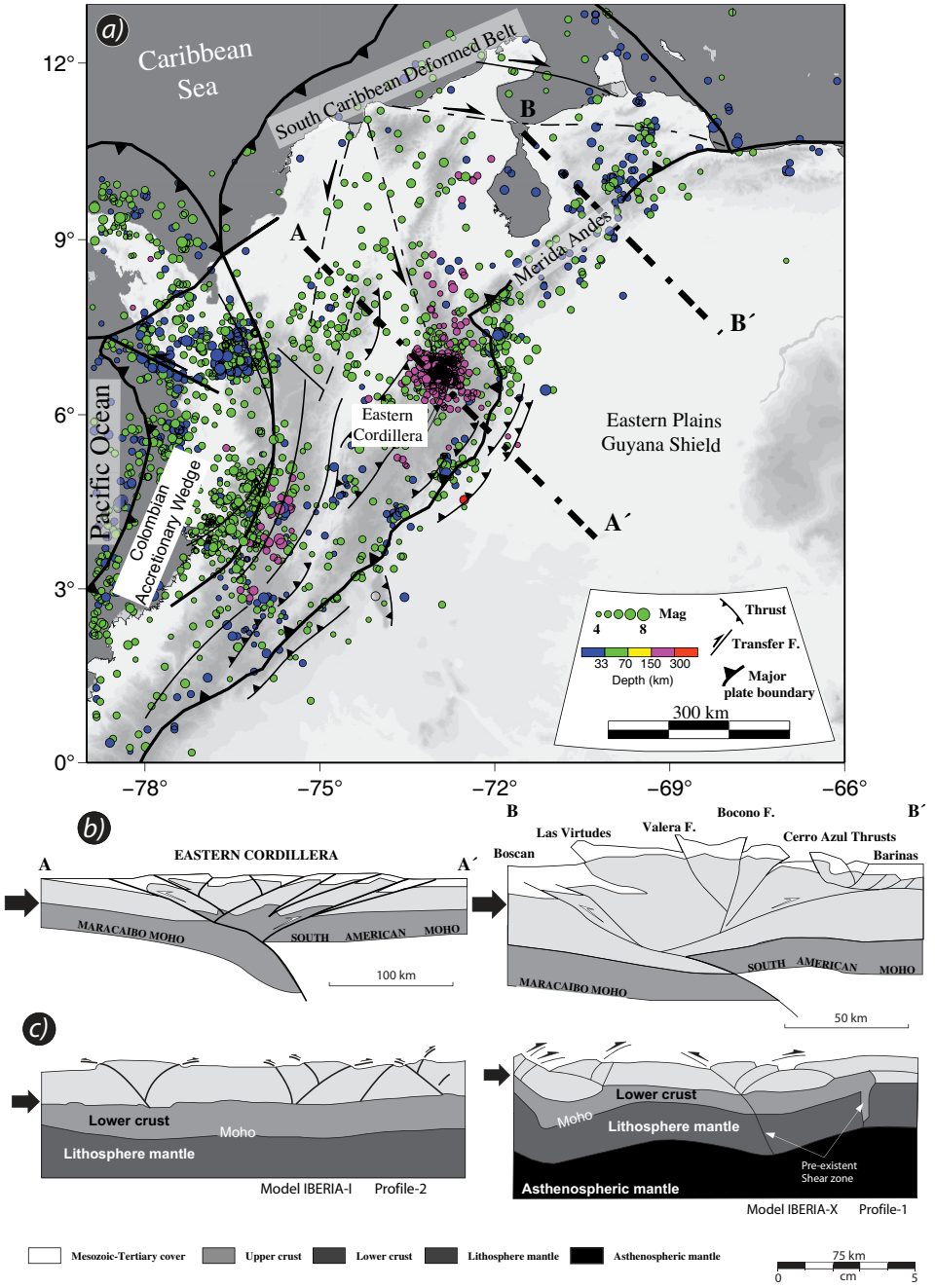

Figure 6.4 *(a) Tectonic map of the Venezuelan Andes showing the main structures. Clusters of epicentres are located towards the western part of the intra-plate chain and the present-day subduction zone. It is worth noticing the presence of seismic alignments following the direction of the main strike-slip fault systems (NW-SE, NE-SW). (b) Cross-sections based on seismic data along two profiles, modified from Colleta et al. (1996) and comparison with (c) analogue model cross-section from models IBERIA-I (Figure 3.29) and IBERIA-X (profile shown in Figure 4.8) Models share similar crustal architecture displaying the effect of pre-existent faults and their contribution to the final distribution of pop-ups and single thrust that led to uplift of the model surface.*

lithosphere led to irregularly distribute crustal folds, whereas the lithospheric mantle was folded in a more regular way (differences in amplitude and wavelength between crustal and mantle folds).

6.3 Crustal architecture of intra-plate folded lithosphere: The role of pre-existent tectonic structures

Analogue experiments provide valuable information on the mode of deformation of the mantle lithosphere and its relation with episodes of thrusting at upper crustal levels. In the following section, I will discuss the implications for crustal architecture and reactivation of pre-existent structures controlled by mantle deformation, in a well-known intra-plate area imaged by gravity and deep seismic data across the Andes of Venezuela.

6.3.1 The Mérida Andes (western Venezuela)

Situated in the north-western part of South-America, the Merida Andes represent an intra-plate chain between the Eastern Cordillera in the south and the South Caribbean transform margin in the north. Unlikely the Central and South Andes, It forms part of the Northern Andes Belt that resulted from Mesozoic and Cainozoic oceanic-continent collision (Jurassic, late Cretaceous, and Palaeogene) prior to the development of the present-day Andes (*Gansser,* 1973).

The Mérida Andes experienced an early episode of extension related to the separation of the North and South American continents that led to the formation of a series of Jurassic basins, striking N-S to NE-SW. During the early-late Cretaceous, an oceanic platform was established on a passive margin, which was coeval with the collision of the Caribbean Plate with the north-western part of Venezuela (Cretaceous sediments were deposited over a Palaeozoic to Precambrian basement previously thinned in the Jurassic) (*Lugo and Mann,* 1995). A subsequent episode of tectonic convergence led to the inversion of pre-existent normal faults during Palaeocene and Miocene, which in turn, uplifted the Mérida Andes (*Colletta et al.,* 1996). The total amount of Tertiary shortening has been estimated to about 60-70 km over the entire range (*Cortés et al.,* 2006). However, the present-day tectonic setting is dominated by superimposed strike-slip faults (*Audemard et al.,* 2005). Balanced geological cross-sections based on reflection seismic profiles have shown the importance of pre-existent fault reactivation (mainly Jurassic and Cretaceous) for the final configuration of the chain. These Mesozoic N-S to NE-SW striking structures may have controlled the vergence of the orogen following the early rift basin pattern (*Cortés et al.,* 2006). Therefore, towards the northeast, underthrusting of the South America craton is taking place beneath the Maracaibo block (crustal indentation), whereas towards the south, the Maracaibo block subducts underneath the craton [Fig.6.4a and b]. The crustal architecture of the chain is delimited by a series of northwest dipping faults to the east and southeast dipping faults to the west defining a broad pop-up that has been interpreted as a crustal-scale flower structure (*Colletta et al.,* 1996; *Audemard et al.,* 2005).

6.3.2 Comparison with Iberia

Comparison with analogue modelling results provides a good understanding of the crustal architecture of intra-plate domains [Fig.6.4b and c]. In this way, the comparison with a model cross-section shown in Figure 3.29, displays a pop-up like structure nucleated at lower crust levels and subsequent thickening of the lower crust below. Moreover, a series of single thrusts account for part of the total amount of shortening. However, the experimental cross-

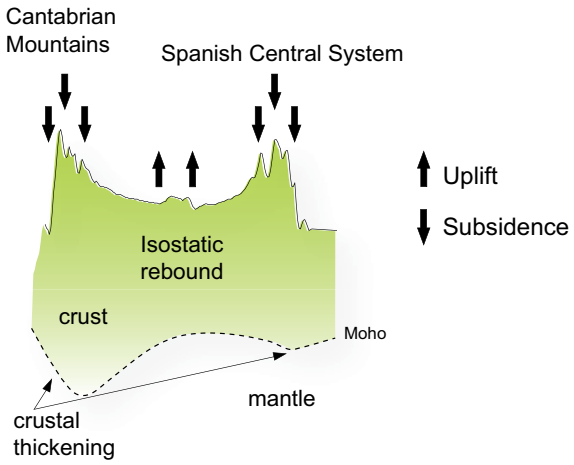

Figure 6.5 *Sketch showing the influence of the combined effect of lithosphere buckling and flexural load of mountain belts on the isostatic bulge that raises the Duero Basin. Areas of subsidence are represented by mountain ranges below which the Moho deepens due to the combined effect of lithosphere folding and the flexural load, whereas domains of induced uplift are found in the central part of the basin, where the Moho is shallow as a result of the isostatic rebound caused by mountain loading in the surroundings.*

section with pre-existent zones of weakness (prior to the onset of shortening) indicates the importance of inherited structures for strain localization and uplift [Fig.6.4c]. This is confirmed by the analysis of horizontal displacement particles described in Chapter 5. Fault reactivation, therefore, may be followed by several tectonic regimes leading to the final configuration of topography.

In Iberia clear examples are the Somolinos Fault, the Vilariça-Bragança Fault System, or the Messejana-Plasencia Fault. All of them resulted from the late-Variscan episode of unroofing under a transtensive tectonic regime that extended from the Appalachian Mountains in USA to the Urals in Russia (*Arthaud and Matte,* 1977). These faults were reactivated during the Mesozoic rifting episode, as follows: Vilariça, during the Jurassic episode of North Atlantic opening; Somolinos at the beginning of the Permo-Triassic and Messejana during the Jurassic (confirmed by the intrusion of a dolerite dike). The analogue modelling results suggest that during N-S compression only those pre-existent faults that were properly oriented under such a stress-field were reactivated. Therefore, only those faults with an obliquity of ca. 20º with the main stress-field were reactivated (i.e. Somolinos and Messejana-Plasencia). This view is in agreement with field observations that suggest that during the Cainozoic, the Messejana Plasencia Fault maintained components of pure thrust- to left-lateral strike-slip movements (*Villamor,* 2002; *Araújo,* 2004). In addition, the Somolinos Fault portrays a similar reactivation history under a regime of transpression leading to dip-slip right-lateral displacements through most of Cainozoic Times (*Bergamin et al.,* 1996; *De Vicente et al.,* 2009b). Recent studies carried out in north-western Iberia by *Martín-González and Heredia* (2010), suggested the possibility that this set of NE-SW oriented faults (Vilariça-Bragança Fault) may have played an important role during the final stages of the Alpine convergence but they were inactive during the Oligocene-Miocene when strain transmission may have transferred into a NW-SE fault systems connected with the Cantabrian off-shore border. This view contradicts previous studies suggesting that the NE-SW trends in western Iberia may have efficiently transferred stress to the plate interior during N-S Alpine convergence (*De Vicente and Vegas,* 2009a). The lithospheric scale models shown in this thesis indicate that such a fault system, striking NE-SW (<40º) possibly has not been re-

activated, emphasizing the role of E-W to NE-SW thrust that may have uplift the surrounding areas. That means that during N-S compression, thrusting in north-western Iberia may have contributed significantly to the present day observed elevation along the Gallician Domain (*Martín-González et al.,* 2006). Therefore, NE-SW trending structures could only be reactivated during the subsequent NW-SE stress-field imposed after the Alboran collision

6.4 Basin response to active intra-plate mantle deformation

Apart from that basins are considered as relative stable areas compared to their surrounding mountain belts, several process have been suggested in order to explain their formation and subsequent sedimentary evolution (*Cloetingh et al.,* 2007). Among the most important mechanisms for intra-plate compressional basin formation are: dynamic or mantle-driven mechanisms (*Allen and Allen,* 2005), lithospheric folding (*Cloetingh and Burov,* 2011), crustal flow (*Li et al.,* 2009) or basin growth by lithospheric flexure (*Watts and Ryan,* 1976; *Watts et al.,* 1982).

None of the above mentioned processes successfully explain the high elevation of the Duero Basin found in Central Spain (~900 m). Instead, the most probable scenario as shown by the analogue modelling results may consist of a combination of lithosphere folds and the flexural load caused by the thickened crust (38-40 km) underneath the Cantabrian Mountains belt. The amplification of a broad lithosphere anticline would lead to uplift of the surface where basins like the Duero may form. For instance, the flexural response triggered by orogenic load of the Central System range in Central Iberia has been correlated with a process of surface extension that evolves with depth into shortening along the Tagus Basin, further south. This idea is supported by the comparison of earthquake focal mechanisms at different depths (*Andeweg et al.,* 1999) [Fig.6.5]. Similar conclusions were obtained in the Betics, where the crustal attenuation of the Internal Betics and the Guadalquivir Basin has been related to a flexural model to explain extension and synchronous uplift of the surroundings based on elastic thickness and gravity studies (*Van der Beek and Cloetingh,* 1992). Estimations of elastic thickness along the border of the Cantabrian-Pyrenees and Spanish Central System fronts indicate 17 to 20 km which may be enough to support the mountain fronts leading to isostatically compensated uplift along the Duero Basin in between.

The combined effect of both mechanisms would also explain the shallow Moho situated below the basin (30-32 km) surrounded by the thickened areas (38-35 km) of the Cantabrian Mountains and Central System (*Banda et al.,* 1981; *Tesauro et al.,* 2008).

6.5 Conclusions: a new model for Intra-plate mountain building and basin development in Iberia.

The purpose of this thesis has been to provide a careful and accurate investigation for the observed pattern of topography and basin evolution in Iberia.

The topography in Spain highlights some peculiarities concerning the overall trend of topography [Fig.6.1]. Western Spain is characterised by a series of E-W, NE-SW oriented mountain ranges regularly spaced towards the northern Atlas (i.e. Cantabrian Mountain, Spanish Central System, Sierra Morena and Moroccan Atlas). This periodicity is hardly seen towards the eastern part of

Iberia where elevated areas follow E-W, NE-SW to NW-SE trends.

In the present study, I have shown that this periodic pattern repeating every 250-300 km is the result of E-W trending folds that affect the entire lithosphere. In some cases, these structures appear to be influenced by pre-existing late-Variscan to Mesozoic structures that were reactivated during N-S compression that gave rise to the formation of the Pyrenees in northern Spain and the stress transmission to the plate interior. However, the presence of a hot and weak lithosphere to the eastern part of Spain (Iberian Range) at the onset of the Cainozoic convergence may have favoured crustal thickening by thrusting at upper crustal levels and ductile flow in the lower crust. As a result, any periodic pattern would finally be destroyed, even though, there is a possibility it was totally absent in this part of Iberia. In any case, the N-S convergence led to tectonic inversion through a series of pre-existent faults that controlled Mesozoic sedimentation. A final stage of extension along the Valencia Trough, related to Miocene to present-day back-arc extension of the western Mediterranean may influence and contribute to the observed differences between eastern and western Spain (*Fontboté et al.,* 1990; *Roca and Guimerá,* 1992; *Janssen et al.,* 1993).

If these lithospheric folds strike from the Pyrenees to the Atlas Mountains in northern Africa, they also could extend laterally along the Atlantic Margin (Galicia Bank, Extremadura Spur and Gorringe Bank).

This thesis aimed in particular to resolve the complexity of the Iberian intra-plate topography, giving a plausible explanation for the observed differences from east to west. Key results are the finding that a single episode of N-S convergence, related to the main stage of Alpine Orogenesis (Pyrenean stage) may have lead to intra-plate mountain building and basin development in Iberia and the Moroccan Atlas. Moreover, the presence of lateral strength changes together with the presence of inherited late-Variscan faults can have actively contributed to the building up of topography and its significant differences from east-west Spain.

The methodology adopted in this thesis (based on analogue modelling, data on the structure of the crust and spectral analysis of topography and gravity from analogue experiments) may help to gain insight into the deep structure of other regions within plate interiors with limited geological and geophysical data (Northern Africa, South Africa, Siberia, etc.). This study, reconciles surface geology with lithospheric-scale processes in order to successfully explain a model for intra-plate mountain building and basin development that took place during most of the Cainozoic Era in Iberia.

References

Abdrakhmatov, K.Y., Aldazhanov, S., Hager, B., Hamburger, M., Herring, T., Kalabaev, K., Makarov, V., Molnar, P., Panasyuk, S. and Prilepin, M., 1996. Relatively recent construction of the Tien Shan inferred from GPS measurements of present-day crustal deformation rates.

Afonso, J.C. and Ranalli, G., 2004. Crustal and mantle strengths in continental lithosphere: is the jelly sandwich model obsolete? Tectonophysics, 394(3-4): 221-232.

Alía-Medina, M., 1976. «Una megaestructura de la Meseta Ibérica: la bóveda Castellano-Extremeña». Estudios Geológicos, 32: 229-238.

Allen, P.A. and Allen, J.R., 2005. Basin analysis: principles and applications. Wiley-Blackwell.

Alonso-Gavilán, G., Armenteros, I., Carballeira, J., Corrochano, A., Huerta, P. and Rodríguez, J., 2004. Cuenca del Duero. Geología de España, Soc. Geol. España, IGME, Madrid: 550-556.

Alonso-Zarza, A., Calvo, J. and García del Cura, M., 1992. Palustrine sedimentation and associated features--grainification and pseudo-microkarst--in the Middle Miocene (intermediate unit) of the Madrid Basin, Spain. Sedimentary Geology, 76(1-2): 43-61.

Álvarez-García, J.A., 2002. Análisis gravimétrico e isostático en el Macizo Hespérico. Tesis de Master: 1-77.

Álvarez-Marrón, J., Pérez-Estaún, A., Danñobeitia, J.J., Pulgar, J.A., Martínez-Catalán, J.R., Marcos, A., Bastida, F., Ayarza-Arribas, P., Aller, J., Gallart, A., 1996. Seismic structure of the northern continental margin of Spain from ESCIN deep seismic profiles. Tectonophysics, 264(1-4): 153-174.

Alvarez-Marrón, J., Rubio, E. and Torné, M., 1997. Subduction-related structures in the North Iberian Margin. Journal of Geophysical Research-Solid Earth, 102(B10).

Álvaro, M., Capote, R. and Vegas, R., 1979. Un modelo de evolución geotectónica para la Cadena Celtibérica: Acta Geológica Hispánica. Homenatge a Lluis Sole i Sabaris, 14: 172-177.

Álvaro, M., 1987. La subsidencia tectónica en la Cordillera Ibérica durante el Mesozoico. Sedimentary Geology, 48: 37-79.

Alves, T.M., Gawthorpe, R.L., Hunt, D.W. and Monteiro, J.H., 2003. Cenozoic tectono-sedimentary evolution of the western Iberian margin. Marine Geology, 195(1-4): 75-108.

Alves, T.M., Moita, C., Cunha, T., Ullnaess, M., Myklebust, R., Monteiro, J. H., Manuppella, G., 2009. Diachronous evolution of Late Jurassic-Cretaceous continental rifting in the northeast Atlantic (west Iberian margin). Tectonics, 28.

Anadón, P., Cabrera, L., Guimerá, J. and Santanach, P., 1985. Paleogene strike-slip deformation and sedimentation along the southeastern margin of the Ebro Basin. Sepm Society for Sedimentary, pp. 303.

Andeweg, B., De Vicente, G., Cloetingh, S., Giner, J. and Muñoz-Martín, A., 1999. Local stress fields and intraplate deformation of Iberia: variations in spatial and temporal interplay of regional stress sources. Tectonophysics, 305(1-3): 153-164.

Andeweg, B., 2002. Cainozoic tectonic evolution of the Iberian Peninsula: causes and effects of

changing stress fields. Unpublished PhD thesis, Vrije Universiteit, Amsterdam.

Araújo, A., 2004. Alpine tectonics in the Juromenha region (Northeast Alentejo). Comunicaciones Geológicas, 91: 17-36.

Arche, A. and López-Gómez, J., 1996. Origin of the Permian-Triassic Iberian Basin, central-eastern Spain. Tectonophysics, 266(1-4): 443-464.

Arthaud, F., 1975. Les décrochements tardi-hercyniens du Sud-Ouest de l´Europe. Géométrie et essai de reconstitution des conditions de la déformation. Tectonophysics, 25: 139-141.

Arthaud, F. and Matte, P., 1977. Late Paleozoic strike-slip faulting in southern Europe and northern Africa: Result of a right-lateral shear zone between the Appalachians and the Urals. Geological Society of America Bulletin, 88(9): 1305.

Audemard, F.A., Romero, G., Rendon, H. and Cano, V., 2005. Quaternary fault kinematics and stress tensors along the southern Caribbean from fault-slip data and focal mechanism solutions. Earth-Science Reviews, 69(3-4): 181-233.

Avouac, J.P. and Tapponnier, P., 1993. Kinematic model of active deformation in central Asia. Geophysical Research Letters, 20(10): 895-898.

Ayarza, P., Álvarez-Lobato, F., Teixell, A., Arboleya, M., Teson, E., Julivert, M. and Charroud, M., 2005. Crustal structure under the central High Atlas Mountains (Morocco) from geological and gravity data. Tectonophysics, 400(1-4): 67-84.

Ayarza, P., Palomeras, I., Carbonell, R., Afonso, J.C. and Simancas, F., 2010. A wide-angle upper mantle reflector in SW Iberia: Some constraints on its nature. Physics of the Earth and Planetary Interiors, 181(3-4): 88-102.

Babault, J., Teixell, A., Arboleya, M.L. and Charroud, M., 2008. A Late Cenozoic age for long wavelength surface uplift of the Atlas Mountains of Morocco. Terra Nova, 20(2): 102-107.

Banda, E.S., Aparicio, A., Sierra, J. and Ruiz de la Parte, E. 1981. Crust and upper mantle structure of the central Iberian Meseta (Spain). Geophysical Journal International, 67(3): 779-789.

Banda, E., Udías, A., Mueller, S., Mezcua, J., Boloix, M., Gallart, J., Aparicio, A., 1983. Crustal structure beneath Spain from deep seismic sounding experiments. Physics of the Earth and Planetary Interiors, 31(4): 277-280.

Banks, C. and Warburton, J., 1991. Mid-crustal detachment in the Betic system of southeast Spain. Tectonophysics, 191(3-4): 275-281.

Barbero, L., Glasmacher, U.A., Villaseca, C., López García, J.A. and Martín-Romera, C., 2005. Long-term thermo-tectonic evolution of the Montes de Toledo area (Central Hercynian Belt, Spain): constraints from apatite fission-track analysis. International Journal of Earth Sciences, 94(2): 193-203.

Barbero, L., Jabaloy, A., Gómez-Ortiz, D., Pérez-Peña, J.V., Rodríguez-Peces, M.J., Tejero, R., Estupiñán, J., Azdimousa, A., Vázquez, M. and Asebriy, L., 2011. Evidence for surface uplift of the Atlas Mountains and the surrounding peripheral plateaux: Combining apatite fission-track results and geomorphic indicators in the Western Moroccan Meseta (coastal Variscan Paleozoic basement). Tectonophysics, 502(1-2): 90-104.

Barrier, L., Nalpas, T., Gapais, D., Proust, J.N., Casas, A. and Bourquin, S., 2002. Influence of syntectonic sedimentation on thrust geometry. Field examples from the Iberian Chain (Spain) and analogue modelling. Sedimentary Geology, 146(1-2): 91-104.

Beekman, F., Bull, J., Cloetingh, S. and Scrutton, R., 1996. Crustal fault reactivation facilitating lithospheric folding/buckling. Geological Society London Special Publications, 99: 251-263.

Beauchamp, W., 2004. Superposed folding resulting from inversion of a synrift accommodation

zone, Atlas Mountains, Morocco. Thrust tectonics and hydrocarbon systems: AAPG Memoir, 82: 635–646.

Benito-Calvo, A. and Pérez-González, A., 2007. Erosion surfaces and Neogene landscape evolution in the NE Duero Basin (north-central Spain). Geomorphology, 88(3-4): 226-241.

Bergamin, J., De Vicente, G., Tejero, R., Sanchez-Serrano, F., Gómez, D., Muñoz-Martín, A. and Perucha, M., 1996. Cuantificación del desplazamiento dextroso Alpino en la cordillera Ibérica a partir de datos gravimétricos. Geogaceta, 20(4): 917-920.

Biot, M., Ode, H. and Roever, W., 1961. Experimental verification of the theory of folding of stratified viscoelastic media. Bulletin of the Geological Society of America, 72(11): 1621.

Bird, P., 1991. Lateral Extrusion of Lower Crust From Under High Topography in the Isostatic Limit. J. Geophys. Res., 96: 10,275-10,286.

Birot, P. and Solé-Sabaris, L., 1954. Investigaciones sobre morfología de la Cordillera Central Española. Madrid, Consejo Superior de Investigaciones Científicas.

Blakely, R., 1996. Potential theory in gravity and magnetic applications. Cambridge Univ. Press., 461 pp.

Boillot, G., and Malod, J.A.,, 1988. The north and north-wes Spanish continental margin: a review. Revista de la Sociedad Geológica de España, 1((3-4)): 295-316.

Bonini, M., 2007a. Deformation patterns and structural vergence in brittle–ductile thrust wedges: An additional analogue modelling perspective. Journal of Structural Geology, 29(1): 141-158.

Bonini, M., Corti, G., Ventisette, C.D., Manetti, P., Mulugeta, G., Sokoutis, D., 2007b. Modelling the lithospheric rheology control on the Cretaceous rifting in West Antarctica. TERRA NOVA-OXFORD-, 19(5): 360.

Bonnet, S., Guillocheau, F., Brun, J.P. and Van Den Driessche, J., 2000. Large-scale relief development related to Quaternary tectonic uplift of a Proterozoic-Paleozoic basement: The Armorican Massif, NW France. J. geophys. Res, 105: 19,273–19,288.

Bonnet, C., Malavieille, J. and Mosar, J., 2007. Interactions between tectonics, erosion, and sedimentation during the recent evolution of the Alpine orogen: Analogue modeling insights. Tectonics, 26(6): TC6016.

Bourgeois, O., Ford, M., Diraison, M., Veslud, C., Gerbault, M., Pik, R., Ruby, N. and Bonnet, S., 2007. Separation of rifting and lithospheric folding signatures in the NW-Alpine foreland. International Journal of Earth Sciences, 96(6): 1003-1031.

Brigham, E.O., 1974. The fast Fourier transform Prentice-Hall, Englewood Cliffs, N.J.

Brun, J., Sokoutis, D. and Van Den Driessche, J., 1994. Analogue modeling of detachment fault systems and core complexes. Geology, 22(4): 319.

Brun, J. and Beslier, M., 1996. Mantle exhumation at passive margins. Earth and Planetary Science Letters, 142(1-2): 161-173.

Brun, J.P., 1999. Narrow Rifts Versus Wide Rifts: Inferences for the Mechanics of Rifting from Laboratory Experiments [and Discussion]. Philosophical Transactions: Mathematical, Physical and Engineering Sciences, 357(1753): 695-712.

Burg, J.P., Peter Nievergelt, P.D., Oberli, F., Seward, D., Diao, Z., and Meier, M., 1997. Exhumation during crustal folding in the Namche-Barwa syntaxis. Terra Nova, 9(2): 53-56.

Burov, E., Kogan, M., Lyon-Caen, H. and Molnar, P., 1990. Gravity anomalies, the deep structure, and dynamic processes beneath the Tien Shan. Earth and Planetary Science Letters, 96(3-4): 367-383.

Burov, E., Lobkovsky, L., Cloetingh, S. and Nikishin, A., 1993. Continental lithosphere folding in

Central Asia. II: Constraints from gravity and topography. Tectonophysics, 226(1-4): 73-87.

Burov, E. and Molnar, P., 1998. Gravity anomalies over the Ferghana Valley (central Asia) and intracontinental deformation. Journal of Geophysical Research-Solid Earth, 103(B8).

Burov, E. and Watts, A.B., 2006. The long-term strength of continental lithosphere: "jelly sandwich" or "crème brûlée"? GSA Today, 16(1): 4-10.

Burov, E. and Cloetingh, S., 2009. Controls of mantle plumes and lithospheric folding on modes of intraplate continental tectonics: differences and similarities. Geophysical Journal International, 178(3): 1691-1722.

Buslov, M., De Grave, J., Bataleva, E. and Batalev, V.Y., 2007. Cenozoic tectonic and geodynamic evolution of the Kyrgyz Tien Shan Mountains: A review of geological, thermochronological and geophysical data. Journal of Asian Earth Sciences, 29(2-3): 205-214.

Cabral, J., 1989. An example of intraplate neotectonic activity, Vilariça Basin, northeast Portugal. Tectonics, 8(2): 285-303.

Calvo, J.P., Ordóñez, S., García del Cura, M., Hoyos, M., Alonso-Zarza, A. M., Sanz-Rubio, E., and Rodríguez Aranda, J. P., 1989. Sedimentología de los complejos lacustres miocenos de la Cuenca de Madrid. Acta Geol. Hispánica, 24: 281-298.

Cann, J.R. and Funnell, B.M., 1967. Palmer Ridge: a Section through the Upper Part of the Ocean Crust? Nature, 213(5077): 661-664.

Capote, R., De Vicente, G. and González-Casado, J.M., 1990. Evolución de las deformaciones alpinas en el Sistema Central Español (SCE). Sedimentology, 33: 33-46.

Casas-Sainz, A.M., 1993. Oblique tectonic inversion and basement thrusting in the Cameros Massif (Northern Spain). Geodinamica Acta, 6(3): 202–216.

Casas-Sainz, A.M. and Gil-Imaz, A., 1994. Evolución tectonosedimentaria de una cuenca extensional intraplaca: la cuenca finijurásica-eocretácica de los Cameros (La Rioja-Soria): Discusión. Revista de la Sociedad Geológica de España, 7(3-4): 337-347.

Casas-Sainz, A.M. and Gil Imaz, A., 1997. Extensional subsidence, contractional folding and thrust inversion of the eastern Cameros basin, northern Spain. Geologische Rundschau, 86: 802-818.

Casas-Sainz, A.M., Cortés, A.L., Liesa, C., Soria, A.R., Terinha, P., Kullberg, J.C., Rocha da, R., 1998. Estudio comparado de la evolución e inversión de distintas cuencas mesozoicas de la Placa Ibérica. Geogaceta, 24: 67-70.

Casas-Sainz, A.M., Cortés-Gracia, A.L. and Maestro-González, A., 2000a. Intraplate deformation and basin formation during the Tertiary within the northern Iberian plate: Origin and evolution of the Almazán Basin. Tectonics, 19(2): 258-289.

Casas-Sainz, A.M., Casas, A., Pérez, A., Tena, S., Barrier, L., Gapais, D., Nalpas, T., 2000b. Syn-tectonic sedimentation and thrust-and-fold kinematics at the intra-mountain Montalbán Basin (northern Iberian Chain, Spain). Geodinamica Acta, 13(1): 1-17.

Casas-Sainz, A.M., and Faccenna, C., 2001. Tertiary compressional deformation of the Iberian plate. Terra Nova, 13(4): 281-288.

Casas-Sainz, A.M., Villalaín, J.J., Soto, R., Gil-Imaz, A., Del Río, P. and Fernández, G., 2009a. Multidisciplinary approach to an extensional syncline model for the Mesozoic Cameros Basin (N Spain). Tectonophysics, 470(1-2): 3-20.

Casas-Sainz, A.M. and De Vicente, G., 2009b. On the tectonic origin of Iberian topography. Tectonophysics, 474(1-2): 214-235.

Cashman, P.H. and Fontaine, S.A., 2000. Strain partitioning in the northern Walker Lane, western Nevada and northeastern California. Tectonophysics, 326(1-2): 111-130.

Choukroune, P. and Team, E., 1989. The Ecors Pyrenean seismic profile reflection data an the overal structure of an orogenic belt. . Tectonics, 8.

Choukroune, P., Roure, F., Pinet, B. and Ecors Pyrenees, T., 1990. Main results of the ECORS Pyrenees profile. Tectonophysics, 173(1-4): 411-418, 421-423.

Choukroune, P., 1992. Tectonic evolution of the Pyrenees. Annual Review of Earth and Planetary Sciences, 20: 143-158.

Civis, J., 2004. Cuencas Cainozoicas: Rasgos generales-estructuración. Geología de España: 531-533.

Cloetingh, S. and Banda, E., 1992. Europe´s lithosphere–physical properties. Mechanical structure. Blundell, D., Freeman, R., Müller, St.(Eds.), A Continent Revealed: The European Geotraverse. Cambridge University Press, Cambridge: 80–91.

Cloetingh, S., D´Argenio, B., Catalano, R., Horvath, F. and Sassi, W., 1995. Interplay of extension and compression in basin formation: introduction. Tectonophysics, 252(1-4): 1-5.

Cloetingh, S. and Burov, E.B., 1996. Thermomechanical structure of European continental lithosphere; constraints from rheological profiles and EET estimates. Geophysical Journal International, 124(3): 695-723.

Cloetingh, S., Burov, E. and Poliakov, A., 1999. Lithosphere folding: Primary response to compression? (from central Asia to Paris Basin): Tectonics, v. 18. doi, 10: 1064–1083.

Cloetingh, S. and Burov, E., Beekman, F., Andeweg, B., Andriessen, P. A. M., García-Castellanos, D., De Vicente, G., and Vegas, R., 2002. Lithospheric folding in Iberia. Tectonics, 21(5): 1041.

Cloetingh, S., Ziegler, P.A., Beekman, F., Andriessen, P.A.M., Matenco, L., Bada, G., Garcia-Castellanos, D., Hardebol, N., Dèzes, P. and Sokoutis, D., 2005. Lithospheric memory, state of stress and rheology: neotectonic controls on Europe´s intraplate continental topography. Quaternary Science Reviews, 24(3-4): 241-304.

Cloetingh, S., Ziegler, P., Bogaard, P., Andriessen, P., Artemieva, I., Bada, G., van Balen, R., Ben-Avraham, Z., Brun, J. and Bunge, H., 2007. TOPO-EUROPE Working Group, 2007, TOPO-EUROPE: The geoscience of coupled deep Earthsurface processes. Global and Planetary Change, 58: 1–118.

Cloetingh, S., Beekman, F., Ziegler, P.A., van Wees, J.D. and Sokoutis, D., 2008. Post-rift compressional reactivation potential of passive margins and extensional basins. Geological Society, London, Special Publications, 306(1): 27-70.

Cloetingh, S. and Burov, E., 2011a. Lithospheric folding and sedimentary basin evolution: a review and analysis of formation mechanisms. Basin Research, 23(3): 257-290.

Cloetingh, S., Gallart, J., de Vicente, G. and Matenco, L., 2011b. TOPO-EUROPE: From Iberia to the Carpathians and analogues. Tectonophysics, 502(1–2): 1-27.

Cobbold, P., 1975. Fold propagation in single embedded layers. Tectonophysics, 27: 333-351.

Colletta, B., Roure, F., De Toni, B., Loureiro, D., Passalacqua, H. and Gou, Y., 1996. Tectonic inheritance and structural styles in the Mérida Andes (western Venezuela).

Corrochano, A. and Armenteros, I., 1989. Los sistemas lacustres de la Cuenca terciaria del Duero. Acta Geológica Hispánica, 24: 259-279.

Cortés-Gracia, A. and Casas-Sainz, A., 1997. Pliegues flexurales asociados al cabalgamiento de la Sierra de la Demanda en el Cerro Peñalba (La Rioja). Geogaceta, 21:85-88.

Cortés, M., Colletta, B. and Angelier, J., 2006. Structure and tectonics of the central segment of the Eastern Cordillera of Colombia. Journal of South American Earth Sciences, 21(4): 437-465.

Cunningham, W.D., Windley, B.F., Dorjnamjaa, D., Badamgarov, J. and Saandar, M., 1996. Late Cenozoic transpression in southwestern Mongolia and the Gobi Altai-Tien Shan connection. Earth and Planetary Science Letters, 140(1-4): 67-81.

Davis, G. and Reynolds, S., 1984. Structural geology of rocks and regions. John Wiley & Sons.

Davy, P. and Cobbold, P.R., 1991. Experiments on shortening of a 4-layer model of the continental lithosphere. Tectonophysics, 188(1-2): 1-25.

De Bruijne, C.H. and Andriessen, P.A.M., 2000. Interplay of intraplate tectonics and surface processes in the Sierra de Guadarrama (central Spain) assessed by apatite fission track analysis. Physics and Chemistry of the Earth, Part A: Solid Earth and Geodesy, 25(6-7): 555-563.

De Bruijne, C.H. and Andriessen, P.A.M., 2002. Far field effects of Alpine plate tectonism in the Iberian microplate recorded by fault-related denudation in the Spanish Central System. Tectonophysics, 349(1-4): 161-184.

De Lamotte, D., Saint Bezar, B., Bracène, R. and Mercier, E., 2000. The two main steps of the Atlas building and geodynamics of the western Mediterranean. Tectonics, 19(4).

De Lamotte, D.F., Leturmy, P., Missenard, Y., Khomsi, S., Ruiz, G., Saddiqi, O., Guillocheau, F., Michard, A., 2009. Mesozoic and Cenozoic vertical movements in the Atlas system (Algeria, Morocco, Tunisia): An overview. Tectonophysics, 475(1): 9-28.

De Vicente, G., González-Casado, J., Bergamín, J., Tejero, R., Babín, R., Rivas, A., Hernández-Henrile, J., Giner, J., Sánchez-Serrano, F. and Muñoz, A., 1992. Alpine structure of the Spanish Central System, pp. 284-288.

De Vicente, G., Giner, J.L., Muñoz-Martín, A., González-Casado, J.M. and Lindo, R., 1996. Determination of present-day stress tensor and neotectonic interval in the Spanish Central System and Madrid Basin, central Spain. Tectonophysics, 266(1-4): 405-424.

De Vicente, G., 2005. First order faults of the Iberian Peninsula: PRIOR project results. Geophysical Research Abstracts, 7(4366).

De Vicente, G., Vegas, R., Muñoz-Martín, A., Silva, P.G., Andriessen, P., Cloetingh, S., González-Casado, J.M., Van Wees, J.D., Álvarez, J. and Carbó, A., 2007. Cainozoic thick-skinned deformation and topography evolution of the Spanish Central System. Global and Planetary Change, 58(1-4): 335-381.

De Vicente, G., Cloetingh, S., Muñoz-Martín, A., Olaiz, A., Stich, D., Vegas, R., Galindo-Zaldívar, J., Fernández-Lozano, J., 2008. Inversion of moment tensor focal mechanisms for active stresses around the Microcontinent Iberia: Tectonic implications. Tectonics, 27(TC1009): 1-22.

De Vicente, G. and Vegas, R., 2009a. Large-scale distributed deformation controlled topography along the western Africa-Eurasia limit: Tectonic constraints. Tectonophysics, 474(1-2): 124-143.

De Vicente, G., Vegas, R., Muñoz-Martín, A., Van Wees, J.D., Casas-Sáinz, A., Sopeña, A., Sánchez-Moya, Y., Arche, A., López-Gómez, J., Olaiz, A. and Fernández-Lozano, J., 2009b. Oblique strain partitioning and transpression on an inverted rift: The Castilian Branch of the Iberian Chain. Tectonophysics, 470(3-4): 224-242.

De Vicente, G., Cloetingh, S., Van Wees, J.D. and Cunha, P.P., 2011. Tectonic classification of Cainozoic Iberian foreland basins. Tectonophysics, 502(1-2): 38-61.

Del Rio, P., Barbero, L. and Stuart, F.M., 2009. Exhumation of the Sierra de Cameros (Iberian Range, Spain): constraints from low-temperature thermochronology. Geological Society, London, Special Publications, 324(1): 153-166.

Díaz, J. and Gallart, J., 2009. Crustal structure beneath the Iberian Peninsula and surrounding

waters: A new compilation of deep seismic sounding results. Physics of the Earth and Planetary Interiors, 173(1-2): 181-190.

Doblas, M., López-Ruiz, J., Oyarzun, R., Mahecha, V., Moya, Y., Hoyos, M., Cebriá, J., Capote, R., Enrile, J. L. H., Lillo, J., Lunar, R., Ramos, A., Sopeña, A., 1994. Extensional tectonics in the central Iberian Peninsula during the Variscan to Alpine transition. Tectonophysics, 238(1-4): 95-116.

Dobretsov, N., Buslov, M., Delvaux, D., Berzin, N. and Ermikov, V., 1996. Meso-and Cenozoic tectonics of the Central Asian mountain belt: effects of lithospheric plate interaction and mantle plumes. International Geology Review, 38(5): 430-466.

Doglioni, C., Mongelli, F. and Fieri, P., 1994. The Puglia uplift (SE Italy): An anomaly in the foreland of the Apenninic subduction due to buckling of a thick continental lithosphere. Tectonics, 13: 1309-1321.

Donath, F. and Parker, R., 1964. Folds and folding. Geological Society of America Bulletin, 75(1): 45.

England, P. and McKenzie, D., 1982. A thin viscous sheet model for continental deformation. Geophysical Journal of the Royal Astronomical Society, 70(2): 295-321.

Farias, P., 1987. La estructura herciniana del sector oriental del Sinclinal de Verín: Los cabalgamientos de Verín y Pradocabalos. Cuadernos Laboratorio Xeolóxico Laxe, 11: 295-303.

Feio, M., 1952. A evolução do relevo do Baixo Alentejo e Algarve: estudo de geomorfologia. Centro de Estudos Geográficos.

Fernández, M., Marzán, I., Correia, A. and Ramalho, E., 1998. Heat flow, heat production, and lithospheric thermal regime in the Iberian Peninsula. Tectonophysics, 291(1-4): 29-53.

Fernández-Lozano, J., Sokoutis, D., Willingshofer, E., Muñoz-Martín, A., De Vicente, G. and Cloetingh, S., 2010. Sobre el origen de la asimetría en el patrón general del relieve en el interior de la Península Ibérica. . Geogaceta, 46.

Fernández-Lozano, J., Sokoutis, D., Willingshofer, E., Cloetingh, S. and De Vicente, G., 2011. Cainozoic deformation of Iberia: A model for intraplate mountain building and basin development based on analogue modeling. Tectonics, 30(1): 1-25.

Fernández-Viejo, G., Gallart, J., Pulgar, J., Gallastegui, J., Dañobeitia, J., Córdoba, D., 1998. Crustal Transition Between Continental and Oceanic Domains Along the North Iberian Margin from Wide Angle Seismic and Gravity Data. Geophys. Res. Lett., 25.

Fernández, M., Marzán, I., Correia, A. and Ramalho, E., 1998. Heat flow, heat production, and lithospheric thermal regime in the Iberian Peninsula. Tectonophysics, 291(1-4): 29-53.

Fitch, T.J., 1972. Plate Convergence, Transcurrent Faults, and Internal Deformation Adjacent to Southeast Asia and the Western Pacific. J. Geophys. Res., 77(23): 4432-4460.

Fitzgerald, P.G., Muñoz, J.A., Coney, P.J. and Baldwin, S.L., 1999. Asymmetric exhumation across the Pyrenean orogen: implications for the tectonic evolution of a collisional orogen. Earth and Planetary Science Letters, 173(3): 157-170.

Fontboté, J., Guimerá, J., Roca, E., Sábat, F., Santanach, P. and Fernández-Ortigosa, F., 1990. The Cenozoic geodynamic evolution of the Valencia trough (western Mediterranean). Revista de la Sociedad Geológica de España, 3: 249-259.

Friend, P.F. and Dabrio, C.J., 1996. Tertiary basins of Spain. Edited by Peter F. Friend and Cristino J. Dabrio, ISBN 0521461715. Cambridge, UK: Cambridge University Press: 399.

Fullea, J., Fernández, M., Zeyen, H. and Vergés, J., 2007. A rapid method to map the crustal and lithospheric thickness using elevation, geoid anomaly and thermal analysis. Application to the Gibraltar Arc System, Atlas Mountains and adjacent zones. Tectonophysics, 430(1-4):

97-117.

Gall, B.L., Piqué, A., Réhault, J.-P., Specht, M. and Malod, J., 1997. Structure et mise en place d´une ride océanique dans un contexte de limite de plaques convergentes: le banc de Gorringe (SW Ibérie). Comptes Rendus de l´Académie des Sciences - Series IIA - Earth and Planetary Science, 325(11): 853-860.

Gallastegui, J., 2000. Estructura cortical de la cordillera y margen continental cantábricos: perfiles ESCI-N. Trabajos de Geología, 22: 9-234.

Gansser, A., 1973. Facts and theories on the Andes: Journal of the Geological Society of London, v. 129. doi, 10: 93–131.

Gao, H., Humphreys, E.D., Yao, H. and Van der Hilst, R.D., 2011. Crust and lithosphere structure of the northwestern US with ambient noise tomography: Terrane accretion and Cascade arc development. Earth and Planetary Science Letters.

García-Castellanos, D., Vergés, J., Gaspar-Escribano, J. and Cloetingh, S., 2003. Interplay between tectonics, climate and fluvial transport during the Cainozoic evolution of the Ebro Basin (NE Iberia). Journal of Geophysical Research, 108(B7): 2347.

Gaspar-Escribano, J., Ter Voorde, M., Roca, E. and Cloetingh, S., 2003. Mechanical (de-) coupling of the lithosphere in the Valencia Trough (NW Mediterranean): what does it mean? Earth and Planetary Science Letters, 210(1-2): 291-303.

Gaspar-Escribano, J., García-Castellanos, D., Roca, E. and Cloetingh, S., 2004. Cainozoic vertical motions of the Catalan Coastal Ranges (NE Spain): The role of tectonics, isostasy, and surface transport. Tectonics, 23(1).

Gerbault, M., Burov, E., Poliakov, A. and Daignieres, M., 1999. Do faults trigger folding in the lithosphere? Geophysical Research Letters, 26(2): 271-274.

Ghorbal, B., Bertotti, G. and Andriessen, P., 2006. On the origin of the anomalous elevation in the Atlas Mountains and adjacent regions (Morocco), European Geosciences Union. Geophysical Research Abstracts, pp. 4315.

Ghorbal, B., Bertotti, G., Foeken, J. and Andriessen, P., 2008. Unexpected Jurassic to Neogene vertical movements in “stable” parts of NW Africa revealed by low temperature geochronology. Terra Nova, 20(5): 355-363.

Gibbons, W. and Moreno, T., 2002. The geology of Spain. Geological Society Pub House.

Gouiza, M., Bertotti, G., Hafid, M. and Cloetingh, S., 2010. Kinematic and thermal evolution of the Moroccan rifted continental margin: Doukkala-High Atlas transect. Tectonics, 29(5): TC5008.

Guimerá, J., Alonso, A. and Mas, J.R., 1995. Inversion of an extensional-ramp basin by a newly formed thrust: the Cameros basin (N. Spain). Geological Society, London, Special Publications, 88(1): 433-453.

Guimerá, J., Salas, R., Vergés, J. and Casas, A., 1996. Extensión mesozoica e inversión compresiva terciaria en la Cadena Ibérica: aportaciones a partir del análisis de un perfil gravimetrico. Geogaceta, 20(7): 7697-7694.

Guimerá, J. and González, Á., 1998. El relieve de la Cadena Ibérica como un producto de la compresión alpina. Geogaceta, 24: 163-166.

Guimerá, A., J, Mas, R. and Alonso, A., 2004. Intraplate deformation in the NW Iberian Chain: Mesozoic extension and Tertiary contractional inversion. Journal of Geological Society, 161(2): 291-303.

Harmand, C. and Cantagrel, J., 1984. Le volcanisme alcalin Tertiaire et Quaternaire du Moyen Atlas (Maroc): chronologie K/Ar et cadre géodynamique. Journal of African Earth Sciences (1983), 2(1): 51-55.

Heiskanen, W.A. and Meinesz, F.A.V., 1958. The earth and its gravity field. McGraw-Hill New York.

Hernández-Pacheco, E., 1923. Edad y origen de la Cordillera Central de la Península Ibérica. Asoc. Española para el Progreso de las Ciencias: 119-134.

Hernando-Costa, S., 1973. El Pérmico en la región de Atienza-Somolinos (provincia de Guadalajara). Boletín Geológico y Minero, 84: 231-235.

Herráiz, M., De Vicente, G., Lindo-Ñaupari, R., Giner, J., Simón, J., González-Casado, J., Vadillo, O., Rodríguez-Pascua, M., Cicuéndez, J.I. and Casas, A., 2000. The recent (upper Miocene to Quaternary) and present tectonic stress distributions in the Iberian Peninsula. Tectonics, 19(4).

Herrero, A., Alonso-Gavilán, G. and Colmenero, J.R., 2010. Depositional sequences in a foreland basin (north-western domain of the continental Duero basin, Spain). Sedimentary Geology, 223(3-4): 235-264.

Horváth, F. and Cloetingh, S., 1996. Stress-induced late-stage subsidence anomalies in the Pannonian basin. Tectonophysics, 266(1-4): 287-300.

Hudleston, P. and Stephansson, O., 1973. Layer shortening and foldshape development in the buckling of single layers. Tectonophysics, 17(4): 299-321.

Hudleston, P.J., 1973. An analysis of "Single-layer" folds developed experimentally in viscous media. Tectonophysics, 16(3-4): 189-214.

Hudleston, P. and Lan, L., 1994. Rheological controls on the shapes of single-layer folds. Journal of Structural Geology, 16(7): 1007-1022.

Hurter, S. and Schellschmidt, R., 2003. Atlas of geothermal resources in Europe. Geothermics, 32(4-6): 779-787.

ITGE, 1990. Documentos sobre la geología del subsuelo de España. VI - Ebro y Pirineos.

Jabaloy, A., Galindo-Zald var, J. and González-Lodeiro, F., 2002. Palaeostress evolution of the Iberian Peninsula (Late Carboniferous to present-day). Tectonophysics, 357(1-4): 159-186.

Jackson, J., 2002a. Strength of the continental lithosphere: Time to abandon the jelly sandwich? GSA Today, 12(9): 4-9.

Jackson, J., 2002b. Faulting, flow, and the strength of the continental lithosphere. International Geology Review, 44(1): 39-61.

Janssen, M.E., Torne´, M., Cloetingh, S. and Banda, E., 1993. Pliocene uplift of the eastern Iberian margin: Inferences from quantitative modelling of the Valencia Trough. Earth and Planetary Science Letters, 119(4): 585-597.

Jarosinski, M., Beekman, F., Matenco, L. and Cloetingh, S., 2009. Mechanics of basin inversion: Finite element modelling of the Pannonian Basin System. Tectonophysics.

Jeng, F. and Huang, K., 2008. Buckling folds of a single layer embedded in matrix–Theoretical solutions and characteristics. Journal of Structural Geology, 30(5): 633-648.

Jiménez-Munt, I., Fernández, M., Torne, M. and Bird, P., 2001. The transition from linear to diffuse plate boundary in the Azores-Gibraltar region: results from a thin-sheet model. Earth and Planetary Science Letters, 192(2): 175-189.

Jiménez-Munt, I., Fernández, M., Vergés, J., Afonso, J.C., García-Castellanos, D. and Fullea, J., 2010. The lithospheric structure of the Gorringe Bank: insights into its origin and tectonic evolution. Tectonics, 29: 1-16.

Jolivet, M., Dominguez, S., Charreau, J., Chen, Y., Li, Y. and Wang, Q., 2010. Mesozoic and Cenozoic tectonic history of the central Chinese Tian Shan: Reactivated tectonic structures and active deformation. Tectonics, 29(6): TC6019.

Jones, R. and Geoff Tanner, P., 1995. Strain partitioning in transpression zones. Journal of Structural Geology, 17(6): 793-802.

Jordan, T., 1995. Retroarc foreland and related basins. Tectonics of sedimentary basins, 9: 331-362.

Junco, F. and Calvo, J., 1983. Cuenca de Madrid. Geología de España, 2: 534-543.

Kampschuur, W. and Rondeel, H.E., 1975. The origin of the Betic orogen, southern Spain. Tectonophysics, 27(1): 39-56.

Kearey, P., Brooks, M. and Hill, I., 2002. An introduction to geophysical exploration. Wiley-Blackwell.

Kidd, R.B., Searle, R.C., Ramsay, A.T.S., Prichard, H. and Mitchell, J., 1982. The geology and formation of King´s Trough, northeast Atlantic Ocean. Marine Geology, 48(1-2): 1-30.

Koons, P.O., 1994. Three-dimensional critical wedges: tectonics and topography in oblique collisional orogens. Journal of Geophysical Research, 99(12): 301–12.

Lankreijer, A., Mocanu, V. and Cloetingh, S., 1997. Lateral variations in lithosphere strength in the Romanian Carpathians: constraints on basin evolution. Tectonophysics, 272(2-4): 269-290.

Le Pichon, X. and Sibuet, J.-C., 1971. Western extension of boundary between European and Iberian plates during the Pyrenean orogeny. Earth and Planetary Science Letters, 12(1): 83-88.

Ledo, J., Jones, A.G., Siniscalchi, A., Campanyà, J., Kiyan, D., Romano, G. and Rouai, M., 2011. Electrical signature of modern and ancient tectonic processes in the crust of the Atlas mountains of Morocco. Physics of the Earth and Planetary Interiors.

Leever, K.A., Gabrielsen, R.H., Sokoutis, D. and Willingshofer, E., 2011a. The effect of convergence angle on the kinematic evolution of strain partitioning in transpressional brittle wedges: Insight from analog modeling and high-resolution digital image analysis. Tectonics, 30(2): TC2013.

Leever, K.A., Gabrielsen, R.H., Faleide, J.I. and Braathen, A., 2011b. A transpressional origin for the West Spitsbergen fold-and-thrust belt: Insight from analog modeling. Tectonics, 30(2): TC2014.

Lefort, J. and Agarwal, B., 2002. Topography of the Moho undulations in France from gravity data: their age and origin. Tectonophysics, 350(3): 193-213.

Lewis, C.J., Vergés, J. and Marzo, M., 2000. High mountains in a zone of extended crust: Insights into the Neogene-Quaternary topographic development of northeastern Iberia. Tectonics, 19(1): 86-102.

Li, D., Xia, Y. and Xu, L., 2009. Coupling and Formation Mechanism of Continental Intraplate Basin and Orogen--Examples from the Qinghai-Tibet Plateau and Adjacent Basins. Earth Science Frontiers, 16(3): 110-119.

Liesa, C.L. and Simón-Gómez, J.L., 2009. Evolution of intraplate stress fields under multiple remote compressions: The case of the Iberian Chain (NE Spain). Tectonophysics, 474(1-2): 144-159.

López-Fernández, C., Pulgar, J.A., Gallart, J., González-Cortina, J.M., Díaz, J., and Ruíz, M., 2008. Seismotectonic zonation of the NW Iberian Peninsula. Geo-Temas 10: 1031-1034.

Lowrie, W., 1997. Fundamentals of geophysics. Cambridge Univ. Press., 354 pp.

Lugo, J. and Mann, P., 1995. Jurassic-Eocene tectonic evolution of Maracaibo basin, Venezuela. Am. Assoc. of Pet. Geol.: 699-699.

Luth, S., Willingshofer, E., Sokoutis, D. and Cloetingh, S., 2009. Analogue modelling of

continental collision: Influence of plate coupling on mantle lithosphere subduction, crustal deformation and surface topography. Tectonophysics, 484: 87-102.

Magistrale, H., 2002. Relative contributions of crustal temperature and composition to controlling the depth of earthquakes in southern California. Geophysical Research Letters, 29(10): 1447.

Makris, J., Demnati, A. and Klussmann, J., 1985. Deep seismic soundings in Morocco and a crust and upper mantle model deduced from seismic and gravity data, pp. 369-380.

Maldonado, A., Somoza, L. and Pallares, L., 1999. The Betic orogen and the Iberian-African boundary in the Gulf of Cadiz: geological evolution (central North Atlantic). Marine Geology, 155: 9-43.

Marques, F.O., Mateus, A. and Tassinari, C., 2002. The Late-Variscan fault network in central-northern Portugal (NW Iberia): a re-evaluation. Tectonophysics, 359(3-4): 255-270.

Martín-González, F., Capote, R., Barbero, L., Insua, J. and Martínez-Díaz, J., 2006. Primeros resultados de huellas de fisión en apatito en el sector Lugo-Ancares (Noroeste de la Península Ibérica). Geogaceta, 40: 79-82.

Martín-González, F., 2009. Cainozoic tectonic activity in a Variscan basement: Evidence from geomorphological markers and structural mapping (NW Iberian Massif). Geomorphology, 107(3-4): 210-225.

Martín-González, F. and Heredia, N., 2011. Complex tectonic and tectonostratigraphic evolution of an Alpine foreland basin: The western Duero Basin and the related Tertiary depressions of the NW Iberian Peninsula. Tectonophysics, 502(1-2): 75-89.

Martín-González, F., Barbero, L., Capote, R., Heredia, N. and Gallastegui, G., 2011. Interaction of two successive Alpine deformation fronts: constraints from low-temperature thermochronology and structural mapping (NW Iberian Peninsula). International Journal of Earth Sciences: 1-12.

Martín-Velázquez, S., De Vicente, G. and Elorza, F., 2009. Intraplate stress state from finite element modelling: The southern border of the Spanish Central System. Tectonophysics, 473(3-4): 417-427.

Martín, S. and De Vicente, G., 1995. Paleoesfuerzos alpinos en el borde suroccidental de la Cuenca de Madrid (Montes de Toledo). Geogaceta, 18: 11–14.

Martinod, J. and Davy, P., 1992. Periodic instabilities during compression or extension of the lithosphere: 1. Deformation modes from an analytical perturbation method. J. geophys. Res, 97: 1999-2014.

Martinod, J. and Davy, P., 1994. Periodic instabilities during compression of the lithosphere, 2, Analogue experiments. J. Geophys. Res, 99: 12057-12069.

Márton, E., Abranches, M.C. and Pais, J., 2004. Iberia in the Cretaceous: new paleomagnetic results from Portugal. Journal of Geodynamics, 38(2): 209-221.

Mata, M., Casas, A., Canals, A., Gil, A. and Pocovi, A., 2001. Thermal history during Mesozoic extension and Tertiary uplift in the Cameros Basin, northern Spain. Basin Research, 13(1): 91-111.

Mattauer, M. and Henry, J., 1974. Pyrenees. Geological Society, London, Special Publications, 4(1): 3-21.

Mauffret, A. and Montadert, L., 1987. Rift tectonics on the passive continental margin off Galicia (Spain). Marine and Petroleum Geology, 4(1): 49-70.

Maus, S. and Dimri, V., 1995. Potential field power spectrum inversion for scaling geology. Journal of Geophysical Research, 100(B7): 12605.

Mazzotti, S., Henry, P., Le Pichon, X. and Sagiya, T., 1999. Strain partitioning in the zone of transition from Nankai subduction to Izu-Bonin collision (central Japan): Implications for an

extensional tear within the subducting slab. Earth and Planetary Science Letters, 172(1-2): 1-10.

McAdoo, D. and Sandwell, D., 1985. Folding of oceanic lithosphere. Journal of Geophysical Research, 90: 8563-8569.

McKenzie, D., 1978. Some remarks on the development of sedimentary basins. Earth and Planetary Science Letters, 40(1): 25-32.

Meinesz, V., 1934. FA Gravity expeditions at sea 1923-1932, vol. 2. Publ. of the Netherlands Geodet. Comm. Delft.

Mézcua, J., Gil, A. and Benarroch, R., 1996. Estudio gravimétrico de la Península Ibérica y Baleares. Instituto Geográfico Nacional, Madrid, 14.

Mickus, K. and Jallouli, C., 1999. Crustal structure beneath the Tell and Atlas Mountains (Algeria and Tunisia) through the analysis of gravity data. Tectonophysics, 314(4): 373-385.

Minster, J.B., and Jordan, T. H., 1978. Present-day plate motions. J. Geophys. Res., 83.

Miranda, R., Valadares, V., Terrinha, P., Mata, J., Azevedo, M.R., Gaspar, M., Kullberg, J.C. and Ribeiro, C., 2009. Age constraints on the Late Cretaceous alkaline magmatism on the West Iberian Margin. Cretaceous Research, 30(3): 575-586.

Missenard, Y., Zeyen, H., Frizon de Lamotte, D., Leturmy, P., Petit, C., Sébrier, M. and Saddiqi, O., 2006. Crustal versus asthenospheric origin of relief of the Atlas Mountains of Morocco. J. Geophys. Res., 111.

Missenard, Y., Saddiqi, O., Barbarand, J., Leturmy, P., Ruíz, G., El Haimer, F.Z. and De Lamotte, D., 2008. Cenozoic denudation in the Marrakech High Atlas, Morocco: insight from apatite fission track thermochronology. Terra Nova, 20(3): 221-228.

Molnar, P. and Tapponnier, P., 1975. Cenozoic tectonics of Asia: effects of a continental collision. Science, 189(4201): 419-426.

Moreira, V.S., 1968. Tsunamis observados em Portugal. Publ. Serviço Meteorológico Nacional, GEO134. Lisbon.

Moreira, V., S., 1985. Seismotectonics of Portugal and its adjacent area in the Atlantic. Tectonophysics, 117(1-2): 85-96.

Morgan, P. and Fernández, M., 1992. Neogene vertical movements and constraints on extension in the Catalan Coastal Ranges, Iberian Peninsula, and the Valencia trough (western Mediterranean). Tectonophysics, 203(1-4): 185-201.

Muñoz, J.A., 1991. Evolution of a continental collision belt: ECORS-Pyrenees crustal balanced cross-section. Thrust tectonics: 235.

Muñoz, J.A., 2002. Alpine tectonics I: the Alpine system north of the Betic Cordillera. The geology of Spain: 367-400.

Muñoz-Martín, A., De Vicente, G. and González-Casado 1994. Análisis tensorial de la deformación superpuesta en el límite oriental de la cuenca de Madrid Cuaderno Lab. Xeolóxico de Laxe, 19: 203-214.

Muñoz-Martín, A. and De Vicente, G., 1998. Cuantificación del acortamiento alpino y estructura en profundidad del extremo sur-occidental de la Cordillera Ibérica (Sierras de Altomira y Bascuñana). Revista de la Sociedad Geológica de España, 11: 233.

Muñoz-Martín, A., De Vicente, G., Fernández-Lozano, J., Cloetingh, S., Willingshofer, E., Sokoutis, D. and Beekman, F., 2010. Spectral analysis of the gravity and elevation along the western Africa-Eurasia plate tectonic limit: Continental versus oceanic lithospheric folding signals. Tectonophysics, 495(3-4): 298-314.

Nikishin, A., Cloetingh, S., Lobkovsky, L., Burov, E. and Lankreijer, A., 1993. Continental

lithosphere folding in Central Asia (Part I): constraints from geological observations. Tectonophysics, 226(1-4): 59-72.

Oberhänsli, H. and Allen, P.A., 1987. Stable isotopic signatures of tertiary lake carbonates, Eastern Ebro Basin, Spain. Palaeogeography, Palaeoclimatology, Palaeoecology, 60: 59-75.

Olivet, J., 1996. La cinématique de la plaque ibérique. Bulletin des Centres de recherches exploration-production Elf-Aquitaine, 20: 131-195.

Oreshin, S., Vinnik, L., Peregoudov, D. and Roecker, S., 2002. Lithosphere and asthenosphere of the Tien Shan imaged by S receiver functions. Geophys. Res. Lett., 29(8): 1191.

Palencia-Ortas, A., Osete, M.L., Vegas, R., Silva, P., 2006. Paleomagnetic study of the Messejana Plasencia dyke (Portugal and Spain): a lower Jurassic paleopole for the Iberian plate. Tectonophysics 420: 455–472.

Palomeras, I., Carbonell, R., Flecha, I., Simancas, F., Ayarza, P., Matas, J., Martínez-Poyatos, D., Azor, A., Gonzáez Lodeiro, F., Pérez-Estaún, A., 2009. Nature of the lithosphere across the Variscan orogen of SW Iberia: Dense wide-angle seismic reflection data. J. Geophys. Res., 114.

Pedreira, D., Pulgar, J.A., Gallart, J. and Díaz, J., 2003. Seismic evidence of Alpine crustal thickening and wedging from the western Pyrenees to the Cantabrian Mountains (north Iberia). J. Geophys. Res., 108.

Pedreira, D., Pulgar, J.A., Gallart, J. and Torné, M., 2007. Three-dimensional gravity and magnetic modeling of crustal indentation and wedging in the western Pyrenees-Cantabrian Mountains. J. Geophys. Res., 112(B12): B12405.

Peltzer, G. and Tapponnier, P., 1988. Formation and evolution of strike-slip faults, rifts, and basins during the India-Asia collision: An experimental approach. Journal of Geophysical Research, 93(B12): 15085-15,117.

Persson, K.S. and Sokoutis, D., 2002. Analogue models of orogenic wedges controlled by erosion. Tectonophysics, 356(4): 323-336.

Pinheiro, L., Wilson, R., dos Reis, R., Whitmarsh, R. and Ribeiro, A., 1996. The Western Iberia Margin: A Geophysical and Geological Overview. Proceedings of the Ocean Drilling Program, 149.

Portero, J. and Aznar, J., 1984. Evolución morfotectónica y sedimentación terciarias en el Sistema Central y cuencas limítrofes (Duero y Tajo). Congr. Esp. Geol. Segovia: 253-263.

Puigdefábregas, C., Muñoz, J. and Vergés, J., 1992. Thrusting and foreland basin evolution in the southern Pyrenees. Thrust tectonics: 247–254.

Pulgar, J., Gallart, J., Fernández-Viejo, G., Pérez-Estaún, A. and Álvarez-Marrón, J., 1996. ESCIN Group, 1996. Seismic image of the Cantabrian Mountains in the western extension of the Pyrenean belt from integrated reflection and refraction data. Tectonophysics, 264: 1-19.

Raffel, M., 2007. Particle image velocimetry: a practical guide. Springer Verlag.

Ramberg, H., 1967. Gravity, deformation and the earth´s crust: as studied by centrifuged models. Academic P.

Ramsay, A.T.S., 1970. The pre-Pleistocene stratigraphy and palaeontology of the Palmer Ridge area (northeast Atlantic). Marine Geology, 9(4): 261-285.

Ramsay, J. and Huber, M., 1987. The techniques of modern structural geology: Folds and fractures. Academic Pr.

Ranalli, G., 1995. Rheology of the Earth. Kluwer Academic Publishers, 413 pp.

Rey-Moral, C., Gómez-Ortiz, D. and Tejero, R., 2000. Spectral analysis and gravity modelling of the Almazán Basin (Central Spain). Revista de la Sociedad Geológica de España, 13(1): 131.

Rey-Moral, C., Gómez-Ortiz, D., Sánchez-Serrano, F. and Tejero, R., 2004. Modelos de densidades de la corteza de la cuenca de Almazán (Provincia de Soria). Boletín Geológico y Minero, 115(1): 137-152.

Rey, P., Vanderhaeghe, O. and Teyssier, C., 2001. Gravitational collapse of the continental crust: definition, regimes and modes. Tectonophysics, 342(3-4): 435-449.

Riba, O., Reguant, S. and Villena, J., 1983. Ensayo de síntesis estratigráfica y evolutiva de la cuenca terciaria del Ebro. Libro homenaje a JM Ríos, Geología de España, 2: 131-159.

Ribeiro, A., Kullberg, M., Kullberg, J., Manuppella, G. and Phipps, S., 1990. A review of Alpine tectonics in Portugal: foreland detachment in basement and cover rocks. Tectonophysics, 184(3-4): 357-366.

Ricard, Y., Froidevaux, C. and Simpson, R., 1987. Spectral analysis of topography and gravity in the Basin and Range Province. Tectonophysics, 133(3-4): 175-179, 183-187.

Rivero, L., Guimerá, J. and Casas, A., 1996. Estructura profunda de la cuenca de Cameros (Cordillera Ibérica) a partir de datos gravimétricos. Geogaceta, 20: 7.

Roca, E. and Guimerá, J., 1992. The Neogene structure of the eastern Iberian margin: structural constraints on the crustal evolution of the Valencia trough (western Mediterranean). Tectonophysics, 203(1-4): 203-218.

Rodriguez-Aranda, J., Martín, A.M., Giner, J. and Cañaveras, J., 1995. Estructuras tectónicas en el basamento de la cuenca de Madrid y su reflejo en la cobertera sedimentaria. Geogaceta, 18:19-22.

Roest, W. and Srivastava, S., 1991. Kinematics of the plate boundaries between Eurasia, Iberia, and Africa in the North Atlantic from the Late Cretaceous to the present. Geology, 19(6): 613.

Rosales-Calvo, F., Carbo-Gorosabel, A. and Cavidad-Camina, S., 1977. Transversal gravimetrica sobre el Sistema Central e implicaciones corticales. Bol. Geol. Min. Inst. Geol. Min. España, 88: 567–573.

Roure, F., Choukroune, P., Berastegui, X., Muñoz, J.A., Villien, A., Matheron, P., Bareyt, M., Seguret, M., Camara, P. and Deramond, J., 1989. ECORS deep seismic data and balanced cross sections: geometric constrains on the evolution of the Pyrenees. Tectonics, 8: 41-50.

Ruíz, J., Gómez-Ortiz, D. and Tejero, R., 2006a. Effective elastic thicknesses of the lithosphere in the Central Iberian Peninsula from heat flow: Implications for the rheology of the continental lithospheric mantle. Journal of Geodynamics, 41(5): 500-509.

Ruíz, M., Gallart, J., Díaz, J., Olivera, C., Pedreira, D., López, C., González-Cortina, J.M. and Pulgar, J.A., 2006b. Seismic activity at the western Pyrenean edge. Tectonophysics, 412(3-4): 217-235.

Salas, R. and Casas, A., 1993. Mesozoic extensional tectonics, stratigraphy and crustal evolution during the Alpine cycle of the eastern Iberian basin. Tectonophysics, 228(1-2): 33-55.

Salas, R. and Guimerá, J., 1996. Rasgos estructurales principales de la cuenca cretácica inferior del Maestrazgo (Cordillera Ibérica oriental). Geogaceta, 20(7): 1704-1706.

Schmalholz, S., Podladchikov, Y. and Burg, J., 2002. Control of folding by gravity and matrix thickness: implications for large-scale folding. Journal of Geophysical Research, 107(B1): 2005.

Schmid, D. and Podladchikov, Y., 2006. Fold amplification rates and dominant wavelength selection in multilayer stacks. Philosophical Magazine, 86(21): 3409-3424.

Schwarz, G. and Wigger, P., 1988. Geophysical studies of the earth´s crust and upper mantle in the Atlas system of Morocco. The Atlas System of Morocco: 339-357.

Searle, R.C. and Whitmarsh, R.B., 1978. The structure of King´s Trough, Northeast Atlantic, from

bathymetric, seismic and gravity studies. Geophysical Journal of the Royal Astronomical Society, 53(2): 259-287.

Sherwin, J.A. and Chapple, W.M., 1968. Wavelengths of single-layer folds; a comparison between theory and observation. American Journal of Science, 266(3): 167.

Simancas, J.F., Carbonell, R., González-Lodeiro, F., Pérez-Estaún, A., Juhlin, C., Ayarza, P., Kashubin, A., Azor, A., Martínez-Poyatos, D., Almodóvar, G.R., Pascual, E., Sáez, R., Expósito, I., 2003. Crustal structure of the transpressional Variscan orogen of SW Iberia: SW Iberia deep seismic reflection profile (IBERSEIS). Tectonics, 22.

Simón-Gómez, J., 1986. Analysis of a gradual change in stress regime(example from the eastern Iberian Chain, Spain). Tectonophysics, 124(1-2): 37-53.

Simón-Gómez, J. and Liesa, C., 2011. Incremental slip history of a thrust: diverse transport directions and internal folding of the Utrillas thrust sheet (NE Iberian Chain, Spain). Geological Society, London, Special Publications, 349(1): 77.

Smit, J.H.W., Brun, J.P. and Sokoutis, D., 2003. Deformation of brittle-ductile thrust wedges in experiments and nature. J. Geophys. Res., 108.

Smit, J.H.W., 2005. Brittle-ductile coupling in thrust wedges and continental transforms. Unpublished PhD thesis, Vrije Universiteit, Amsterdam: 115.

Smith, R., 1975. Unified theory of the onset of folding, boudinage, and mullion structure. Bulletin of the Geological Society of America, 86(11): 1601.

Smith, R., 1977. Formation of folds, boudinage, and mullions in non-Newtonian materials. Bulletin of the Geological Society of America, 88(2): 312.

Sokoutis, D., Burg, J.P., Bonini, M., Corti, G. and Cloetingh, S., 2005. Lithospheric-scale structures from the perspective of analogue continental collision. Tectonophysics, 406(1-2): 1-15.

Sokoutis, D. and Willingshofer, E., 2011. Decoupling during continental collision and intra-plate deformation. Earth and Planetary Science Letters, 305(3–4): 435-444.

Sopeña, A., López, J., Arche, A., Pérez-Arlucea, M., Ramos, A., Virgili, C. and Hernando, S., 1988. Permian and Triassic rift basins of the Iberian Peninsula. Triassic-Jurassic rirting. Developments in Geotectonics, Amsterdam, Elsevier, 22: 757-786.

Soto, R., Villalán, J.J. and Casas-Sainz, A.M., 2008. Remagnetizations as a tool to analyze the tectonic history of inverted sedimentary basins: A case study from the Basque-Cantabrian basin (north Spain). Tectonics, 27:1-16pp. TC1017, doi:10.1029/2007TC002208,

Souriau, A., 1984. Geoid anomalies over Gorringe Ridge, North Atlantic Ocean. Earth and Planetary Science Letters, 68(1): 101-114.

Srivastava, S.P., Sibuet, J.C., Cande, S., Roest, W.R. and Reid, I.D., 2000. Magnetic evidence for slow seafloor spreading during the formation of the Newfoundland and Iberian margins. Earth and Planetary Science Letters, 182(1): 61-76.

Stapel, G., Cloetingh, S. and Pronk, B., 1996. Quantitative subsidence analysis of the Mesozoic evolution of the Lusitanian basin (western Iberian margin). Tectonophysics, 266(1-4): 493-507.

Stapel, G., 1999. The nature of isostasy in West Iberia and its bearing on Mesozoic and Cenozoic regional tectonics. Published PhD thesis, Vrije Universiteit Amsterdam, the Netherlands.

Stephenson, R. and Lambeck, K., 1985. Isostatic response of the lithosphere with in-plane stress: application to central Australia.

Stephenson, R., Ricketts, B., Cloetingh, S. and Beekman, F., 1990. Lithosphere folds in the Eurekan orogen, Arctic Canada? Geology, 18: 603-606.

Stephenson, R. and Cloetingh, S., 1991. Some examples and mechanical aspects of continental

lithosphere folding. Tectonophysics, 188: 27-37.

Stich, D., Ammon, C.J. and Morales, J., 2003. Moment tensor solutions for small and moderate earthquakes in the Ibero-Maghreb region. J. Geophys. Res., 108(B3): 2148.

Stich, D., Mancilla, F.d.L. and Morales, J., 2005. Crust-mantle coupling in the Gulf of Cadiz (SW-Iberia). Geophys. Res. Lett., 32(13): L13306.

Storti, F., Holdsworth, R.E. and Salvini, F., 2003. Intraplate strike-slip deformation belts. Geological Society, London, Special Publications, 210(1): 1-14.

Stüwe, K., 2007. Geodynamics of the lithosphere: An introduction. Springer Verlag.

Surinach, E. and Vegas, R., 1988. Lateral inhomogeneities of the Hercynian crust in central Spain. Physics of the Earth and Planetary Interiors, 51: 226-234.

Tapponnier, P. and Molnar, P., 1979. Active faulting and Cenozoic tectonics of the Tien Shan, Mongolia, and Baykal regions. Journal of Geophysical Research, 84(B7): 3425-3459.

Talwani, M., Worzel, J.L. and Landisman, M., 1959. Rapid Gravity Computations for Two-Dimensional Bodies with Application to the Mendocino Submarine Fracture Zone. J. Geophys. Res., 64(1): 49-59.

Talwani, M. and Heirtzler, J., 1964. Computation of magnetic anomalies caused by two-dimensional structures of arbitrary shape. Computers in the mineral industries, 9: 464-480.

Teixell, A., 2000. Geotectónica de los Pirineos. Investigación y Ciencia, 288: 54-65.

Teixell, A., Arboleya, M., Julivert, M. and Charroud, M., 2003. Tectonic shortening and topography in the central High Atlas (Morocco). Tectonics, 22(5): 1051.

Teixell, A., 2004. Estructura cortical de la Cordillera Pirenaica. Geología de España, SGE-IGME, Madrid: 321-321.

Tejero, R. and Ruíz, J., 2000. Transición dúctil-frágil en la corteza de la zona central de la Península Ibérica. Geogaceta: 163-166.

Tejero, R. and Ruíz, J., 2002. Thermal and mechanical structure of the central Iberian Peninsula lithosphere. Tectonophysics, 350(1): 49-62.

Tejero, R., González-Casado, J., Gómez-Ortiz, D. and Sánchez-Serrano, F., 2006. Insights into the "tectonic topography" of the present-day landscape of the central Iberian Peninsula (Spain). Geomorphology, 76(3-4): 280-294.

Tejero, R., Garzón-Heydt, G., Babín-Vich, R. and Fernández-García, P., 2010. Long-term evolving tectonic landscapes within intra-plate domains: the Iberian Peninsula. In: Horizons in Earth Science Research, 2: 103-123.

Ter Borgh, M., Oldenhuis, R., Biermann, C., Smit, J. and Sokoutis, D., 2010. The effects of basement ramps on deformation of the Prebetics (Spain): A combined field and analogue modelling study. Tectonophysics, 502(1-2): 62-74.

Tesauro, M., Kaban, M.K., Cloetingh, S.A.P.L., Hardebol, N.J. and Beekman, F., 2007. 3D strength and gravity anomalies of the European lithosphere. Earth and Planetary Science Letters, 263(1-2): 56-73.

Tesauro, M., Kaban, M.K. and Cloetingh, S.A.P.L., 2008. EuCRUST-07: A new reference model for the European crust. Geophys. Res. Lett., 35.

Tesauro, M., Kaban, M. and Cloetingh, S., 2010. Thermal and rheological model of the European lithosphere. In: New Frontiers in Integrated Solid Earth Sciences: 71-101.

Thatcher, W. and Pollitz, F.F., 2008. Temporal evolution of continental lithospheric strength in actively deforming regions. GSA Today, 18(4/5): 4.

Tikoff, B. and Teyssier, C., 1994. Strain modeling of displacement-field partitioning in transpressional orogens. Journal of Structural Geology, 16(11): 1575-1588.

Tikoff, B. and Maxson, J., 2001. Lithospheric buckling of the Laramide foreland during Late Cretaceous and Paleogene, western United States. Rocky Mountain Geology, 36(1): 13-35.

Tikoff, B., Teyssier, C. and Waters, C., 2002. Clutch tectonics and the partial attachment of lithospheric layers. EGU Stephan Mueller Special Publication Series, 1: 57-73.

Treagus, S., 1973. Buckling stability of a viscous single-layer system, oblique to the principal compression. Tectonophysics, 19: 271-289.

Treagus, S. and Fletcher, R., 2009. Controls of folding on different scales in multilayered rocks. Journal of Structural Geology.

Truyols, J., Ramos, J., Cladellas, L. and Llopis, J., 1991. El terciario de los alrededores de Oviedo. Acta Geológica Hispánica, 26(3-4).

Ubanell, A., 1981. Características principales de la fracturación tardihercínica en un segmento del Sistema Central español.

Ubanell, A.G., 1994. Los modelos tectónicos del Sistema Central Español Tectonic models of Spanish Central Range. Cuaderno do Laboratorio Xeolóxico de Laxe, 19: 249-260.

Ulomov, V., 1974. Dynamics of the Earth´s Crust in Central Asia and Earthquake Prediction. FAN, Tashkent, Uzbekistan (in Russian).

Van der Beek, P. and Cloetingh, S., 1992. Lithospheric flexure and the tectonic evolution of the Betic Cordilleras (SE Spain). Tectonophysics, 203(1-4): 325-344.

Van Wees, J.D. and Stephenson, R.A., 1995. Quantitative modelling of basin and rheological evolution of the Iberian Basin (Central Spain): implications for lithospheric dynamics of intraplate extension and inversion. Tectonophysics, 252(1-4): 163-178.

Van Wees, J.D. and Cloetingh, S., 1996. 3D flexure and intraplate compression in the North Sea Basin. Tectonophysics, 266(1-4): 343-359.

Van Wees, J.D., Arche, A., Beijdorff, C., López-Gómez, J. and Cloetingh, S., 1998. Temporal and spatial variations in tectonic subsidence in the Iberian Basin (eastern Spain): inferences from automated forward modelling of high-resolution stratigraphy (Permian–Mesozoic). Tectonophysics, 300(1-4): 285-310.

Vargas, H., Gaspar-Escribano, J. M., López-Gómez, J., Van Wees, J.D., Cloetingh, S., de La Horra, R. and Arche, A., 2009. A comparison of the Iberian and Ebro Basins during the Permian and Triassic, eastern Spain: A quantitative subsidence modelling approach. Tectonophysics, 474(1-2): 160-183.

Vauchez, A., Tommasi, A. and Barruol, G., 1998. Rheological heterogeneity, mechanical anisotropy and deformation of the continental lithosphere. Tectonophysics, 296(1-2): 61-86.

Vázquez, J.T., Medialdea, T., Ercilla, G., Somoza, L., Estrada, F., Fernández-Puga, M. C., Gallart, J., Grácia, E., Maestro, A., Sayago, M., 2008. Cainozoic deformational structures on the Galicia Bank Region (NW Iberian continental margin). Marine Geology, 249(1-2): 128-149.

Vegas, R., 1975. Wrench (transcurrent) fault System of the southwestern Iberian Peninsula, paleogeographic and morphostructural implications. Geologische Rundschau, 64(1): 266-278.

Vegas, R. and Suriñach, E., 1987. Engrosamiento de la corteza y relieve intraplaca en el centro de Iberia. Geogaceta, 2: 40–42.

Vegas, R., Vázquez, J., Surinach, E. and Marcos, A., 1990. Model of distributed deformation, block rotations and crustal thickening for the formation of the Spanish Central System. Tectonophysics, 184(3/4): 367-378.

Vegas, R., 2000. The intrusion of the Plasencia (Messejana) dyke as part of the Circum-Atlantic Early Jurassic magmatism: tectonic implications in the southwester Iberian Peninsula.

Geogaceta: 175–178.

Vegas, R., De Vicente, G., Muñoz-Martín, A. and Palomino, R., 2004. Los corredores de fallas de regua-Verín y Vilariça: zonas de transferencia de la deformación intraplaca en la península ibérica. Geotemas, 6(5): 245–249.

Vegas, R., 2005a. Deformación alpina de macizos antiguos. El caso del Macizo Ibérico (Hespérico). Boletín de la Real Sociedad Española de Historia Natural. Sección Geológica, 100(1-4): 39-54.

Vegas, R., De Vicente, G., Muñoz-Martín, A., Olaiz, A., Palencia, A., and Osete, M.L., 2005b. Was the Iberian Plate moored to Africa during the Tertiary, pp. 06769.

Vegas, R., Medialdea T. and Vázquez J.T., 2008. On the nature of the present-day plate boundary between the Iberian Peninsula and northern Africa. Geo-Temas, 10: 1535-1538.

Vera, J., 1998. El Jurásico de la Cordillera Bética: Estado actual de conocimientos y problemas pendientes The Jurassic of the Betic Range: State ofthe art and open questions. Cuadernos de Geología Ibérica: 17-42.

Vergés, J., Millán, H., Roca, E., Muñoz, J.A., Marzo, M., Cirés, J., Bezemer, T.D., Zoetemeijer, R. and Cloetingh, S., 1995. Eastern Pyrenees and related foreland basins: pre-, syn-and post-collisional crustal-scale cross-sections. Marine and Petroleum Geology, 12(8): 903-915.

Vergés, J. and Fernández, M., 2006. Ranges and basins in the Iberian Peninsula: their contribution to the present topography. Memoirs-Geological Society of London, 32: 223-234.

Villamor, M., 2002. Cinemática Terciaria y Cuaternaria de la Falla de Alentejo-Plasencia y su influencia en la peligrosidad sísmica del interior de la Península Ibérica, Tesis Doctoral. Universidad Complutense de Madrid, Madrid.

Vinnik, L.P., Reigber, C., Aleshin, I.M., Kosarev, G.L., Kaban, M.K., Oreshin, S.I. and Roecker, S.W., 2004. Receiver function tomography of the central Tien Shan. Earth and Planetary Science Letters, 225(1-2): 131-146.

Watts, A. and Ryan, W., 1976. Flexure of the lithosphere and continental margin basins. Tectonophysics, 36(1-3): 25-44.

Watts, A., 1978. An analysis of isostasy in the world´s oceans: 1. Hawaiian-Emperor seamount chain. J. geophys. Res, 83(B12): 5989-6004.

Watts, A.B., Karner, G.D. and Steckler, M.S., 1982. Lithospheric Flexure and the Evolution of Sedimentary Basins. Philosophical Transactions of the Royal Society of London. Series A, Mathematical and Physical Sciences, 305(1489): 249-281.

Watts, A. and Torné, M., 1992. Subsidence history, crustal structure, and thermal evolution of the Valencia Trough: A young extensional basin in the western Mediterranean. Journal of Geophysical Research, 97(B13): 20021-20,041.

Weijermars, R. and Schmeling, H., 1986. Scaling of Newtonian and non-Newtonian fluid dynamics without inertia for quantitative modelling of rock flow due to gravity (including the concept of rheological similarity). Physics of the Earth and Planetary Interiors, 43(4): 316-330.

Weissel, J.K., Anderson, R.N. and Geller, C.A., 1980. Deformation of the Indo-Australian plate. Nature, 287(5780): 284-291.

Welch, P., 1967. The use of fast Fourier transform for the estimation of power spectra: a method based on time averaging over short, modified periodograms. IEEE Transactions on Audio and Electroacoustics, 15(2): 70-73.

Westerweel, J., 1997. Fundamentals of digital particle image velocimetry. Measurement Science and Technology, 8: 1379.

Wigger, P., Asch, G., Giese, P., Heinsohn, W.D., Alami, S.O. and Ramdani, F., 1992. Crustal

structure along a traverse across the Middle and High Atlas mountains derived from seismic refraction studies. Geologische Rundschau, 81(1): 237-248.

Williams, P.F. and Jiang, D., 2001. The role of initial perturbations in the development of folds in a rock-analogue. Journal of Structural Geology, 23(6-7): 845-856.

Willingshofer, E. and Sokoutis, D., 2009. Decoupling along plate boundaries: Key variable controlling the mode of deformation and the geometry of collisional mountain belts. Geology, 37(1): 39-42.

Won, I. and Bevis, M., 1987. Computing the gravitational and magnetic anomalies due to a polygon: Algorithms and Fortran subroutines. Geophysics, 52(2): 232–238.

Woodcock, N.H. and Daly, M., 1986. The Role of Strike-Slip Fault Systems at Plate Boundaries [and Discussion]. Philosophical Transactions of the Royal Society of London. Series A, Mathematical and Physical Sciences, 317(1539): 13.

Zeyen, H., Ayarza, P., Fernández, M. and Rimi, A., 2005. Lithospheric structure under the western African-European plate boundary: A transect across the Atlas Mountains and the Gulf of Cadiz. Tectonics, 24(2): TC2001.

Ziegler, P.A., Cloetingh, S. and van Wees, J.D., 1995. Dynamics of intra-plate compressional deformation: the Alpine foreland and other examples. Tectonophysics, 252(1-4): 7-22.

Ziegler, P.A., Van Wees, J.-D. and Cloetingh, S., 1998. Mechanical controls on collision-related compressional intraplate deformation. Tectonophysics, 300(1-4): 103-129.

Ziegler, P.A. and Dèzes, P., 2006. Crustal evolution of Western and Central Europe. Geological Society, London, Memoirs, 32(1): 43-56.

Ziegler, P.A., Bertotti, G. and Cloetingh, S., 2002. Dynamic processes controlling foreland development–the role of mechanical (de) coupling of orogenic wedges and forelands. Stephan Mueller Special Publication Series, 1: 17-56.

Ziegler, P.A. and Dèzes, P., 2007. Cainozoic uplift of Variscan Massifs in the Alpine foreland: Timing and controlling mechanisms. Global and Planetary Change, 58(1-4): 237-269.

Zitellini, N., Gràcia, E., Matias, L., Terrinha, P., Abreu, M. A., DeAlteriis, G., Henriet, J. P., Dañobeitia, J. J., Masson, D. G., Mulder, T., Ramella, R., Somoza, L., Diez, S., 2009. The quest for the Africa-Eurasia plate boundary west of the Strait of Gibraltar. Earth and Planetary Science Letters, 280(1-4): 13-50.

Zoback, M.L., Zoback, M.D., Adams, J., Assumpcao, M., Bell, S., Bergman, E.A., Blumling, P., Brereton, N.R., Denham, D., Ding, J., Fuchs, K., Gay, N., Gregersen, S., Gupta, H.K., Gvishiani, A., Jacob, K., Klein, R., Knoll, P., Magee, M., Mercier, J.L., Muller, B.C., Paquin, C., Rajendran, K., Stephansson, O., Suarez, G., Suter, M., Udias, A., Xu, Z.H. and Zhizhin, M., 1989. Global patterns of tectonic stress. Nature, 341(6240): 291-298.

Summary

Long-term topography in Europe results from the interaction between Alpine continental collision and anomalously raising mantle material. The Alpine belt runs from southern Europe all the way to the Himalayas along thousands of kilometres. It resulted from the closure of oceanic realms and subsequent continental subduction and collision (Pyrenees, Alps, Carpathians, Dinarides, and Himalayas). However, far from the suture zone, little is known about the mountain building processes within plate interiors. For this reason, new research projects such as Topo-Europe (see Cloetingh et al., 2011b, in Topo-Europe Tectonophysics volume) and Topo-Iberia have recently arisen under international cooperation. The aim of these multi-scale investigations is to add new insights into deep Earth and surface processes.

Following this line of research, this thesis builds on analogue modelling and spectral analysis of topography and gravity data, aiming to portray and discuss the mechanisms of mountain building in intra-plate settings. More specifically the research focuses on the evolving topography and formation of related basins in Iberia, although the results can be extrapolated to other intra-plate areas where geophysical and geological data are scarce.

As is evident from aerial pictures, western Iberia is characterised by a regular pattern of topography from the Cantabrian Mountains in the north to the Sierra Morena Mountains in the south, following E-W to NE-SW trends. This periodic pattern has been linked to large-scale folds affecting the entire lithosphere. In contrast, in the Eastern part of the Peninsula topography relief follows E-W, NW-SE and NE-SW trends without any observable regularity. Although many theories have been formulated to explain these differences, none of them reconcile surface topography with deep earth processes. Among the questions that have not been answered yet by previous studies in Iberia the following stand out: what is the nature of the lithosphere in terms of possible strength variations inherited from different episodes of mountain building (Variscan) or rifting (Mesozoic); what are the process of intra-plate mountain development and the high elevation of the Duero Basin, or the Cainozoic influence of pre-existent late-Variscan tectonic structures over present-day topography.

The models presented in this thesis are based on geological and geophysical data available from Spain. The first series of models aims to understand the mechanism behind intra-plate mountain building and basin development in Iberia by testing two different lithosphere set-ups. I describe favourable conditions for the evolution of lithosphere folds that led to present-day topography. A de-coupled lithosphere where strength resides in the upper crust and mantle seems to be the key for the evolution of large-scale folds. However, the Iberian lithosphere is far from being homogenous in terms of lithospheric strength. Inherited structures stemming from Variscan phases of deformation as well as the weakening of the lithosphere related to Mesozoic extension possibly affected deformation during Cainozoic times. Therefore, a new set of experiments was carried out in order to study the mode of deformation under different thermo-mechanical conditions prior to the onset of Alpine shortening. Since analogue experiments allow the direct observation of the lithosphere after deformation, I established a new approach in order to reconcile surface and deep earth architecture through the study of gravity and topography.

Digital elevation models obtained from the model surface, together with the theoretical gravity data calculated from digitized model cross-sections, were analysed in terms of spectral analysis and compared with the Moho depth maps. This analysis allowed differentiating between periodic and non-periodic signals, which may explain the mechanism of mountain building (folding versus crustal thickening, respectively). Finally, models with heterogeneous lithosphere were implemented with the addition of pre-existent late-Variscan faults which may have influenced the position of the lithosphere folds and in turn the final configuration of topography. In order to study the influence of these tectonic structures, surface particle displacement field techniques were performed (Particle Image Velocimetry or PIV). PIV, therefore, aimed to discriminate between re-activation of old structures and neo-formed tectonic structures. The results of analogue models were compared with fieldwork carried out along the boundary between the Spanish Central System and the Iberian Range, where interfering structures (E-W to NE-SW oriented) are coeval with NE-SW, NW-SE and E-W striking structures in Central Spain. Interestingly, field data and analogue modelling concluded that different topographic trends can be caused by folding of the lithosphere with laterally different thermo-mechanical conditions under a single N-S stress field during the Pyrenean stage of the Alpine Orogeny.

Chapter 1 provides a brief introduction of the observed topographic trends and introduces the main theories concerning mountain building in Iberia. In *chapter 2*, I summarise the principal mechanisms for single and multi-layer folding, studying the existing relationships between faulting and folding at large-scale. Moreover, I review the differences and similarities between folding of oceanic and continental lithosphere on the basis of areas where lithospheric folding has been described.

The tectonic evolution of the Iberian Peninsula is presented in *chapter 3*, where geological and geophysical data has been compiled in order to describe the rheology and evolution of the Iberian lithosphere. A series of analogue models are shown where I investigate folding of a de-coupled lithosphere and the associated uplift of the northwestern corner of Iberia (Galicia Massif) related to the opening of the Kings Trough in the Atlantic offshore.

Chapter 4, addresses the new methodology carried out on the analogue experiments combining the calculation of the theoretical gravity and spectral analysis of topography from model cross-sections. The results show differences on mode of deformation between a simple scenario comprising a homogeneous strong and cold (Variscan in age) lithosphere and a weak and hot heterogeneous lithosphere, representing lateral variations in strength from western to eastern Iberia. The results show similar wavelengths of gravity and topography between models and nature (short ~50 km and long ~250km), indicating the presence of periodic signals to the west. Therefore, the regular pattern of topography can be related to folding of the Variscan lithosphere, whereas the lack of hardly any periodicity to the eastern part of Iberia can be related to other processes like crustal thickening by thrusting and lower crustal flow processes.

Chapter 5 shows the surface particle displacement field analysis carried out on the analogue experiments comparing the results with the intra-plate configuration of topographic reliefs in Spain. The influence of lateral lithosphere strength variations and pre-existent tectonic structures on strain localization and the surface expression of deformation is investigated. The structural interpretation of modelling results displacement vector field indicates re-activation of pre-existent structures (NE-SW and NW-SE oriented) during uni-directed N-S compression illustrating a scenario of strain partitioning that may favour the observed differences of present-day topographic trends in Iberia.

Finally, in *Chapter 6*, I provide the summary and conclusions. A brief discussion between well-known areas affected by lithospheric folding is shown. Moreover, I argue about

the connection between regular E-W, NE-SW trends of topography observed in western Spain with those along the Moroccan Atlas in northern Africa. Similar discussion is focussed on the area of the Tian Shan and Pamir mountains in Central Asia, where long-term topography has been linked to lithosphere folds. A synthesis concerning the influence of pre-existent faults on the final configuration of a deformed intra-plate area is compared with the tectonic structures from models and the Merida Andes in Venezuela, illustrating the main differences and similarities related to intra-plate reactivation of inherited tectonic structures.

Samenvatting

Lange termijn topografie in Europa is het gevolg van de interactie tussen botsende continenten en het opreizen van mantel materiaal. Het Alpine gebergte loopt van Zuidwest Europa helemaal tot aan het Himalaya gebergte in het Verre Oosten. Deze keten is het gevolg van het sluiten van verschillende oceanen en de daarop volgende botsing tussen continenten. De Pyreneeën, Alpen, Karpaten, Dinariden, en de Himalaya maken deel uit van deze keten. Onderzoek naar het ontstaan van deze verschillende gebergten heeft al veel opgeleverd. Echter, de meeste studies richtte zich op de botsing gerelateerde deformatie direct rond de verschillende tektonische plaatgrenzen en in mindere mate op het deformeren van het continent zelf. Om deze reden zijn recentelijk nieuwe internationale onderzoeksprojecten opgezet, zoals Topo-Europe (zie Cloetingh et al., 2011b, in Tectonophysics volume) en Topo-Iberia, met als doel inzicht te verkrijgen in de relatie tussen de diepe Aarde en oppervlakte processen.

Binnen deze context wordt in dit proefschrift doormiddel van een integratie tussen analoge modellen en geologische/geofysische data het mechanisme achter gebergte- en bekkenvorming midden op het continent (intra-plate setting) nader onderzocht. Vervolgens worden de resultaten vergeleken met de grootschalige deformatie patronen die kenmerkend zijn voor intra-plate regionen en in het bijzonder het Iberisch schiereiland.

Het westelijk deel van het Iberisch schiereiland wordt gekenmerkt door een regelmatig patroon van O-W tot NO-ZW georiënteerde topografie, met het Cantabrisch gebergte als noordelijke grens. Dit patroon is in samenhang gebracht met een grootschalige plooi structuur van de gehele plaat (lithosfeer). In het oostelijk deel van het schiereiland daarin tegen, strekt de topografie overheersend O-W, NW-ZO, of NO-ZW en zonder duidelijke regelmaat. Alhoewel verschillende theorieën dit verschil proberen te verklaren omvat geen enkele een samenhang tussen de topgrafie en de diepere processen. Hierdoor zijn de volgende vragen nog steeds onbeantwoord: In welke mate is de sterkte van de Iberische lithosfeer bepaald door de verschillende periode van gebergtevorming (Varistisch) en rek (Mesozoïcum)? Welke processen zijn verantwoordelijk voor intra-plate gebergtevorming en de uiteindelijke opheffing van het Duero bekken? Wat is de invloed geweest van de al bestaande Laat-Varistische structuren op de huidige topografie?

De opbouw van de analoge modellen in dit proefschrift zijn gebaseerd op de geologische en geofysische gegevens van Spanje. Een eerste serie experimenten is erop gericht de mechanismes achter intra-plate gebergtevorming en bekken ontwikkeling op het Iberisch schiereiland beter te begrijpen. Hierin staat de relatie tussen het plooien van de gemodelleerde lithosfeer en de topografie centraal. Het blijkt dat een ontkoppeling tussen een relatief sterke bovenkorst en mantel lithosfeer noodzakelijk is voor het ontwikkelen van grootschalige plooistructuren.

Desalniettemin is de Iberische lithosfeer in termen van sterkte niet homogeen. Verschillende fases van vervorming (Varistisch) en verzwakking (Mesozoïcum) gingen vooraf aan de deformatie tijdens het Cenozoïcum. De invloed van deze opeenvolgingen op het

huidige deformatiepatroon en topografie wordt aan de hand van een tweede serie experimenten bestudeerd. Tevens worden de experimenten voor het eerst geanalyseerd door het combineren van hoogte modellen (DEM´s), en synthetische gravitatie; bepaald doormiddel van gedigitaliseerde profielen. Op deze manier worden signalen van het oppervlak en op diepte gecombineerd en kunnen worden vergeleken met zowel de topografie en Moho patronen van het Iberisch schiereiland. Het wordt daardoor mogelijk periodiek van non-periodieke signalen te scheiden om zo uiteindelijk de achterliggende processen van gebergtevorming te bepalen (plooiing of korstverdikking).

Een laatste uitbreiding van de modellen betreft het implementeren van reeds bestaande zwakte zones als zijnde een analoog voor Laat-Varistische breuken. Deze structuren beïnvloeden mogelijkerwijs het grootschalige plooiingspatroon en de uiteindelijke topografie. Om de bewegingen langs oude en nieuwe structuren te kunnen onderscheiden is gebruik gemaakt van Particle Image Velocimetry (PIV). Deze resultaten zijn vervolgens vergeleken met veldgegevens van het grensgebied tussen het Spaans Middengebergte en het Iberisch Massief, waar O-W en NO-ZW structuren gelijktijdig zijn gevormd met NO-ZW, NW-ZO en O-W structuren in centraal Spanje. Uit deze vergelijking tussen veld- en modeleer gegevens kan geconcludeerd worden dat de verschillende topografische oriëntaties het gevolg zijn van plooiing van een lithosfeer met laterale sterkte verschillen. In dit scenario kunnen de diverse oriëntaties gevormd zijn onder enkel N-Z verkorting gedurende de Pyrenean stage van de Alpine gebergtevorming.

Hoofdstuk 1 bestaat uit een korte introductie van de geobserveerde topografie en beschrijft de verschillende theorieën van gebergtevorming op het Iberisch schiereiland. In *hoofdstuk 2* worden de basis mechanisme achter plooiing van zowel enkele als meerder lagen en de relatie tussen breuken en plooien kort samengevat. Tevens wordt het verschil tussen het plooien van oceanische- en continetale lithosfeer toegelicht.

De tektonische evolutie van het Iberisch schiereiland wordt beschreven in *hoofdstuk 3*. Een overzicht van de geologische en geofysische data geeft inzicht in de rheologische ontwikkeling van de Iberische lithosfeer. De resultaten van een eerste serie experimenten worden gepresenteerd en vergeleken met de plooiing van een ontkoppelde lithosfeer en geassocieerde opheffing van NW Spanje (Galicia Massief) in relatie tot het openen van de King slenk.

In *hoofdstuk 4* wordt een nieuwe methode besproken waarin synthetische gravitatie en spectrum analyse van de topografie van de modellen worden gecombineerd. De resultaten laten het verschil zien tussen de deformatie van een homogene, sterke, en koude lithosfeer enerzijds, en de deformatie van een heterogene, zwakke, en warme lithosfeer anderzijds. De golflengten van de gravitatie en topografie komen overeen met westelijk Iberia (kort ~50 km en lang ~250 km), en zijn gerelateerd aan plooiing van de Varistische lithosfeer. Echter, de afwezigheid van periodiciteit in het oostelijk deel van Iberia kan zijn veroorzaakt door korstverdikking door middel van overschuivingen of het vloeien van de onderkorst.

In *hoofdstuk 5* worden aan de hand van Particle Image Velocimetry (PIV) de analoog modeleer resultaten vergeleken met veldgegevens afkomstig uit centraal Spanje. Dit gebied wordt gekenmerkt door overlappende topografische patronen welke op grote schaal typerend zijn voor het gehele Iberisch schiereiland. De mogelijke invloed van een laterale sterkte variatie in the lithosfeer en de aanwezigheid van bestaande tektonische structuren op deze complexe topografie is nader onderzocht. Uit de modeleer resultaten blijkt dat reactivatie van NO-ZW en NW-ZO georiënteerde structuren onder een N-Z verkorting inderdaad de topografische patronen op het Iberisch schiereiland kan verklaren.

In *hoofdstuk 6* zijn de belangrijkste conclusies uit dit onderzoek samengevat. Tevens

worden de mogelijke toepassingen van de bevindingen op andere gebieden waar plooiing van de lithosfeer plaatsvindt besproken. Een mogelijke verbinding tussen de grootschalige topografische patronen in het westelijk deel van het Iberisch schiereiland en de topografie van de het Marokkaanse Atlas gebergte in noordwest Afrika wordt beargumenteerd. Ook wordt de samenhang tussen topografie en plooiing van de lithosfeer in the Tian Shan en Pamir gebergte in Centraal Azië bediscussieerd aan de hand van de conclusies. De invloed van bestaande breuken op de configuratie van een deformerende plaat wordt verder verduidelijkt door een vergelijking tussen de modeleer resultaten en structurele interpretaties van de Merida Andes in Venezuela.

Resumen

A largo plazo, la topografía en Europa es el resultado de la interacción entre la colisión continental Alpina y la presencia de una anomalía mantélica ascendente hacia la superficie terrestre. El cinturón Alpino se extiende desde el sur de Europa hacia los Himalayas a lo largo de miles de kilómetros. Esta masa montañosa resulta del cierre de océanos y la posterior subducción de los mismos, provocando una colisión continental (como por ejemplo, los Pirineos, Alpes, Cárpatos, Dinarides e Himalayas). Sin embargo, lejos de la zona de sutura, en el interior de las placas tectónicas, se conoce muy poco sobre los procesos de formación del relieve. Por esta razón, nuevos proyectos como Topo-Europe (ver Cloetingh et al., 2011b, en el volumen especial de Tectonophysics) y Topo-Iberia han surgido como resultado de una estrecha colaboración científica internacional. Los nuevos proyectos surgidos permitirán obtener nuevos conocimientos sobre el interior terrestre y los procesos que operan en la superficie.

Siguiendo esta linea de investigación, en esta Tesis se establece una relación entre modelación análoga y análisis espectral de datos de topografía y anomalía de la gravedad, permitiendo conocer y discutir los mecanismos de formación de relieves montañosos en zonas de interior de placas. De modo más específico, la investigación se centra en la evolución de la topografía y la formación de cuencas adyacentes en la Península Ibérica, aunque los resultados pueden extrapolarse a otras zonas intra-placa, donde la ausencia de datos geológicos y geofísicos impiden el estudio del interior terrestre.

Como evidencian las fotos aéreas, la zona occidental de la Península Ibérica se caracteriza por un patrón regular de la topografía que se extiende desde la Cordillera Cantábrica en el norte, hacia Sierra Morena en el sur, siguiendo una dirección E-O a NE-SO. Este patrón periódico ha sido relacionado con la presencia de unos pliegues que afectan a toda la litosfera (corteza superior, inferior y manto superior litosférico). En cambio, hacia la parte oriental de la Península, el relieve topográfico sigue un patrón E-O, NO-SE y en algunas ocasiones NE-SO sin que pueda observarse regularidad alguna. Aunque se han postulado muchas teorías para explicar estas diferencias, ninguna de ellas establece una relación sostenible entre los procesos de modelado del relieve superficial y del interior terrestre. Entre algunas de las cuestiones no resueltas, en la actualidad, destacan: la naturaleza de la litosfera en términos de posibles variaciones de resistencia, heredados de episodios disferentes de formación de montañas (Orogenia Varisca) y extensión tectónica (rifting Mesozoico); conocer los procesos intra-placa que dan lugar a la elevada topografía que se observa en la Cuenca del Duero, así como la influencia de estructuras tectónicas post-Variscas durante el Cenozoico (Terciario), que podrían haber jugado un papel importante en la disposición del relieve topográfico Peninsular actual.

Los modelos presentados en esta Tesis Doctoral están basados en un extenso conocimiento geológico y en los datos geofísicos disponibles en España. La primera serie de modelos ayuda a comprender el mecanismo que está detrás de la formación del relieve topográfico y la evolución de cuencas sedimentarias que los acompañan en el interior de placa, mediante la comparación de dos modelos litosféricos con distintas caracterísitcas de partida. Se describen las condiciones favorables para la evolución de pliegues litosféricos que llevan a la

topografía actual. Una litosfera des-acoplada donde la resistencia reside en la corteza superior y el manto parece ser la clave para la evolución de grandes pliegues litosféricos. Sin embargo, la litosfera Ibérica presenta heterogeneidades en términos de resistencia litosférica. La presencia de estructuras tectónicas heredadas de las fases Variscas de deformación, así como el debilitamiento de la litosfera relacionado con la extensión litosférica Mesozoica, han jugado un papel muy importante durante la deformación Cenozoica. Por ello, se realizaron una serie de modelos para estudiar el modo de deformación bajo condiciones tectono-termales distintas de la litosfera, anteriores al comienzo del acortamiento Alpino. Como los experimentos análogos permiten la observación directa de la litosfera tras la deformación, se ha establecido una nueva metodología que permite el estudio de la litosfera superficial y profunda a través de la comparación de datos topográficos y de anomalía de la gravedad. Para ello se obtuvieron los Modelos Digitales de Elevaciones (DEMs) de la superficie de los experimentos, y se calculó la anomalía de la gravedad teórica a partir de la digitalización de los perfiles obtenidos tras la deformación de los modelos.

Finalmente estos datos se analizaron mediante la obtención del análisis espectral que se comparó con los mapas de profundidades del Moho. Este análisis sistemático permitió diferenciar entre señales periódicas y no periódicas, que pudiesen explicar el mecanismo de formación del relieve (plegamiento litosférico/engrosamiento cortical). Así mismo, los modelos con una variaciones de resistencia litosférica fueron completados con la presencia de estructuras tectónicas pre-existentes de edad post-Varisca, las cuales pudieron haber influenciado la posición de los pliegues que afectan a la litosfera, así como la configuración final de la topografía.

Para estudiar esta influencia, se estudió mediante una nueva técnica, conocida como "Campo de Velocidades de Partícula en Superficie" (con su acrónimo anglosajón PIV), la evolución cinemática de las fallas originadas en el modelo. El PIV, por tanto, permitió discriminar entre re-activación de antiguas estructuras y la neo-formación de estructuras tectónicas. Los resultados de los modelos análogos fueron comparados con estudios de campo llevados acabo en la zona de enlace entre el Sistema Central y la Cordillera Ibérica, donde interfieren estructuras tectónicas con direcciones variadas (E-O y NE-SO, típicas del Sistema Central) coetáneas con estructuras de dirección NE-SO, NO-SE y E-O Ibéricas. Sorprendentemente, los datos de campo y la modelación análoga concluyen que los distintos patrones topográficos observados resultan de una litosfera con diferencias termo-mecánicas laterales intersectada por fallas de orientaciones diversas que favorece los procesos de plegamiento litosférico y el engrosamiento cortical por inversión tectónica bajo un campo de esfuerzos N-S Pirenaico, que tuvo lugar durante gran parte de la Orogenia Alpina.

El *capítulo 1* proporciona una breve introducción a los patrones del relieve observados y sirve de introducción a las principales teorías propuestas sobre el origen de la formación de las cadenas montañosas en la Península Ibérica. En el *capítulo 2* hago un resumen de los principales mecanismos de plegamiento para una o múltiples capas, estudiando la relación existente entre plegamiento y fracturación a gran escala. Además, llevo a cabo una revisión de las diferencias y similitudes entre el plegamiento de la litosfera oceánica y la continental, en base a las zonas donde se ha descrito el proceso de plegamiento litosférico en nuestro planeta.

La evolución tectónica de la Península Ibérica se presenta en el *capítulo 3*, donde se han recogido datos geológicos y geofísicos para describir la reología y evolución de la litosfera Ibérica. Una serie de modelos análogos donde se investiga el plegamiento de una litosfera des-acoplada, así como el origen del levantamiento propuesto en la zona noroccidental de España (Macizo Galaico), como consecuencia de la apertura del Surco de King en la plataforma Atlántica.

En el *capítulo 4*, se recoge una nueva metodología llevada a cabo en la modelación

análoga, que combina el cálculo de la anomalía de la gravedad teórica y el análisis espectral junto con la topografía, a lo largo de perfiles tomados de los modelos tras la deformación. Los resultados muestran diferentes modos de deformación entre un escenario de escasa complejidad que comprende una litosfera homogénea y resistente (de edad Varisca) y una litosfera heterogénea, caliente y débil, que representan las variaciones laterales en resistencia litosférica encontradas en la parte occidental y oriental, respectivamente en la Península Ibérica. Los resultados indican longitudes de onda para la gravedad y la topografía muy similares entre los modelos y la naturaleza (una corta ~50 km y una larga ~250 km), indicando la presencia de un patrón periódico hacia el oeste peninsular (Macizo Ibérico). Por tanto y como sugieren los modelos, este patrón regular de la topografía parece estar relacionado con el plegamiento de una litosfera estable, Varisca, mientras que la falta de periodicidad hacia el este peninsular podría estar relacionado con otros procesos como engrosamiento cortical por inversión tectónica (a través de cabalgamientos que engrosan la corteza), y por un proceso de flujo en la corteza inferior.

El *capítulo 5*, muestra el análisis llevado a cabo sobre la superficie de los modelos, basado en el estudio del campo de desplazamiento de partículas, que permitió la comparación de los resultados en la zona central de España. La importancia de esta zona reside en los distintos patrones observados en la topografía, los cuales reproducen, en una pequeña área, la multitud de orientaciones observadas, en general, en toda la Península. Se investiga la influencia de los cambios laterales de resistencia litosférica, así como la presencia de estructuras tectónicas pre-existentes y su influencia en la localización de la deformación y en la expresión final en superficie de dicha deformación. La interpretación estructural de los vectores de campo de partículas en superficie indican la reactivación de dichas estructuras pre-existentes con orientaciones principales NE-SO y NO-SE bajo un acortamiento dirigido N-S, mostrando un escenario de partición de la deformación que podría haber favorecido la formación de este patrón singular observado en la topografía actual de la Península Ibérica.

Finalmente, en el *capítulo 6*, proporciono un resumen y las conclusiones. Una breve discusión entre zonas donde se ha reconocido la presencia de pliegues litosféricos. Además, argumento sobre la conexión existente entre los patrones regulares E-O y NE-SO observados en la zona occidental de España y los relieves que forman el Atlas marroquí en el norte de África. Una discusión similar es propuesta para el área del Tien-Shan y la Cordillera del Pamir en Asia Central, donde la topografía a largo plazo ha sido relacionada con pliegues litosféricos. Una sintesis sobre la influencia de las fallas pre-existentes en la configuración final de la deformación de áreas intra-placa se presenta mediante la comparación de estructuras tectónicas de los modelos y un ejemplo en los Andes de Merida, Venezuela, mostrando las principales diferencias y similitudes en la reactivación de estructuras tectónicas heredadas en un entorno intra-placa.

Acknowledgements

First of all, I would like to thank my promotors Prof. Dr. Sierd Cloetingh and Prof. Dr. Gerardo de Vicente for their support to complete this Thesis. I wish also to thank my supervisors Dimi and Ernst, who were the objective view of my thoughts. Without you, this would not have been possible.

Life is a hard and a bumpy track that we all walk from childhood to elderly. The first pilgrims should have travelled around Europe opening new roads and building tracks thousands of years before us. They used maps that aimed to find their routes and understand the world as we know it today. In my way to the completion of this PhD Thesis, I wish particularly to thank my good friend, confident and colleague Stefan, because you were the map that made easy this route, and above all, we shared emotions, wishes and words. The world is small enough to meet each other again soon. Es importante también para mí, el papel que ha jugado tanto en mi vida personal como académica, mis padres, Esther y David, sin los cuales este sueño no hubiese sido posible. Gracias por todo. Deseo agradecer especialmente a Cristina, que ha dado "color" a esta Tesis. También a Nina y mis amigos Paquito, Miguel, Jalil y Raquel, al igual que a Belén, sin su empujón, esto hoy, no se hubiese hecho realidad. Quiero agradecer en estas líneas a Miguel, porque también estuvo allí, correr no solo nos hace fuertes: Impossible is nothing.

In addition, I would like to thank Alfonso and Andrei, because they contributed actively with their knowledge and advise, inproving this manuscript. I also thank Marten, David, Inge, Antonio, Manel, Jose Luis, Pilar, Ramón, Antonio and Endre who have been there, even when things were not so easy. To Marious, John and Dave with whom I have enjoyed nice scientific discussions in the field. I would also like to express in words my gratitude to my reading committee: Prof. Dr. Manel Fernández, Prof. Dr. Jan-Diederik Van Wees, Prof. Dr. Evgenii Burov, Dr. Antonio Casas and Dr. Fred Beekman.

My special thanks go to my girls Irene, Raheleh and Esther and my good friend Roozbeh, I am sure we will meet each other again. I spent a wonderful time in Amsterdam with all of you.

In addition, I cannot leave behind those people who made my stay in Amsterdam comfortable: Andrea, Ioan, Ward, Magdala, Mélody, Mohammed, Suzane, Marteen, Felipe, Karen, Tadashi, Antonio, Maria, Nico, Bernd, Moud, Ibrahim, Silvan, Aud, Wiebcke, Ron, Arno, Nynke, Boro, and Anna. I am also very greatful to people from Utrecht University, among others: Ria, Margot, Miranda and Karin who gave me their support. Unfortunately, I am sure that I forget more people that pushed me to the end of this adventure, you are also in the list.

Thanks to you all.